

THE HIGH PERFORMANCE LIQUID CHROMATOGRAPHY AND  
DETECTION OF PHOSPHOLIPIDS AND TRIGLYCERIDES

by



Bruce Jon Compton .

A Thesis Submitted to the Faculty of Graduate Studies  
and Research in Partial Fulfillment of the Requirement  
for the Degree of Doctor of Philosophy

Department of Chemistry  
McGill University  
Montreal, Quebec, Canada

September 1980

# 7

## ABSTRACT

Work on developing an instrumental system for total analysis of triglycerides and phospholipids is presented. Initial chromatographic analysis using reversed-phase high performance liquid chromatography on C<sub>6</sub>-bonded, 5  $\mu$ m silica stationary phase and acetonitrile-water (and dilute phosphoric acid with phospholipids) mobile phase is demonstrated. The Kovats index is shown to allow correlation of structure to retention behavior. An ultraviolet absorbance detector ( $\lambda_{195\text{nm}}$ ) and novel post-column reaction detector (p.c.r.) based on saponification, periodate oxidation and derivatization using a new class of reagents are used for detection. The p.c.r. is shown to be sensitive to samples in the lower nanomole-per-injection range.

A novel transport-thermal ionic detector for organophosphorus compounds and a new class of aldehyde reagents are introduced. The detector is capable of detecting some pesticides in the lower nanogram-per-injection range. The aldehyde reagents, called the Fluorals, of which Fluoral-P (4-amino-3-penten-2-one) is studied extensively, have promise of being useful for selective, rapid and sensitive (sub-nanomoles formaldehyde) determinations.

## RESUME

Le travail sur le développement d'un système instrumental permettant l'analyse totale d'espèces moléculaires de triglycérides et de phospholipides est présenté. Le système impliquait une analyse initiale par chromatographie à haute performance en phase inverse sur phase stationnaire de silice 5  $\mu\text{m}$  sur laquelle sont fixés des hydrocarbures  $\text{C}_6$ , et phase mobile d'acétonitrile/eau (et d'acide phosphorique dans le cas de phospholipides). L'index Kovats fût utilisé pour corrélérer la rétention à la structure. La réponse d'un détecteur d'absorbance ultraviolet (à 195 nm) et celle d'un détecteur de réaction post-colonne (r.p.c.) basé sur la saponification, l'oxydation et la dérivatisation des lipides fût étudiée. Il a été constaté que le détecteur r.p.c. pouvait détecter des échantillons dans les régions de nanomoles par-injection.

Un détecteur impliquant une nouvelle combinaison de détection par transport et par ionization thermique fût aussi développé pour les composés organo-phosphore et une nouvelle classe de réactifs aldéhydes. Il a été constaté que ce détecteur était capable de détecter des pesticides organo-phosphorés dans les régions de nanomoles-par-injection. Le fluoral-P (4-amino-3-penten-2-one) qui fait partie de cette nouvelle classe de réactifs aldéhydes appelés fluorals, fût étudié extensivement et pourrait s'avérer utile dans les déterminations fluorométriques et colorimétriques sélectives et rapides des aldéhydes. Le fluoral-P fût utilisé pour déterminer la formaldéhyde à un niveau de 3 nanomoles par injection.

To my parents, Duane and Alice  
and to Janice



#### ACKNOWLEDGEMENTS

I would like to express my gratitude to Professor William C. Purdy for the support, guidance and patience he has given me during the course of this work.

Special appreciation is also extended to: M. Mancini, J. Honek and G. Lajoie, Jr. for helpful discussions concerning the organic synthetic work,

Drs. G. Just, T.-H. Chan, D.N. Harpp and B. Belleau for making available key equipment and allowing freedom of movement in their laboratories,

J.R. Weber for years of interesting conversation and Assunta Cerrone for the helpful typing of this manuscript.

TABLE OF CONTENTS

	<u>PAGE</u>
ACKNOWLEDGEMENTS .....	i
TABLE OF CONTENTS .....	ii
LIST OF FIGURES .....	vii
LIST OF TABLES .....	xii
PREFACE .....	xv
1. <u>INTRODUCTION</u> .....	1
1.1 SIGNIFICANCE OF TRIGLYCERIDES AND PHOSPHOLIPIDS	1
1.2 STRUCTURE OF TRIGLYCERIDES AND PHOSPHOLIPIDS ...	2
1.3 HIGH PERFORMANCE LIQUID CHROMATOGRAPHY .....	3
1.4 THE CHROMATOGRAPHIC SYSTEM .....	8
1.5 THE ANALYTICAL METHOD APPLIED HERE .....	13
REFERENCES .....	16
2. <u>THE REVERSED-PHASE CHROMATOGRAPHIC BEHAVIOR OF TRI- GLYCERIDES AND PHOSPHOLIPIDS</u> .....	18
2.1 INTRODUCTION .....	18
2.1.1 Modern Aspects of Lipid Separations .....	21
2.2 THEORETICAL CONSIDERATIONS AND THE KOVATS INDEX	23
2.3 EXPERIMENTAL .....	29

	<u>PAGE</u>
2.3.1 Instrumentation .....	29
2.3.2 Materials .....	33
2.4 RESULTS AND DISCUSSION .....	38
2.4.1 Preliminary Study and the Adsorptive Role	38
2.4.2 Studies on the Partition Role in the Reversed-Phase Mode .....	44
REFERENCES .....	57
 3. <u>PHOSPHORUS SENSITIVE DETECTION: MODIFICATION OF A TRANSPORT FLAME IONIZATION TO THE THERMAL IONIZATION MODE</u> .....	 61
3.1 INTRODUCTION .....	61
3.2 METHODS AND MATERIALS .....	62
3.3 RESULTS .....	71
3.3.1 Selectivity .....	75
3.3.2 Sensitivity .....	81
3.4 DISCUSSION .....	82
REFERENCES .....	86
 4. <u>DEVELOPMENT AND DESIGN OF A POST-COLUMN REACTOR FOR HIGH PERFORMANCE LIQUID CHROMATOGRAPHY</u> .....	 88
4.1 GENERAL INTRODUCTION .....	88
4.2 INSTRUMENTAL DESIGN CONSIDERATIONS .....	95

	<u>PAGE</u>
4.2.1 Introduction .....	95
4.2.2 Choice and Evaluation of Components .....	100
4.2.2.1 The bubbler .....	100
4.2.2.2 Ancillary tubing and some pressure considerations .....	113
4.2.2.3 Ancillary equipment, pull- through and the segmentation gas .....	120
4.2.2.4 The de-bubbler .....	122
4.2.2.5 Sampler(s) and the detector ....	124
4.3 CHEMISTRY OF THE REACTOR .....	125
4.3.1 The Chromophore Developing Reagents: Introduction, Stage I .....	128
4.3.2 Preliminary Studies: Introduction .....	131
4.3.2.1 Experimental .....	133
4.3.2.2 Results and discussion .....	136
4.3.3 Detailed Studies: Introduction .....	139
4.3.3.1 Experimental .....	143
4.3.3.2 Results and discussion .....	150
4.3.4 Characterization of Fluoral-P: Introduction .....	163
4.3.4.1 Experimental .....	163
4.3.4.2 Results and discussion .....	166
4.3.5 Chemistry of the Reactor, Stages II and III .....	173
4.3.5.1 Experimental .....	176
4.3.5.2 Results and discussion .....	179

	<u>PAGE</u>
4.4 OPTIMIZATION OF THE POST-COLUMN REACTOR .....	187
4.4.1 General Introduction .....	187
4.4.2 The Optimization Scheme Based on Stop- Flow Analysis .....	188
4.4.3 Experimental .....	192
4.4.4 Results and Discussion .....	194
4.5 DESCRIPTION OF THE TOTAL OPTIMIZED CONTINUOUS FLOW ANALYZER-POST COLUMN REACTOR SYSTEM .....	196
REFERENCES .....	199
APPENDIX 4-A .....	207
APPENDIX 4-B .....	208
5. <u>EVALUATION AND COMPARISON OF CHROMATOGRAPHIC DETECTORS     FOR THE DETERMINATION OF TRIGLYCERIDE AND     PHOSPHOLIPIDS</u> .....	210
5.1 INTRODUCTION .....	210
5.2 THE ULTRAVIOLET ABSORBANCE DETECTOR .....	210
5.2.1 Selectivity .....	214
5.2.2 Sensitivity .....	217
5.2.3 The Linear Dynamic Range .....	218
5.2.4 Operating Characteristics .....	220
5.3 THE POST-COLUMN REACTOR .....	220
5.3.1 Selectivity .....	226
5.3.2 Sensitivity .....	227

	<u>PAGE</u>
5.3.3 The Linear Dynamic Range .....	228
5.3.4 Operating Characteristics .....	229
5.4 COMPARISON OF THE DETECTOR RESPONSES .....	230
5.5 EXPERIMENTAL .....	234
5.5.1 Equipment .....	234
5.5.2 Chemicals .....	234
5.5.3 Methods .....	235
5.6 RESULTS AND DISCUSSION .....	240
5.6.1 Origins of Noise .....	240
5.6.2 Sources of Background and the Effects on Detection Limit .....	246
5.6.3 Comparison of the Absorbance and Fluorescence Response for Use with the Post-Column Reactor .....	247
5.6.4 Evaluation of Bubbled and Debubbled Response .....	249
5.6.5 Evaluations of the Detectors for Triglycerides and Phospholipids .....	256
REFERENCES .....	271
APPENDIX 5-A .....	272
CLAIMS TO ORIGINALITY .....	274

LIST OF FIGURES

<u>CHAPTER 1</u>	<u>DESCRIPTION</u>	<u>PAGE</u>
1-1	Schematic representation of the general h.p.l.c. ....	10
 <u>CHAPTER 2</u>		
2-1	Schematic representation of the experimental h.p.l.c. ....	30
2-2	Separation of triglycerides ....	30
2-3	Irreversible retention of PC ....	39
2-4	Separation of PC and diolein ....	39
2-5	Comparison of PC-C <sub>18:2</sub> and C <sub>18:2</sub> diglyceride	43
2-6	Retention <u>versus</u> % H <sub>3</sub> PO <sub>4</sub> for PC ....	43
2-7	Retention <u>versus</u> I for TG ....	46
2-8	Retention <u>versus</u> I and I <sub>corr.</sub> for PL ....	48
2-9	Retention <u>versus</u> D <sub>b</sub> for PL ....	48
2-10	Retention <u>versus</u> I and I <sub>corr.</sub> for TG ....	55
 <u>CHAPTER 3</u>		
3-1	The transport detector ....	64
3-2	The modified f.i.d. ....	65
3-3	i <sub>B.C.</sub> <u>versus</u> i <sub>B</sub> for days one and ten ....	65
3-4	i <sub>B.C.</sub> <u>versus</u> nitrogen, air and hydrogen flow rates ....	73
3-5	Detector response <u>versus</u> pyrolysis over temperature ....	78

<u>CHAPTER 3</u>	<u>DESCRIPTION</u>	<u>PAGE</u>
3-6	Response, noise and SNR <u>versus</u> $i_{B,C}$ .....	78
3-7	Response of the t.i.d. to a wide range of malathion, .....	83
 <u>CHAPTER 4</u>		
4-1	Comparison of c.f.a. and f.i.a. ....	94
4-2	Development of dispersion in a flow system .	94
4-3	Gas segmented plug flow in the c.f.a. ....	97
4-4	Optimum $d_t$ , $n$ and $F_R$ to give $\sigma_t$ .....	97
4-5	The c.f.a. system .....	101
4-6	The bubbler .....	101
4-7	The bubbler pattern .....	104
4-8	The bubble evaluation system .....	104
4-9	Correlation of A and C .....	109
4-10	Relation of $n$ to $F_{H_2O}$ .....	109
4-11	Relation of $V_b$ to $F_g$ .....	111
4-12	Relation of $n$ to $F_g$ .....	111
4-13	Relation of $n$ to $E$ .....	112
4-14	Minimum $L$ for various $n$ and tubing diameters and $F_T$ .....	112
4-15	The debubbler .....	123
4-16	TG analysis .....	123
4-17	Preliminary reactions of 1,3-diketones, ammonium acetate and formaldehyde, .....	137



<u>CHAPTER 4</u>	<u>DESCRIPTION</u>	<u>PAGE</u>
4-18	Intermediates and reaction paths investigated for the Nash reagent .....	140
4-19	The reactions and intermediates of the Sawicki method .....	142
4-20	Absorbance and fluorescence <u>versus</u> pH for IV and IX .....	149
4-21	Occurrence of II and IV in the Nash reagent	151
4-22	Comparison of fluorescence intensity of IV and IX .....	152
4-23	Excitation and emission spectra of IV and IX	152
4-24	Initial reaction rate of reaction between II or VI with formaldehyde <u>versus</u> pH .....	155
4-25	Initial reaction rate and hydrolysis rate for II <u>versus</u> pH .....	155
4-26	Reaction rate of Sawicki reagent <u>versus</u> pH	156
4-27	h.p.l.c. separation of intermediates of the Nash reagent .....	156
4-28	Adsorption t.l.c. of the Sawicki intermediates .....	157
4-29	h.p.l.c. of the Sawicki reagent intermediates .....	157
4-30	Absorbance and fluorescence intensity of the formaldehyde Fluoral-P reaction .....	170
4-31	SNR of absorbance and fluorescence <u>versus</u> amount of formaldehyde .....	170
4-32	Production and destruction of lutidine .....	182
4-33	Absorbance <u>versus</u> phosphoglycerol concentration .....	182
4-34	Decrease in signal <u>versus</u> periodate concentration .....	183

<u>CHAPTER 4</u>	<u>DESCRIPTION</u>	<u>PAGE</u>
4-35	h.p.l.c. of saponification samples and products .....	183
4-36	$W_{1/2}$ and H <u>versus</u> reactor temperature .....	186
4-37	Flr-intensity <u>versus</u> conc. perchloric acid ..	186
4-38	s.f.a. optimization method .....	191
4-39	c.f.a. reaction manifold and ancillary equipment .....	191
4-40	s.f.a. results for detector optimization ....	195
4-41	s.f.a. of the optimized system at 120 s .....	195
4-42	Photograph of the c.f.a. manifold .....	197

#### CHAPTER 5

5-1	Schematic of the Schoeffel SF770 .....	212
5-2	The "Zee" cell design .....	212
5-3	Schematic of the FS970 .....	224
5-4	Schematic of the frontal fluorescence cell ..	224
5-5	Recorder traces of some noise patterns .....	241
5-6	Noise due to successive addition of reagents	241
5-7	Noise and baseline at different dilutions ...	243
5-8	Baseline and noise at successive addition of reagents .....	243
5-9	Direct comparison of absorbance and fluorescence detection .....	248
5-10	Fluorescence response at different $\tau$ values .	248
5-11	H and $W_{1/2}$ <u>versus</u> $\tau$ .....	254

<u>CHAPTER 5</u>	<u>DESCRIPTION</u>	<u>PAGE</u>
5-12	2 $\sigma$ noise versus $\tau$ .....	255
5-13	Absorbance response of triolein .....	259
5-14	p.c.r. response of triolein and trilinolein .....	259
5-15	Absorbance response of PC-dilinoleoyl and dilinenoyl .....	260
5-16	p.c.r. response of PC-dilinoleoyl and dilinenoyl .....	260
5-17	$R_{\text{PCR}}^{\text{UV}}$ versus $D_b$ .....	266
5-18	h.p.l.c. of TG with absorbance and p.c.r. detection .....	269
5-19	h.p.l.c. of PL with absorbance and p.c.r. detection .....	270

LIST OF TABLES

<u>CHAPTER 2</u>	<u>DESCRIPTION</u>	<u>PAGE</u>
2-1	List of triglyceride standards .....	35
2-2	List of phosphatidylcholine standards .....	36
2-3	Molar concentrations of TG and PC standards	37
2-4	Summary of the effect of mobile phase modifiers .....	42
2-5	TG $k'$ data for various mobile phases .....	45
2-6	PC $k'$ data in 90% $\text{CH}_3\text{CN}/10\% \text{H}_2\text{O}-\text{H}_3\text{PO}_4$ .....	49
2-7	Summary of $\log k'$ <u>versus</u> $I$ linear regression data .....	50
2-8	$I_{\text{calc.}}$ values for unsaturated standards .....	53
2-9	$C$ values of unsaturation effects on $I$ .....	54
 <u>CHAPTER 3</u>		
3-1	Comparison of standards f.i.d. to t.i.d. responses .....	76
3-2	Comparison of pesticides f.i.d. to t.i.d. response .....	80
 <u>CHAPTER 4</u>		
4-1	Optimum $V_b$ for various tube diameters .....	106
4-2	Optimum $n$ for the B and measuring tube .....	106
4-3	$P_T$ specifications .....	115
4-4	Backpressure values for some tubing .....	119

<u>CHAPTER 4</u>	<u>DESCRIPTION</u>	<u>PAGE</u>
4-5	Summary of literature conditions for TG analysis .....	126
4-6	Lutidine equivalence background for some 2,4-pentanedione sources .....	138
4-7	Retention data for Nash and Sawicki reagents	154
4-8	Spot test results for Fluoral-P selectivity	168
4-9	Formaldehyde content of some laboratory solvents .....	172
4-10	Experimental conditions used to evaluate deacylation .....	180
4-11	Results of deacylation experiments .....	181
4-12	Summary of the optimized p.c.r. system .....	193

CHAPTER 5

5-1	Absorptivities of some polyenes .....	216
5-2	Operating characteristics of the UV absorption detector .....	221
5-3	Operating characteristics of the Schoeffel SF770 .....	222
5-4	Reported detection limits for h.p.l.c. detectors .....	231
5-5	Summary of detection limit and response expressions .....	232
5-6	Triglyceride and phospholipid standards used for the detector evaluations .....	236
5-7	Chromatographic conditions used to evaluate the detectors .....	238
5-8	Comparison of detector modifications on $W_{1/2}$ and H .....	251

<u>CHAPTER 5</u>	<u>DESCRIPTION</u>	<u>PAGE</u>
5-9	Linear regression analysis summary of data from Figures 5-13 to 5-16 .....	258
5-10	Detection limits $C_{SDL}^D$ .....	262
5-11	Detector response ratios .....	264
5-12	Molar response ( $R_{Flr}$ ) of the p.c.r. measured as area .....	268

APPENDIX 5.

5-A	Detector monochrometer calibrations .....	272
-----	---	-----

## PREFACE

Phospholipids and triglycerides are both major lipid classes which contain a diverse population of molecular species. The analytical techniques normally utilized for studying occurrence of these molecular species are destructive in nature and lose much information. The procedures are also very tedious to execute. Clearly, alternative methods are needed.

Recent advances in the field of liquid chromatography have made it at least conceivable that a total lipid analysis system can be developed.

By combining multiple detection with high efficiency chromatography this thesis lays the foundation for a total lipid analyzer.

BJC, 1980.

## 1. INTRODUCTION

### 1.1 SIGNIFICANCE OF TRIGLYCERIDES AND PHOSPHOLIPIDS

The definition of lipids as a chemical family can be based on the purely physiochemical property of solubility in organic solvents. While the field is diverse, general references on the nomenclature (1,2), chromatography (3,4), and chemistry (1,5,6), have been of aid in giving it definition. The foundations of phospholipid research have also been given some attention (1,7).

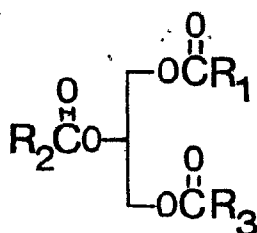
This work is concerned with the development of high performance liquid chromatographic techniques for quantitating the separate molecular species of two members of the lipid family, triglycerides and phospholipids. The triglycerides make up a major portion of the body's adipose tissue and are constituents of the class of bio-macromolecular complexes, the lipoproteins (8). Phospholipids are the major biological membrane constituents (9), lung surfactants (10) and the subject of much research interest. Both of these classes of compounds make up major portions of the biomass of any organism, are major classes of biomolecules, and are of at least peripheral interest to most biochemists. Also, they represent very diverse classes of complex molecules and are interesting to study from an analytical



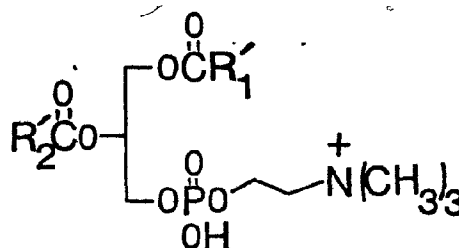
chemistry viewpoint.

## 1.2 STRUCTURES OF TRIGLYCERIDES AND PHOSPHOLIPIDS

The terms triglyceride (TG) and phospholipid (PL) refer to the triacyl derivative of glycerol and diacyl derivative of phosphatidylcholine, respectively. Recommended TG (Structure I) and PL (Structure II) nomenclature has been



I.



II.

proposed (2,11,12) and is used when specifically needed. The lipids used in this study are all non-stereospecifically substituted synthetic and symmetrical (i.e. all R's equal) molecular species. Thus little ambiguity should exist when referring to them.

The term "acyl glyceride(s)" is used to mean, collectively, the mono-, di- and triacyl derivatives of glycerol regardless of substitution position. Phosphatidyl-

choline (PC) is a member of the diverse class of phosphatides and was used as a model compound because it is readily available as a pure synthetic material.

The terms phospholipid, phosphatide and lecithin are used interchangeably and all refer to the general class of 1,2-diacylglycerol-3-phospho derivatives with the understanding that PC was used as the model. In most cases specific lipid molecular species are referred to by trivial name and a number identifying the lipid.

### 1.3 HIGH PERFORMANCE LIQUID CHROMATOGRAPHY

The spectacular advances and acceptance of high performance liquid chromatography (h.p.l.c.) as an analytical tool in the last ten years has made a discussion of this technique more a review rather than an introduction. The terminology used in this field generally follows that recommended for the closely related gas chromatography by the American Society for Testing Materials (13). The exceptions are that  $k$  is designated  $k'$  and  $n$  by  $N$ . A review of the terms encountered in this work is presented as follows.

#### Review of Terms

It is recalled that all chromatographic techniques are based on the differential affinity of a solute for a

mobile phase versus a stationary phase. This can be expressed by the equilibrium partition coefficient  $K$ ;

$$K = \frac{C_s}{C_m} \quad (1-1)$$

where  $C_s$  = concentration of  $x$  in the stationary phase,

$C_m$  = concentration of  $x$  in the mobile phase.

While  $K$  can be determined from extraction data and applied to liquid-liquid chromatography, the value  $k'$ , where

$$k' = K \frac{V_s}{V_m} \quad (1-2)$$

( $V_s$  and  $V_m$  are the volumes of stationary and mobile phases respectively) is of more practical interest. The value  $k'$  is termed the capacity factor, capacity of the stationary phase versus mobile for a given solute.

Another way of expressing  $k'$  is

$$k' = \frac{t_R - t_0}{t_0} \quad \text{or} \quad k' = \frac{V_R - V_0}{V_0} \quad (1-3)$$

$t_R$  = Retention time of solute, i.e., time to elute solute from column.

$t_0$  = Retention time for unretained solute, or the so-called void volume, the time required to elute one column plus

fittings volume of solvent.

$V_R$  = Retention volume calculated from  $t_R \cdot v$ ,  $v$  being flow rate of solvent.

$V_0$  = Retention time of unretained solute or the actual void volume.

It is important to note that  $k'$  is a measure of the partitioning of solute between stationary and mobile phase relative to time units, or

$k' = 0$ , solute spends all its time in the mobile phase.

$k' = 1$ , solute is equally partitioned and spends half its time adsorbed to stationary phase and half its time in the mobile phase.

The values  $k' = 1$  to 10 represent the optimum  $k'$  range ( $k' \approx 4$  optimized for a given solute) for a given mixture. For  $k' > 10$  time of elution may be too long (14).

Another parameter of importance is  $R$ , resolution between two eluting solute bands. Since time and separation ability are of importance in any chromatographic system,  $R$  as well as  $k'$  must be described.  $R$  is defined as

$$R = \frac{t_1 - t_2}{\frac{1}{2}(w_1 + w_2)} \quad (1-4)$$

where  $t_1$  and  $t_2$  are retention times for two solutes (1 and 2, respectively) of interest and  $w_1$  and  $w_2$  their respective baseline band widths.

To effectively evaluate one's chromatographic system (i.e. the column) the number of theoretical plates  $N$ , where  $N = 16(t_R/w_R)^2$ ,  $t_R$  again retention time for solute  $R$  and  $w_R$  its baseline band width, is of practical importance. The equation for  $N$  given above is a convenient method for estimating the overall efficiency (resolution, time) of a system.

A further quantity is

$$\alpha = \frac{k'_1}{k'_2} \quad (1-5)$$

the ratio of two solute capacity factors (note: base width not accounted for) which describes the differential selectivity of a given solvent-stationary phase system for two solutes.

The terms  $k'$ ,  $\alpha$  and  $N$  all contribute to the central objective of chromatography, solute separation. The measure of separation of two bands is their resolution, predicted by (15)

$$R = \frac{\sqrt{N}}{4} \left( \frac{\alpha-1}{\alpha} \right) \left( \frac{k'_2}{1+k'_2} \right) \quad (1-6)$$

which states that greater resolution  $R$  can be attained between two solute bands by increasing  $N$ , increasing  $\alpha$  (note  $\alpha = 1$ ,  $R = 0$ ,  $\alpha$  term  $\rightarrow 1$  for  $\alpha \rightarrow \infty$ ) and increasing  $k'$  of the second (last) band.

The  $N$  term represents hydrodynamic efficiency which can be increased by increasing column length  $L$  (a linear relationship, slope unity) or decreasing mobile phase velocity (from the Van Deemter equation (16)) directly or changing the column packing and mobile phase viscosity.

The selectivity term ( $\alpha$ ) represents different selectivity of the mobile or stationary phase for a given pair of solutes. It does not consider band width since it merely describes solvent selectivity and  $N$  is required to determine true resolution.

The capacity factor ( $k'$ ) term represents the solvent polarity in an overall sense since changing solvent polarity usually results in overall changes in  $k'$  for all solute peaks. This is in contrast to changing solvent selectivity, where one band  $k'$  is moved with respect to the other band  $k'$ . The net result of this is the change of  $\alpha$ , a measure of solvent selectivity.

The usual steps involved in developing a chromatographic separation are to find the right solvent polarity to bring the solutes off the column in a reasonable amount of time ( $k' < 15$ ), then either vary solvent selectivity

while leaving polarity constant or increasing system efficiency by increasing N. In this study the chromatographic behavior of TG and PL molecular species rather than any given separation was studied. Examples of specific studies are presented in Chapter 4.

A final topic is the two types of chromatographic modes, reversed-phase and normal phase, used in this work. The normal phase mode involves a polar stationary phase and less polar mobile phase. The stationary phase used routinely is silica or alumina. The term "adsorption chromatography" is also used to mean the normal phase mode. In the reversed-phase mode the stationary phase is less polar than the mobile phase. Thus typically a silica support onto which is chemically bonded n-octadecyl or some other alkyl moiety is used as stationary phase, and aqueous alcohol or acetonitrile mixtures are used as mobile phases. Normal-phase is characterized as useful for separations of lipid classes while the reversed-phase mode shows selectivity based on the hydrocarbon substitution of a lipid class and thus is useful for molecular species separations. The reversed-phase mode is used extensively in this work.

#### 1.4 THE CHROMATOGRAPHIC SYSTEM

A schematic representation of the components and

their interrelationship in h.p.l.c. are shown in Fig. 1.1. The basic instrument utilized the same eluent reservoir, pump, pressure gauge, injector and recorder, regardless of the general application or chromatographic mode used. The main exception to this is when using the system for preparative isolation: this involves scale-up of all components. The column and detector are the most variable of components and are chosen to match the chromatographic mode (reversed or normal-phase for column) and solute-mobile phase (this with respect to the detectors compatibility with both).

In this work the chromatographic detector is of greatest interest because it is normally the limiting component in the system. For instance, the chromatography of most compounds is easily accomplished but adequate detection to the desired sensitivity is usually difficult. Lipids are a prime example of detector limitations because as a class they lack physiochemical properties such as fluorescence, absorbance or electrochemical activity to allow easy detection by commercially available detectors. Some aspects of detectors of interest in this work are as follows.

#### Chromatographic Detectors

What is meant by a detector is anything which is used to monitor the effluent of a chromatographic system.



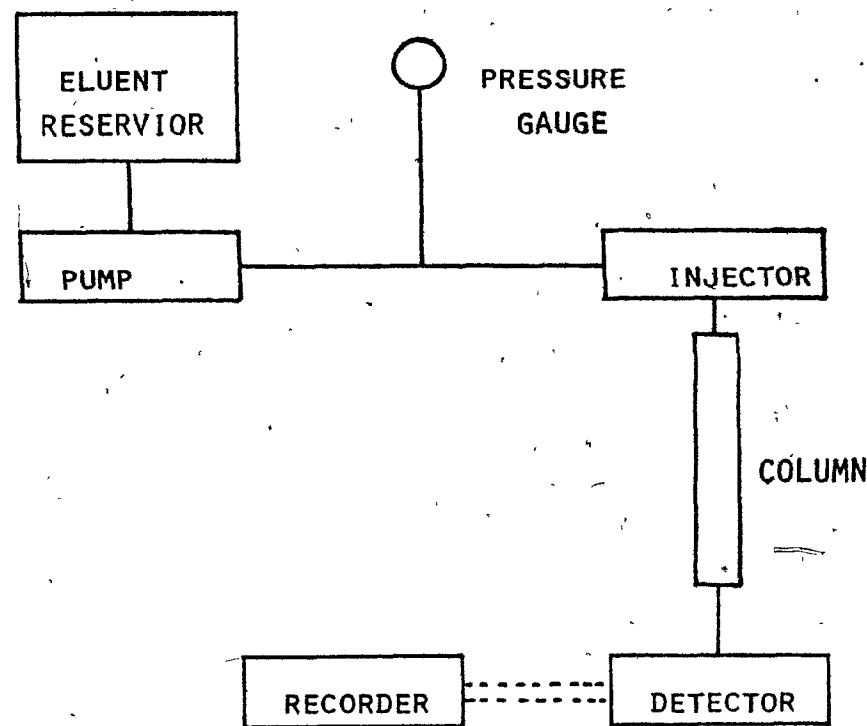


Figure 1-1. Schematic representation of the general h.p.l.c. and relation of components.

Detectors have characteristics which can be described by certain terms and the concepts they represent. Since no accepted terminology is used in the field, the following relates only to this specific work. General terms used to describe detector performance are found in two books on detectors (17, 18).

#### Selectivity ( $R_D$ )

Selectivity is the term used to describe the detector's responsiveness to different compounds. It is thus a measure of relative sensitivity of the detector and a rectilinear plot of detector response to amount of solute has a slope that is one measure of selectivity.

#### Sensitivity ( $C_{SDL}^D$ )

Like selectivity, sensitivity is a measure of the detector's responsiveness to different compounds. Sensitivity however is further defined by the ability of the detector to measure low amounts of a compound, the so-called "lower-detection limit". This limit is defined by the detector's response (dependent on the detector selectivity) and noise (output that can be mistaken for signal). The detection limit is defined as that amount of solute that gives signal-to-noise ratio (SNR) of 2.

#### Linear-Dynamic Range

The upper concentration range is the upper detection limit and the concentration extremes between the upper and

lower limits delineates the detector's linear-dynamic range.

The upper detection limit is defined by when detector selectivity deviates by  $\pm 5\%$ . Thus a rectilinear plot of signal to concentration above the upper range is non-linear.

### Noise

In this work noise is defined as detector output which is not due to controlled input into the system. The features of noise are frequency, amplitude and purity. Noise is best classified in the frequency-purity context.

a)  $1/f$  noise: noise at very low frequency whose amplitude varies as  $1/f$ . The alternative terms of drift and flicker apply, as well as pink noise.

b) white noise: noise that has equal power throughout the entire frequency spectrum. This noise is also called background or, in discrete sampling, signal blank.

c) interference noise: noise with relative spectral purity in that its main power is centered within a narrow frequency range. This noise is often easy to diagnose because it can be correlated to some external source (example is 60 Hz line noise) but may be difficult to locate if internal in origin (example due to electronic component interactions generating unwanted harmonics).

Noise can be measured in a variety of manners. In this application baseline peak-to-peak noise is used. The

amplitude of this type of noise is measured directly off a detector output amplitude versus time trace. Two parallel lines are drawn such that they enclosed 95% of the noise over a period of at least 3 peak base widths. This noise is referred to as  $2\sigma$  noise. An alternative SNR can be calculated from the mean signal to standard deviation of the measured signal. This expression is used in Chapter 4 for a special application because of baseline effects that were encountered in the application.

The main concern in chromatography is with  $2\sigma$ -noise in the frequency range less than 1 Hz. Band elution normally takes from 10-100s (0.1-0.01 Hz) and thus  $1/f$  and periodic interference at low frequency are a major concern.

#### 1.5 THE ANALYTICAL METHOD APPLIED HERE

The objective of this work was to develop an analytical system based on chromatography and on-line detection for quantitating, at the nanomole level, the separate TG and PL molecular species. Because of the diversity of lipid molecular species and the desire to quantitate them intact, high performance liquid chromatography was required. Also detection as molar quantities of material eluted from the chromatographs was desired. This "molar sensitive" detection has the advantage of not requiring

detector calibration for each molecular species. The entire separation-detection system was also envisioned as having information gathering capabilities sufficient to allow total characterization of the TG or PL sample. Thus, the molecular species present and their molar quantities could be determined.

With reference to the TG and PL general structures, it is seen that R determines the identity of the molecular species while all TG's and PL's have glycerol and glycerol-3-phosphate in common, respectively. Thus dual detection, one to detect R, the other the glycerol or phosphoglycerol moiety (the molar sensitive detector), was needed. Also, since retention behavior in the reversed-phase chromatograph contains information on R, the h.p.l.c. of TG's and PL's was studied.

The chromatography of TG and PL was first examined in Chapter 2, to test the usefulness of h.p.l.c. and to aid in detector design. Following this, two detectors, one based on detecting the substituted orthophosphate of PL (i.e. only sensitive to PL, Chapter 3) and the other on detecting glycerol or phosphoglycerol (Chapter 4), were developed. A commercially available ultraviolet absorption detector was also evaluated for its usefulness in determining the degree of unsaturation of R, an aid in assigning molecular species identity. The final work (Chapter 5) dealt with

combining the chromatography and detection methods. Since this work was concerned with analytic instrumental development, applications were not included.

REFERENCES

1. Ansell, G.B. and Hawthorne, J.N., "Phospholipids: Chemistry, Metabolism, and Function", B.B.A. Library, Vol. 3, Elsevier, N.Y., 1964.
2. IUPAC-IUP Commission on Biochemical Nomenclature: The Nomenclature of Lipids, Biochem. J., 105 (1967) 897.
3. Marinetti, G.V., "Lipid Chromatographic Analysis", Vol. 1, Marcel Dekker, N.Y., 1967.
4. Litchfield, C., "Analysis of Triglycerides", Academic Press, New York, 1972.
5. Gunstone, F.D., "An Introduction to the Chemistry and Biochemistry of Fatty Acids and Their Glycerides", Chapneau and Hall, London, 1967.
6. Gurr, M.I. and James, A.T.J., "Lipid Biochemistry: An Introduction", Cornell University Press, Ithaca, N.Y., 1971.
7. Wittcoff, H., "The Phosphatides", Reinhold, N.Y., 1951.
8. Tietz, N.W., in "Fundamentals of Clinical Chemistry", W.B. Saunders, Co., Philadelphia, 1976, p. 482.
9. Overath, P., Schairer, H.-U., Hill, F.F. and Lamnek-Hirsch, I., in "The Dynamic Structure of Cell Membranes", (D.F.H. Wallach and H. Fisher, eds.) Springer-Verlag, N.Y., 1971, p. 149.
10. Freer, D.E., Statland, B.E. and Sher, G., Clin. Chem., 25 (1979) 960.
11. IUPAC-IUP Commission on Biochemical Nomenclature, "Nomenclature of Lipids (Recommendations 1976)", reprinted in Lipids, 12 (1977) 455.
12. IUPAC-IUP, "Nomenclature of Phosphorus-Containing Compounds of Biochemical Importance (Recommendations 1976)", Proc. Natl. Acad. Sci. USA, 74 (1977) 2222.
13. ASTM, "Gas Chromatography Terms and Relationships", ASTM: E355-68, reprinted in J. Gas Chromatogr., 6 (1968) 1.

14. Snyder, L.R. and Kirkland, J.J., in *"Introduction to Modern Liquid Chromatography"*, 2nd Ed., J. Wiley & Sons, N.Y., 1979, p. 23.
15. Ibid., p. 36.
16. Keller, R.A. and Giddings, J.C., in *"Chromatography"*, (E. Heftmann, ed.), Van Nostrand Reinhold Co., N.Y., 1975, p. 115.
17. Sevcik, J., *"Detectors in Gas Chromatography"*, Elsevier Sci., N.Y., 1976.
18. Scott, R.P.W., *"Liquid Chromatography Detectors"*, Elsevier Sci., N.Y., 1977.



## 2. THE REVERSED-PHASE CHROMATOGRAPHIC BEHAVIOR OF TRIGLYCERIDES AND PHOSPHOLIPIDS

### 2.1 INTRODUCTION

The use of chromatography for the class separation of lipids usually follows a separation from non-lipid material based on the extraction method of Folch (1). After this method is applied, chromatographic techniques involve samples in their native or chemically modified form. In the former case the selectivity of the chromatographic technique and natural physiochemical properties of the sample determine the success of the procedure. In the latter case the chemical nature of the lipid sample is more fully exploited to aid in the separation. Chemical treatment is also done to enable the use of a specific method (such as the esterification of fatty acids prior to gas liquid chromatography) or to aid in detection after chromatography.

An example of chemical treatment is in the separation of three closely related phosphoglycerol derivatives, the plasmalogens (1-alk-1'-enyl-2-acyl-), 1-alkyl-2-acyl-, and diacylphosphatides. These are only separated after acetolysis of the ortho-phosphate group (2) since the chromatography is no longer dominated by the presence of the polar constituent. Some acyl migration occurs (3,4). Acid hydrolysis on the

other hand enables separation of plasmalogens (their vinyl ether portions are very acid labile) from the diacyl phosphatides (5). Base hydrolysis (saponification) or metholysis (transesterification) also enable separation of the diacyl phosphatides from the base-resistant sphingomyelins (6) and plasmalogens (7).

Unmodified lipids can often be separated by class using thin-layer chromatography (t.l.c.) or column chromatography. The first separations of PS from PE (8) and PC from Sph. (9) used base-modified silicic acid columns. Many variations on multiple development in t.l.c. using silica (10,11) or 2-dimensional development (12,13,14) have also appeared. Molecular-class separations were also greatly dependent on either t.l.c. or column argentation chromatography (15,16,17,18).

The role of t.l.c. as a separation and quantitation tool cannot be over emphasized. No other technique has the flexibility of containing for easy inspection the entire capacity of the system ( $k'$  of zero to infinity). Also, the options of reversed and normal-phase, multiple development, etc. and the wide choice of general or specific post-separation chromophore developing agents make this technique very useful.

The introduction in the mid-1950's of commercial gas

chromatographs allowed rapid quantitation of the acyl portions of phospholipids and glycerides. Recent column developments have enabled determinations of underivatized fatty acids and even moderately high molecular weight glycerides (19). The use of gas chromatography for fatty acid analysis is not likely to be superseded in the near future since the field is still under active development (20,21).

Because the general trend in analysis is towards more automated and sensitive techniques, since 1970, high performance liquid chromatography (h.p.l.c.) has developed at a spectacular rate. This technique is well suited for lipid analysis, being useful for highly polar and non-volatile compounds. Instrument advances have made molecular species separations possible with short analysis times. This type of advance can be illustrated by example. In 1956 Rhodes and Lea (22) showed that "enrichment" of the more unsaturated phosphatidylcholine of rat liver occurred in the column chromatographic band on silica. This behavior was opposite to what was expected since unsaturation tends to increase retention. What was found was that unsaturation was accompanied by an increase in acyl methylene group number that more than compensated for the unsaturation effects. Recent work in triglyceride analysis has led to the ability to totally separate, in the normal phase mode, glycerides according to chain length or degree of saturation (23). This type of

separation was normally only accomplished in the reversed-phase mode, with band enrichment seen in the normal-phase mode only under the unusual circumstances found by Rhodes and Lea.

The difference between the classical column method of Rhodes and Lea and the newer methods of h.p.l.c. is in column technology. With greater chromatographic efficiency the need for chromatographic diversity is diminished. While h.p.l.c. is not likely to be a total lipid analysis system, it is a step in that direction. A recent review on routine techniques used in lipid research laboratories (24) will have to be revised in the near future to accommodate these advances in column technology.

#### 2.1.1 Modern Aspects of Lipid Separations

The h.p.l.c. of triglycerides and phospholipids can be grouped as either concerned with molecular species or class separations. Molecular species are usually separated using the reversed-phase mode while class separations are done using the more familiar normal-phase mode, a direct extrapolation from adsorption chromatography used since the 1930's.

Two very comprehensive reviews (25,26) on lipid analysis using h.p.l.c. have recently appeared. The separations accomplished with the column technology used in

the reviewed studies were impressive since in most cases complete class separation of neutral and polar lipid was demonstrated. The use of Simplex optimization (27) has also been applied to PL class separations. One application of a commercial preparative instrument has been given for purification of egg lecithin (28).

The molecular species separation of triglycerides in the normal-phase mode has been mentioned (23). Most complete separation of TG molecular species has been done using reversed-phase h.p.l.c. and in one case with solvent selectivity enhanced with silver salts (29), separations of cis-trans isomers were possible.

Separation of lipids must be discussed in the context of detection since this is a main source of instrumental limitation. Most recent work has utilized low wavelength (195-205 nm) ultraviolet absorption detection (30,31,32) in the normal-phase mode for phospholipid class separations. Low wavelength detection has also been applied to molecular species separations in the ion-paired reversed-phase mode (30) and for the study of the autooxidation of linolenic acid (34,35). Usually the refractive index detector (RI) is preferred in the reversed-phase mode (36-38) because of the limited UV transparency of most solvents used for lipid analysis (notably chloroform).

Detection problems have led to some novel detector

developments such as liquid chromatography-mass spectroscopy (39), infrared absorption (40), and the transport-flame ionization detectors (25,41-44) investigated in Chapter 3. Pre-column derivatization of PE and PS to their biphenyl carbonyl derivatives (45) or fatty acids to their p-bromophenacyl esters (26) or phenylacyl esters (46) have also been used for detection at 254 nm, a common detection wavelength.

When the lipid of interest has ultraviolet absorbance such as sorbic acid triglycerides of aphids (47), the detection problem does not exist. Only some of the lipids studied in this chapter had ultraviolet absorbance (at 195-210 nm) and thus both the refractive index and ultraviolet detection methods were used. Chromatographic mobile-phase selection was purposely limited to those which were ultraviolet transparent at low wavelengths and for reasons presented in Chapter 4, were low in aldehydes.

## 2.2 THEORETICAL CONSIDERATIONS AND THE KOVATS INDEX

Studies of the processes occurring in reversed-phase h.p.l.c. have ranged from fundamental, to semi-empirical and empirical in nature. The fundamental studies have attempted to develop methods for a priori predictions of solute retention behavior based on physio-chemical relationships. Notable amongst these attempts are those of Horvath and

co-workers (48-51) and Riedman (52). Other approaches are based on the solubility parameter concept of Hildebrand and Scott (53,54); a useful review of this concept is presented by Barton (55). Recent attempts at simplifying the parameter approach for h.p.l.c. (56,57) has done little to actually aid practicing chromatographers.

A more useful approach involves the alternative empirically derived methods. These have the advantage of being easily related to the well established Kovats Index (58,59) used in gas-liquid chromatography and further give predictive information without great effort on the chromatographer's part. The Kovats retention index (58,59) states that  $k'$  and retention index ( $I$ ) are related by:

$$\log k' = BI + A \quad (2-1)$$

where  $k'$  has the usual meaning of  $\frac{V_R - V_0}{V_0}$ ,

$B$  = slope of the Kovats retention index parameter,  
a measure of the selectivity of the system.

$I = 100 n$  where  $n$  is the carbon number (number of methylene groups) in the standard series (usually  $n$ -alkanes or alcohols, ketones, etc.).

$A$  = system characteristic, a measure of the capacity factor of the system and thus its overall polarity.

When a chromatographic system has been characterized using the Kovats retention index, any other compound D can be indexed using Eqn. (2-1) or, with appropriate standards, by the equation

$$I = \frac{100 \times \log k'_D - \log k'_n}{\log k'_{n+x} - \log k'_n} + 100n \quad (2-2)$$

where n and n+x are the standards which bracket D such that  $k'_n \leq k'_D \leq k'_{n+x}$ . In gas chromatography, I varies approximately 30-60 units over a 100°C temperature range (60) and is thus not constant for wide ranging conditions.

When applied to h.p.l.c., Baker and Ma (61) showed that the use of Kovats index can be very useful and regardless of the class (hydrocarbon, alcohol, ketone or carboxylic acid) B was approximately the same. Experimentally derived relationships were that I decreased 18 per 10% increase in methanol and replacing methanol with acetonitrile reduced  $k'$  by approximately 50%. The overall effects of increasing the organic content of the mobile phase was thus a decrease in the free energy change associated with each methylene group in the chromatographic process. This effect was, as studied by another group, also approximately proportional to the amount of water in the mobile phase (62).

Other uses of the Kovats Index in h.p.l.c. involve



n-alkyl homologous series. In a study of argentation-h.p.l.c. (29), work on  $C_{18:1}$  and  $C_{18:2}$  triglyceride isomers, in the context of changing I by addition to the mobile phase of silver salts, showed I could be greatly changed by mobile phase variations.

The role of mobile phase in RP-h.p.l.c. has been given some attention in recent years and can be fitted into the framework of the Kovats index. A general paper (63) on developing a "Elutropic Series" for RP-h.p.l.c. showed that the Kovats index relationship held for n-alcohols and phenol on both  $C_4$  and  $C_{18}$  stationary phases and in this instance water/methanol content was varied (i.e. B was found to be approximately independent of mobile-phase composition).

Using the slope B of the Kovats index as a general measure of selectivity of a solvent with methanol, acetonitrile, ethanol, dioxane, 2-propanol and tetrahydrofuran as solvents, and n-alkanes, n-alcohols, ethers, esters, amides and ketones as solutes, Hoffman and Liao (64) showed that acetonitrile gave the greatest B and thus was the best solvent for isocratic elution work. A trend in the mode of separation from reversed- to normal-phase was noted as the solvent series went from methanol through ethanol to 2-propanol. Mixed mode retention was seen especially for amides and alcohols. In fact, using the same mobile phases as in their reversed-phase studies, they showed that significant retention occurs on the silica stationary phase for the two classes

of compounds.

Since the Kovats Index is very general for homologous series studies and especially systems having n-alkyl substituents, some work on triglycerides and phospholipids has been interpreted by a similar index. A very recent work (38) on PC involved the use of a parameter called E.C. (effective carbon number). The derived relationship for Lecithins on a Waters proprietary "Fatty Acid" column was

$$.042 \text{ E.C.} = \log(\text{retention volume})$$

or in other words their work can be related to the present by noting that E.C. is 0.01 I. The value E.C. was used because the authors were concerned with molecular species of PC containing varying degrees of unsaturation. They subtracted a factor of 1 E.C. (i.e. I = 100) per double bond in the acyl portion of the PC species and noted relatively close agreement with retention expected for saturated molecular species used as standards.

The analysis of triglycerides (36) in acetonitrile-acetone mobile phases on a Bondapak C<sub>18</sub> column has also been studied. In this case a correction for double bonds of 1 double bond  $\approx$  200 (I) was applied, or

$$I_{\text{corr.}} = I - C N_{\text{db}} \quad (2-3)$$

$I_{\text{corr.}} = I_{\text{corrected}}$  as experimentally derived.

$I = I$  for the parent alkane.

$N_{\text{db}}$  = Number of double bonds in the compound of interest.

$C = 200 I$ .

In this chapter the reversed-phase h.p.l.c. of triglyceride and phospholipid molecular species using Kovats indexing will be attempted, with particular interest placed on the double bonds' effect on  $I_{\text{corr.}}$ .

It was noted that most authors use refractive index, the transport-FID or infrared absorption detectors in the reversed-phase mode for triglycerides and phospholipids. This is because limited sample solubility dictates the use of ultraviolet absorbing solvents (34,38). In the present study dual detector of absorbance in the region 190-200 nm and refractive index is accomplished using mobile phases normally avoided. This was possible since very small (nanomolar) quantities of sample and high column temperature eliminated most solubility problems. Some limitations on sample size were noted, but the chromatographic system used was developed primarily for use with a novel detector described in Chapters 4 and 5 and the sample size limitation was required.

## 2.3 EXPERIMENTAL

### 2.3.1 Instrumentation

The chromatographic system used in this study is schematically represented in Fig. 2-1. A Waters 6000A solvent delivery system (P), U6K injector (I) and differential refractive index detector ( $D_2$ ) model R-401, all from Waters Scientific Ltd., Mississauga, Ontario, and a laboratory designed column (C) and Schoeffel SF770 variable wavelength detector ( $D_1$ ) from Schoeffel Instrument Corp., Westwood, N.J. was used.

The 6000A pump unit worked on the basis of constant flow (0.1-9.9 mL/min) delivery of liquid against pressure drops up to 6000 p.s.i. Delivery rates of the pump, measured using a volumetric flask (5 mL) - stop watch, were within  $\pm 5\%$  of rated flow for the range 0.5-2.0 mL/min. Due to the finite compressibility of liquids this flow rate was system dependent, compensated for by a multi-turn potentiometer on the pump. For any given solvent the pump was found to have between-run flow variance of less than 1%. Retention data were usually reproducible to standard deviations of less than 1% between runs.

The injector (I) was found to be reliable once familiarity with its operation was gained. Injection reproducibility routinely had a relative standard deviation

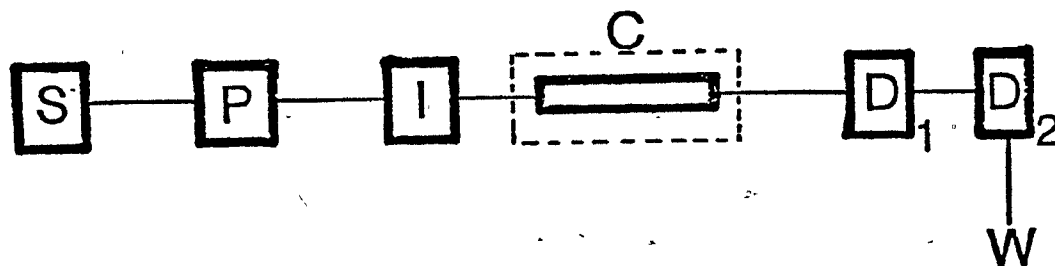


Figure 2-1. Schematic representation of the h.p.l.c. experimental system used. See text for explanation of abbreviations.

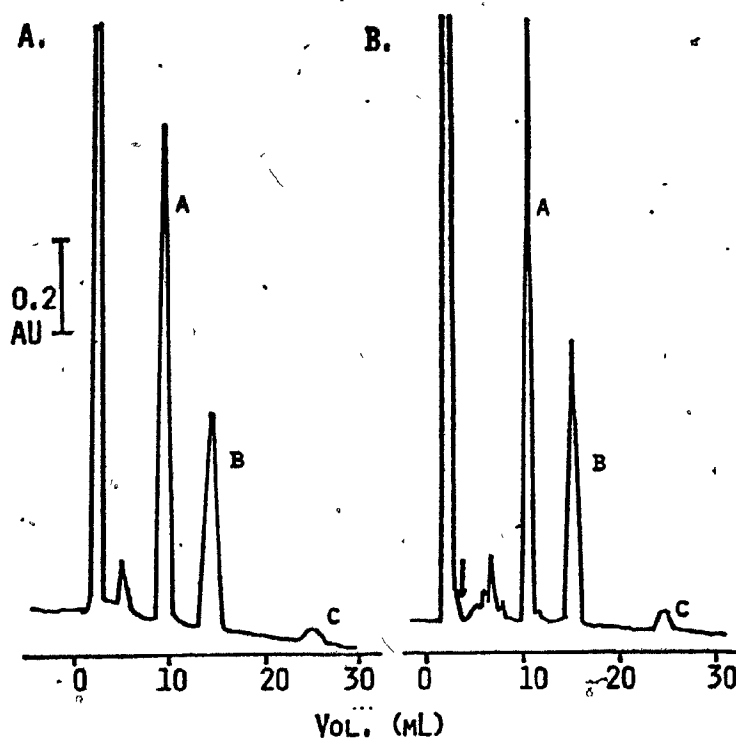


Figure 2-2. (A.) Separation of a)  $C_{18:3}$ , b)  $C_{18:2}$ , and c)  $C_{18:1}$  triglycerides, 250  $\mu\text{g}$  of each  $C_{18:1}$  per injection. Methanol flow rate was 1 mL/min using the Altex 10- $\mu\text{m}$  particle size column. (B.) Same as for (A.) except the initial portion of the separation was run at 30°C and then stepped as indicated by arrow to 60°C.

of less than 3% and with care, less than 1% was obtained.

The absorbance detector is described thoroughly in Chapter 5. It utilizes a variable wavelength 5 nm half width band pass source passing through two 8- $\mu$ L, 1.0-cm long flow cells (reference and sample). Maximum sensitivity was 0.01 AU full-scale deflection (FSD) and range was up to 2 AU FSD.

The refractive index detector R-401, optimized for high efficiency separations by using 0.009-inch I.D. inlet tubing, could be used from flow ranges of 0.03-20 mL/min. The detector contained two back-to-back 45° cells which had poor wash out characteristics and outlet tubing of large diameter (0.040" I.D.). The nominal detector signal range was from  $3 \times 10^{-3}$  -  $6 \times 10^{-6}$  RI units full-scale deflection depending on the attenuation used. This detector worked on the principle of differential refractive index changes between the two cells and had an absolute requirement that the reference cell be filled with mobile phase. Once turned on the unit required at least 2 h to reach thermal equilibrium.

The columns used varied from commercial to in-lab designed systems. The lab-designed columns are described in detail below. The commercial columns used were Waters  $\mu$ -Bondapak ODS ( $C_{18}$ , 10  $\mu$ m, Waters Scientific), Altex LiChrosorb  $C_{18}$  5  $\mu$ m (10 x 0.32 cm) and an Altex LiChrosorb  $C_{18}$  10  $\mu$ m (25 x 0.32 cm, Aviation Electronics, Ltd., St. Laurent,

Quebec).

The lab-designed columns were made of S.S. 316, 2-mm I.D. standard 1/4"-O.D. tubes specially honed and polished for this application. The column outlet frit was a stainless steel (S.S.) 316, nominal pore size 0.2  $\mu\text{m}$ , 3.0 mm by 1.65 mm disc, force fitted into an equally thick S.S. 316 collar 6.20 mm in diameter. This assembly and the inlet disc were maintained in place with 1/4" Swaglok<sup>®</sup> fittings modified to hold the unit with no dead volume. Standard compression units and ferrels were used to secure connecting tubing to the column.

The column inlet was modified to be low dead volume by adding a spacer disc of identical dimensions as the exit disc. No inlet frit was used and the center of the disc contained a .015" diameter hole bored through. This inlet design decreased dead volume by allowing the column connecting tubing from injector to butt directly against the entrance disc.

The columns were packed with bonded phase  $\text{C}_6$  5  $\mu\text{m}$  silica (Sp-6, a hexyl stationary phase on 5  $\mu\text{m}$  spherical silica support from Phase Separation, 255 Oser Ave., Hanpage, N.Y.) using the equal-density method (65). This involved suspending the packing in a degassed 1:3 isooctane-chloroform liquid phase and immediate packing into the column

at 12,000 p.s.i.

The columns were thermostated with water to  $60 \pm 1^\circ\text{C}$  using a lab-designed water jacket. In the reversed-phase mode, there is an absolute requirement for maintaining column temperatures isothermal.

All solvents were degassed using the helium displacement technique (66). This was essential when using elevated column temperatures to prevent degassing of the mobile phase at the column exit. Also, degassing has been reported to extend column life (67) and, when using a fluorescence detector, the elimination of oxygen was of importance in minimizing quenching (Chapter 5).

Temperature changes in the solvent system were observed as a baseline shift in the SF 770 detector. The post-column-to-detector connector was thus thermostated using an ice bath to minimize long-term baseline drift associated with heating bath cycling.

### 2.3.2 Materials

Solvents used for the mobile phases were spectro-grade methanol (American Chemicals, Ltd., Montreal, P.Q.), LiChrosorb acetonitrile (British Drug House, Montreal, P.Q.) and double distilled (in glass) water. The acids utilized were from American Chemicals, Ltd. (Montreal, P.Q.) while



diethyl phosphate was purchased from Eastman Kodak Co.  
(Rochester, N.Y.).

The lipid standards were purchased from one of two sources. Acyl glycerides and fatty acids or their methyl esters were obtained from Sigma Chemical Co. (St. Louis, Missouri) while the synthetic phosphatidylcholines were purchased from Serdary Research Laboratories (London, Ontario). The lipid standards were certified by the manufacturers as being pure by t.l.c. (two mobile phases) and were found by h.p.l.c. to be free of any extraneous material. The exception to this was the sample of PC-dilinolenoyl which characteristically contained low carbon number autooxidation products, a subject of some interest in the lipid research field (34,35) since these products are associated with rancidity of oils.

The lipid standards were dissolved in chloroform-methanol to give standards with concentrations in Tables 2-1 to 2-3. Amounts injected and chromatographic conditions varied and are presented in the text.

All mobile phases were made up volume-to-volume to 1% of the stated value and those using polar modifiers were made such that one modifier was added directly to the prepared aqueous-organic solution. The only exception was the case of triethylammonium sulfate (Eastman Kodak) where a 0.1% (v/v) suspension of the amine in water was acidified to pH 2.10 with conc. sulfuric acid. This solution was used to

Table 2-1: List of triglyceride standards, their acyl carbon numbers, trivial and systematic names, and Kovats index of the saturated samples.

N	TN	ACN:D <sub>b</sub>	acyl	I
1	Tricaproin	C <sub>6</sub>	n-hexanoic	1800
2	Tricaprylin	C <sub>8</sub>	n-octanoic	2400
3	Tricaprin	C <sub>10</sub>	n-decanoic	3000
4	Trilaurin	C <sub>12</sub>	n-dodecanoic	3600
5	Trimyristin	C <sub>14</sub>	n-tetradecanoic	4200
6	Tripalmitin	C <sub>16</sub>	n-hexadecanoic	4800
7	Tristearin	C <sub>18</sub>	n-octadecanoic	5400
8	Triarachidin	C <sub>20</sub>	n-eicosanoic	6000
9	Tribehenin	C <sub>22</sub>	n-docosanoic	6600
10	Tripalmitolein	C <sub>16:1</sub>	cis-9-hexadecenoic	
11	Trilinolein	C <sub>18:2</sub>	cis,cis-9,12-octadecadienoic	
12	Trielaidin	C <sub>18:1 t</sub>	trans-9-octadecenoic	
13	Triolein	C <sub>18:1 Δ9</sub>	cis-9-octadecenoic	
14	Tripetroselinin	C <sub>18:1 Δ6</sub>	cis-6-octadecenoic	
15	Trierucin	C <sub>22:1</sub>	cis-13-docosenoic	

N = standard number.

TN = trivial name.

ACN:D<sub>b</sub> = acyl carbon number: number of double bonds (D<sub>b</sub>), t = trans, all others are cis, 13 and 14 are isomers Δ9 and Δ6 double bond placement.

acyl = refers to the systematic name in 1,2,3-triacylglycerol.

I = Kovats retention index.

Table 2-2: List of phosphatidylcholine (PC) standards,  
their acyl carbon number, trivial and systematic  
names, and Kovats index of the saturated samples.

N	TN	ACN:D <sub>b</sub>	acyl	I
1	Dicaproyl lecithin	C <sub>6</sub>	n-hexanoic	1200
2	Dicapryloyl "	C <sub>8</sub>	n-octanoic	1600
3	Dicaprinoyl	C <sub>10</sub>	n-decanoic	2000
4	Dilauroyl	C <sub>12</sub>	n-dodecanoic	2400
5	Dimyristoyl	C <sub>14</sub>	n-tetradecanoic	2800
6	Dipalmitoyl	C <sub>16</sub>	n-hexadecanoic	3200
7	Distearoyl	C <sub>18</sub>	n-octadecanoic	3600
8	Dioleoyl	C <sub>18:1</sub>	cis-9-octadecenoic	
9	Dilinoleoyl	C <sub>18:2</sub>	cis,cis-9,12-octadecadienic	
10	Dilinolenoyl	C <sub>18:3</sub>	cis,cis,cis-9,12,15-octadecatrienoic	

Table 2-3: Molar concentrations of the standards (N), listed in Table 2-1, used in these studies. Samples were dissolved in chloroform-methanol. Details are presented in the text.

<u>Triglyceride Concentrations</u>		<u>Phospholipid Concentrations</u>	
N	conc (M) x 10 <sup>3</sup>	N	conc [M] x 10 <sup>3</sup>
1	10.3	1	11.0
2	8.50	2	9.77
3	7.20	3	8.79
4	6.26	4	8.46
5	5.53	5	6.76
6	4.95	6	6.88
7	4.49	7	11.3
8	4.10	8	6.34
9	3.77	9	6.37
10	4.99	10	6.40
11	4.60		
12	4.50		
13	4.50		
14	4.52		
15	3.79		

make up the 95% aqueous methanol mobile phase.

## 2.4 RESULTS AND DISCUSSION

### 2.4.1 Preliminary Study and the Adsorption Role

The separation of triglycerides can be accomplished with high efficiency as shown in Fig. 2-2a, where equal amounts of trilinolenin (tri-C<sub>18:3</sub>), trilinolein (tri-C<sub>18:2</sub>), and triolein (tri-C<sub>18:1</sub>) were injected into a mobile phase of methanol. Figure 2-2b shows the same sample injected under identical conditions except that the initial portion of the separation is run at 30°C and then stepped to 60°C to increase both resolution and efficiency without loss of time.

The plate count realized for a typical 10  $\mu$ m reversed-phase packing for tri-C<sub>18:3</sub> was measured to be as high as 16,000 plates/meter and typically greater than 6,000 plates/meter.

When using similar mobile phases for determination of phosphatidylcholines, very low efficiencies were observed. This is illustrated in Fig. 2-3 for acetonitrile and methanol mobile phases. The PC-C<sub>18:3</sub> is either completely retained on the column (A) or tailed severely (B).

Figure 2-4 illustrates a more dramatic example of the problems found with PC samples. In Fig. 2-4a a mixture

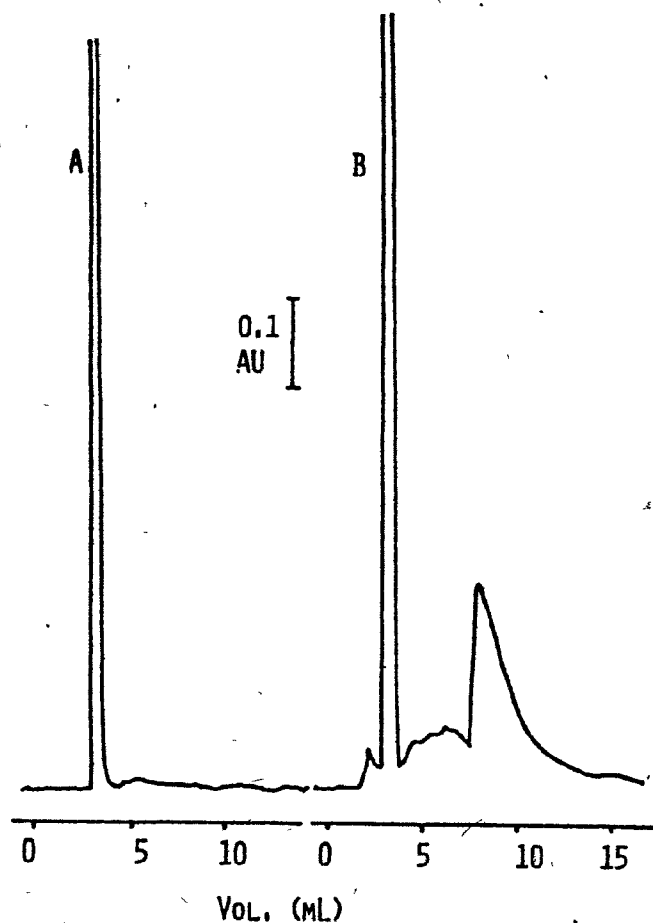


Figure 2-3. (A.) Irreversible retention of 50 ug PC-C<sub>18:3</sub> using acetonitrile as mobile phase. Flow rate was 1 mL/min using the Altex 10-um particle size column. (B.) Same as (A.) but using methanol as eluent.

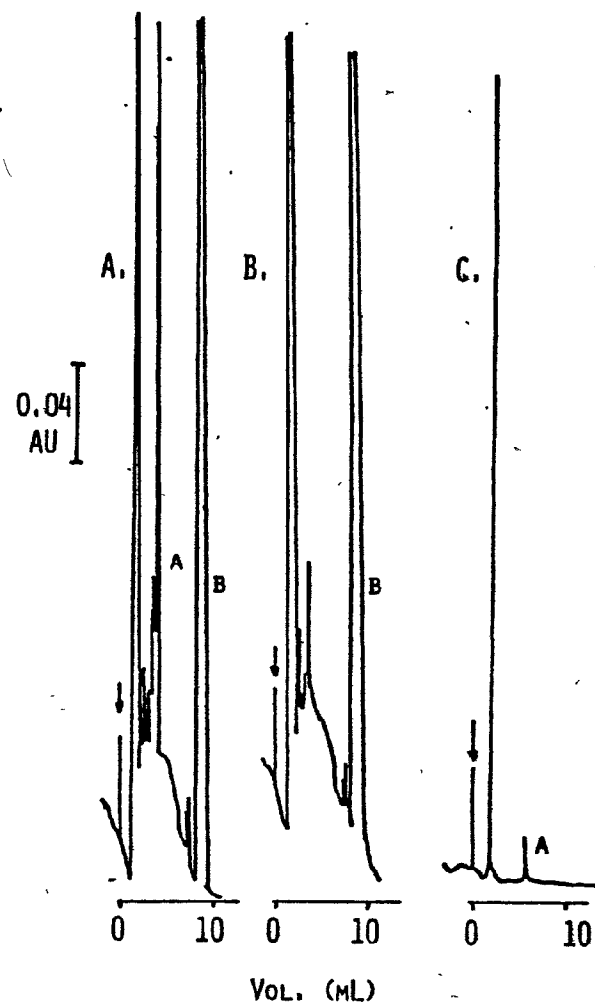


Figure 2-4. (A) Separation of a mixture of PC-C<sub>18:1</sub> (a) and diolein (b). All other bands represent degradation products of diolein. Mobile phase 95% aqueous methanol-diethylphosphoric acid, 1 mL/min using the 5-um Altex column. (B) Identical to (A) except phosphoric acid is eliminated from the mobile phase. (C) Chromatogram of the fraction collected when switching to 95% aqueous methanol-phosphoric acid, 1 mL/min. Band (a) corresponds to PC-C<sub>18:1</sub>.

of the diglyceride diolein and PC dioleoyl was run using first 95% aqueous methanol-diethylphosphoric acid. Figure 2-4B shows the chromatogram for the same system except that the diethylphosphoric acid has been eliminated from the mobile phase. When comparing the two chromatograms it is apparent that peak-for-peak every component except for phosphatidylcholine dioleoyl is present in Fig. 2-4B.

When switching from the mobile phase containing diethylphosphoric acid to that lacking any mobile phase modifier, no baseline shift corresponding to an eluting band is seen. However, when changing solvent systems in the reversed order after injecting PC samples into the aqueous methanol mobile phase, an eluting band is observed. This band corresponds to the missing PC shown in Fig. 2-4B, for upon collection and injection into a 95% aqueous methanol-0.1%-phosphoric acid mobile phase, the chromatogram Fig. 2-4C shows the corresponding PC sample (highly diluted). In these studies diethylphosphoric acid and phosphoric acid were found to be interchangeable with respect to eluting off lost PC bands. The ratio of  $k'$  for diolein to that of PC dioleoyl were nearly identical for either orthophosphoric acid or diethylphosphoric acid as modifiers and were 0.39 versus 0.35, respectively.

To increase the reversed-phase chromatographic efficiency of PC, other modifiers to the aqueous methanol

mobile phase system were investigated. Their effects are summarized in Table 2-4. The use of nitric acid was not attempted since it has high UV absorbance in the region (200 nm) of interest. Acetic acid was not useful for increasing efficiency even in a concentration as high as  $5 \times 10^{-2}$  M. Of the strong mineral acids, phosphoric acid consistently gave efficiencies comparable to the triglycerides. Tailing and general peak asymmetry were eliminated. The use of ion-pairing agents has been reported for phospholipids (33). The one used here, triethylammonium sulfate (pH 2.10), gave results illustrated in Fig. 2-5; PC-C<sub>18:2</sub> had similar chromatographic efficiency to di-C<sub>18:2</sub>, the diglyceride analog to the phosphatidylcholine.

One mode of action of the modifier is thought to be in masking highly adsorptive sites of the stationary phase. This is possible due to the relatively high modifier concentration and suppression of ionization of the solute of interest. Support for this mode of action is that the actual tailing and overall inefficiency of phospholipid chromatography has been observed to be a function of the course and history of the column as well as mobile phase composition. Generally, newer and reconditioned columns have given worse chromatographic efficiency. One example is for a Waters  $\mu$ Bondapak C<sub>18</sub> column, the adsorptive sites on the support could be 'titrated'. That is, PC bands start to elute off the column only after a



Table 2-4: Summary of the mobile phase modifiers used in the preliminary studies on absorption in phospholipid reversed-phase chromatography.

Modifier Added <sup>1</sup>	$N_{PC}/N_{DG}$ <sup>2</sup>	Effect
Nitric acid	-	Not useful due to UV cutoff
Acetic acid	-	Not useful at $5 \times 10^{-2}$ M
Sulfuric acid	0.60	Some tailing observed
Perchloric acid	0.34	Some tailing observed
Phosphoric acid	1.65	Very useful, no tailing
Diethylphosphoric acid	1.88	Very useful, no tailing
Triethylammonium sulfate <sup>3</sup>	1.06	Very useful, no tailing

<sup>1</sup>Mobile phase composition  $1 \times 10^{-2}$  M except for triethylammonium sulfate.

<sup>2</sup>Plate count for PC/plate count for the analogous diglyceride.

<sup>3</sup>See text for concentration.

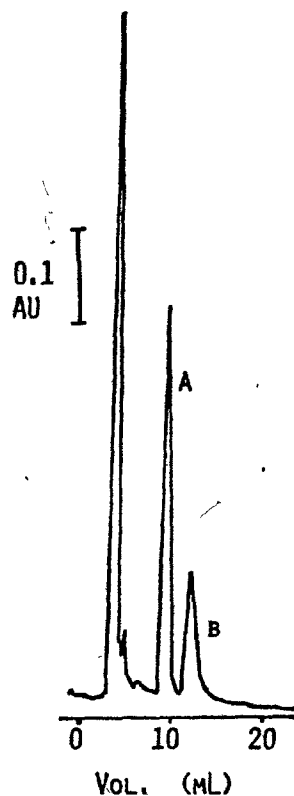


Figure 2-5. Comparison of band shapes of (a) PC-C<sub>18:2</sub> versus (b) C<sub>18:2</sub> diglyceride using t-ethylammonium sulfate (pH 2.10 1% v/v in 95% methanol). Flow rate was 1 mL/min using the Altex 10-um column.

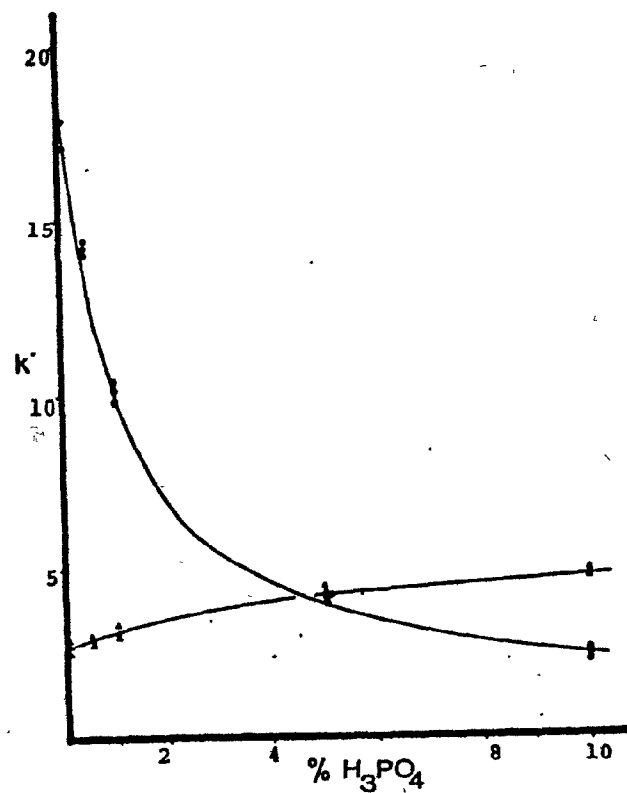


Figure 2-6. Retention changes of PL standard N=10 (•) and TG standard 1,2-dioleoylglycerol (▲) of varying phosphoric acid content of the mobile phase.

number of injections had been made. Also, the  $k'$  ratios of PC dioleoyl over diolein were approximately the same for diethylphosphate and orthophosphate.

As shown in Fig. 2-6, varying the phosphoric acid concentration of the mobile phase had opposite effects on the retention behavior of phospholipid and triglyceride. This very large effect on retention behavior is not accountable by the reversed-phase mode. The role of ionic modifiers in "ion-suppression" chromatography of peptides and proteins has been the subject of great interest in recent years (68-71). An undeniable increase in retention, however, is normally observed to occur as increasing acid content protonates acidic substituents on these compounds. The role of adsorptive chromatography in the reversed-phase mode is thus undeniable with respect to phospholipids. The extreme polarity of the orthophosphate group makes such suppression difficult with normal mobile phase composition and 0.1% (v/v) phosphoric acid was used consistently to give improved separation and efficiency in these systems.

#### 2.4.2. Studies on the Partition Role in the Reversed-Phase Chromatography

The reversed-phase h.p.l.c. retention behavior of triglycerides is given in Table 2-5 and Fig. 2-7 for various

Table 2-5: Triglyceride retention data ( $k'$ ) for various mobile phase compositions.

N	I ( $D_b$ )	$k'$ for % $\text{CH}_3\text{CN}$				
		80	85	90	95	100
1	1800	- NR -				
2	2400					
3	3000					
4	3600					
5	4200	11.20	6.51	2.63		
6	4800		17.87	7.44	1.97	
7	5400			20.60	4.71	
8	6000	- ND -				P
9	6600					P
10	4800 (3)		17.28	6.69	1.78	0
11	5400 (6)		22.54	7.63	1.94	0
12	5400 (3) <sub>t</sub>			-	4.32	0
13	5400 (3) $\Delta_9$			18.75	3.59	0.94
14	5400 (3) $\Delta_6$			-	4.03	0
15	6600 (3)				-	2.79

N = Standard number. Sample volumes injected were 1-5  $\mu\text{L}$ .

I = Kovats index for 1-9. For 10-15 the values are uncorrected and the values in parentheses are the total number of double bonds in the molecule.

NR (or 0 for 10-15) = not retained,  $k' = 0$

ND (or (-) for 10-15) = not detected.

P = Detector response indicates precipitation and very asymmetric band shape. The lines represent the upper and lower chromatographic boundaries for retention and detection, respectively.

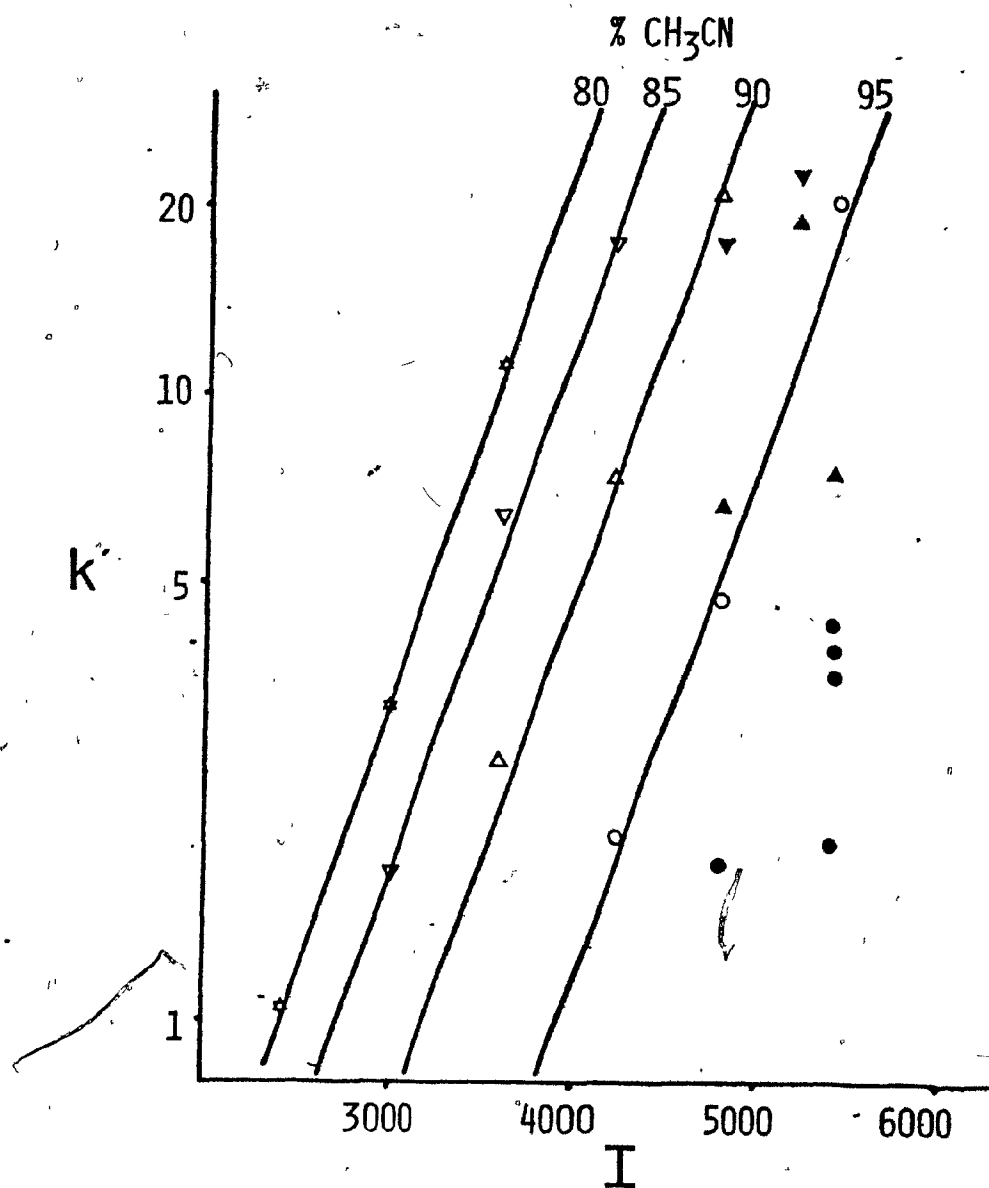


Figure 2-7. Relationship of  $-\log k'$  to  $I$  for triglyceride standards from data presented in Table 2-5. Open symbols are for saturated and closed for unsaturated standards.  
 ( ☆ = 80, ▽ = 85, Δ = 90, and ○ = 95%  $\text{CH}_3\text{CN}$ )

concentrations of acetonitrile-water mobile phases. The phospholipid results are presented in Table 2-6 and Fig. 2-8. Linear-regression analysis of the data presented in Tables 2-5 and 2-6 for the saturated lipids are summarized in Table 2-7. The retention data for the unsaturated phospholipids and phospholipid standard 7 are plotted as shown in Fig. 2-8 and its linear regression analysis presented in Table 2-7.

The use of acetonitrile as the organic constituent in the mobile phase was prompted by the greater selectivity (64), lower aldehyde content (Chapter 4 and 5) and lower solubility for silica (with concomitant longer column life) than methanol. The retention behavior of triglycerides in this mobile phase on the C-6 5  $\mu$ m column conformed to the Kovats retention index equation 2-1. Since the relationship between  $k'$  and  $I$  is logarithmic, limited  $I$  ranges for TG but not PC were noted for any given %  $\text{CH}_3\text{CN}$ . This suggests that the isocratic mode is not too useful for triglyceride samples of wide ranging  $I$ . The useful range, presented in Table 2-5, is about 1200  $I$  or 3 methylene units per acyl portion of a triglyceride. Also, acetonitrile was not useful for triglycerides with  $I$  greater than 6000, precipitate formation occurring for these high molecular weight lipids.

The effect on  $B$ , the selectivity factor, of varying acetonitrile concentration was found to be negligible and no apparent trend is seen in Table 2-7. This suggests that

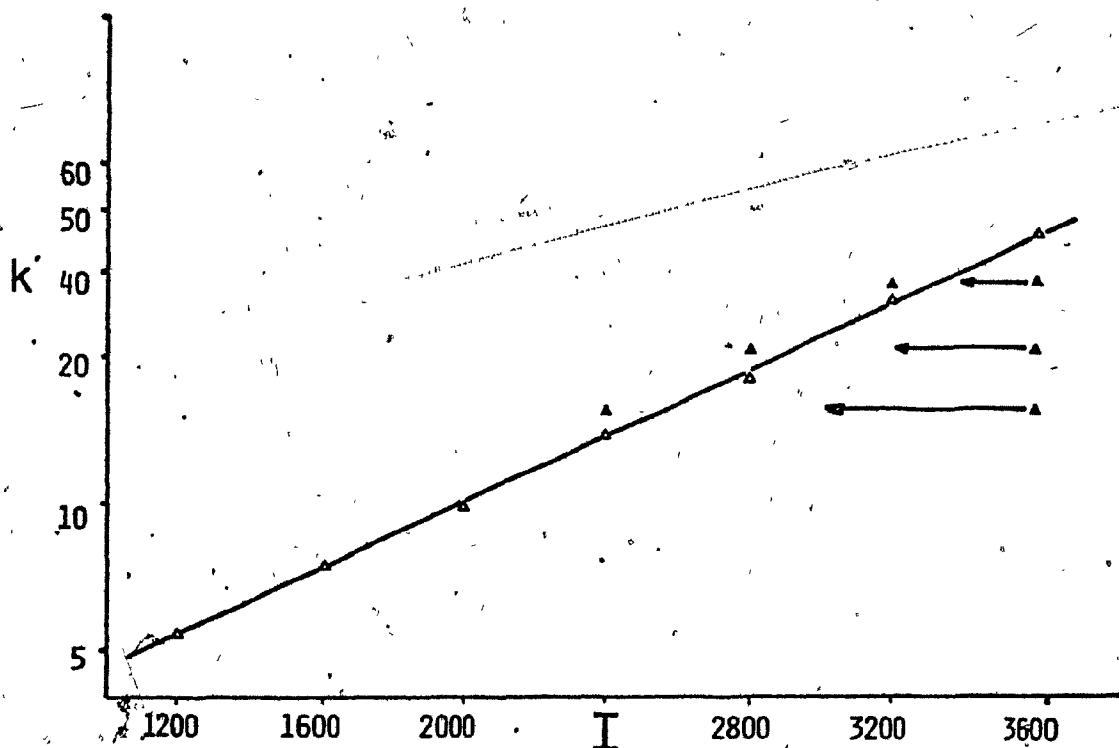


Figure 2-8. Relationship of  $\log k'$  to  $I$  and  $I_{\text{corr}}$  for phospholipid standards plotted from data presented in Tables 2-6 and <sup>corr</sup> 2-9. Open symbols are for saturated and closed for unsaturated standards. The arrows show the change in  $I$  to  $I_{\text{corr}}$  when  $C$  is taken as 200.

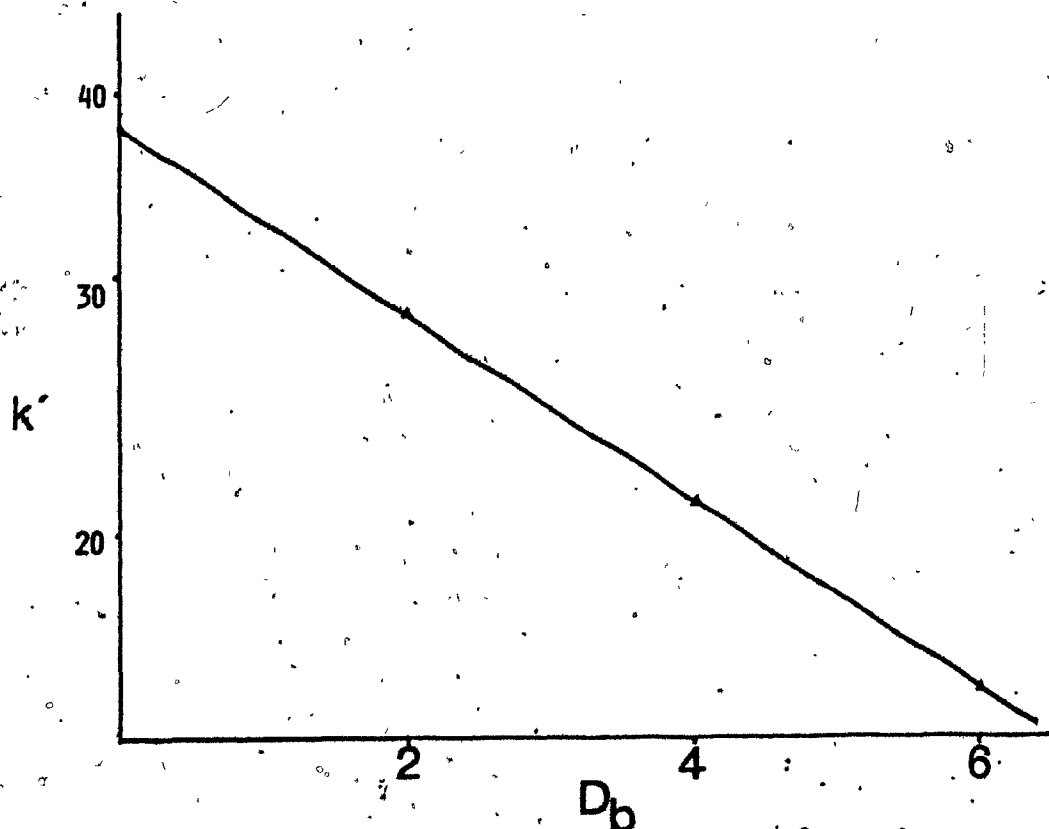


Figure 2-9. Relationship of  $\log k'$  to  $D_b$ , the total number of double bonds of the phospholipid acyl portion of standards 7-10, from Table 2-6.

Table 2-6: Phosphatidylcholine retention data ( $k'$ ) for 90%  
CH<sub>3</sub>CN/10% H<sub>2</sub>O (0.1% conc.) H<sub>3</sub>PO<sub>4</sub>.

N	I (D <sub>b</sub> )	$k'$ for 90% CH <sub>3</sub> CN - 0.1% conc. H <sub>3</sub> PO <sub>4</sub>
1	1200	5.5
2	1600	7.6
3	2000	9.7
4	2400	13.9
5	2800	17.5
6	3200	27.0
7	3600	38.0
8	3600 (2)	28.4
9	3600 (4)	20.9
10	3600 (6)	15.7

N and I are as for Table 2-5. Sample volume injections were  
1-5  $\mu$ L.



Table 2-7: Summary of linear-regression analysis of data from Tables 2-5 and 2-6 (plotted in Figures 2-7 to 2-9) interpreted using equation 2-1.

Triglyceride

% CH <sub>3</sub> CN	B	A	Linear Corr. Coeff.
80	8.57 ( $\pm 0.12$ ) $\times 10^{-4}$	-2.05 ( $\pm 0.12$ )	0.9989
85	8.43 ( $\pm 0.20$ ) $\times 10^{-4}$	-2.27 ( $\pm 0.24$ )	0.9971
90	7.47 ( $\pm 0.02$ ) $\times 10^{-4}$	-2.26 ( $\pm 0.00$ )	1.0000
95	8.47 ( $\pm 0.37$ ) $\times 10^{-4}$	-3.30 ( $\pm 0.60$ )	0.9893

Phospholipid

% CH <sub>3</sub> CN	B	A	Linear Corr. Coeff.
----------------------	---	---	---------------------

Saturated (For Figure 2-8)

90	3.46 ( $\pm 0.11$ ) $\times 10^{-4}$	3.12 ( $\pm 0.29$ ) $\times 10^{-1}$	0.9973
----	--------------------------------------	--------------------------------------	--------

Unsaturated (For Figure 2-9)

90	3.21 ( $\pm 0.00$ ) $\times 10^{-4}$	4.24 ( $\pm 0.09$ )	0.9999
----	--------------------------------------	---------------------	--------

A and B are coefficients in Equation 2-1.

the role of acetonitrile and water, the two constituents of the mobile phase, are non-selective and further implies that the only molecular interactions occurring are dispersion interactions. The effect of increasing acetonitrile concentration in the reversed-phase mode is to decrease the strength of the mobile phase. This results in less solute retention and less capacity (lower  $k'$ ) of the system. The polarity role of the mobile phase can be conceptually separated from the selectivity role as  $A$  in Eqn. 2-1. With triglycerides the expected decrease of capacity ( $k'$ ) with decrease in mobile phase polarity (increase in %  $\text{CH}_3\text{CN}$ ) is observed. The data are not sufficiently refined to make further analysis other than that when the results for 90%  $\text{CH}_3\text{CN}$  are neglected, linear-regression analysis of %  $\text{CH}_3\text{CN}(X)$  and  $A(y)$  gives  $y = -0.0861x + 4.925$ , correlation coefficient being 0.9859. Linear-regression analysis on  $\text{CH}_3\text{CN}(X)$  and  $|\log A(y)|$  gives  $y = -0.8297x + 0.01414$ , correlation coefficient being 0.9917. The effects on phospholipid retention of varying %  $\text{CH}_3\text{CN}$ , are similar in trend with the triglyceride results. The phosphoric acid modifier was added for the reasons presented in the initial part of this discussion.

The saturated triglyceride and phospholipid standards can be used to define a Kovats index scale for investigating the effects of unsaturation on retention. In section 2.2

reported unsaturation effects were that one double-bond approximated 1 methylene group ( $C = 100 I$  in Eqn. 2-3) for a fatty acid column (38) or 2 methylene groups (36) for a Waters  $C_{18}$  column. The  $C_6$  column investigated here showed effects similar to the  $C_{18}$  in that when  $C$  in Eqn. 2-3 was taken as approximately 200  $I$ , the relationship between  $I_{\text{corr.}}$  and  $\log k'$  for phospholipids (Fig. 2-8) or triglycerides (Fig. 2-10) was approximately the same as for the standards.

A more quantitative treatment is to use Eqn. 2-1 and the linear-regression analysis data of the saturated standards (Table 2-7). The Kovats index is thus calculated for each unsaturated lipid. These values ( $I_{\text{calc.}}$ ) calculated from Tables 2-5 and 2-6, are presented in Table 2-8. The  $I_{\text{calc.}}$  values, when applied to Eqn. 2-3, give values for  $C$  shown in Table 2-9. The values for  $I_{\text{corr.}}$  average  $221 \pm 27.8$  for triglycerides and  $165 \pm 13.0$  for phospholipids (mean  $\pm$  standard deviation). There are no apparent trends in the triglyceride or phospholipid data; the only obvious relationship is that the effect of double bonds on triglyceride retention is greater than on phospholipid retention. Placement and orientation of double-bond (standards 12-14) gave no significant difference in  $C$  but the effects were not systematically studied. The role of the double bond is seen to decrease  $I$  compared to the saturated standard. As implied by Eqn. 2-3, the effect is systematic and a  $\log k'$  versus  $D$

Table 2-8: Calculated Kovats index values (I calc.) for unsaturated standards.

<u>Triglycerides</u>		<u>% CH<sub>3</sub>CN</u>		
N	I (D <sub>b</sub> )	85	90 I calc	95
10	4800 (3)	4158	4131	4193
11	5400 (6)		4209	4239
12	5400 (3) <sub>t</sub>			4647
13	5400 (3) <sub>Δ9</sub>		4731	4626
14	5400 (3) <sub>Δ6</sub>			4614

Phospholipids

8	3600 (2)	3299
9	3600 (4)	2914 <sub>n</sub>
10	3600 (6)	2555

Table 2-9: Calculated correction factors (C) of equation  
(2-3) for unsaturation effects on I.

<u>Triglycerides</u>		<u>% CH<sub>3</sub>CN</u>		
N		85	90	95
			<u>C</u>	
10	4800 (3)	214	223	202
11	5400 (6)	184	199	194
12	5400 (3) <sub>t</sub>			251
13	5400 (3) <sub>Δ9</sub>		223	258
14	5400 (3) <sub>Δ6</sub>			262

Phospholipids

8	3600 (3)	150
9	3600 (6)	171
10	3600 (9)	174



plot for phospholipids gives the results shown in Fig. 2-9 with linear-regression analysis in Table 2-7. The physico-chemical mechanism responsible for the double-bond effect on I is not known. Two possibilities are that the mobile phase-solute-stationary phase interactions are changed such that double bonds cause the solute to have:

- 1) Greater affinity for the mobile phase and equal or less affinity for the stationary phase.

- 2) Greater or less affinity for the mobile phase and stationary phase such that the partition coefficient gives greater affinity for the mobile phase. None of these mechanisms can be eliminated based on the data presented here. The actual phenomena responsible for the double bond effects are an active field of research.

The work presented here is directed towards developing an empirically based method for total molecular species quantitation. Two previously cited references have also discussed this (36,38) but neither were fully successful. The detectors developed and characterized in the following chapters add another dimension and a major step towards total lipid analysis. The work presented here was used mainly to augment the investigations on the detectors but can also be interpreted as the basis for more detailed studies.

REFERENCES

1. Fölch, J., Lees, M. and Stanley, G.H.A., J. Biol. Chem., 226 (1957) 497.
2. Renkonen, O., Acta Chem. Scand., 18 (1964) 271.
3. Nutter, L.J. and Privett, O.S., Lipids, 1 (1966) 234.
4. Renkonen, O., Lipids, 1 (1966) 160.
5. Debuch, H., Z. Physiol. Chem., 304 (1956) 109.
6. Schmidt, G., Benatti, J., Hershman, B. and Thannhanser, J.J., J. Biol. Chem., 166 (1946) 505.
7. Hanahan, D.J. and Watts, R., J. Biol. Chem., 236 (1961) PC59.
8. Rouser, G., O'Brien, J. and Heller, D., J. Amer. Oil Chemists' Soc., 39 (1961) 14.
9. Rouser, G., Kritchevsky, G., Heller, D. and Lieber, E., J. Amer. Oil Chemists' Soc., 40 (1963) 425.
10. Morris, L.J., J. Lipid Res., 7 (1966) 717.
11. Neskovie, N.M. and Kostic, D.M., J. Chromatogr., 35 (1968) 297.
12. Lepage, M., J. Chromatogr., 13 (1964) 99.
13. McKillican, M.E., J. Amer. Oil Chemists' Soc., 41 (1964) 554.
14. Skidmore, W.D. and Entenman, C., J. Lipid Res., 3 (1962) 471.
15. Morris, L.J., J. Lipid Res., 7 (1966) 717.
16. DeVries, B., Chem. Ind. (London) 1962, 1049.
17. Cubero, J.M. and Mangold, H.K., Mikrochem. J., 9 (1965) 227.
18. Haverkate, F. and Van Deenen, L.L.N., Biochem. Biophys. Acta, 106 (1965) 78.



19. van Vleet, E.S. and Quinn, J.G., *J. Chromatogr.*, 151 (1978) 396.
20. Kuksis, A., Myher, J.J., Geher, K., Skaikh, N.A., Breckenridge, W.C., Jones, G.J.L. and Little, J.A., *J. Chromatogr.*, 182 (1980) 1.
21. Haan, G.J., Heide, S.V.D. and Wolthens, B.G., *J. Chromatogr.-Biomed. Appl.*, 162 (1979) 261.
22. Renkonen, O., *Adv. Lipid Res.*, 5 (1967) 329.
23. Plattner, R.D. and Payne-Wahl, K., *Lipids*, 14 (1979) 152.
24. Kuksis, A., *J. Chromatogr.-Biomed. Appl.*, 143 (1977) 3.
25. Aitzetmuller, K., *J. Chromatogr. Sci.*, 13 (1975) 454.
26. Pei, P.T.-S., Kossa, W.C., Ramachandran, S. and Henley, R.S., *Lipids*, 11 (1976) 814.
27. Rainey, M.L. and Purdy, W.C., *Anal. Chim. Acta*, 93 (1977) 211.
28. Patel, K.M. and Sparrow, J.T., *J. Chromatogr.*, 150 (1978) 542.
29. Vonach, B. and Schomburg, G., *J. Chromatogr.*, 149 (1978) 417.
30. Hax, W.M.A. and Geurts Van Kessel, W.S.M., *J. Chromatogr.*, 142 (1977) 735.
31. Geurts Van Kessel, W.S.M., Hax, W.M.A., Demel, R.A. and De Gier, J., *Biochim. et Biophys. Acta*, 486 (1977) 524.
32. Jungalwala, F.B., Evans, J.E. and McCluer, R.H., *Biochem. J.*, 155 (1976) 55.
33. Rivier, J.E., *J. Liq. Chrom.*, 1 (1978) 343.
34. Chan, H.W.-S. and Levett, G., *Lipids*, 12 (1977) 837.
35. Neff, W.E., Frankel, E.N., Schofield, C.R. and Weisleder, D., *Lipids*, 13 (1978) 415.
36. Plattner, R.D., Spencer, G.F. and Kleiman, R., *J. Amer. Oil Chemists' Soc.*, 54 (1977) 511.

37. Pei, P.T.-S., Henly, R.S. and Ramachandran, S.,
38. Porter, N.A., Wolf, R.A. and Nixon, J.R., *Lipids*, 14 (1979) 20.
39. Erdahl, W.L. and Privett, O.S., *Lipids*, 12 (1977) 797.
40. Parris, N.A.; *J. Chromatogr.*, 149 (1978) 615.
41. Stolyhwo, A. and Privett, O., *J. Chromatogr. Sci.*, 11 (1973) 20.
42. Worth, H.G.J. and MacLead, M., *J. Chromatogr.*, 40 (1969) 31.
43. Lieberman, S.L., U.S. Patent 3,128,619 (March 24, 1961).
44. Kinchi, K., Ohta, T. and Ebina H., *J. Chromatogr.*, 133 (1977) 226.
45. Jungalwala, F.B., Turel, R.J., Evans, J.E. and McCluer, R.H., *Biochem. J.*, 145 (1975) 517.
46. D'Amborse, M. and Gendreau, H., *Analyt. Letts.*, 12 (1979) 381.
47. Fallon, W.E. and Shimizu, Y., *Lipids*, 12 (1977) 765.
48. Horvath, C. and Melander, W., *J. Chromatogr. Sci.*, 15 (1977) 393.
49. Horvath, C., Melander, W. and Molnar, I., *J. Chromatogr.*, 125 (1976) 129.
50. Horvath, C., Melander, W. and Molnar, I., *Anal. Chem.*, 49 (1977) 142.
51. Melander, W., Campbell, D.E. and Horvath, C., *J. Chromatogr.*, 158 (1978) 215.
52. Riedman, M., *Z. Anal. Chem.*, 279 (1976) 154.
53. Hildebrand, J.H. and Scott, R.L., *"The Solubility of Non-Electrolytes"*, Dover, N.Y., 1964.
54. Hildebrand, J.H., Prausnitz, J.M. and Scott, R.L., *"Regular and Related Solutions"*, Van Nostrand-Reinhold, N.Y., 1970.

55. Barton, A.F.M., Chem. Rev., 75 (1975) 731.
56. Tijssen, R., Billiet, H.A.H., and Schoenmakers, P.J., J. Chromatogr., 122 (1976) 185.
57. Karger, B.L., Snyder, L.R., and Eon, C., J. Chromatogr., 125 (1978) 71.
58. Kovats, E., Helv. Chim. Acta, 41 (1958) 1915.
59. Kovats, E., Advanc. Chromatogr., 1 (1965) 229.
60. Tate, M.S., Advanc. Drug. Res., 6 (1971) 1.
61. Baker, J.K. and Ma, C.-Y., J. Chromatogr., 169 (1979) 107.
62. Tanaka, N. and Thornton, E.R., J. Am. Chem. Soc., 99 (1977) 7300.
63. Karch, K., Sebastian, I., Halasz, I. and Engelhardt, H., J. Chromatogr., 122 (1976) 171.
64. Hoffman, N.E. and Liao, J.C., Anal. Letts., 11 (1978) 287.
65. Krull, I.S., Wolf, M.H. and Ashworthy, R.B., Amer. Laboratory, May (1978) 45.
66. Bakalyar, S.R., Bradley, M.P.T. and Honganen, R., J. Chromatogr., 158 (1978) 277.
67. Personal communication with J.J. Kirkland, Montreal, 1978.
68. Pickart, L.R. and Thaler, M.M., Prep. Biochem. 5 (1975) 397.
69. Schechter, I., Anal. Biochem., 58 (1974) 30.
70. Hancock, W.S., Bishop, C.A., Hearn, M.T.W., FEBS Letts. 72 (1976) 139.
71. Kikta, E.J. and Grushka, E., J. Chromatogr., 135 (1977) 367.

3. PHOSPHORUS SENSITIVE DETECTION: MODIFICATION OF A  
TRANSPORT FLAME IONIZATION TO THE  
THERMAL IONIZATION MODE

3.1 INTRODUCTION

Since Karmen and Giuffrida (1) first described a hydrogen flame doped with alkali metal vapor as being sensitized to phosphorus, numerous variations of this class of gas chromatographic (g.c.) detector have been reported (2). The thermal ionic detector (t.i.d.) described here is of the rubidium silicate variety which is reported to give relative ease of operation (3,4,5). A description of this type of t.i.d. (3,4), its possible mechanism (5), and investigations of its operating parameters (6) have been described. Also, a study of the composition of the essential element of this detector, the glass bead, has been presented (7,8,9).

Julin et al. (10) developed a phosphorus- and sulfur-sensitive detector for h.p.l.c. not requiring a transport interface. They utilized a special burner and monitored the HPO (Salet phenomena) and S<sub>2</sub> emission with a filter photometer. The detector was utilized for the assay of 5'-monophosphate nucleotides but was limited to reverse-phase solvent systems since emission quenching, CH<sub>2</sub> background interference, and,

soot formation were all associated with high concentrations of hydrocarbon solvents at such low flame temperatures. Due to the transport mechanism the detector described in this chapter is compatible with all solvent systems.

Slais and Krejci (11) have described a similar system of h.p.l.c.-t.i.d. using a totally redesigned two-stage burner-detector system and Balaukin et al. (12) described a detector where the wire was transported through the t.i.d. flame. The former detector was used to detect halogen derivatives of tetrahydrofurans but both detectors required totally redesigned burner systems in order to allow the detectors to operate as t.i.d.'s.

The modification described here can be applied to any existing flame ionization detector (f.i.d.) of similar configuration to the Pye-Unicam f.i.d. and requires no permanent modification of the f.i.d. In fact, interconversion from the t.i.d. to f.i.d. requires only about five minutes time. Also, by proper adjustment of the bead height,  $H_2$ - and air-flow rates, the detector should be sensitive to nitrogen- and sulfur-containing compounds (3-6).

### 3.2 METHODS AND MATERIALS

The W.G. Pye Liquid Chromatograph Detector (W.G. Pye & Co., Ltd., Cambridge, England) used here is schematically

represented in Fig. 3-1. This system, the Model 1, works on the principle of interfacing via a moving wire transport mechanism (feed spool and collecting spool) a f.i.d. normally used with gas chromatography to the h.p.l.c. The point of contact between the chromatograph and the interface is the coating block where, after effluent coats the wire, volatile solvent is evaporated in the evaporation oven and the remaining non-volatile solute enters the pyrolyzer oven. After conversion to a detectable form, the pyrolyzed solute is swept into the detector by the nitrogen purge gas. The modified Pye-Unicam f.i.d. (detector in Fig. 3-1) described here is shown in Fig. 3-2. It consists of an electrically insulated burner with permanent nozzle, a cylindrical collector electrode assembly maintained in position by a ceramic disk and a glow plug igniter. An exit port is located next to the glow plug igniter. The addition to the f.i.d. which converts it to a t.i.d. is the bead holder and rubidium silicate bead, the bead holder extending from the glow plug body through the collector electrode in such a way that the bead is positioned above the burner nozzle.

Nitrogen or air is used to purge the pyrolysis oven of the moving-wire portion of the detector and is premixed with hydrogen before introduction to the burner. Air is introduced to the detector through a side port in the detector body. The introduced air sweeps down to the burner

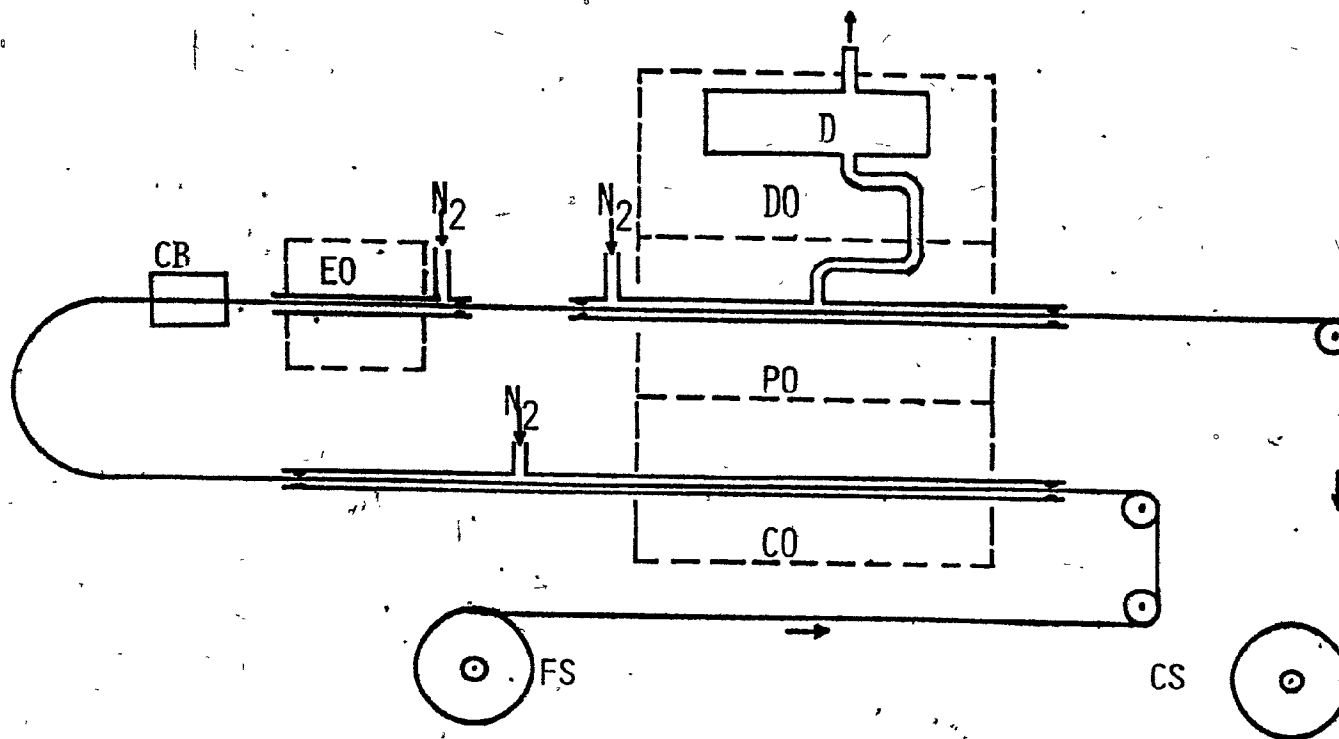


Figure 3-1. Schematic diagram of the W.G. Pye Liquid Chromatographic Detector Model 1. CB = coating block; EO = evaporator oven; N<sub>2</sub> = nitrogen, the purge gas; DO, PO, and CO = detector, pyrolysis and cleaner oven, respectively; D = Detector; and FS and CS = Feed and Collector spool, respectively.

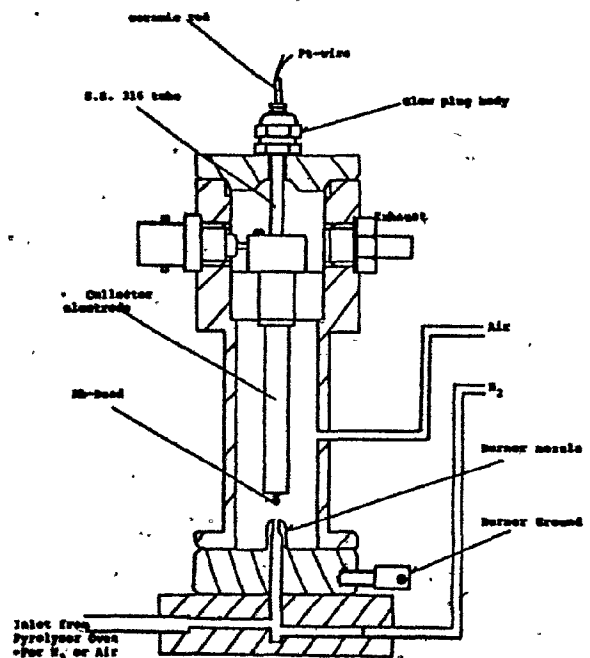


Figure 3-2. The modified Pye-Unicam f.i.d. Additions made were the ceramic rod, stainless steel 316 (S.S. 316) tube of bead holder, rubidium silicate bead (Rb-Bead) and platinum wire (Pt-wire) leading to the Rb-Bead. Figure was modified from LC Technical Manual (System 2) with permission of W.G. Pye & Co., Ltd.

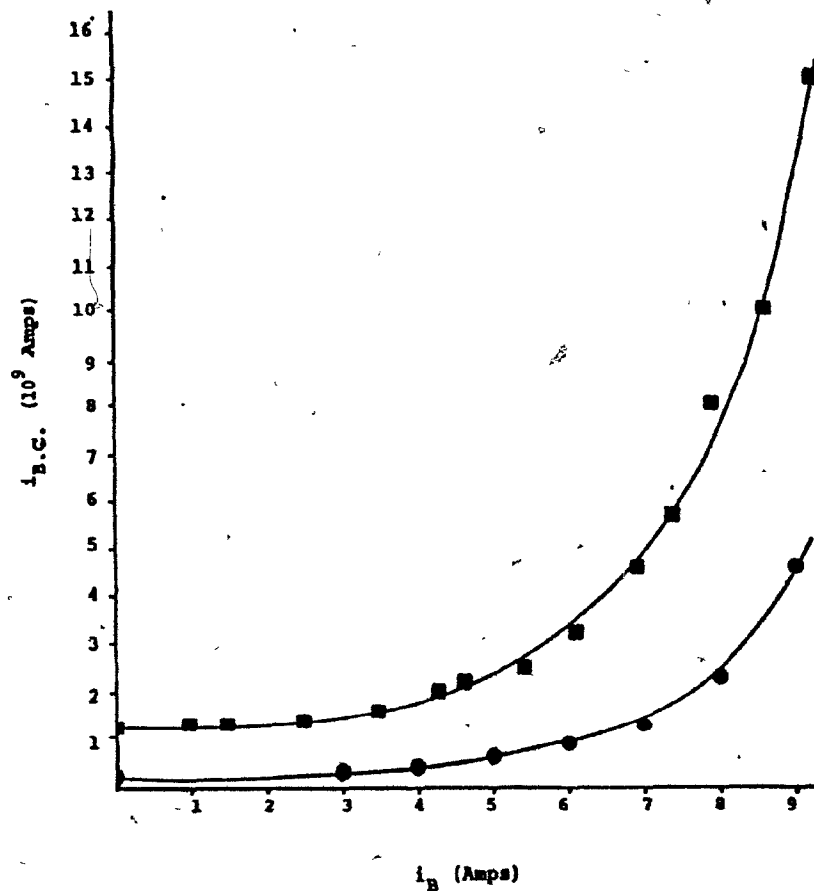


Figure 3-3. Ionization background current ( $i_{B.C.}$ ) versus bead heating current ( $i_B$ ) for two separate days. ■ = day one, ● = day ten. (Air = 590 mL/min,  $H_2$  = 35 mL/min,  $H_2$  = 30 mL/min, detector oven = 200°C.)



from the exterior portion of the collector electrode and then up through the center of the electrode along with exhaust products from the burner.

In modifying the f.i.d. to a t.i.d., placement of the rubidium silicate bead directly and reproducibly over the burner is necessary. This is accomplished by converting the existing glow plug body of the f.i.d., which is centrally located over the burner, to a bead holder. Also, the bead holder described allows use of an externally applied current to heat the bead and thus gives flexibility in generating the ionization background current ( $i_{B.C.}$ ) important to the sensitivity of this detector (3-7).

With reference to Fig. (3-2), the necessary modifications made to the glow plug are:

- 1) The attachment of a 4.3-cm long 316 stainless steel tube (0.47-cm O.D.; 0.28-cm I.D.) to a glow plug body,
- 2) The placement of a 7.5-cm long ceramic rod (0.275 cm O.D., Omegatite 350 two hole round thermal-couple insulator, TRA04018, Omega Engineering, Inc.) containing two parallel bores through this stainless steel tube and,
- 3) The threading of an 18-cm long, 0.5 mm diameter platinum wire (Fisher Scientific Co., Ltd.) through the bores in the ceramic rod in such a way that a 3-mm loop is left at one end of the ceramic rod. To this loop is attached the rubidium silicate bead (see below).

With the tubing size used in constructing the bead holder, the holder is able to fit through the collector electrode and is held in place by the glow plug body. The bead height above the burner is adjusted by sliding the ceramic rod with respect to the stainless steel tubing mounted into the glow-plug body. An Allen screw is used to secure the position of the rod once an optimum height of bead above the burner is attained. In this study the rubidium bead is placed 5 mm above the burner. This region corresponds to a flame temperature zone of 700-800°C (depending on flame conditions) as measured with a differential thermocouple (10-560-10, Fisher Scientific Co., Ltd).

One centimeter of the collector electrode is removed so that no collector area will be below the level of the bead. In this way separation of f.i.d. from t.i.d. response is assured (13,14).

To electrically heat the bead, two in-parallel 10 Amp maximum Powerstats (Superior Electric Company) are used and connected to the platinum leads extending from the ceramic rod above the glow-plug body. One Powerstat is used for coarse and the other for fine adjustment of the bead heating current ( $i_B$ ). A Wilbac (model ACA15) 0-15 Amp AC ammeter is used in series with the Powerstats and stabilized using a Sola Constant Voltage Transformer (Type CVH). A maximum

of 10 Amp can be applied to heat the bead.

The final modification involves the burner polarizing voltage (-170 V) delivered from the Pye-Unicam ionization amplifier. A four-pole double-throw switch is used to connect the polarizing voltage and ground, so that in one direction the burner is at ground and the platinum lead to the bead is polarized. This is necessary since polarization of the bead is the normal t.i.d. configuration (3,5). For f.i.d. operation the bead is removed and the switch thrown in the other direction, thus polarizing the burner.

The Pye-Unicam ionization amplifier and dual-temperature controller are used to monitor the response from the detector and maintain constant pyrolysis and detector-oven temperatures, respectively. The solvent-evaporator oven of the moving-wire detector is not used, the detector oven is maintained at 200°C, and the pyrolysis-oven temperature is varied when appropriate.

A Honeywell Electronik 196 (10 mV full scale deflection) recorder is used to record the amplifier-output responses and noise measurements.

The alkali-metal source, a rubidium silicate glass bead, was fabricated according to Lubkowitz et al. (7,8). Since they mentioned that a more complete study was underway to optimize the composition of the alkali source, only one bead composition was used. The bead contained 17% by weight

RbCl to Corning 7740 glass (Pyrex). Ground glass and RbCl were mixed and placed in a 15-mL Coors porcelain crucible. While stirring continuously with a quartz rod, a butane-oxygen rich flame was used to melt the mix. Once a melt was formed a strand was pulled and, using a smaller flame, attached to the bead holder platinum wire loop. One bead, 1.9 mm diameter, was used for this entire study. Once attached and centered on the wire the bead was aged glowing red in the flame for ten minutes and then annealed for another 10 min in a sooty flame. After placement in the detector, a high bead heating current (9.0 Amp) was applied through the bead until a stable ionization background current was attained (approximately 5 h). A properly aged bead should give a  $i_{B.C.}$  of around 1 pA at high bead current (7), i.e., enough to cause the bead to glow red.

The evaluation of the detector involved first relating the rubidium silicate bead response to variations in  $H_2$ , air, and  $N_2$  flow rates and bead-heating current. Since the Pye system did not provide an adequate means of quantitating gas flow rates, Brooks flow controllers and rotameters (Emerson Electric Co., Hatfield, Penn.) were used. These were modified for the flow-rate ranges used. All gases were of "Zero Gas" purity (Linde Specialty Gases) and further purified by passing through filters of Drierite (Anachemia Chemicals Ltd., Montreal, P.Q.) and molecular sieve (Type

3A, Matheson, Coleman, and Bell, Norwood, Ohio). At a constant  $i_B$  evaluation of the bead response involved varying the  $H_2$ , air or  $N_2$  flow rate while keeping the other two rates constant and measuring  $i_{B.C.}$ . These measurements were repeated at different bead-heating currents.

To evaluate the response of the detector to selective standards, samples in a 0.5 mL/min methanol (Spectrograde, American Chemicals, Ltd.) stream were delivered to the coating block of the moving-wire portion of the detector with a Milton Roy Minipump (Model 396, Laboratory Data Control), homemade pulse-damping system (15) and a Valco 3000 psig valve with 20- $\mu$ L sample loop (Valco Instrument Co., Inc.). As a substitute for a column, four feet of connecting tubing (1/16-inch O.D.; 0.030-inch I.D.) were used between the injector and detector to allow some band broadening.

The standards evaluated were reagent grade chloro- and nitrobenzene (Fisher Scientific Co., Ltd.), aniline and octanoic acid (Baker Analyzed Reagent), hexadecane (Eastman Organic Chemicals), tri-n-butyl phosphate (Fisher Scientific Co., Ltd.), PC-distearoyl (Standard 7, Chapter 2) and organophosphorus pesticides (Supelco Inc., Bellefonte, Penn.). Working standards were made of chloro- and nitrobenzene, aniline, octanoic acid and hexadecane to correspond to a 10-mg sample delivered to the detector coating block. These roughly corresponded to 10 mL of standard in 15 mL of hexane

(Spectrograde, American Chemicals Ltd.). Tri-n-butyl phosphate and phosphatidycholine solutions were made with methanol to correspond to a 20-mg sample delivered to the coating block while the pesticides were as 50% solutions in methanol (Spectrograde, American Chemicals, Ltd.). The malathion standards for the evaluation of linearity and sensitivity of the detector were made by appropriate serial dilution in methanol.

### 3.3 RESULTS

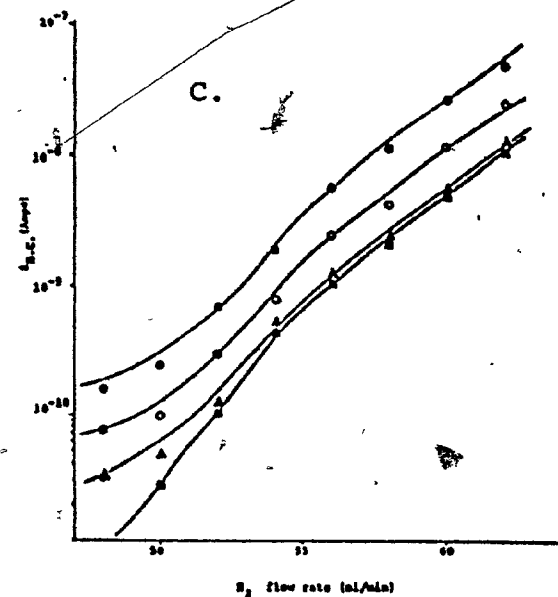
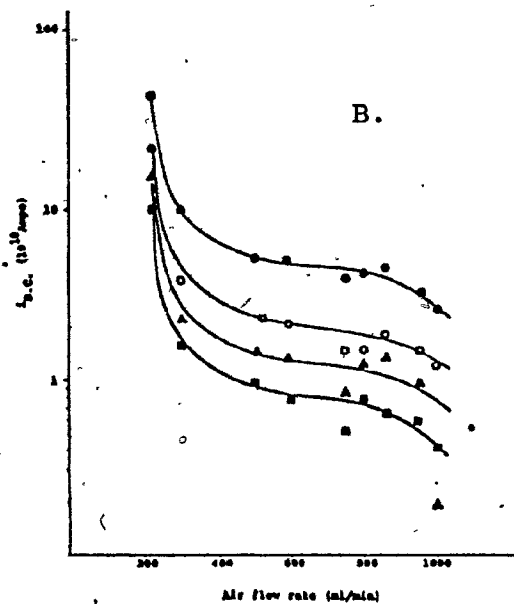
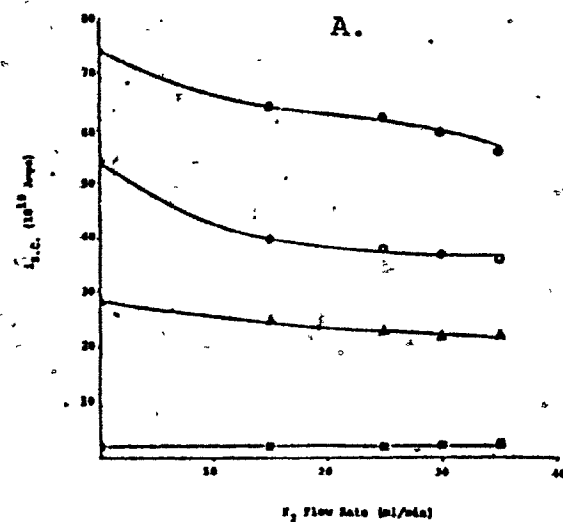
While this detector is similar in operation principle to one previously described (3-5), it varies considerably in burner design. A series of experiments was conducted to compare the operating parameters ( $i_B$ , and  $N_2$ , air, and  $H_2$  flow rates) of the present detector with a similar study reported for the previously described detector. The detectors were not expected to be directly comparable but general similarities were expected to be found.

Lubkowitz et al. (6) found ionization background current to be a function of bead heating current, and as the bead aged greater  $i_B$  was required to attain the same  $i_{B.C.}$ . Figure 3-3 shows  $i_{B.C.}$  versus  $i_B$  for our bead. As can be seen, a significant decline in  $i_{B.C.}$  was observed after ten days usage. The  $i_B$  required to attain a given  $i_{B.C.}$  was

significantly higher in our system, presumably due to the large bead size used and the necessity of heating the bead holder.

The dependence of  $i_{B.C.}$  on nitrogen, hydrogen and air flow rates was also investigated. This was done because the sensitivity of the TID is a function of  $i_{B.C.}$  and numerous ways of attaining the same  $i_{B.C.}$  are possible. Figures (3-4A), (3-4B) and (3-4C) show that a different dependence of  $i_{B.C.}$  was observed for  $N_2$ , air and  $H_2$  at different  $i_B$ . For  $N_2$  flow rates from 0 to 34 mL/min (Fig. (3-4A)) the effect was not dramatic and, as expected from a previous study (6), at increasing  $N_2$  flow rates  $i_{B.C.}$  was observed to decrease. The reason for this decrease is not known but has been attributed to cooling of the bead by convection (6). Using a platinum-platinel thermocouple, we measured an increase in the temperature of the zone where our bead was placed. This observation warrants further investigation.

Figure (3-4B) shows that by increasing air flow rates from 220 to 1000 mL/min, ionization decreased more significantly than for  $N_2$  changes over its entire range. The nitrogen flow rate was normally left constant at 30 or 35 mL/min while the air-flow rate was varied from 300 to 500 mL/min. For  $N_2$  a high flow rate is required to prevent tail skewing of injected samples. Air-flow rates have the similar effect of preventing mishaped peaks and so must be



Figures 3-4A,B and C. Ionization background current ( $i_{B.C.}$ ) as a function of changes in nitrogen (A), air (B), and hydrogen (C) flow rate and bead heating current. (Unless otherwise stated,  $H_2 = 51$  mL/min, Air = 300 mL/min, and  $N_2 = 35$  mL/min).  $\blacksquare = i_B$  of 0 Amps,  $\blacktriangle = i_B$  of 3 Amps,  $\bigcirc = i_B$  of 5 Amps, and  $\bullet = i_B$  of 7 Amps.



maintained at a rather high value.

Figure (3-4C) shows that  $H_2$  flow rates from 48 to 64 mL/min play the most significant role of the three. As expected an increasing  $H_2$  flow rate increased  $i_{B.C.}$  due to direct heating. What was unexpected was how large a dependence  $i_{B.C.}$  had on the  $H_2$  flow rate. Figure (3-4C) indicates that very careful control of the  $H_2$  flow rate is required to prevent considerable low frequency noise. Because the ionization process responsible for maintaining  $i_{B.C.}$  (i.e., Rubidium loss from the bead) occurs on the bead surface, fluctuations in the  $H_2$  flow rate are expected to make a greater contribution to noise than  $i_B$ . The bead-heating current heats through the center of the bead, where the bead-heat capacity can buffer any short term fluctuations in current. A voltage stabilizer for the bead heater is still required since line-voltage fluctuations, without the stabilizer, cause significant low frequency fluctuations in  $i_{B.C.}$  and baseline drift at low attenuations.

The gas-flow rates used in these studies represent the upper and lower limits of combustion with the burner system used and are quite different from those given in the comparison study (6). This is expected because of the totally different burner designs employed by the Pye and Perkin-Elmer systems.

### 3.3.1 Selectivity

One problem associated with evaluating a t.i.d. using a wire transport interface is the uncertainty of the amount of sample reaching the detector (11). In order to test the selectivity of this modified detector the transport mechanism was first run with the f.i.d. in place. Nitrogen was used as the purge gas from the pyrolysis oven for nitrobenzene, chlorobenzene, aniline, t-butyl phosphate, hexadecane, octanoic acid, and phosphatidylcholine. The results are presented in Table 3-1. As indicated by Slais and Krejic (11) the response from a detector of this sort is complicated by the wire-transport system, pyrolysis process, and gas-phase transfer of pyrolysis products to the sensing element. All results in Table 3-1 corresponded to injections of a 10-mg sample except for t-butyl phosphate and phosphatidylcholine which were 20 µg: peak heights rather than areas were cited since no columns were used. For comparison to the other standards, the t-butyl phosphate and phosphatidylcholine responses were multiplied by a factor to correspond to an injected sample of 10 mg.

The f.i.d. and t.i.d. responses for chlorobenzene, aniline and nitrobenzene were either not detectable or very small. It was assumed that a lack of wire coating was the main reason that these compounds were not detectable. For

Table 3-1: Comparison of f.i.d. to t.i.d. Responses for Standards

STANDARD	f.i.d. RESPONSE* (Amp)	t.i.d. RESPONSE (Amp)	
		AIR***	N <sub>2</sub>
Hexadecane	$2 \times 10^{-9}$	$1.1 \times 10^{-12}$	$2.8 \times 10^{-10}$
Octanoic acid	$1.2 \times 10^{-9}$	$1.3 \times 10^{-12}$	$1.4 \times 10^{-10}$
t-butyl phosphate	$1.3 \times 10^{-9}$	$1.5 \times 10^{-11}$	$1.0 \times 10^{-10}$
Chlorobenzene	N.R.**	N.R.	N.R.
Nitrobenzene	$3 \times 10^{-13}$	N.R.	N.R.
Aniline	N.R.	N.R.	N.R.
Phosphatidylcholine	$5 \times 10^{-10}$	N.R.	$7.5 \times 10^{-10}$

\* See text for sample amounts.

\*\* No response above noise.

\*\*\* Air was substituted for N<sub>2</sub> as purge gas from pyrolysis oven.

H<sub>2</sub> = 32 mL/min.

Air = 590 mL/min.

N<sub>2</sub> = 35 mL/min.

Wire speed = 6 cm/sec.

Pyrolysis oven = 700°C.

the f.i.d. mode, hexadecane, octanoic acid, and t-butyl phosphate gave approximately equal responses while phosphatidylcholine gave a slightly reduced response compared to the three detectable standards. The  $i_{B.C.}$  used to generate the data in Table 3-1 was  $8 \times 10^{-9}$  Amp. Using  $N_2$  as purge gas and the t.i.d. mode, t-butyl phosphate and phosphatidylcholine gave responses approximately equal in magnitude to the non-phosphorus containing standards, hexadecane and octanoic acid.

To further investigate the similarity of response between the non-phosphorus containing and phosphorus containing standards, a study involving f.i.d. and t.i.d. response as a function of pyrolysis oven temperature was conducted. As illustrated by Fig. 3-5, the response of t-butyl phosphate in the f.i.d. and t.i.d. modes was found to be dependent on pyrolysis-oven temperature. As the pyrolysis-oven temperature was increased, response in the f.i.d. mode increased slightly, while t.i.d. response decreased significantly (over 140 times). At  $400^\circ C$ , octanoic acid and hexadecane gave no response above noise with the t.i.d. detector. Also, the phosphatidylcholine response did not increase with a decrease in oven temperature. Thus it was concluded that for relatively volatile standards such as hexadecane, octanoic acid and t-butyl phosphate, compared to phosphatidylcholine, a large portion of the sample coated on the wire can be transported to the detector sensor. Some compounds such as

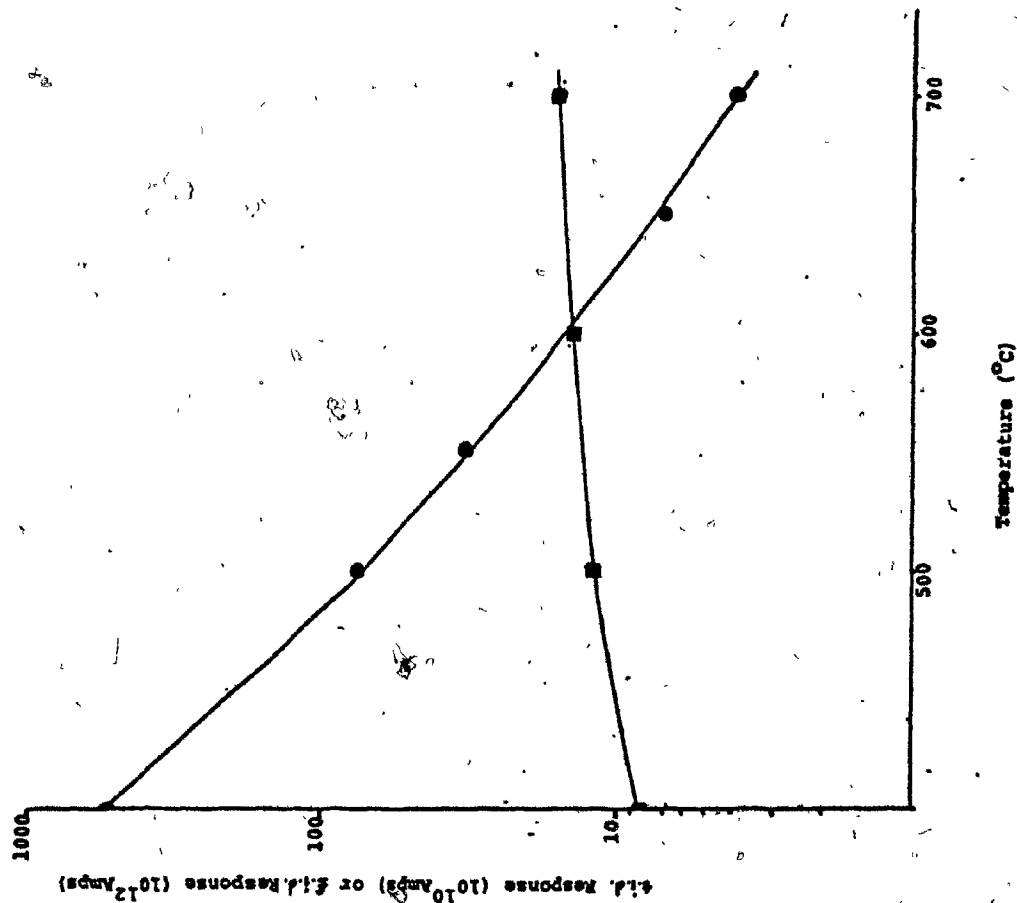


Figure 3-5. Detector response as a function of pyrolysis oven temp., for 20 ug t-butyl phosphate.  $\circ$  = t.i.d.,  $\square$  = f.i.d.,  $H_2$  = 35 mL/min, air = 590 mL/min,  $H_2$  = 35 mL/min, and wire speed = 6 cm/sec.)

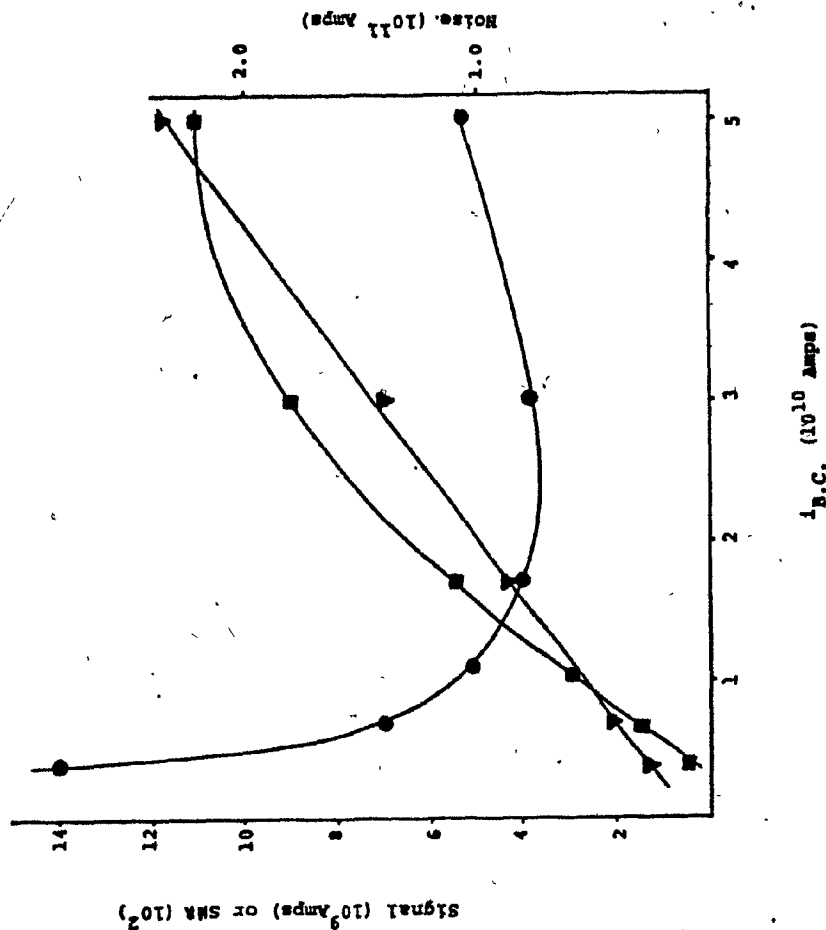


Figure 3-6. t.i.d. response, noise, and signal-to-noise ratio (SNR) for 20-µgm t-butylphosphate as a function of varying  $i_{B.C.}$  by changing head current.  $\circ$  = response,  $\square$  = noise, and  $\triangle$  = SNR.

( nitrobenzene, chlorobenzene, and aniline were not detectable, apparently due to a transport problem. Furthermore, the detector is species selective for phosphorus. Care must be taken in controlling pyrolysis-oven temperature as too high a temperature appears to be associated with a transport problem to the t.i.d. sensor, possibly by formation of some refractory phosphate species.

High molecular weight compounds such as phospholipids were not detectable at low levels presumably due to their low vapor pressure. The low vapor pressure of phosphatidylcholine necessitated high pyrolysis-oven temperature, causing the same transport problem associated with t-butyl phosphate.

The response of organophosphorus pesticides was also tested. These compounds are similar to t-butyl phosphate, the model compound used to develop this detector. The response of the pesticides tested is given in Table 3-2 as a t.i.d.-f.i.d. ratio. The enhanced sensitivity for this class of compounds indicates again that a relatively high vapor pressure (compared with phosphatidylcholine) is necessary for response. Pyrolysis-oven temperature was 500°C for this study, but could be optimized for any given pesticide of interest.

C

Table 3-2: Comparison of f.i.d. to t.i.d. Responses from Organo-Phosphorus Pesticides

SAMPLE	RESPONSE f.i.d./t.i.d.
DDVP	367
DIAZINION	182
PHORATE	252
m-SYSTON	200
MALATHION	219
PARATHION	167
VALED	476
DI-SYSTON	238
PHOSDRIN	222
ETHION	243

### 3.3.2 Sensitivity

The original purpose for detector modification was the determination of phospholipids. As modified, the detector is incapable of any enhanced sensitivity over the Pye Unicam LCM2 system (16,17) for this class of compounds for reasons cited previously. However, the detector may be useful for other classes of organophosphorus compounds, such as pesticides. Therefore, sensitivity for malathion was studied. The relationship of response to background ionization for the t.i.d. is well documented (6,18,19). Figure (3-6) illustrates that while the signal does increase with an increase in  $i_{B.C.}$ , the t-butyl phosphate noise also increases. The signal-to-noise ratio (S/N) curve illustrates that an optimum S/N is obtained at lower  $i_{B.C.}$ . For this study  $i_{B.C.}$  was varied by changing the bead current  $i_B$ ; however,  $i_{B.C.}$  could also be changed by varying the  $H_2$ - or air-flow rate. Lubkowitz et al. (6) illustrate the signal and noise dependence of this type of detector on  $H_2$ , air,  $N_2$  and  $i_B$ .

Optimization of  $H_2$ , air, and  $i_B$  as well as wire speed, which also affects sensitivity and noise, can be done but requires a complicated optimization format. No such technique was applied here. When this detector is to be used for quantitating a specific solute, simplex optimization



(20,21) may be employed. Thus the responses given are not optimum with respect to the signal-to-noise ratio.

In Fig. (3-7) is plotted ~~amount~~ of malathion injected versus response as peak height. As can be seen the response of the modified detector is linear over at least four orders of magnitude; the detector has the capability of detecting 35 ng of malathion. The detection limit is defined (Chapter 1) as the amount of malathion producing a signal twice the peak-to-peak noise as measured over three times the peak base width. Similar detection limits are expected for the other pesticides monitored as well as other organophosphorus compounds exhibiting some volatility.

### 3.4 DISCUSSION

The objective of this study was to modify a simple transport f.i.d. to give enhanced sensitivity for organophosphorus compounds. The data in Figs. (3-4A) to (3-4C) illustrate that different burner configurations require different operating ranges for  $H_2$ , air, and carrier gas (purge gas,  $N_2$ ) flow rates. Also, the sensitivity of  $i_{B.C.}$  to varying  $H_2$  flow rates was greater than expected, and demonstrates that the  $H_2$  flow rate must be controlled more carefully than either the air or the purge gas-flow rate. Finally, while bead current  $i_B$  can be used to establish

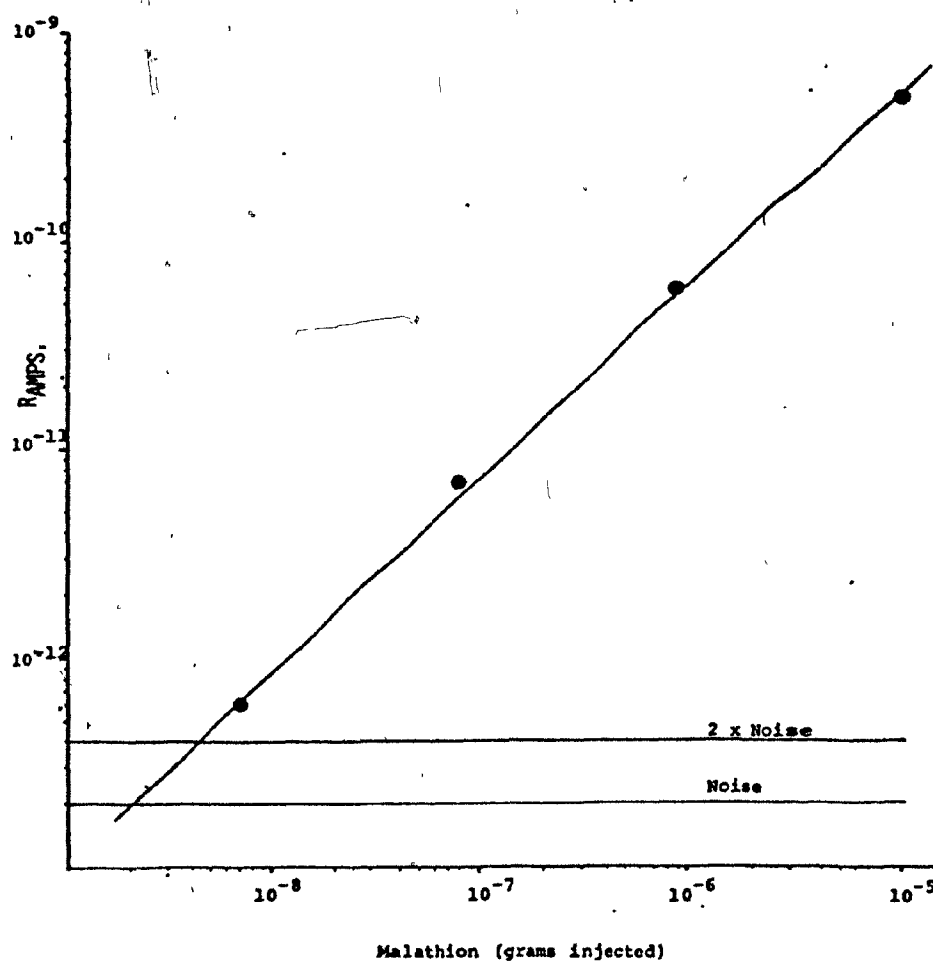


Figure 3-7. Response ( $R_{AMPS}$ ) of the t.i.d. to varying amounts of malathion. Conditions as in Figure 3-6 with pyrolysis oven temperature 500°C and  $i_{B.C.}$  of 35 picoamps. Linear regression analysis gave response =  $4.67 (+ 0.121) \times 10^{-5}$  moles malathion +  $7.07 (+ 6.05) \times 10^{-12}$  (+ 1 S.D.).


a given  $i_{B.C.}$ , the  $H_2$  flow rate has a larger effect and must be used initially to establish the lower limit of  $i_{B.C.}$ .

The sensitivity and selectivity of the detector were difficult to evaluate and could not be compared with other reported gas chromatographic detectors because of the different transport mechanism. The response of the detector was due to two phenomena: transportation of the solute to the detector-sensing element and response of the sensing element. When compared to an f.i.d. using the same transport mechanism, the t.i.d. showed enhanced sensitivity for certain organophosphorus pesticides ranging up to 500 times (and presumably greater if properly optimized). The detection of phospholipid by this detector was not possible. This was primarily because of the inability of the transport mechanism to transport the most important portion of the molecule, the phosphate diester, into the flame.

The transport mechanism used here was first developed by James et al. (22) and the entire detector was later improved significantly by Scott and Lawrence (23) with the addition of a reduction unit before the f.i.d. which converted the oxidation products from the pyrolysis oven to methane. This later model (not used here) is useful as a detector for hydrocarbon species but detection limits for phospholipids below one microgram are not possible (18,19).

An additional modification to circumvent the

transport problems observed with phosphatidylcholine would be to place the transport wire through the t.i.d. flame as done by Balaukin et al. (11). This modification was attempted, but increased noise, as seen in another study (27), made this configuration useless for detection purposes. The next chapter describes the design of a detector based on an entirely different principle of operation.



REFERENCES

1. A. Karmen and L. Giuffrida, Nature (London), 201 (1964) 679.
2. U.U. Brazhinkov, M.V. Gurev, and K.I. Sakodinsky, Chromatogr. Rev., 12 (1972) 1.
3. B. Kolb and J. Bischoff, J. Chromatogr. Sci., 12 (1974) 625.
4. B. Kolb and J. Bischoff, U.S. Patent 3852037 (1974).
5. B. Kolb, M. Auer and P. Pospisil, J. Chromatogr. Sci., 15 (1977) 53.
6. J.A. Lubkowitz, J.L. Glajek, B.P. Semonian and L.B. Rogers, J. Chromatogr., 133 (1977) 37.
7. J.A. Lubkowitz, B.P. Semonian, J. Galodardes and L.B. Rogers, Report for ERDA, SRO-854-15, May 1977.
8. J.A. Lubkowitz, B.P. Semonian, J. Galobardes, and L.B. Rogers, Anal. Chem., 50 (1978) 672.
9. R. Greenhalgh, J. Muller and W.A. Aue, J. Chromatogr. Sci., 16 (1978) 8.
10. B.G. Julin, H.W. Vanderborn and J.J. Kirkland, J. Chromatogr., 112 (1975) 443.
11. K. Slais and M. Krejcek, J. Chromatogr., 91 (1974) 181.
12. A.A. Balaukin, B.C. Utorov, O.I. Kalmanouskii, and A.A. Chernokozhin, Patent USSR 370520 (1973).
13. F.P. Speakman and K. Waring, Column, 2 (1968) 2.
14. B. Kolb, M. Linder and B. Kempken, App. Chromatogr., 21E (1974) 1.
15. D.H. Freeman and W.L. Zielinski, Jr., NBS Technical Note, 589 (July 1970 to June 1971).
16. K. Kinchi, T. Ohta and H. Ebine, J. Chromatogr., 133 (1977) 226.

17. M.L. Rainey and W.C. Purdy, Anal. Chim. Acta, 93 (1977) 211.
18. M. Dressler and J. Janak, Collection Czechoslov. Chem. Commun., 33 (1968) 3960.
19. M. Dressler and J. Janak, Collection Czechoslov. Chem. Commun., 33 (1968) 3870.
20. D.E. Long, Anal. Chim. Acta, 46 (1969) 193.
21. S.N. Deming and S.L. Morgan, Anal. Chem., 45 (1973) 278A.
22. A.T. James, J.R. Revenhill and R.P.W. Scott, Gas Chromatography, 1964 (1965) 197, London: Inst. Petroleum.
23. R.P.W. Scott and J.G. Lawrence, J. Chromatogr. Sci., 8 (1970) 65.
24. E. Haati, J. Nikkari, and J. Karkkainen, Gas Chromatography, 1964 (1965) 190, London: Inst. Petroleum.

#### 4. DEVELOPMENT AND DESIGN OF A POST-COLUMN REACTOR FOR HIGH PERFORMANCE LIQUID CHROMATOGRAPHY

##### 4.1 GENERAL INTRODUCTION

Alternative detectors for high performance liquid chromatography (h.p.l.c.) have been discussed in Chapters 1 and 2. In this chapter a detector based on quantitating the 1-phosphoglycerol portion of a phospholipid or the glycerol portion of triglyceride molecular species is described.

The determination of total triglycerides in serum is often done in clinical laboratories by one of two methods. One method is based on classical chemical reactions, the other newer method is based on enzymatic reactions.

The development of the classical method covered the period of 1964 to 1975 beginning with its introduction by Lofland (1,2), and Kessler and Lederer (3). This method has the advantage of cost effectiveness but lacks selectivity. All classical methods for triglycerides require extensive sample pre-treatment to separate triglycerides from phospholipids.

The enzyme-based alternative method was developed after 1973 (4,5) and is now used almost exclusively. Enzymatic selectivity eliminates the need for sample pre-treatment. The NAD-NADH couple, a common denominator in many clinical

analyses, is the final end product for UV-spectrophotometric quantitation. Enzyme-based methods have very recently been extended to phospholipid determinations (6,7,8) and are similar in approach to the triglyceride methods.

In comparing the two triglyceride methods, in the context of use with chromatography, the enzyme method's main advantage of selectivity is not important. Furthermore, interfacing an enzyme system with either normal or reversed-phase chromatographic units raises a compatibility problem that greatly restricts the choice of mobile phase. The classical method, on the other hand, is reasonably liberal with regards to compatibility with various mobile-phase systems. Thus, the classical method was chosen to be investigated as a possible basis for a liquid chromatographic detector.

In order to effectively couple the classical method, essentially a series of chemical reactions, to the effluent of an h.p.l.c., a marriage between the h.p.l.c. and some mechanized chemical system, a Post-Column Reactor (p.c.r.), is needed. Mechanized chemical systems can be divided into two general types: discrete analyzers and flow analyzers. With discrete analyzers, mechanization is accomplished on the principle of the robot-chemist where the sample is placed in a container (sample cup, test tube, etc.) and chemical



manipulations are carried out in a discrete manner. With continuous flow systems, the sample is injected or aspirated into a continuously moving reagent stream and additional chemical manipulations such as heating, delay, irradiation, or addition of other reagents, occur at various stages in the reactor.

A comparison of each general method shows that the discrete analyzer, by definition, is characterized by good sample integrity, but suffers from the need for complex mechanical design and close tolerance construction. The flow analyzer, on the other hand, does not guarantee sample integrity and may consume more reagent, but the design is simple and is more flexible with respect to adaptations or additions. When used as a p.c.r., the flow analyzer more faithfully reproduces the continuous functions generated by chromatographic processes, while the discrete analyzer gives averaged results in a histogram form whose resolution is limited by the incrementation process of discrete sampling.

The choice of which class of analyzer was based on the application and on the resources available. While examples of both classes of analyzers are in commercial production at this time, the system that appeared best suited for the problem of phospholipid and triglyceride analysis was the flow analyzer. Two systems using discrete analysis for detection of phosphorus after column chromatography were

mentioned in the literature (9,10).

The recent general reviews on h.p.l.c.-p.c.r. work (11,12,13) indicate that flow analyzers are well suited for p.c.r. work. Flow analyzers were used for fluorimetric derivatization methods (14) and electrochemical detection (15). Some recent work on p.c.r.'s emphasized the fundamental sources of band-broadening in flow analyzers (16,17). Because these p.c.r. detectors offer selectivity and sensitivity based on the wealth of classical chemical techniques presently available, conceivably any compound can be detected using p.c.r.

Three types of flow analyzers have been reported for use in p.c.r. systems. These are:

- 1) Segmented flow systems (continuous flow analysis, c.f.a.): Characterized by gas segmentation involving plugged flow of the reactor stream using low pressure peristaltic pumps. They are useful for almost any reaction sequence. This is the most established of all flow analysis methods and the basis of a large part of the clinical chemistry industry (18).
- 2) Non-segmented flow systems (flow injection analysis, f.i.a.): Characterized by non-segmented reactor streams and the use of relatively precise pumps. These systems have gained recent popularity due to the simple design features and wide applicability of the technique to common analysis

problems. It is suitable for reactions with very fast reaction rates, generally coming to completion within 30 sec (19).

3) Packed-bed reactors (p.b.r.): Characterized by the use of a wide diameter column containing inert packing as the reaction delay-mixing unit. One publication (20) has reported using this method. This system is limited in use to special applications.

A common denominator between them is that they all represent designs of on-line reactors which attempt to maintain sample integrity by limiting dispersion while simultaneously allowing enough delay time in their systems for reactions to occur to the desired degree.

The theory of dispersion in each system has been the subject of much study and is a very active field of research at this time. For instance, at a recent international symposium totally dedicated to flow analysis (21), 25% (7 out of 28) of the papers were concerned with dispersion in different flow analysis systems. This can be compared to the relatively small number (less than 0.2% out of 7,870) of earlier papers theoretically oriented, mentioned in one review (11).

Reactors based on c.f.a. are identical in concept to the widely used Technicon clinical chemistry analyzers (Technicon International, Tarrytown, New York) and are discussed in the context of the p.c.r. in Section 4.2.1. Detectors based on f.i.a. are in common usage and the theory

of dispersion in these systems has been well developed (22). The mechanism of dispersion in the p.b.r. is analogous to column chromatography dispersion and a useful discussion is presented in Refs. 20 and 23.

In terms of choosing between the various systems, the p.b.r. is immediately rejected because of the requirement for high-pressure pulseless pumps at each stage in the reactor. A choice between c.f.a. and f.i.a., (i.e. segmented versus non-segmented flow) is made possible by knowledge of the advantages and limitations of these systems. While it would be highly desirable to use f.i.a., because of its simplicity of design, appreciable band dispersion is anticipated for reactors which require multi-step addition of reagents and long (greater than 60 sec) delay times (24). An illustration of this is shown in Fig. 4-1 where repetitive injections of the chromophore 3,5-diacetyl-2,6-dihydrolutidine made into a f.i.a. and c.f.a. system monitored by absorbance and fluorescence are compared. The f.i.a. and c.f.a. systems were identical except that water replaced air segmentation in the f.i.a. system. Thus the system of choice for use as the p.c.r. in this application (reaction sequence shown in Fig. 4-16) is c.f.a.

In this chapter the development of the chemistry and hardware of the p.c.r. are described in detail. These two lines of work were carried out in parallel because of the

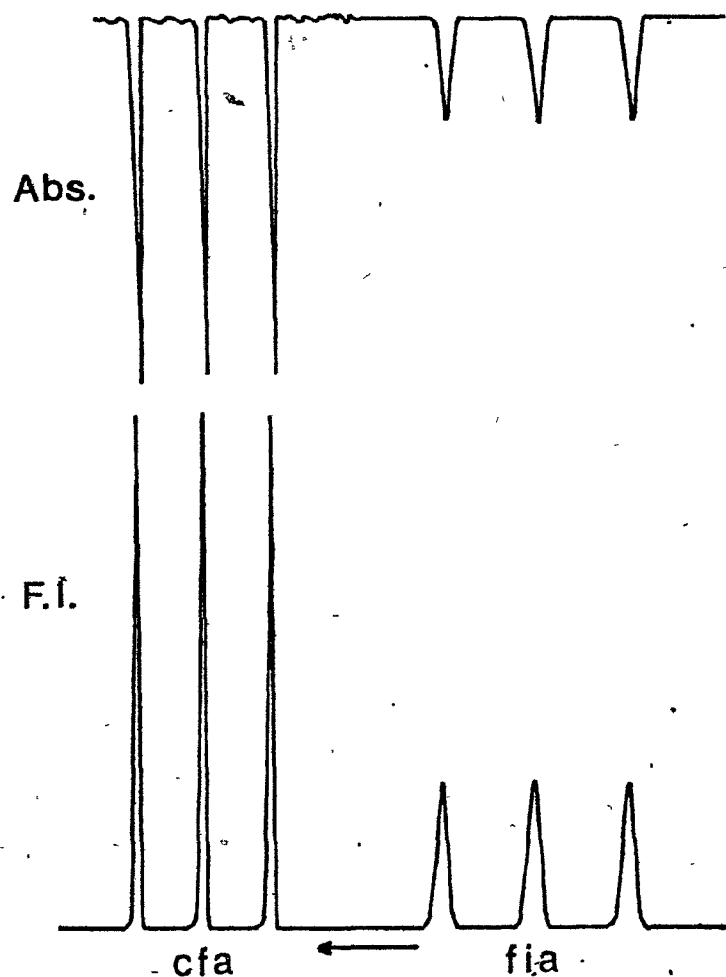


Figure 4-1. Continuous flow analysis (c.f.a.) and flow injection analysis (f.i.a.) band dispersion. See section 4.2. for details of the system used.

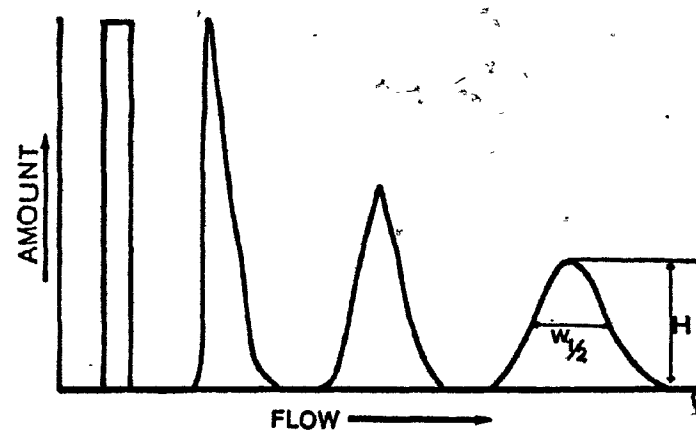


Figure 4-2. Development of dispersion in a flow analysis system with transition from rectangular bolus shape through Poisson to a Gaussian distribution. The last band shows the relation between band half width and band height ( $\sigma$  = width at 0.61  $H$ ).

need for compatability.

#### 4.2 INSTRUMENTATION DESIGN CONSIDERATIONS OF CONTINUOUS FLOW ANALYSIS SYSTEMS

##### 4.2.1 Introduction

The field of continuous flow analysis includes a large quantity of literature (7,870 references between 1957 and 1974 , (25)<sup>6</sup>) and a large number of determinations done each year using instrumentation based on this method. This subject is reviewed in two places rather exhaustively (11,26).

One of the most important aspects of c.f.a. is band dispersion of a sample as it is processed by the analyzer. Early work on this subject was based on an empirical approach (27-32) while more recent work (33-35) has been of a fundamentally derived nature. This work has culminated in a theoretically derived expression for predicting band dispersion from experimental conditions (36) and thus a firm basis for instrumental design in this field is now possible.

##### 4.2.1.1 Mechanisms of dispersion in continuous flow analysis

The mechanism of band dispersion in c.f.a. is best introduced by regression to the simpler case of f.i.a. (i.e. non-segmented flow analysis). It is recalled that the model

Poiseuille flow distribution of a fluid in the tube results in a bolus with its fastest linear velocity ( $v_{\max}$ ) in the center, the velocity dropping off in a parabolic fashion to  $v = 0$  at the walls of the tubes.

The tube material is, for hydrodynamic reasons, always assumed to be wetted and the flow is assumed to be both steady and laminar. What results from this flow model is a bolus with infinite tailing. This is not seen to occur in practice and in fact a bolus traveling through a tube undergoes band dispersion (shown in Fig. 4-2) with transition from a rectangular to a Poisson and then a Gaussian distribution (22). This dispersion pattern is explained by the phenomena of Taylor flow (37) where molecular diffusion across the tube averages the parabolic flow velocity distribution in the tube and in doing this, limits dispersion. The attainment of even linear flow velocity throughout the cross-section of the tube results in dispersion of a bolus by the mechanism of molecular diffusion, and in liquids can lead to quite low dispersion.

To radically alter the velocity distribution pattern in the flowing stream, Skeggs (18) introduced bubbles (as plugged flow) and thus compartmentalized the stream into separate segments. This is schematically represented in Fig. 4-3 where it is seen that a finite amount of liquid, due to wall wetting, is transferred from one liquid segment to another.

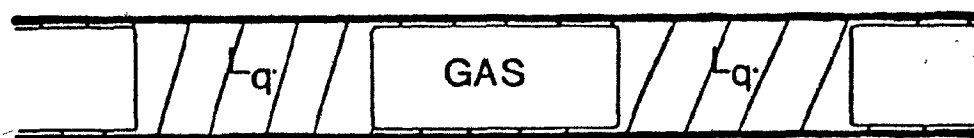


Figure 4-3. Schematic representation of bubbles (gas) segmenting the liquid stream ( $Lq.$ ) as plugged flow in the c.f.a. system. Liquid wets the tube wall and contributes to sample dispersion.

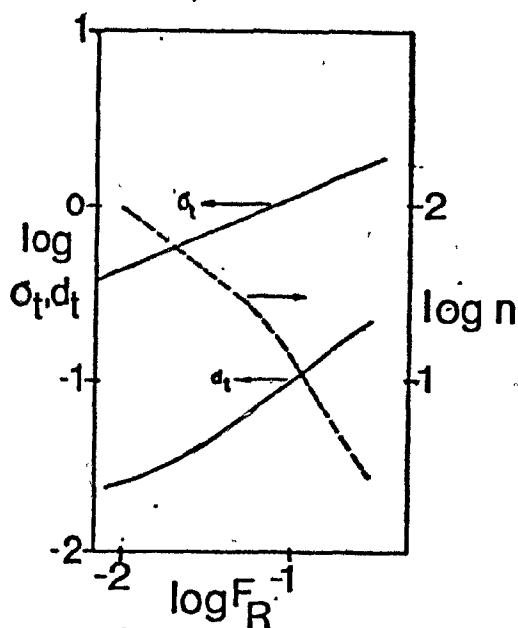


Figure 4-4. Optimum values for  $d_t$ ,  $n$  and  $F_R$  giving values of  $\sigma_t$ . Taken from <sup>1</sup>refer-36.  
where  $D_{w,25} = 0.00035$ ,  $\eta = 0.004P$ ,  $\gamma = 25$  dynes/cm and  $t = 100$  s.



The plugged flow forms the basis for c.f.a. systems. Dispersions in these systems occur because of the wall wetting, a hydrodynamic requirement for steady laminar flow. Thus, while plugged flow disrupts the Poiseuille flow velocity distribution, a mechanism still exists for dispersion. This amount of dispersion in c.f.a. systems can be predicted by Snyder's equation (36).

#### 4.2.1.2. Snyder's equation

Starting with a definition of dispersion (Gaussian distribution) of a bolus,

$$\sigma_t = \sigma_v / F_R \quad (4-1)$$

where  $\sigma_t$  = dispersion in time units (s) and is measured as the peak width at 0.61 peak height,  $\sigma_v$  is dispersion in volume units (mL) and  $F_R$  is liquid flow rate (mL · sec<sup>-1</sup>), the expression for the dispersion of band in a c.f.a., in terms of the parameters most often encountered in chromatography is

$$\sigma_t^2 = \left[ \frac{538 d_t^{2/3} (F_R + 0.92 d_t^3 n)^{5/3} n^{2/3}}{\gamma^{2/3} F_R D_{w,25}} + \frac{1}{n} \right] \left[ \frac{2.35 (F_R + 0.92 d_t^3 n)^{5/3} n^{2/3} t}{\gamma^{2/3} F_R d_t^{4/3}} \right] \quad (4-2)$$

where  $d_t$  = tube diameter (cm)  
 $\gamma$  = liquid surface tension (dynes  $\cdot$  cm $^{-1}$ )  
 $\eta$  = liquid viscosity (p)  
 $D_{w,25}$  = mass transfer coefficient in water at 25°C  
 $n$  = bubble frequency (sec $^{-1}$ )  
 $t$  = reaction residence time (sec).

This equation, as derived and confirmed by Snyder (24,36), can be used to predict  $\sigma_t^2$  and thus determine a priori the best design characteristics needed to build a low-dispersion c.f.a.-p.c.r. system.

One example of the use of this equation for use in the p.c.r. application is shown in Fig. 4-4 where the optimum values of  $d_t$ ,  $n$  and  $F_R$  resulting in the respective  $\sigma_t$  is shown. The optimum bubble frequency (obtainable in practice) is generally in the range of 1-10 sec $^{-1}$ ,  $F_R$  in the range 0.01-0.1 mL $\cdot$ sec $^{-1}$  (0.6-6.0 mL $\cdot$ min $^{-1}$ ) and  $d_t$  of less than .2 cm. Under these conditions and if each parameter is optimized with respect to one another,  $\sigma_t$  can be less than 1 s. When one considers the contribution of other components in the h.p.l.c. and the dispersion due to connector tubing this value is well within the tolerable limits of most modern chromatographic systems (36). For instance, 1 s for a typical flow of 1.0 mL $\cdot$ min $^{-1}$  or 0.0033 mL $\cdot$ sec $^{-1}$  corresponds to 0.0033 mL dead volume. The typical column void volume

is around 2 mL and thus 0.0033 mL is small in comparison.

The values for  $n$ ,  $F_R$  and  $d_t$  mentioned above were used as general guides in developing the c.f.a. system described next. Some practical limiting values of  $n$ ,  $L$ ,  $F_R$  and  $d_t$  were found to be important considerations in designing the c.f.a.

#### 4.2.2 Choice and Evaluation of c.f.a. Components

The components of a c.f.a. and their relationship to one another are schematically represented in Fig. 4-5. Each component is discussed below.

##### 4.2.2.1 The bubbler (B)

The distinguishing feature of c.f.a. is plugged flow gas segmentation of the moving stream. The requirements of a gas bubble introduction system (bubbler) are that it delivers:

- 1) The optimum number of bubbles per unit length of reactor stream (i.e. correct bubble frequency).
- 2) The optimum bubble size.
- 3) A uniform bubble distribution.

Also, the bubbler should have low dead-volume and good purge characteristics.

The optimum bubble size is that the bubble length  $L$

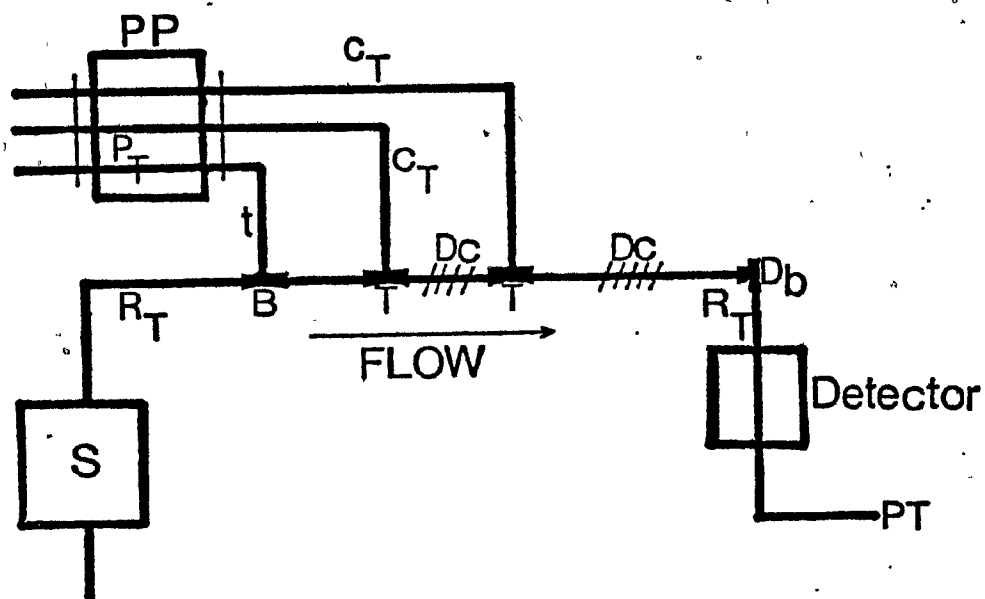


Figure 4-5. Schematic representation of the c.f.a. Refer to text for explanation of abbreviations.

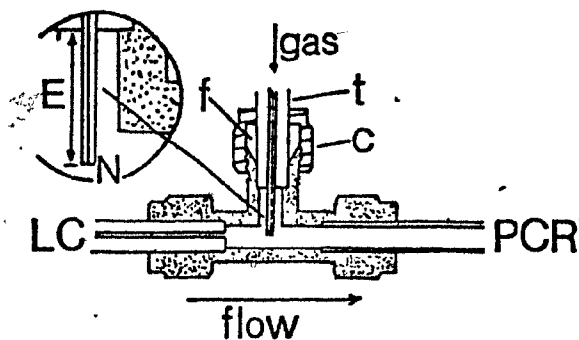


Figure 4-6. The bubbler (B) developed and characterized for use with the c.f.a. Scale enlargement is included in the offset to show needle (N) displacement (E) from the gas connection tubing (t). Consult text for details.

is 1.5 times the diameter of the tube (36). Shorter bubble lengths are unsuitable and give unstable bubbles that allow excess carry-over between each segment; longer bubble lengths on the other hand are inefficient since excessive reactor-tube length is required to achieve equivalent delay times. Uniform bubble distribution is required to minimize short term noise by enabling uniform proportioning of reagents in the reactor. Low bubbler dead volume is required to prevent excessive band dispersion before and while segmentation occurs.

#### Bubbler design

Special consideration was given to the bubbler as it, more than any other part, determines the efficiency of the system.

The bubbler design which evolved from preliminary work is represented in Fig. 4-6. The body of the bubbler was made from a 0.159 cm (1/16") stainless steel Swagelok<sup>®</sup> Tee fitting utilizing standard compression nuts (C) as connectors. The gas inlet connecting tube (T) was 0.159-cm O.D., 0.0254-cm I.D. Teflon construction and connected to the peristaltic pump tubing with 30 cm of length. To prevent leakage around the connecting tube a silicon ferrel (f) made from pump tubing was used to seal T to the body of the bubbler. A 0.045-cm O.D., 0.0015-cm I.D. (25-gauge) stainless steel needle (N) was force fitted into the tube T and extended a distance E into the bubbler.

The utilization of very narrow diameter connecting tubing and the needle overcame one serious problem often associated with bubblers which is due to the compressible nature of the segmenting gas. The backpressure of the c.f.a. built up a resistor-capacitor (RC) hydraulic analog when large volumes of gas were present in the bubbler lines, which caused non-uniform addition of bubbles due to the gas compression and discharge (gas surging). Thus, gas surging was eliminated by decreasing the volume of the gas-connecting tube T so that the effective time constant of the RC hydraulic system was very low. Surging still occurred with this arrangement but when observed was diagnostic of unusually high back pressures in the c.f.a., due usually to precipitate formation.

This bubbler was found to be very reliable and as shown in Fig. 4-7, gave a uniform bubble pattern.

#### Evaluation of the Bubbler

As mentioned previously, the optimum bubble is one which has length  $L = 1.5 d_t$ , where  $d_t$  is the tube diameter (36). The volume ( $V_B$ ) of such a bubble is calculated from the volume of an ellipsoid as

$$V_B = (7/24) \pi d_t^3 \quad (4-3)$$

$d_t$  being the interior diameter of the tube (cm),  $V_B$  having

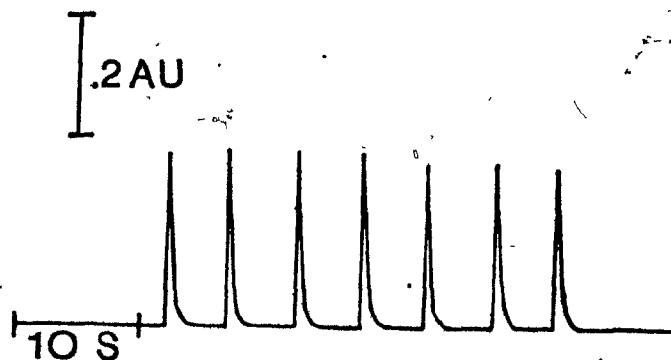


Figure 4-7. Schaeffel SF770 display of the bubble pattern produced by B, Figure 4-5.

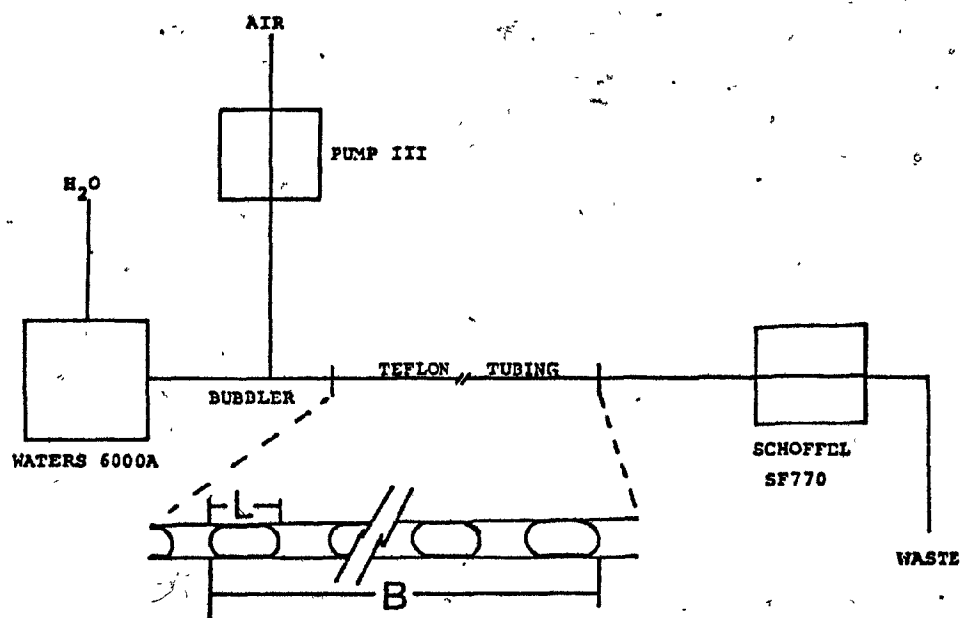


Figure 4-8. Schematic representation of the experimental system used to evaluate the bubbler. The value B was measured over a length of 10 bubbles.

units  $\text{cm}^3 \cdot \text{bubble}^{-1}$ . The choice of frequency of bubble injection ( $n$ ) depends on other experimental parameters as mentioned in the context of Snyder's equation (Eqn. 4-2). For any given gas flow rate ( $F_g$ ) and tube diameter, an optimum frequency  $n$  will occur based on the optimum bubble size and the equation

$$F_g = nV_B \quad (4-4)$$

Combining with Eqn. 4-3, gives

$$F_g = (7\pi/24) d_t^3 n \quad (4-5)$$

which takes into account the optimum bubble size for the tube diameter used in the c.f.a.

Representative optimum bubble volumes for various commercially available tube diameters are given in Table 4-1. Some theoretically optimum bubble rates are given in Table 4-2. These rates shall be discussed later in the context of evaluating the bubbler design.

The experimental parameters of interest with respect to their effect on  $V_B$  and  $n$  are:

- 1) Reagent-flow rate ( $F_R$ ).
- 2) Gas-flow rate ( $F_g$ ).
- 3) Position of bubbler needle ( $E$ ).



Table 4-1: Optimum bubble volume for various tube diameters.

dt(cm)	$V_B$
0.0254	$1.5 \times 10^{-5} \text{ cm}^3$
0.0761	$4.0 \times 10^{-4} \text{ cm}^3$
0.100	$9.6 \times 10^{-4} \text{ cm}^3$
0.200	$7.3 \times 10^{-3} \text{ cm}^3$

Table 4-2: Theoretical optimum bubble frequency (n) for the bubbler (B) and the Teflon measuring tube (Figure 4-8).

Fg	n(Teflon tube, $r = 0.08 \text{ cm}$ )	n(B, $r = 0.132 \text{ cm}$ )
0.03	1.0	0.23
0.10	3.6	0.80
0.16	5.7	1.28
0.23	8.1	1.80
0.32	11.3	2.51
0.60	21.3	4.75
0.80	28.3	6.31
1.00	35.6	7.92

Evaluation of these three variables was done with the system represented in Fig. 4-8. Bubble frequency and  $V_B$  were determined by measuring:

- 1) Bubbles per cm (B) from the length of tubing required to contain a segment of liquid stream containing 10 bubbles.
- 2) Individual bubble length (L) using the length of at least ten bubbles sighted through a transparent 0.08-cm I.D. Teflon tube.
- 3) Frequency directly using a photometric detector with low (8  $\mu$ L) dead volume. This system was found to be inadequate for measuring bubble frequencies greater than  $n = 3 \text{ sec}^{-1}$  and thus was used principally for gathering data for display (example Fig. 4-7).

Bubble volumes were calculated using the equation

$$V_B = L\pi r^2 \quad (4-6)$$

where  $r = 0.04 \text{ cm}$ . This equation assumes the bubbles are cylindrical and does not correct for rounding effects at the bubble ends. The use of narrow diameter Teflon tubing (0.04-cm radius) for measurements of B and L allowed this approximation to be made (estimated error < 10%).

Bubble frequencies were calculated from the following

$$n = BF_T/V_T \quad (4-7)$$

where  $F_T$  and  $V_T$  are total flow rate (i.e.  $F_R + F_g$ ) and unit tube volume ( $\text{cm}^2$ ), respectively.

The effect of reagent flow rate on  $n$  was tested by varying flow rate  $F_R$  over the range  $0.5\text{--}7.0 \text{ mL}\cdot\text{min}^{-1}$ . The effect on  $V_B$  and  $n$  of varying  $F_g$  over the range  $0.030$  to  $1.0 \text{ mL}\cdot\text{min}^{-1}$  was investigated and the effect of position of bubble needle (E) on bubble frequency  $n$  was investigated by varying E. In all cases  $V$  and  $n$  were calculated using Eqn. 4-6 and Eqn. 4-7.

To test the validity of this experimental approach a relationship between the dependent and independent variables was derived such that

$$A = BV_B/V_T \quad \text{and} \quad C = F_A/F_R \quad (4-8)$$

and

$$A = C$$

A rectilinear plot of  $A$  versus  $C$  is given in Fig. 4-9 and shows that the experimental approach was valid over the flow ranges tested and lacked obvious systematic error.

The effect of varying  $F_R$  (presented as  $F_{\text{H}_2\text{O}}$ ) on  $n$  is shown in Fig. 4-10 and indicates that this variable has

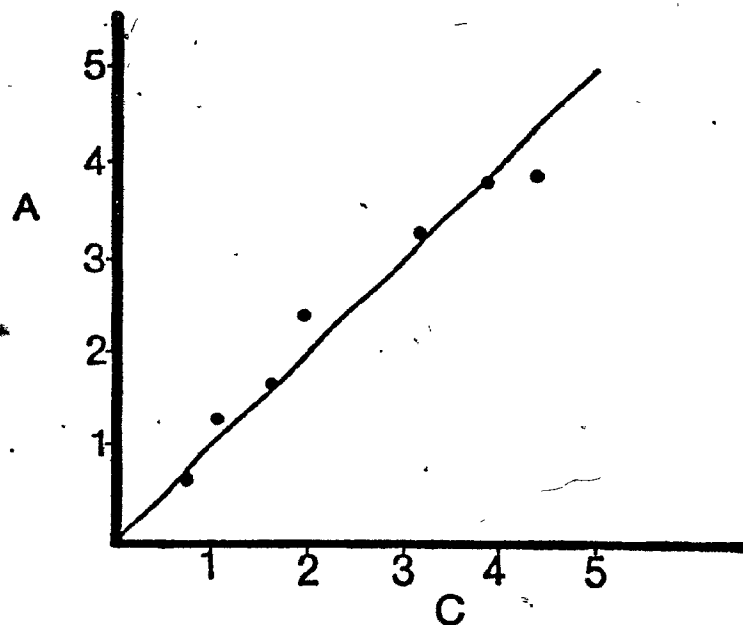


Figure 4-9. Correlation of A and C for seven separate experiments over a wide range of conditions.

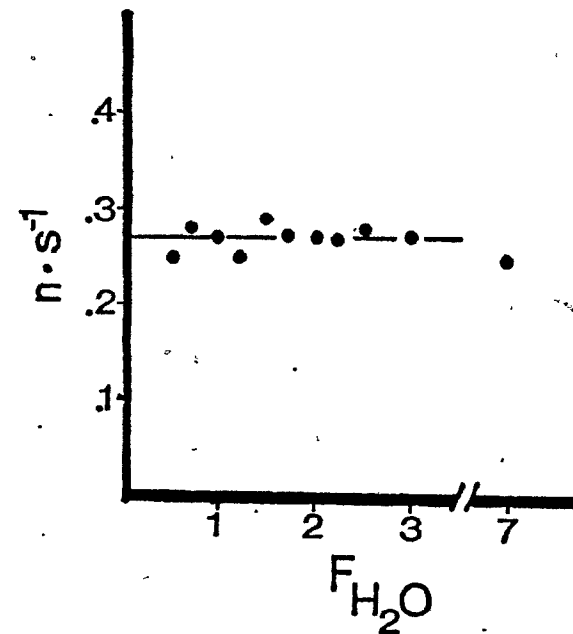


Figure 4-10. Relationship of  $n$  to the liquid flow rate ( $F_{H_2O}$ ) for the bubbler B.

little effect on  $n$  and  $V_B$  over the range investigated.

The effect of varying  $F_g$  on  $V_B$  and  $n$  is shown in Fig. 4-11 and 4-12. These results are for two positions of the bubble needle,  $E = 0.4$  and  $E = 0.8$  cm. The bubble frequencies and volumes are in the desired ranges discussed in the presentation of Snyder's equation and Tables 4-1 and 4-2. The effect of varying needle position,  $E$ , is shown in Fig. 4-13 and shows that  $E$  affects  $n$  insofar as for  $E$  less than 0.5 cm,  $n$  is independent of  $E$  and for  $E$  greater than 0.5 cm,  $n$  is dependent on  $E$ . Thus the bubbler has some adjustability and can be operated at either low (less than 0.5 cm) or high (greater than 0.5 cm) frequency.

For  $E$  in the range 0.8 cm, the bubble volume  $V_B$  is seen to be in the range  $1-2 \times 10^{-3} \text{ cm}^3$ . This range corresponds to the optimum  $V_B$  for c.f.a. reactor tubing of diameter 0.1 cm. Furthermore, this diameter tubing was found to be well suited for the specific c.f.a. developed here as will be shown in the following sections.

The optimum bubble rate ( $n$ ) depends on many parameters but the range of  $1-10 \text{ sec}^{-1}$  covers the usual optimum range for p.c.r. work. Thus the bubbler used here was well suited for use in the c.f.a. system. As will be seen, a significant amount of dispersion in the c.f.a. occurs due not to bubbling or extended reactor delay times, but rather to sources not accounted for in Snyder's equation. These other sources of

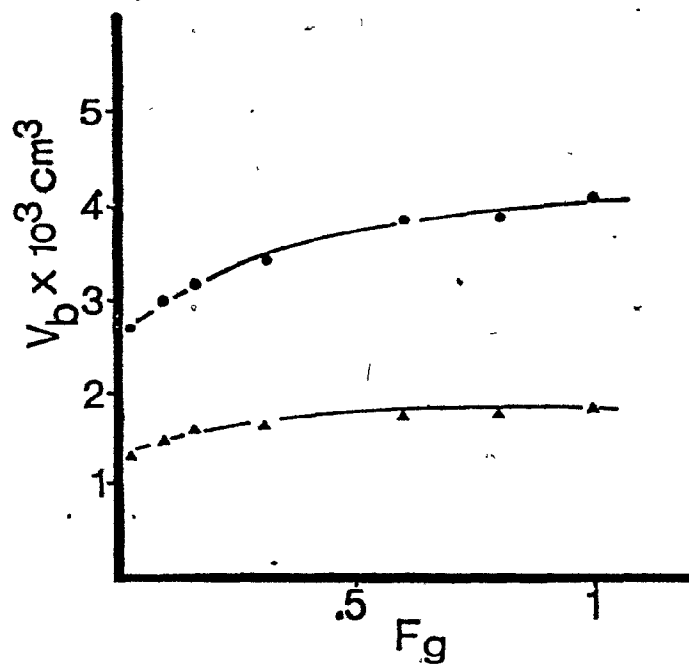


Figure 4-11. Affect on  $V_b$ , the bubble volume, of variations in  $F_g$ , the injected gas flow rate.  $E = 0.4 \text{ cm}$  (•) and  $0.8 \text{ cm}$  (Δ).

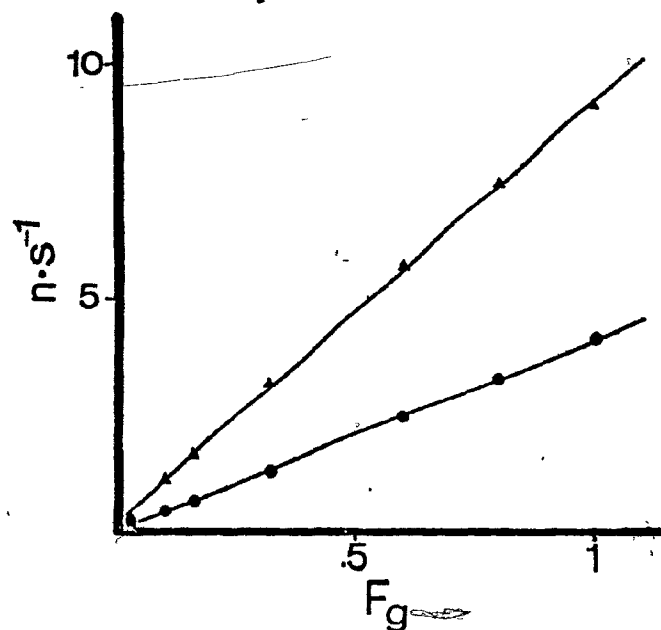


Figure 4-12. Affect on  $n$ , the bubble frequency, of variations in  $F_g$ . Data is taken from the same set as in Figure 4-11.  $E = 0.4 \text{ cm}$  (•),  $0.8 \text{ cm}$  (Δ).

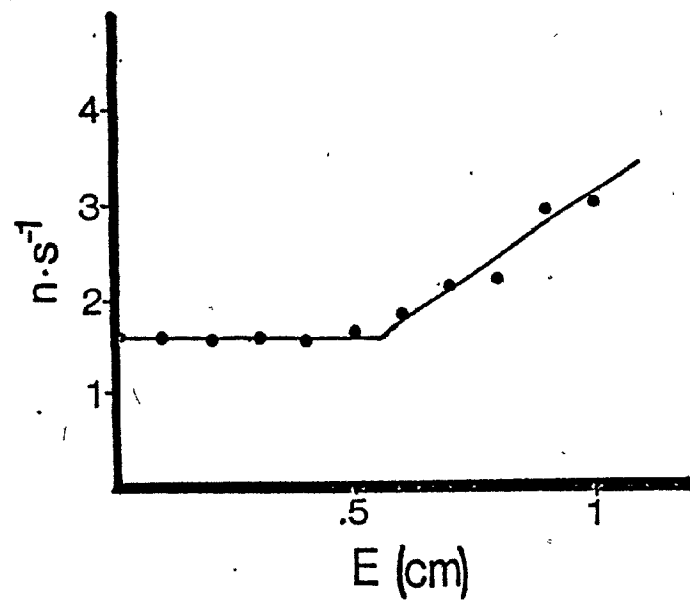


Figure 4-13. Affect on  $n$  of varying needle position  $E$ .

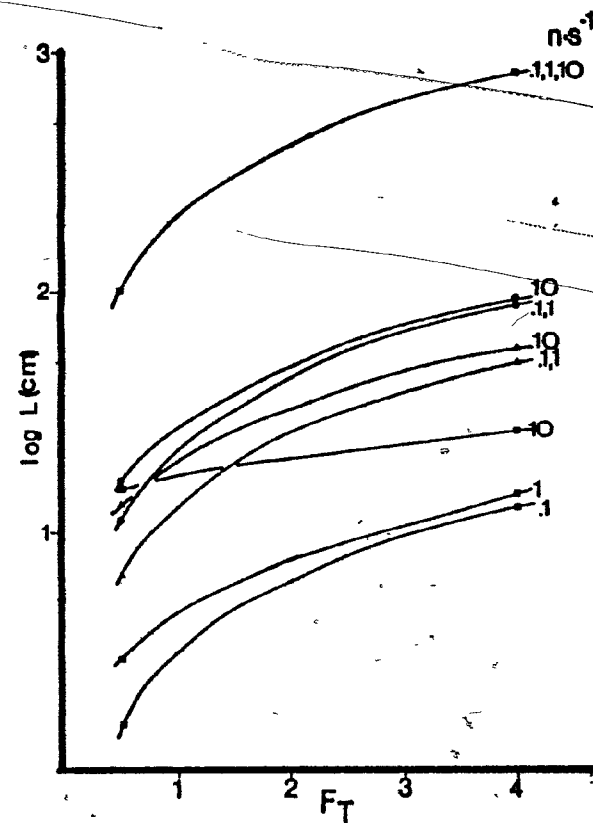


Figure 4-14. Calculated DC ( $L$ ) as a function of total flow rate ( $F_T$ ) for 0.20 (■), 0.10 (▲), 0.76 (●) and 0.025 (□) cm I.D. tubing at the bubble frequencies ( $n$ ) shown.

dispersion are the connecting tubing and the debubbler-detector connection dead volume, which are discussed in the following section.

#### 4.2.2.2 Ancillary tubing and some pressure considerations

##### Connector tubing ( $C_T$ )

This tubing is used to make connections between components of the c.f.a. and the peristaltic pump. Except for the case of the bubbler, the only requirement of this tubing is that it exhibit chemical inertness and be of low dead-volume, an aid when changing composition of the reagents. A 0.159-cm O.D. and 0.076-cm I.D. Teflon tubing was used for  $C_T$ .

##### Reactor tubing ( $R_T$ )

This tubing is used to make connections between on-line components of the c.f.a. where no segmentation occurs and thus must be of low dead volume as well as be chemically inert. The band broadening associated with connecting tubing has been described (38). The connections between the sampler (h.p.l.c.) and bubbler as well as debubbler and detector were made using 0.159-cm O.D., and 0.0254-cm I.D. Teflon tubing and were held in place with standard Swagelok<sup>®</sup> stainless steel ferrels and compression nuts.



### Pump tubing ( $P_T$ )

This tubing was specialized and matched the peristaltic pump being used. For a constant speed multi-channel pump, changes in tube interior diameter are used to vary the flow rate of a given channel. For instance, Table 4-3 shows the various diameters, nominal flow rates and measured flow rates for the  $P_T$  used in this work. The flow rates are expected to vary  $\pm 5\%$  between tubing.

In addition to a characteristic interior diameter, pump tubing also exhibits different chemical properties. Commonly used tubes are made of heavily plasticized polyvinyl chloride, polyurethane or silicon. Their physical and chemical properties have been reviewed elsewhere (39). For this study one of the major problems associated with using the post-column reactor was finding the proper pump tube for the reagents being pumped. It was found that all solutions containing acetonitrile required silicon pump tubing. Other reagents were pumped with the polyvinyl chloride pump tubing. All tubing was purchased from Technicon Corp. (Tarrytown, New York) for use on the peristaltic pump (PP), the Technicon Pump III, used during the course of these studies.

### Delay coils (DC)

The requirements of a delay coil are that it shows:

Table 4-3: Color code, reported (manufacturers) delivery rates and measured delivery rates for  $P_T$ .

Color Code	I.D. (cm)	Nominal Delivery Rate (mL/min)	Measured* Delivery Rate (mL/min)
orange-red	0.019	0.05	0.03
orange-yellow	0.051	0.21	0.16
orange-white	0.064	0.30	0.23
orange	0.089	0.49	0.42
white	0.102	0.66	0.60
red	0.114	0.83	0.80
gray	0.130	1.00	1.00
purple	0.206	2.44	2.50

\* Measured using a 5 mL volumetric flask and stop-watch.

- 1) Chemical and thermal inertness.
- 2) Hydrodynamic compatibility with the moving stream (i.e. wet ability).
- 3) Mechanical properties assuring easy handling.
- 4) Proper diameter ( $d_t$ ) for minimum band broadening.
- 5) Proper total volume for sufficient delay time at the reagent flow rates being used.

Of all the materials tested (Teflon, Polyvinyl chloride, polyethylene, glass and stainless steel 316) stainless steel was found to be the most useful and fulfilled requirements 1-3. One of the limitations of stainless steel was the relative incompatibility of this material with halides but otherwise the overall chemical and mechanical properties made it a useful material.

With respect to the choice of proper diameter and volume of the delay coil referral to the work of Snyder (section 4.2.1.2) was of aid, but only when considered in the context of the practical aspects of choosing reactor tubing. The overall flow balance of the c.f.a. is

$$F_T = F_R + F_g \quad (4-9)$$

where  $F_R = \sum F_{Rn}$  and  $F_T$ ,  $F_g$  and  $F_{Rn}$  are the total, gas and individual reagent flow rates, respectively. By substituting Eqn. (4-5) into Eqn. (4-9) and also allowing for the reaction

delay time to determine  $F_T$ , the resulting expression is

$$\frac{\pi d_t^2 L}{4t} \geq F_R + \frac{7\pi}{24} d_t^3 n \quad (4-10)$$

and thus

$$L \geq \frac{4tF_R}{\pi d_t^2} + (7/6) d_t n t \quad (4-11)$$

where  $t$  is the required reaction time. When  $L$  was evaluated for the wide ranging conditions of:

$d_t = 0.0254, 0.761, 0.10,$  and  $0.20$  (cm, all commercially available).

$F_R = 0.0083, 0.017, 0.033,$  and  $0.0667$  mL·sec<sup>-1</sup>.

$t = 60$  sec.

$n = 0.1, 1.0, 10.0$  (sec<sup>-1</sup>).

The results, shown in Fig. 4-14, allowed judgement on which conditions were practically attainable. For instance, using the tube size 0.025 (0.010" I.D.) at a  $F_T$  of 1 mL/min requires a minimum of 20 meters of reactor tubing for 60 sec of delay time. This length of tubing is not practical for use in a c.f.a. The diameter tubing of practical usefulness as well as having moderately narrow interior diameter for band broadening is either the 0.05- or 0.1-cm I.D. tubing.

The 0.1-cm tubing allows more flexibility in choice of  $F_T$ ; the relatively high flow rate of 4 mL/min required only 4 meters tubing for 60-sec delay.

#### Some pressure considerations

Back pressure considerations are important with respect to the action of the peristaltic pump (PP) and the bubbler (B). Using the Waters 6000A pump and a strip-chart recorder connected to the output of the pump's pressure transducer allowed measurement of the back pressure developed when distilled water (22°C) was pumped through various tubing diameters and lengths. The results, presented in Table 4-4, were derived from plots of back pressure developed in 3-m segments of the tubing over the range 0.5-9.0 mL/min. Linear relationships were seen between length of tubing and pressure drop recorded. The results indicate that 0.1-cm I.D. tubing has low enough pressure drop to be useful over a wide range of conditions.

The tubing used for the DC of the c.f.a. was 0.10-cm I.D., 0.159-cm O.D. (standard 0.030" I.D., 1/16" O.D.) stainless steel 316 tubing. The coil diameter of the tubing was 1 cm as measured from the exterior of the tubing.

Table 4-4: Back pressure associated with various internal tube diameters of some commercially available stainless steel tubing.

Tube I.D. (cm)	$\frac{\Delta P (\text{psi}) \cdot \text{mL}}{\text{M} \cdot \text{s}}$
0.025	100 psi
0.076	~ 10 psi
0.170	~ 5 psi

#### 4.2.2.3 Ancillary equipment, pull-through and the segmentation gas

##### Proportioning pumps (PP)

For the low-pressure application of c.f.a. a linear peristaltic pump, Technicon Pump III, (leased from Technicon Instrument Corp. Tarrytown, New York, 10591) capable of delivering 23 flow channels in the flow range 0.015 to 3.90 mL/min/channel was used. This pump came equipped with an air bar used to synchronize the bubbler with lift-off of the pump rollers but was not used in the application described here. Also, the pump runs at two speeds, normal for reagent delivery and a pre-timed fast for wash out of the c.f.a. When the system was shut down the c.f.a. was washed out with distilled water using the fast cycle. The entire system was periodically washed with 10% nitric acid solution.

##### Tees (T)

The requirements of the tee connectors were that they enable different liquid streams to merge without disruption of the bubble segmentation pattern or excessive band broadening of sample. The stainless steel Tee connector used for the bubbler (standard SwageLok<sup>®</sup> design) was also used for all other tee junctions. The advantage in this was that all connections were made with standard material of low dead volume capable of withstanding high temperature and pressure (8,000 psi max).

### Pull-through (PT)

The pull-through was used in conjunction with a debubbler and was required to sample the c.f.a. segmented stream. The main requirement was that the maximum PT be attained while still enabling the debubbler to reject bubbles. This value for maximum PT is normally taken (36) as having a value of  $0.7 F_T$ .

The PT must, however, be adjusted to a particular system. During the course of this study various pull-throughs were utilized (from 0.42 to 1.0 mL/min) depending on the reagent composition of the reactor, and were accomplished by using one channel of the peristaltic pump with appropriate sized tubing.

### Segmentation gas

All reagents and the mobile phase of the h.p.l.c. (sampler, S) were degassed continuously using the helium displacement method. Segmentation was also done using helium. This prevented:

- 1) Dissolution of segmentation gas into the reagent stream.
- 2) Interaction of segmentation gas chemically with the reagent stream.
- 3) Bubble formation in the detector cell due to partial-pressure degassing of the pull-through line.

The final point of preventing micro-bubble formation



in the detector cell will be discussed in detail in a following section. The use of helium was only partially successful in accomplishing this goal.

Helium was sampled directly from the h.p.l.c. mobile phase reservoir since this was a convenient source of the gas presaturated with acetonitrile.

#### 4.2.2.4 The de-bubbler (Db)

Numerous debubbler designs have been proposed (40). In all cases the debubbler was used in conjunction with the pull-through to remove the segmentation gas from the c.f.a. stream just prior to detection. The main function and feature of the debubbler was thus:

- 1) Efficient gas removal with no breakdown.
- 2) Low dead-volume and good purge characteristics.

The debubbler used here, schematically represented in Fig. 4-15, was a standard unmodified stainless steel Swagelok<sup>®</sup> Tee connector such as used in the bubbler and was chosen because it possessed low dead volume and convenient hook-up to the c.f.a.

The normal method of removing excess sample and bubbles from the debubbler is to allow the debubbler waste to flow directly into a waste container. This is not efficient since a different back pressure occurs at the

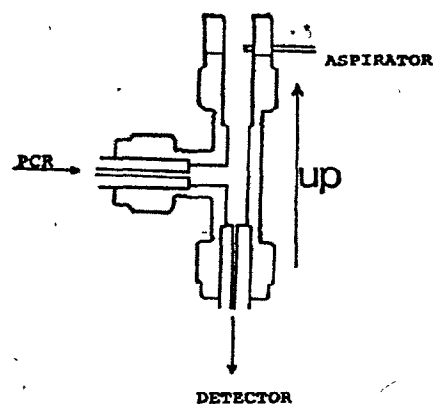


Figure 4-15. Schematic representation of the debubbler developed and used in the study. p.c.r. refers to the rest of the p.c.r., detector refers to either the Schoffel SK770 or PS 970 as well as the direction of flow from the pull through (PT). The aspirator needle removed waste fluid not directed by the PT through the detector.

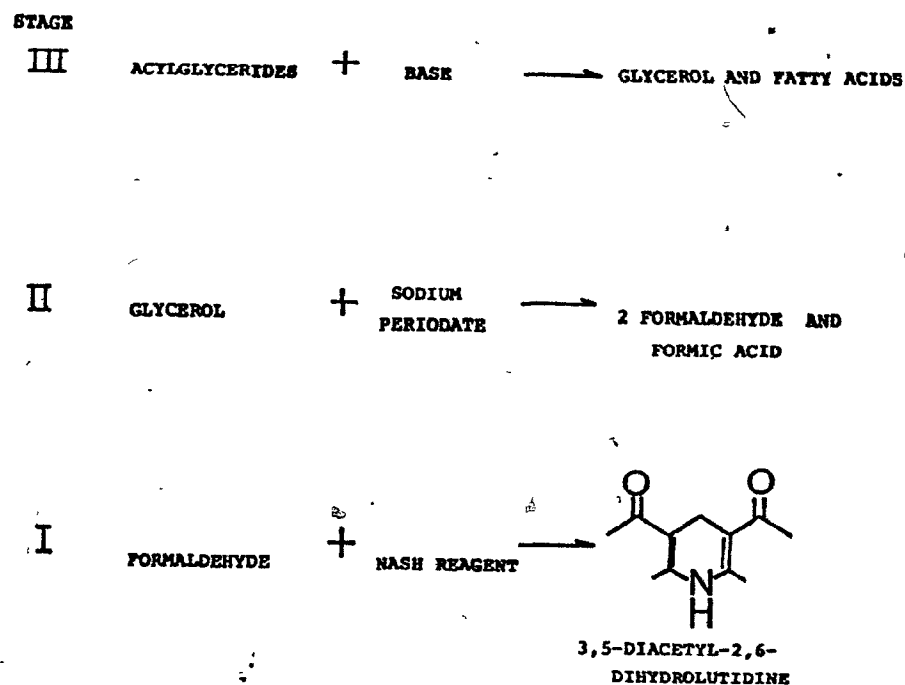


Figure 4-16. Triglyceride analysis using sequential reactions. Details are presented in Table 4-9 and the text. The reversed numbering is used in conjunction with the optimization of the reaction sequence.

debubbler depending on the state of the waste line, positioning of the line with respect to the container, and the level of waste in the waste container. To circumvent all these problems the top of the debubbler was capped with a 1-cm tall piece of Tygon<sup>®</sup> tubing punctured at the base with a needle connected to the peristaltic pump. With this aspiration (2.5 mL/min) the debubbler worked efficiently and independent of the waste line.

The need for a debubbler can be eliminated in certain instances. Alternatives to debubbling are the use of analog electronic debubbling (36,41,42) or digital debubbling (43). In both cases the bubble is allowed to pass through the detector cell but the signal from the bubble is discriminated against and not recorded. Another alternative developed specifically for the application described here is presented in a following section.

#### 4.2.2.5 Sampler (S) and the detector

The sampler used in these studies depended on the application. In Chapter 5 the c.f.a. is evaluated for use as a p.c.r. and thus the h.p.l.c. system used in Chapter 2 was used. For optimization of the analyzer, the PP was used to aspirate sample into the c.f.a. in a fashion identical to reagent addition. Another sampler system used the Waters

6000A pump and UK6 injector (Section 4.3.4) for sample addition. This was used in an application ancillary to the c.f.a. and involved f.i.a.

The detector used in these studies also depended on the application. When high sensitivity was required, the Schoffel FS970 spectrofluorimeter was used. For applications requiring low sensitivity the SF770 spectrophotometer was used. Often both detectors were used in series to check each others' operation. These detectors are described in detail in Chapter 5 and are identified here when used.

#### 4.3 THE CHEMISTRY OF THE POST-COLUMN REACTOR SYSTEM, STAGE I

The general reaction steps required to quantitate triglycerides and phospholipids is presented in Fig. 4-16, where the following occurs:

##### Stage.

- (III) Saponification of the triglyceride to glycerol.
- (II) Oxidation of glycerol to formaldehyde.
- (I) Chromophore development based on formaldehyde.

A summary of the conditions used for triglyceride analysis by eight of the more widely cited papers dealing with this method is presented in Table 4-5. The concentrations presented are not those reported in the original references

Table 4-5: Summary of the experimental conditions used by various authors to determine triglycerides.

Extraction Solvent <sup>1</sup>	III <sup>2</sup> Reagent	Solvent <sup>1</sup>	II Conc. NaIO <sub>4</sub>	Solvent <sup>3</sup>	Conc. 2,4-pent. I	Conc. NH <sub>4</sub> Ac	Temp. (C) <sup>4</sup>	Det. (F) or (A) <sup>5</sup>	Auto. or Man.	Comment	Ref.
1. I	0.29M KOH	I	0.025M	A	0.025M	0.7M	50	F	A	original system, see refs. 1 & 2	3
2. C-M	0.4M KOH	E	0.0045M	S	0.72M	1.0M	V	A	M	procedure incomplete	44
3. IN	0.084M NaOMe	I	0.0074M	A	0.09M	0.05M	50	F	A	Reagent I is used after 1 h and within two days	45
4. IN	0.012M KOH	I	0.003M	A	0.0005M	0.37M	50	F	A		46
5. IN	0.0028M NaOMe	H <sub>2</sub> O	0.005M	H <sub>2</sub> O	0.017M	0.44M	50	F	A		47
6. IN	0.05M NaOEt	I	0.001M	S	0.0025M	1.5M	60	A F	M	Reagent I is used within 1 h	48
7. IN	$\frac{1}{2}$ SAT'D NaOMe	IN	0.014M	A	0.10M	1.6M	RT	A	A		49
8. IN	0.05M KOH	E	0.017M	H	0.035M	1.0M	60	A	A		50

<sup>1</sup>I = isopropanol, n = n-nonane, E = ethanol and C-M = HCCl<sub>3</sub>-MeOH.

<sup>2</sup>All molarities are given as concentrations of the reagent described in the reaction mixture.

<sup>3</sup>A = acetic acid, S = sulfuric acid, H = hydrochloric acid.

<sup>4</sup>RT = room temperature, V = varied with each step.

<sup>5</sup>F = fluorescent detection at  $\sim \lambda_{410}^{410}$ , A = absorbance at  $\sim \lambda_{400-420}^{410}$ .

but derived by multiplying the reported values by a dilution factor that accounts for the different reagent and total reactor flow rates reported. All concentrations are thus directly comparable.

The following trends are discernable from Table 4-5 and the original references:

1) Extraction methods have been favored over column techniques for separating triglycerides from phospholipids. Isopropanol-n-nonane is efficient in separating these neutral lipids from the polar phospholipids, which remain in a dilute sulfuric acid layer.

2) Saponification and transesterification have been used for hydrolysis, the conditions being variable involving a variety of reagent-solvent combinations.

3) Oxidation has always been accomplished with sodium periodate in acidic medium. The periodate concentration ranges from  $1 \times 10^{-3}$  to  $2.5 \times 10^{-2}$  M.

4) Chromophore development utilized the Nash reagent in a wide range of concentrations of 2,4-pentanedione ( $5 \times 10^{-4}$  - 0.72 M) and high concentrations of ammonium acetate (0.44 - 1.6 M). Also, many observations on the stability of the Nash reagent were reported. While it was normally observed that the reagent was usable for one week after preparation, in one case (45) the reagent was discarded after 2 days, in another after 1 h (48).

All work emphasized developing a method having wide linear range with particular emphasis on extending the upper rather than lower range of the method. This is because only high concentrations of triglycerides in serum have clinical significance.

The chemistry of the p.c.r. was investigated in two stages. First, alternative chromophore developing agents were studied to increase the efficiency of stage I of the reactor. Then stages II and III were investigated to determine the optimum reagent compositions and concentrations. All stages were then joined and optimized with respect to one another by a novel method developed for this study. The total (chemistry and hardware) is evaluated in the next chapter.

#### 4.3.1 The Chromophore Developing Reagents

##### Introduction

Reagents for formaldehyde, a major constituent of combustion gases and polluted air (51), are of general interest because of the significant irritation (52-54) and recently discovered carcinogenic (55-57) properties of this aldehyde. The latest recommendations on formaldehyde concentration are for the "lowest practicable concentrations in indoor residential air" (57). Thus, this topic is of

significant contemporary interest as well as being of interest from the standpoint of detecting phospho- and acyl-glycerides. Also, since many other classes of compounds such as carbohydrates can be converted to formaldehyde by oxidation (58-61), this reagent would be of interest for use in either bench methods or in a p.c.r. for h.p.l.c. detection of other presently poorly quantifiable compounds.

The colorimetric and fluorometric methods for detecting formaldehyde have been comprehensively reviewed in a recent series (62). The method of Nash (63) and the more recently introduced method of Sawicki and Carnes (64,65) both enable formaldehyde detection under relatively mild reaction conditions. They are related since both involve a condensation reaction between formaldehyde and a reagent consisting of a 1,3-diketone and ammonium acetate. In the Nash method, based on the Hantzsch pyridine synthesis (66,67) formaldehyde reacts with a reagent consisting of 2,4-pentanedione and concentrated (approximately 2 M) ammonium acetate. The chromophore developed is 3,5-diacetyl-2,6-dihydrolutidine, which also exhibits fluorescence (68). The method of Sawicki and Carnes (63,64) uses dimedone (5,5-dimethyl-1,3-cyclohexanedione) or 1,3-cyclohexanedione as the 1,3-diketone. The reaction of formaldehyde, cyclic 1,3-diketone and ammonium acetate was first described by Vorländer (69-71).

Dimedone (as the Vorländer reagent (71-73)) or



1,3-cyclohexanedione (74) has also been used for the gravimetric analysis of formaldehyde (with no ammonium acetate present) and was at one time the only reliable method for quantitating formaldehyde. The reagent was also used as a spot test for aldehydes after condensation to the aldol product (74) and further oxidation to red or brown compounds. Formaldehyde was also determined by quantitating, amperometrically, excess dimedone indirectly using sodium nitrate as the electrochemically active agent (75). In the original description of the use of chromotropic acid for determinations of formaldehyde in biological samples, Vorländer's reagent was used for standardization and comparison (76). After the introduction of chromotropic acid, colorimetric analysis became more established for formaldehyde determinations but dimedone was still used as an aldehyde trapping agent, after which the aldol derivatives were hydrolyzed under alkaline conditions and the released aldehydes determined with 2,4-dinitrophenylhydrazine (77). With the introduction of gas (78,79) and liquid chromatographic techniques (80-82) the selectivity problems associated with 2,4-dinitrophenylhydrazine have been eliminated. Thus dimedone's use for quantitating aldehydes has declined.

When trying to apply either the reagents of Nash or Sawicki to continuous automated determinations of formaldehyde it was found that they were both unsuitable for

a variety of reasons. Due to the presence of high concentrations of ammonium acetate, high viscosity and poor mixing of the reagent with the other components of the reactor were noticed. Also, long reaction times (up to 30 min) and high reagent background readings made these methods inefficient for the high efficiency continuous flow reactor developed here.

This section deals with the development of a reagent which is selective for formaldehyde and well suited for continuous-flow analysis. The ideal reagent for this application would have the following properties:

- 1) Extremely large reaction rate giving a chromophore which possesses a property that can be selectively detected (e.g. fluorescence, absorbance, etc.)
- 2) Specific for the compound of interest
- 3) Stable as a reagent
- 4) Low viscosity and is easy to mix with other reagents in the systems
- 5) Low background signal.

The reagent developed for use in the reactor was designed to have all of these properties (83,84).

#### 4.3.2 Preliminary Studies: Introduction

These studies involved some classical chemical investigative work on the Nash and Sawicki reagents. First,

the reactions of some 1,3-diketones, ammonia and formaldehyde were investigated. Then high sources of background in the Nash reagent was followed. Then the reagents of Nash and Sawicki were studied using thin-layer chromatography for clues to their mechanism of reaction with formaldehyde. Alternate 1,3-diketones were investigated because of the observation that the product of the Sawicki reagent was 100 times more fluorescent than the Nash reagent product (64).

The Nash reagent was investigated for sources of background contamination since one of the striking features of the reagent was its color. When an old sample of 2,4-pentanedione (Baker analyzed, source 3) was added to 2 M ammonium acetate solution, the diketone dissolved to give a yellow solution. The compound responsible for this yellow color was indicated by thin-layer chromatography (t.l.c.) to be the product of the reaction of condensation with formaldehyde (yellow in color with green fluorescence) and thus a large source of formaldehyde contamination was present in the reagent. Another feature of the reagent was that the diketone was seen to be insoluble in water but soluble with heating in ammonium acetate solution. It is well known that 2,4-pentanedione reacts with ammonium hydroxide or ammonia gas to form the ammonium 2,4-pentanedionate which then undergoes internal reaction to 4-amino-3-penten-2-one (85,86). Thus it was thought that the Nash reagent was simply

a more tedious synthetic route to this product and that all of the reagents containing 1,3-diketone and ammonium acetate had as their active forms the iminodiones.

#### 4.3.2.1 Experimental

The reactions of the 1,3-diketones (0.1 M in methanol, 1.0 mL):

- 1) 2,4-pentanedione.
- 2) Dimedone (5,5-dimethyl-1,3-cyclohexanedione).
- 3) 1,3-Cyclohexanedione.
- 4) 1,3-Cyclopentanedione.
- 5) 1,3-Cyclopent-4-enedione.

(all purchased from Aldrich Chemicals Co., Milwaukee, Wis.) with 2.0 M ammonium acetate (1.0 mL in H<sub>2</sub>O) and 36% formaldehyde (100  $\mu$ L) were run in a fluorescence cell and the fluorescence monitored. They were also followed by thin-layer chromatography (silica coated plates, ethyl acetate: methanol mobile phase).

These reactions were investigated further by t.l.c. and preparative syntheses:

- 1) The reaction involving 2,4-pentanedione was run as described by Erikson and Biggs (87). When monitored with thin-layer chromatography this reaction gave one fluorescent product ( $R_f$  0.85 in chloroform, methanol, ammonium hydroxide

1/1/1, on silica plates) yield 90% and m.p. 204-205°C (c.f. 201-205°C (87)) after recrystallization in methanol.

2) The reaction involving dimedone was run using the procedure of Sawicki and Carnes (64): to 7 g dimedone dissolved in 20 mL ethanol was added 38.5 g ammonium acetate and 20 mL glacial acetic acid diluted 1/1 (v/v) with water. After heating to 80°C rapid addition of 2.1 mL 36% formaldehyde gave a white precipitate which when isolated was found to be 2,2'-methylene-bis-(5,5-dimethyl-3-amino-cyclohex-2-en-1-one), in almost quantitative yield (m.p. 241-242°, c.f. 242° (88)). With dropwise addition of formaldehyde the fluorescent product was isolated in 10% yield, m.p. 298-230°C (c.f. 296-297° (70)) after recrystallization in acetone.

3) 1,3-Cyclohexanedione (5.6 g) replaced dimedone in (2). Rapid addition of formaldehyde gave a precipitate of clear crystalline sheets with m.p. 130-133°C. When formaldehyde was added dropwise the fluorescent product was isolated, m.p. greater than 300°C, yield 20%.

4&5) The reactions involving the cyclopentane- and pentenediones went as followed with t.l.c., to a very small extent and with low yields which were not isolated.

For the background studies 2,4-pentanedione was purchased from the following sources:

1) Sigma Chemical Co. (St. Louis, Mo., USA), two grades, one reagent (A3511) and the other their special grade

(405-4) for triglyceride analysis.

2) Fisher Scientific (Fairlawn, NJ, USA) Reagent chemical 761510.

3) "Baker Analyzed" (J.T. Baker Chemical Co., Phillipsburg, NJ), Reagent 99.0%.

4) Aldrich Chemical Co. (Milwaukee, Wis.), Gold Label 99+%.

These were assayed for fluorescence background by adding 5  $\mu$ L of the respective 2,4-pentanedione to 2.0 mL 2 M ammonium acetate. After 30 min the fluorescence (excitation 410 nm, emission 510 nm) of the solution was measured.

The investigation of the condensation reactions involved addition of 1,3-diketone to 2 M ammonium acetate and then heating to 80°C for 24 h while periodically monitoring, using thin-layer chromatography, the reaction mixtures. Thus to 20 mL 2 M ammonium acetate (in 50/50 v/v H<sub>2</sub>O/methanol) was added either 1 mL of 2,4-pentanedione or 1 g of dimedone. After 24 h the starting 1,3-diketones were not detectable by the chromatographic process but a new major and many minor bands were observed. When an aliquot of the reaction mixture was treated with a drop of 36% formaldehyde, chromophore development was immediately evident by the color change and thin-layer chromatography showed that the original major product band was no longer present. Also, when the developed thin-layer plates of the reaction mixtures

were sprayed with a dilute formaldehyde solution the band comprising of the major product of the 1,3-diketone and ammonium acetate became fluorescent.

#### 4.3.2.2 Results and discussion

The reactions occurring between the 1,3-diketones, ammonia and formaldehyde are shown in Fig. 4-17. Except for case 4, all product structures were confirmed as presented in the following sections. The use of 1,3-cyclopentanedione and 1,3-cyclopent-4-enedione as the basis for aldehyde reagents was abandoned at this preliminary stage; their reactivities were very low.

In the background study, the fluorescence intensities, when compared to a standard curve made up by measuring fluorescence versus concentration of 3,5-diacetyl-2,6-dihydrolutidine in methanol (measured to be stable for at least 7 months when stored in the dark (Appendix 4A)) gave the results shown in Table 4-6. One of the main sources of formaldehyde contamination was thus found to be the 2,4-pentanedione itself. Vorländer (72,73) mentioned that dimedone was easily oxidized to formaldehyde and thus 2,4-pentanedione may also have this property.

The other source of formaldehyde contamination was undoubtedly the ammonium acetate which was present in very

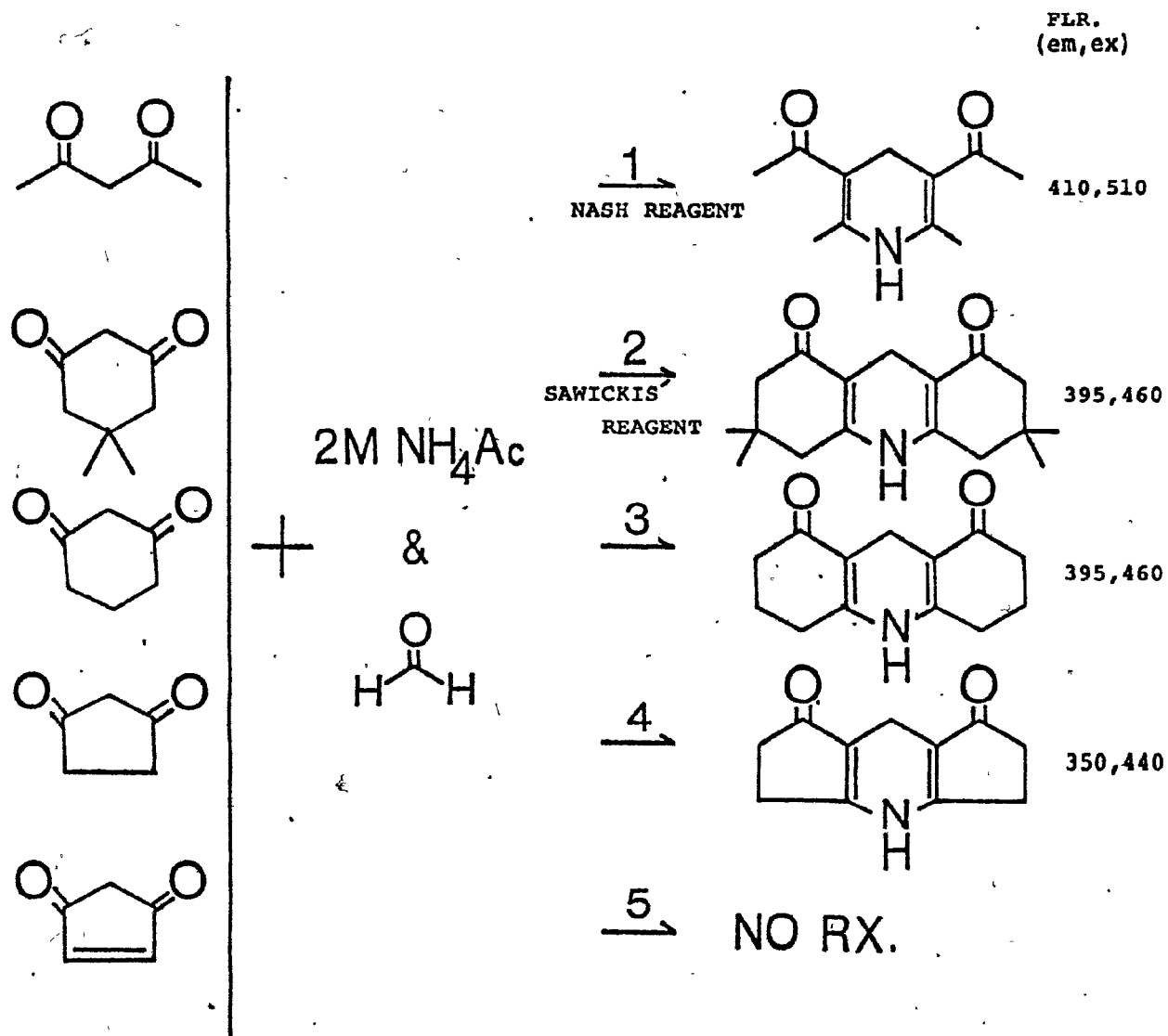


Figure 4-17. Preliminary reactions involving some 1,3-diketones, ammonium acetate, and formaldehyde. Details are presented in the text.



Table 4-6: Lutidine molar equivalence for various sources of 2,4-pentanedione.

Source	Lutidine molar equivalent*
Sigma a) Regular (A3511)	$7.6 \times 10^{-5}$ M
b) Triglyceride (405-4)	$6.7 \times 10^{-5}$ M
Fisher	$1.1 \times 10^{-4}$ M
Baker Analyzed	$8.5 \times 10^{-5}$ M
Aldrich Gold Label	$3.3 \times 10^{-5}$ M

\* Assuming 100% reaction, is equal to the formaldehyde contamination in the system.

high concentrations.

Aldrich Gold Label 2,4-pentanedione was used for the rest of these studies and as a precautionary measure was stored at  $-20^{\circ}\text{C}$  in the dark when not in use.

The t.l.c. studies indicated that there occurred in situ in the formaldehyde reagents a product of ammonium acetate and 1,3-diketone. This product, an iminodione, was most likely the actual agent in the reagents under investigation. Thus a more detailed investigation of the reagents' chemistry was initiated since, if the iminodiones were usable isolated, much of the high blank and mixing problems encountered in the original reagents could be eliminated. The detailed chemistries are described next.

#### 4.3.3 Detailed Studies: Introduction

The chemistry of the Nash reagent was investigated using preparative synthetic techniques and an h.p.l.c. method. This reagent was mentioned as being based on the Hantzsch pyridine synthesis. The mechanism of this reaction was reported as not being well understood just two years prior to Nash's development of his reagent (89). This situation has not improved since then. However, this investigation has relied heavily on previous work (89).

Fig. 4-18 shows the various intermediates and reaction

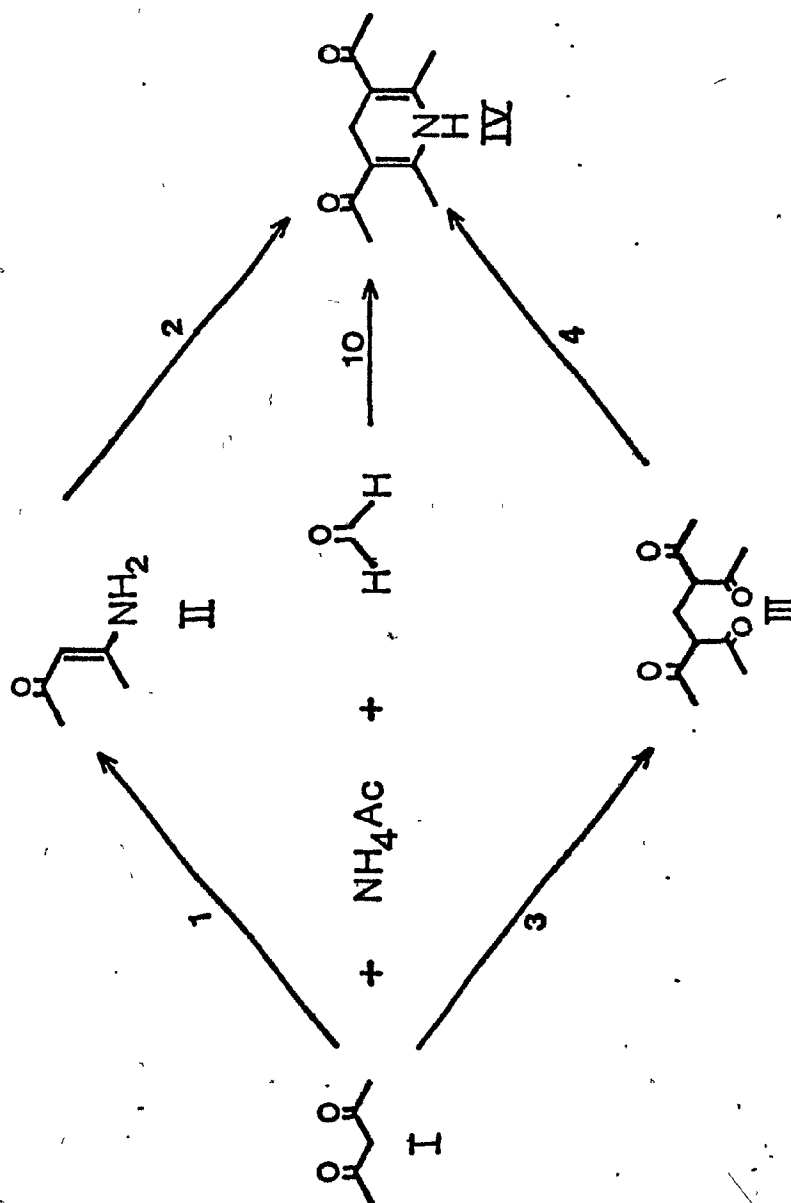


Figure 4-18. Intermediates and reaction paths investigated for the Mash reagent.

pathways which were investigated. In reference to Fig. 4-18 reaction 1 is the reaction of ammonia with 2,4-pentanedione. Reaction 2 is the condensation of two moles of iminodione with one mole of formaldehyde to form the fluorescent lutidine product. Reaction 3 is the reaction of formaldehyde with 2,4-pentanedione to form the bis-methylenedione. Reaction 4 is the bis-methylenedione reacting with ammonia to form the lutidine chromophore.

In order to show that each reaction could occur under conditions of the analytical assay (i.e. conditions of the Nash reagent) the intermediates II and III were synthesized using conditions similar to those found in the Nash reaction. These were then shown to react further to give the lutidine chromophore. Following this, an h.p.l.c. method was developed to quantitate simultaneously compounds II-IV and this procedure was used to further investigate the reactions involved in the Nash procedure.

The study of the Sawicki and Carnes reagent (64) paralleled the study of the Nash reagent and an identical experimental approach was taken. Thus, reactions 5-9 in Fig. 4-19 were investigated as possible pathways for the Sawicki reaction by both synthetic and chromatographic means.

Reaction 5 is the reaction of dimedone with ammonia to form the endogenous iminodione mentioned in the preliminary study. Reaction 6 is the condensation of two iminodiones

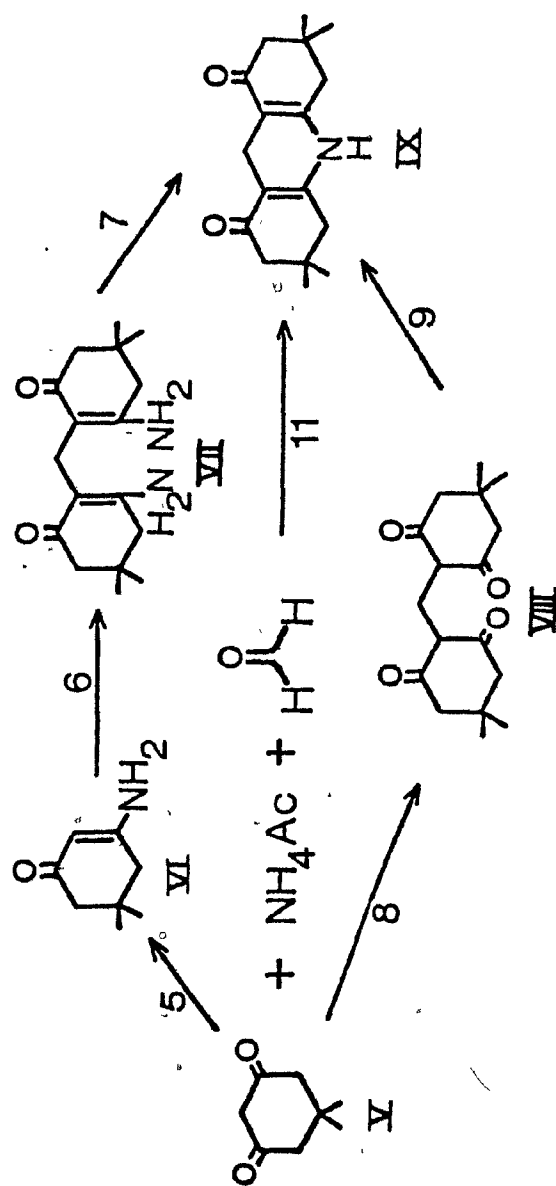


Figure 4-14. The reactions and intermediates found in the Sawicki method.

with formaldehyde to form the compound referred to as the bis-iminodione. Reaction 7 is the acid catalyzed ring closure of the bis-iminodione to form the fluorescent product of the Sawicki and Carnes reaction, here called the acridine-dione. Reaction 8 is the classical reaction of Vörlander, historically used for the gravimetric analysis of formaldehyde. The product, bis-(4,4-dimethyl-2,6-dioxocyclohexyl)methane, is also known as aldol. Reaction 9 is the reaction of aldol and ammonia to form the acridinedione chromophore of the Sawicki reaction.

These reactions have been partly described in various places in the literature (see synthetic procedures, below).

None of the reactions have been previously discussed with reference to the reagent of Sawicki and Carnes nor with reference to the original reactions of Vörlander.

The comparison of the Nash and Sawicki reactions was done by referring to some studies on the pH dependency of the reagents' reaction rates. These are also reported.

#### 4.3.3.1 Experimental

##### Synthetic procedures

Compound I: 2,4-pentanedione was investigated as mentioned in the introduction.

Compound II: 4-amino-3-penten-2-one (Fluoral-P in

the reagent form). Twenty mL of 2,4-pentanedione in 50 mL of 4 M ammonium acetate, pH 5.5, was heated to 80°C for 3 h, extracted into chloroform and vacuum distilled (bulb-to-bulb, 5 mm, 64°C) to give a clear viscous liquid which solidified upon cooling (yield 32%, 5.66 g; m.p. 45°C; recrystallized from ethyl acetate:petroleum ether). Structural assignment was based on chemical (conversion of II to IV with formaldehyde) and spectral data (n.m.r.:  $H_{200MHz}^1$ , D-chloroform;  $\delta$  2.75 (3), 2.87 (3), 5.87 (2), 8.10 (1), all singlets; m.s.: 99.0674- $C_5H_9NO$ ; i.r.: chloroform; 3500 (s), 3120-3440 (b), 3200 (s), 1624 (s), 1597 (s)), and microanalysis C 61.03 (60.61), H 9.30 (9.09), N 14.38 (14.31), theoretical in parentheses.

This compound was also synthesized on large scale (kg) by an alternative route modified from the literature (86). This involved adding cold ammonium hydroxide to cold 2,4-pentanedione with stirring until no more ammonium 2,4-pentanedionate formed. The large amounts of heat given off required that the ammonia was added very slowly and with constant cooling in ice. The ammonium 2,4-pentanedionate was next stirred for 4 h at room temperature. The reaction mixture was then extracted three times with ether and the recrystallized (from cold ether) 4-amino-3-penten-2-one was recovered in 70-80% yield, m.p. 45°C. The recrystallized product was suitable for use as a reagent but vacuum sublimation at room temperature was found to be useful when

sensitive determinations were required.

Compound III: 3,3'-methylene-bis-(2,4-pentanedione). To 1 mL of 2,4-pentanedione in 20 mL of 99% methanol: 1% acetic acid was added 4 mL of 37% formaldehyde. After 10 min of stirring and evaporation, a white crystalline mass was isolated; this was recrystallized from ethyl acetate (yield 89%, 0.923 g; m.p. 140-142°C). Structural assignment was based on chemical (conversion of III to IV with addition of ammonium acetate) and spectral data (i.r.; 3200-3600 (b), 1695 (s); n.m.r.:  $\delta$  1.3 (3), 2.2 (3), 2.6 (1), 3.6 (2), all singlets; m.s. 212, 150, 112, 109, 43 (base)). The melting point data indicate that the di-intramolecular hydrogen-bonded species was isolated since the free and mono-intramolecular hydrogen-bonded species have already been assigned different melting points (90).

Compound IV: 3,5-diacetyl-1,4-dihydro-2,6-lutidine. The method of Erikson and Biggs (87) was used. Also, II was employed by reaction of formaldehyde in pH 2.25 phosphate buffer or III with molar ammonium acetate, pH 6.0, after 30 min of stirring. All products were recrystallized from methanol, m.p. 204-205°, c.f. 200° (63) or 201-205° (87), with yields greater than 90%.

Compound VI: 5,5-dimethyl-3-aminocyclohex-2-en-1-one. The method of Greenhill (88) was used (yield 81%) as well as a method similar to that described for II (yield 27%, m.p.



166.5-167°, c.f. 164-165° (88)).

Compound VII: 2,2'-methylene-bis-(5,5-dimethyl-3-aminocyclohex-2-en-1-one). The method of Greenhill (88) was used. In addition, this compound was isolated whenever attempts were made to convert VI to IX by the rapid addition of formaldehyde (m.p. 241-242°, c.f. 242° (88)).

Compound VIII: Bis-(4,4-dimethyl-2,6-dioxocyclohexyl) methane. The method of Horning and Horning (91) was used (yield 95%). Also this product was isolated when following the synthetic method of Sawicki and Carnes (62) for IX formaldehyde is added at a rate faster than dropwise (m.p. 191-191.5°, c.f. 189-190° (92), 191-191.5° (91)).

Compound IX: 3,3,6,6-tetramethyl-1,2,3,4,5,6,7,8,9,10-decahydro-1,8-acridinedione. The method of Sawicki and Carnes (64) was used and the product was recrystallized from acetone (yield 10%; m.p. 298-301°, c.f. 296-297° (93)). Also IX was synthesized by heating VIII in 2 M ammonium acetate (pH 5.5) for 3 h at 80°C or directly from VI or VII by modifying the alternate method for VII to include overnight heating at 80°C.

#### Chromatography studies

The chromatographic assay used the equipment described in Chapter II except that the normal rather than reversed-phase mode was used. The following conditions were adhered to:

Nash Reagent

Mobile phase: Ethyl acetate:petroleum ether:acetic acid

(59:40:1, v/v/v).

Column: Waters u-Porasil (Waters Associates, Milford, Conn.).

Flow rate: 2 mL min<sup>-1</sup>.

Detector settings: 254, 285 or 410nm.

Injection volumes: 25 µL.

Standard concentration ranges: 10<sup>-9</sup>-10<sup>-6</sup> moles·injection<sup>-1</sup>.

Temperature: ambient.

Sawicki Reagent

Mobile phase: Ethyl acetate:petroleum ether:methanol

(60:40:0.5 v/v/v).

Detector settings: 254 and 397 nm.

Standard concentration ranges: 2 x 10<sup>-9</sup> to 2 x 10<sup>-8</sup> mole·  
injection<sup>-1</sup>.

All other conditions as with the Nash Reagent.

pH studies

The pH dependency of the reaction rate of both reagents for formaldehyde was investigated.

For the reagents, the pH range from 4.3 to 11.3 was investigated by adjusting 1.0 M ammonium acetate to the desired pH using either acetic acid or ammonium hydroxide. The reactions were initiated by addition of 100 µL 1.2 x 10<sup>-2</sup> M

formaldehyde to 2.1 mL  $9.5 \times 10^{-4}$  M 2,4-pentanedione or dimedone in 1 M ammonium acetate solution (23°C). The reaction was monitored by fluorescence at their characteristic excitation and emission wavelengths. Initial rates were measured for each pH run and reported in relative units as the mean of triplicate determinations. The rates were corrected for differences in fluorescence intensity as a function of pH as shown in Fig. 4-20. The rates were normalized such that the maximum rate was given a value of 1.00.

The relative reaction rate dependence on pH between compound II or VI and formaldehyde was investigated and reported in a similar manner. Thus, initial rates were corrected for the difference in fluorescence of the chromophores as a function of pH and reported as normalized to a maximum of 1.00. The reaction conditions were to 1.0 mL of  $4.4 \times 10^{-3}$  M II or VI in methanol was added 1.0 mL of 0.25 M phosphate buffer (sodium salt in the pH range of 2-9) and after mixing, and incubation for 5 min at 25°C, 1.0 mL of  $6.0 \times 10^{-2}$  M formaldehyde in methanol was added. Methanol was used as the solvent to decrease the hydrolysis of the iminodiones (94).

The investigation of reaction 10 was carried out by pre-incubating (either 5 or 30 min) a mixture of 0.1 M 2,4-pentanedione (1 mL in methanol) and molar ammonium

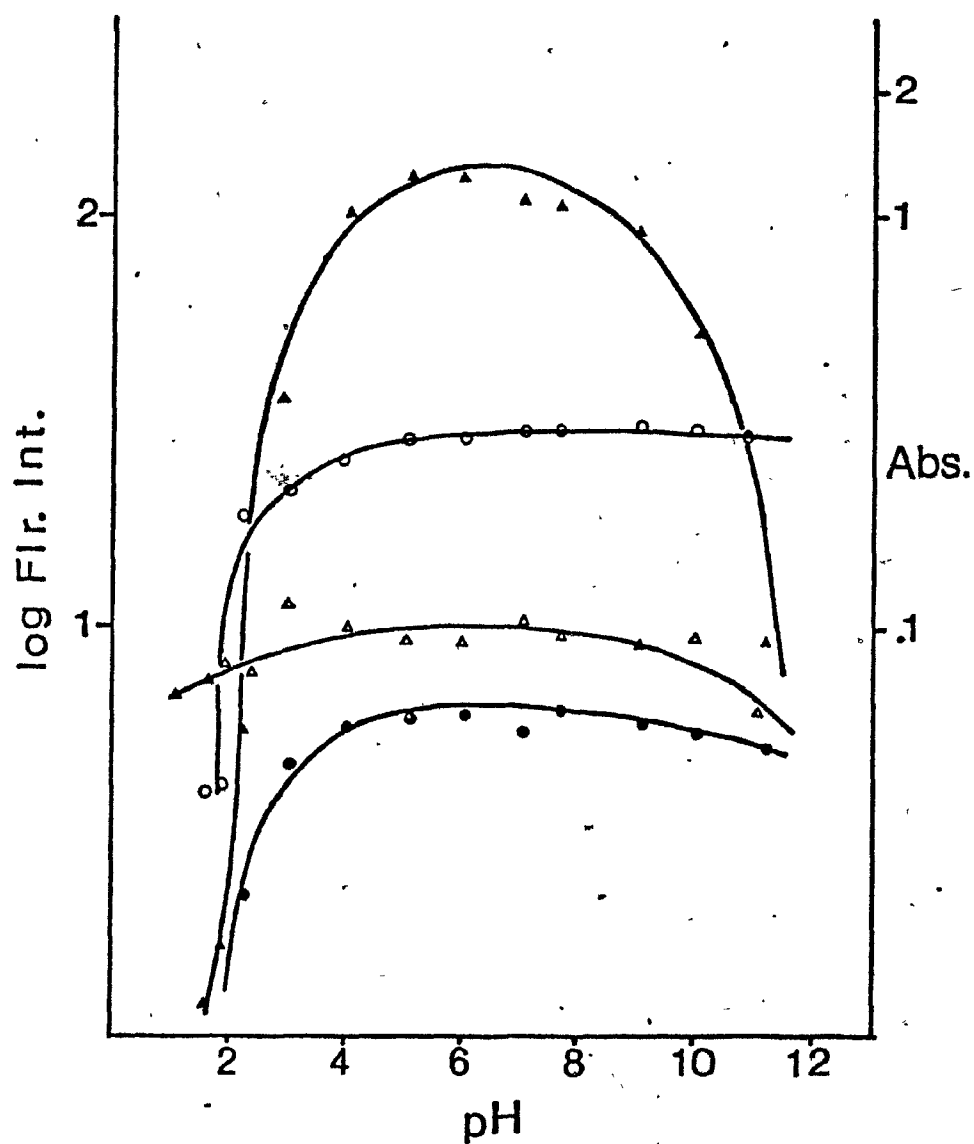


Figure 4-20. Absorbance of IV ( $\Delta$ , 410 nm) and IX ( $\circ$ , 315 nm) and fluorescence intensity of IV ( $\circ$ , 410, 510 nm) and IX ( $\Delta$ , 395, 460 nm) as a function of pH.

acetate (2 mL at pH 5.5) at 22°C and then adding to this 1 mL of  $1.26 \times 10^{-2}$  M formaldehyde. Samples were introduced directly from the reaction mixture into the chromatographic system at the times indicated in Fig. 4-21.

Investigation of the reagent of Sawicki and Carnes was carried out under conditions similar to that used for the Nash reagent except that the reagent concentrations were slightly changed and involved 1 mL of .1 M formaldehyde, 1 mL of 2.0 M ammonium acetate, pH 5.5, and 1 mL of 1.0 M dimedone in methanol. Pre-incubation was carried out for 5 min and after addition of formaldehyde a white precipitate (compound VIII) formed and dissolved during the course of the investigation.

The conversion of VI to IX was studied using 25  $\mu$ L of  $1.0 \times 10^{-3}$  M VI in methanol added to 1 mL of  $1.24 \times 10^{-1}$  M formaldehyde and 1 mL of a 0.5 M phosphate buffer, pH 2.25. The mixture was incubated at 22°C and assayed after 1 h.

#### 4.3.3.2 Results and discussion

One of the main features of the reagents is the difference in fluorescence efficiency of their products IV versus IX as shown in Fig. 4-22. Since the excitation and emission spectra of the two compounds are fairly similar (Fig. 4-23) the response of the fluorometer can be assumed to

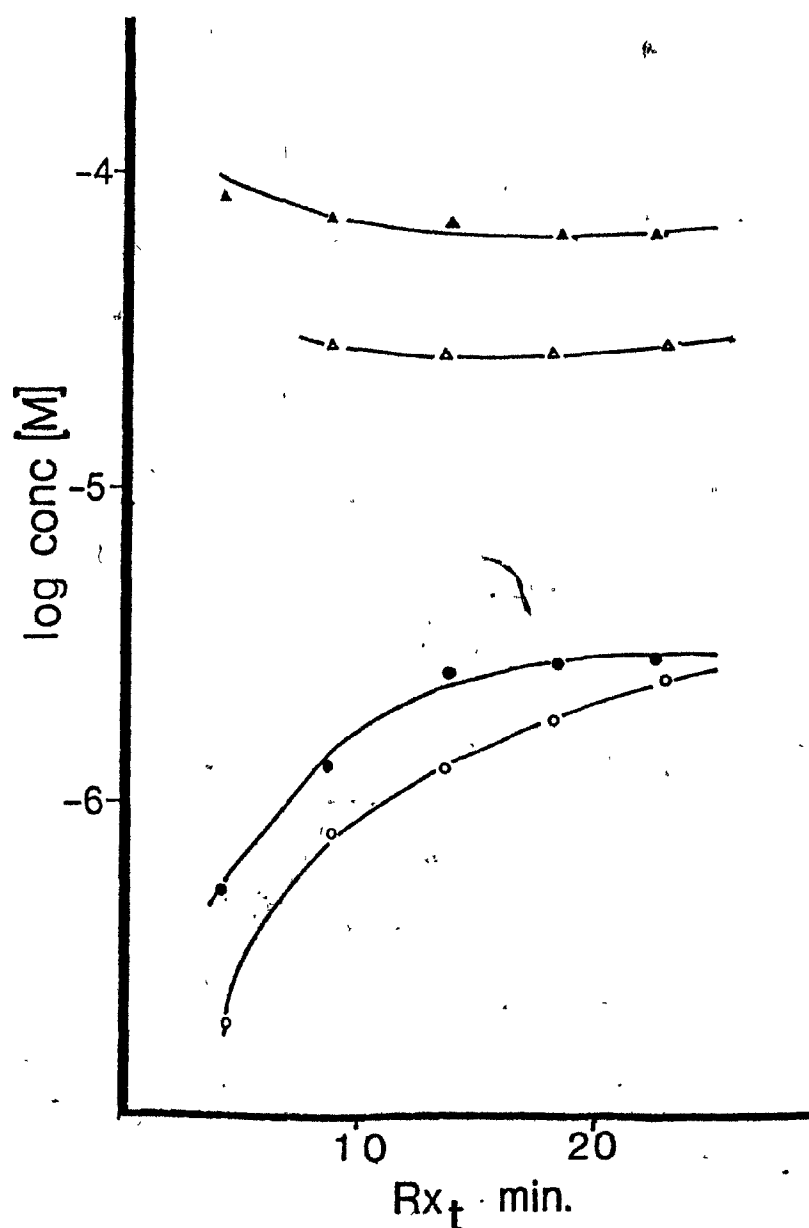


Figure 4-21. Effect of pre-incubation and formaldehyde addition on the concentration of Fluoral-P (II) and the formation of IV. ( $\circ$  = IV, 5 min. incubation time,  $\bullet$  = IV, 30 min. incub.;  $\Delta$  = II, 5 min. incub.,  $\Delta$  = II, 30 min. incub.)

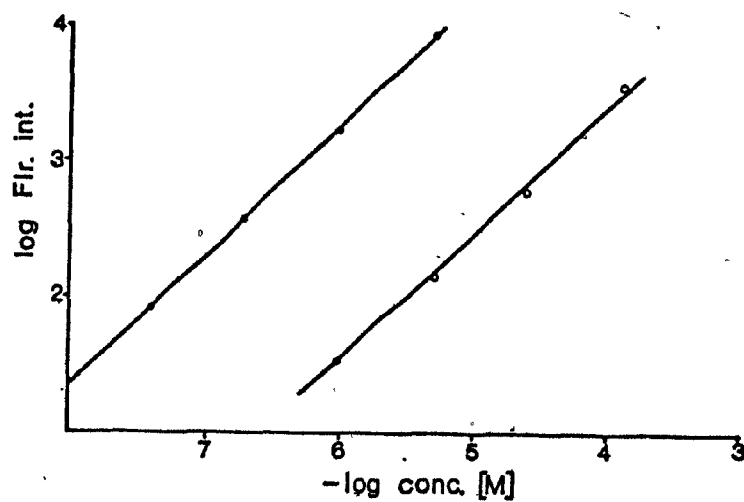


Figure 4-22. Comparison of fluorescence intensity versus concentration for IV (○) and IX (●).

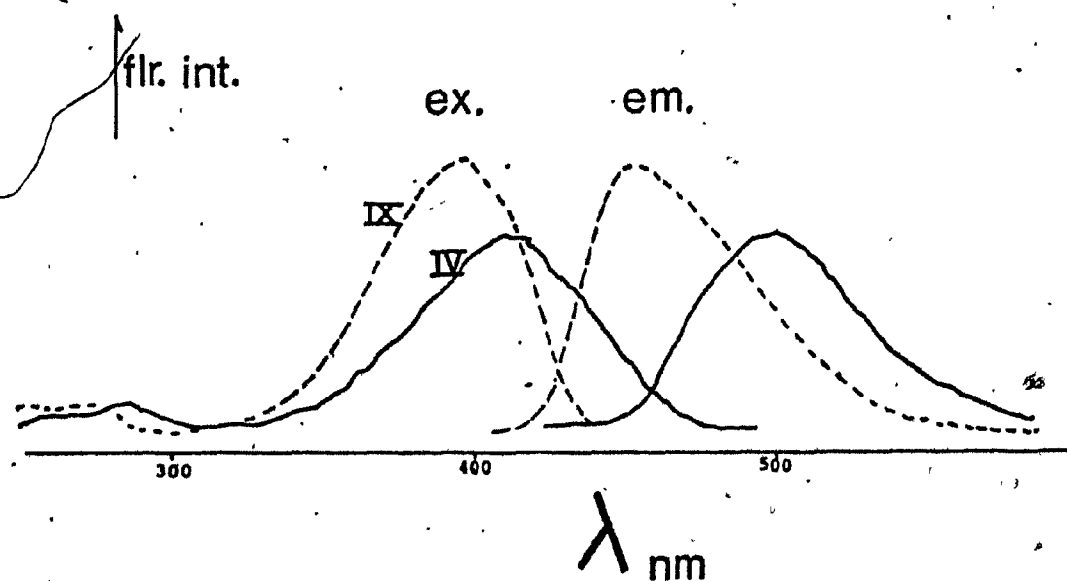


Figure 4-23. Excitation (ex.) and emission (em.) spectra for compounds IV and IX.

be approximately the same for both compounds and the difference in quantum efficiency is such that IX is seventy times more fluorescent than compound IV.

The study on pH versus reaction rate gave the results presented in Fig. 4-24 for the reactions of II or III with formaldehyde. Figs. 4-25 and 4-26, are results for the Nash or Sawicki reagent, respectively, over the pH range 5.0-8.0. Also, hydrolysis data for compound II has been taken from a study on the subject (94), normalized so that the maximum reported rate was given the value 1.00, and plotted along with the reaction data in Fig. 4-25.

Unfortunately, no hydrolysis data for compound VI have been reported; however, inspection of the results of the source of the data on II (94) indicates that the hydrolysis of VI should be similar to II.

The chromatographic retention data are reported in  $k'$  units in Table 4-7. A typical chromatogram of the Nash reagent constituents is shown in Fig. 4-27 as an aid to those interested in determining formaldehyde in complex reaction or environmental samples. Due to the complexity of the reaction mixture, the separation of the Sawicki products was more involved than for the Nash reaction system. However, thin-layer chromatography (retention data shown in Fig. 4-28, using silica glass backed plates) enabled direct extrapolation to the h.p.l.c. system; a representative chromatogram is



Table 4-7: Chromatographic retention data for the intermediates and products of the Nash and Sawicki reagents.

Compound	k'
II	2.3
III	1.4
IV	3.2
V	3.0
VI	6.0
VII	2.0
VIII	0.0
IX	1.5

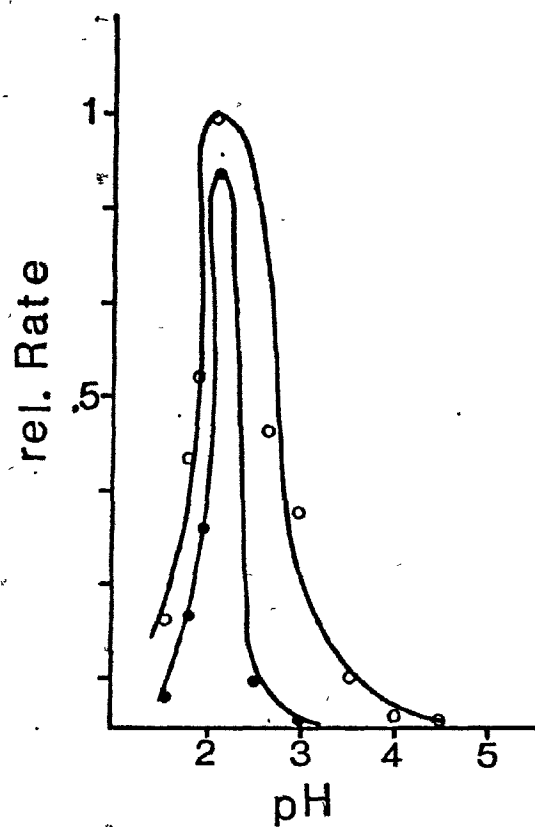


Figure 4-24. Initial reaction rate of the reaction of II (●) or VI (○) with formaldehyde as a function of pH. Results are off-set for clarity.

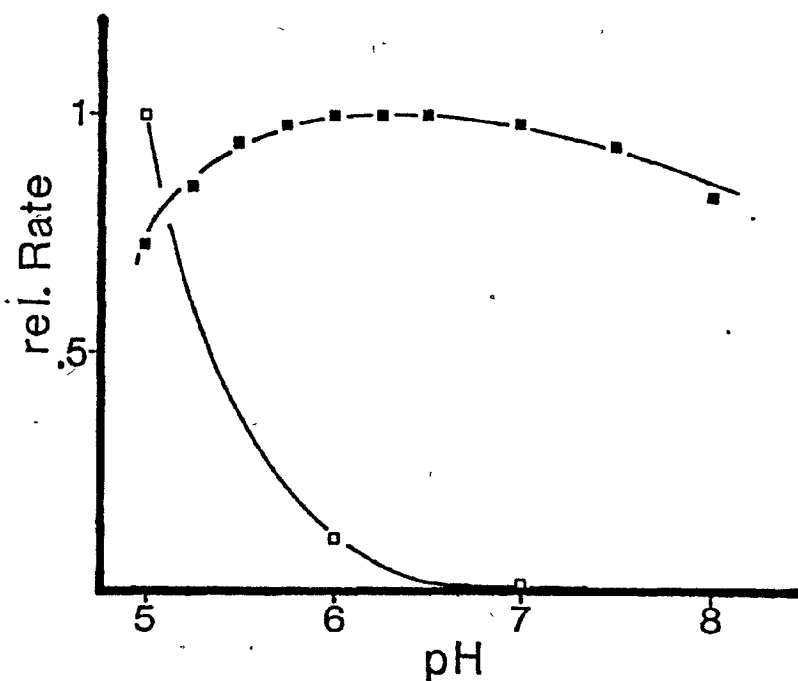


Figure 4-25. Initial reaction rate (■) and rate of hydrolysis (□) for the Nash reagent and compound II, respectively. Hydrolysis data was taken from refer. 14.

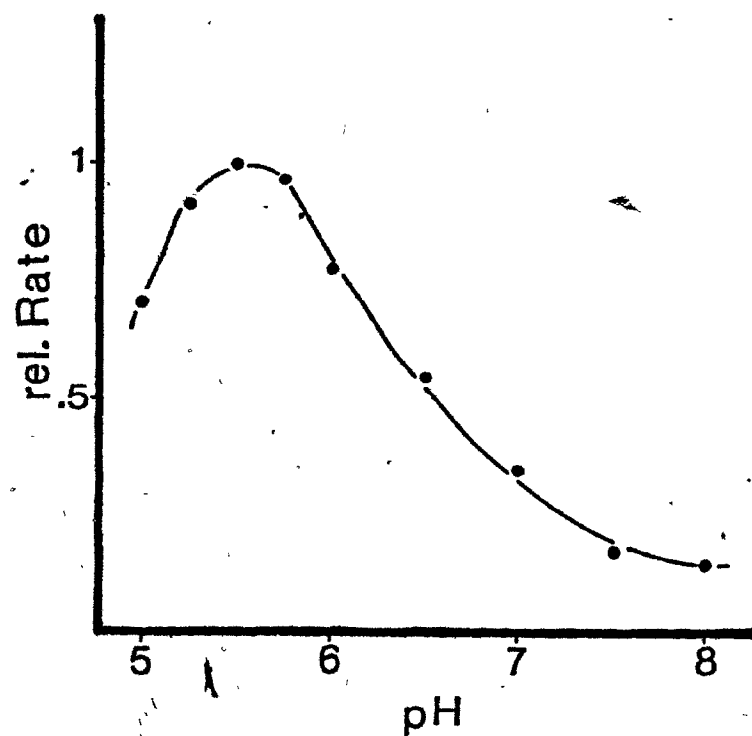


Figure 4-26. Initial reaction rate for the reagent of Sawicki and Carnes as a function of pH.

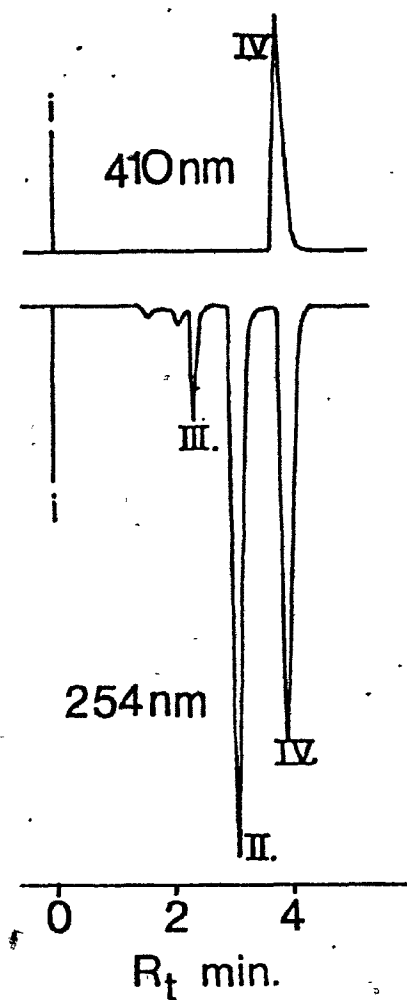


Figure 4-27. h.p.l.c. normal-phase separation of the intermediates (Figure 4-18) of the Nash reagent. (i) indicates sample injection time  $R_t = 0$  min.

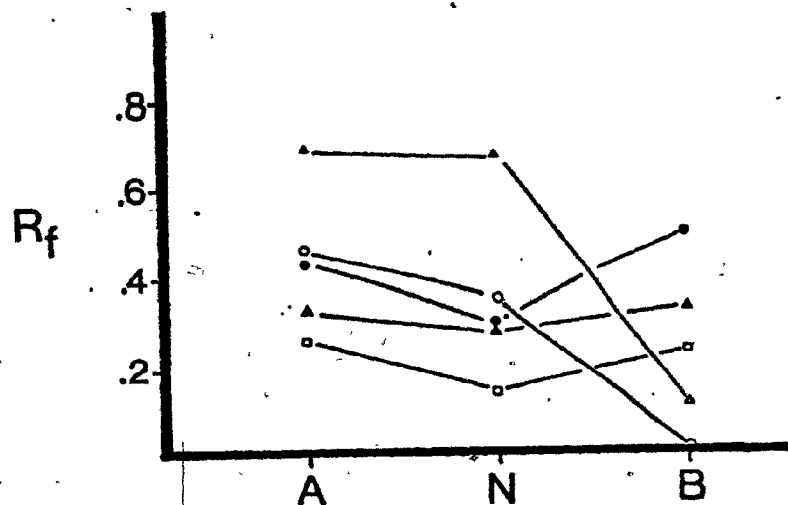


Figure 4-28. Adsorption on silica t.l.c. retention data for V (◐), VI (◑), VII (◒), VIII (◔) and IX (◕) where h.p.l.c. mobile phase was acidified (with 1% acetic acid (A)), left with no polar modifier (N) or made basic (with 1% ammonium hydroxide (B)).  $R_f$  refers to the retention of solute band and is related to  $k'$  by  $k' = (1-R_f)/R_f$ .

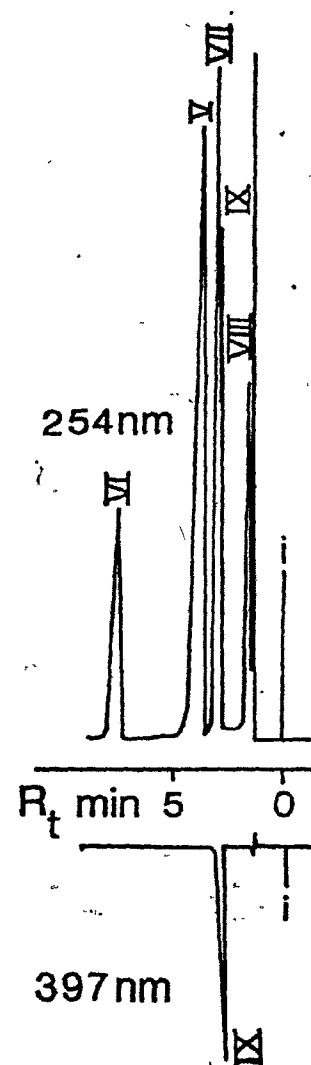


Figure 4-29. h.p.l.c. (normal phase) separation of the intermediates and products of the Sawicki and Carnes reagent. The numerals refer to those in Figure 4-19. (1) is where sample was injected.

shown in Fig. 4-29. Note that dual wavelength detection was used because VII and IX were not fully resolved.

The h.p.l.c. assay system indicated that in the Nash method the formation of II occurred in situ. Thus, as can be seen from Fig. 4-21 compound II was already present at time  $t = 0$  due to the 5 min pre-incubation of 2,4-pentanedione with ammonium acetate. Upon addition of formaldehyde there was a decrease in the concentration of II and the appearance and increase in the concentration of IV to a steady state. This confirms the preliminary thin-layer chromatography studies. Fig. 4-24 shows a duplicate experiment in which the 2,4-pentanedione was pre-incubated with ammonium acetate for 30 min. Greater concentrations of II and a faster rate of formation of IV were noted. The results for the Sawicki reagent study indicated that compound VIII was formed immediately upon addition of formaldehyde to the Sawicki reagent and then with further incubation the acridinedione chromophore (IX) formed. No other reaction intermediates were detected. Upon condensation with formaldehyde, compound VI formed the bis-iminodione (VII), and then the final product IX was detected.

One of the interesting aspects of the two reagents studied was the recommendation given in the literature for their preparation and storage. A general discussion of this and the results given in the previous sections is now possible.

In Nash's original communication (63) he describes the shift of the "first ultraviolet absorption band" which stabilized 24 h after the reagent was made at a position approximately 18 nm higher in wavelength. This bathochromic shift of the ammonium acetate shoulder can be attributed to the formation of compound II in solution ( $\lambda_{\text{max}} = 271.7 \text{ nm}$ ,  $\log a = 3.43$ ). Nash shows further that the reaction rate for the condensation reaction (he assumed first-order conditions), when measured for a 1-day-old reagent, gave during the course of the reaction two distinctive rate constants. The initial rate was very fast relative to the second and the inflection point between the two rates was, with respect to the degree of reaction, the same at temperatures  $5^\circ$  and  $37^\circ\text{C}$ . This was the first and last detailed study of the reagent but the necessary data to predict that the iminodione was the active reagent in the Nash reagent were shown in this contribution. The formation of the iminodione explains the many different recommendations given in the literature for the preparation and storage of the reagent. The slow but progressive formation of the iminodione during the course of an experiment must certainly have given non-reproducible results.

The reagent of Sawicki and Carnes (64) was also interestingly described with respect to preparation. When cyclohexanedione was used as the 1,3-diketone, Sawicki and Carnes recommended allowing the reagent to stand overnight

before using. The reagent, when prepared with dimedone was, on the other hand, reported to be stable for only six hours after preparation. This advice is very difficult to rationalize when one considers that the chemistry of these two compounds was found to be almost identical throughout this study. The main differences were that cyclohexanedione was found to be relatively heat sensitive (and is supplied as stabilized with 3% NaCl, recrystallized from toluene and stored at  $-20^{\circ}\text{C}$  in these studies) while dimedone was found to be stable to heating up to  $80^{\circ}\text{C}$ . Spectroscopic studies and molecular models of dimedone (95) and cyclohexanedione indicated that some steric effects of the 5-methyl groups of dimedone decrease its reactivity. This was found to be the case in that when preparing the iminodione of dimedone the reaction was run at  $80^{\circ}\text{C}$  for up to 16 h while for cyclohexanedione the conditions were milder ( $22^{\circ}\text{C}$ ) and the reaction was completed in approximately 12 h. No explanation can be given for the recommendations given by Sawicki and Carnes.

The reagent of Sawicki and Carnes is very similar to the Nash reagent but because of the slower reaction of ammonia with dimedone relative to 2,4-pentanedione, the reaction of the former reagent with formaldehyde proceeds through the bis-methylene derivative VIII and thus through

reactions 8 and 9. Since the reagent involving cyclohexanedione was recommended by Sawicki and Carnes to be allowed to stand overnight before use, the reaction in this case would most likely proceed through the iminodione of cyclohexanedione (i.e. reactions 5-7). The actual pathways that are followed in the Sawicki and Carnes reagent depend on the history of the reagent.

No conditions were found for making a reagent based on the cyclic iminodiones and this was attributed to a variety of reasons. The pH profile for the reaction of the Sawicki reagent with formaldehyde (Fig. 4-17) was found to coincide with the general stability of the iminodiones reported in the literature (94). To further complicate the situation, the intermediate VII was found to be stable and easily isolated. Thus while much data could be gathered for reactions involving the cyclic iminodiones with high concentrations of formaldehyde, low concentrations of formaldehyde and the resulting slower condensation rates gave no measurable product IX.

The advantages of using a reagent consisting of the iminodione rather than the original 1,3-diketone-ammonium acetate mixture are:

- 1) the iminodiones can be isolated and purified to give a reagent with very low background thus greater sensitivity,



2) the reaction between reagent and formaldehyde can be run at the pH most suited for rapid reaction (low pH) and thus greater reaction rates and decreased analysis time are seen, and

3) eliminating ammonium acetate from the reagent aids in the mixing of the reagent with a moving stream in a continuous flow reactor.

The iminodione of the Nash reagent was shown to be formed in situ under the conditions of its use and was investigated in more detail. By using the iminodione at the pH where the fastest reaction occurs with formaldehyde, (pH 2.3), a reagent was developed that had remarkable reactivity. The rate of hydrolysis versus pH profile (Fig. 4-25) was found to coincide in an inverse relationship with the maximum of the reaction profile for the Nash reagent. The reason for this is evident from the data on the reaction of iminodione II with formaldehyde. It is reasonable to assume that by virtue of the fact that a reagent based on the iminodione II was developed that could be used at pH 2.3, the rate of hydrolysis of the iminodione is slow relative to the reaction of the iminodione with formaldehyde. This hydrolysis of II, however, means that in order to use the reagent under conditions of its fastest reaction rate, prior adjustment of the sample to a low pH is required. This was the only limitation found for the reagent.

The rest of this section will be devoted to reporting the characteristics and use of the reagent based on II. This reagent is referred to as Fluoral-P.

#### 4.3.4 Characterization of Fluoral-P as a Reagent for Aldehydes and Specifically Formaldehyde

##### Introduction

4-Amino-3-penten-2-one, which we shall call Fluoral-P in the reagent form, has been utilized previously as a synthetic intermediate (96,97), a complexing agent for metals (98), and a model compound for investigating imine-enamine equilibrium (99). Here it is investigated for use as an aldehyde reagent.

##### 4.3.4.1 Experimental

The Fluoral-P reagent was made by dissolving 1.8 g of 4-amino-3-penten-2-one (sublimated) in 100 mL of acetonitrile to give a 0.18 M Fluoral-P reagent. This solution was stored refrigerated in an amber bottle.

The reagent was characterized as chromophore-producing by studying (i) its long-term stability, (ii) its general reactivity and selectivity, and (iii) its absorbance and fluorescence response to a range of formaldehyde concentrations.

Stability studies on Fluoral-P solutions were

conducted in three ways. Initial reaction rates were measured for different ages of Fluoral-P solutions in a manner identical to the pH studies. The reagent was analyzed directly using gas chromatography (OV-101, 100-200°C, 15°C min<sup>-1</sup>, FID) when made up in distilled water, 0.1 M phosphate buffer (pH 2.25), and acetonitrile. The background fluorescence and absorbance were noted for different batches of reagent made up in different solvents.

The reactivity of Fluoral-P to various compounds was determined in a series of test tube experiments. To one drop of the compound under study, one drop of Fluoral-P reagent, one drop of 0.5 M phosphate buffer (pH 2.25) and a small amount of acetone (to aid miscibility) was added. Qualitative evaluation of reactivity was based on either a positive or negative response. Positive responses were subdivided into instantaneous reaction at room temperature (fast), reaction in less than 1 min (moderate) and those which took longer than 1 min to react (slow). In all cases the Fluoral-P derivatives were yellow in color and gave crystalline products.

The linear dynamic range of the reaction between Fluoral-P and formaldehyde was determined by measuring the fluorescence and absorbance of the reaction mixture as a function of formaldehyde concentration. This was accomplished by reacting 1.0 mL of the appropriate aqueous formaldehyde

standard (Appendix 4B) with 2.0 mL of 0.125 M phosphate buffer (pH 4.0) and 100  $\mu$ L of Fluoral-P reagent in acetonitrile. Fluorescence and absorbance measurements were made between 5 and 30 min of mixing of solution; however, the lutidine product was stable in solution for many hours.

The lower limit of detection of this reagent was investigated using a continuous-flow system based on the concepts of flow-injection analysis (19). The hardware used in the analysis system involved two Waters 6000A solvent delivery systems (Waters Associates, Waltham, Mass.) and a Waters U6K sample injector. The reactor was constructed of 1/16" stainless steel 316 tubing with I.D. measured as 1.0 mm. Reagents from the two pumps were mixed in a 1/16" tee connector (Swagelok<sup>®</sup>) just prior to the injector. Sample volumes of 25  $\mu$ L were added to the analyzer stream. The Spectroflow monitor SF 770 (set at 410 nm, 0.4 AUFS) and FS970 L.C. Fluorimeter (excitation 410 nm, emission 470+550 cut-off filters) were connected in series to the exit of the reactor delay tubing. The Fluoral-P reagent was added through one pump with 0.125 M phosphoric acid through the other. The reactor was run at room temperature, 20°C. Both pumps were operated at 0.5 mL/minute: total delay time to the fluorimeter was 70 sec.

Since the lower concentration range of formaldehyde was of interest, formaldehyde concentrations between  $1.0 \times 10^{-3}$

and  $1.0 \times 10^{-5}$  M were used. Absolute amounts of formaldehyde injected corresponded to  $2.5 \times 10^{-8}$  to  $1.25 \times 10^{-9}$  moles.

One application of this analysis system was to investigate formaldehyde concentrations in the solvents and water used during the course of these studies. This was done by injecting 25  $\mu$ l of the solvent of interest taken from four separate containers. These results are reported as an application of the reagent in automated analysis.

#### 4.3.4.2 Results and discussion

The discussion presented here will be directed toward the use of this reagent in an automated chemical reactor.

##### pH Dependency

One of the more interesting and important aspects of this reagent is the pH dependency of its reaction with formaldehyde. In Fig. 4-24 was shown the relative reaction rate for the production of the lutidine product as a function of pH. This pH dependency must be described as sharp. Optimum reaction conditions for using this reagent in continuous flow analysis would try to favor a fast reaction between Fluoral-P and formaldehyde. Thus the reagent must be used in the pH range of 2.0 to 2.5. Also, because of hydrolysis of 4-amino-3-penten-2-one, a continuous flow system which utilizes the Fluoral-P reagent must contain at

least two channels, one for the reagent and the other for acidic buffer.

#### Stability of Fluoral-P

The hydrolysis of enaminones in acidic media has been described elsewhere (94). When Fluoral-P reagent was made up in aqueous pH 2.25, 0.1 M phosphate buffer, no color development was found after 1 h. Closer examination with gas chromatography showed that 4-amino-3-penten-2-one was hydrolyzed to 2,4-pentanedione within 15 min, was stable in neutral aqueous solution for at least 1 h, and, based on fluorescence and absorbance measurements, was stable for at least one month in acetonitrile. It is concluded that acetonitrile is the solvent of choice for preparing this reagent.

#### Reactivity and selectivity of Fluoral-P

The general reactivity of Fluoral-P was evaluated as described in the Experimental Section. All reactions which were positive gave a yellow product. The results are given in Table 4-8.

Among all the compounds tested, the reagent condenses fastest with formaldehyde. It should be noted that only the product from the formaldehyde reaction is expected to give appreciable fluorescence (63). Thus, while the reagent reacts generally with aldehydes, some selectivity for formaldehyde is possible by using fluorescence rather than

Table 4-8: Results of spot tests between Fluoral-P and some common chemicals.

Compounds, which react fast

Formaldehyde  
Acetaldehyde  
Propanol  
Pentanal  
3-Methylbutanal  
Hexanal  
Octanal  
Nonanal  
Decanal  
Hendecanal  
Dodecanal  
Tridecanal  
Tetradecanal  
Benzaldehyde

Compounds which do not react

Ethyl methyl ketone  
Acetic anhydride  
Ethyl acetate  
Ethylene glycol  
N,N-Dimethylaniline  
o-Nitrotoluene  
1,1,1-Trichloroethane  
Formic acid  
2,4-Pentanedione  
N,N-Dimethylacetamide  
Triethylamine  
Acetone  
Phenyl isocyanate

Moderate

Anisaldehyde  
Cinnamaldehyde  
Phenylpropionaldehyde  
Hydrocinnamic aldehyde

Slow

Cuminaldehyde  
Isobutyraldehyde

absorbance as a means of detection in an automated system.

Linearity and analytically useful range of Fluoral-P  
for reaction with formaldehyde

This aspect of Fluoral-P was expected to be very similar to that for the Nash reagent except in the lower concentration region where Fluoral-P, due to lower background, was expected to be a more sensitive reagent. The absorbance (410 nm) and fluorescence (excitation 410 nm, emission 510 nm) versus concentration of formaldehyde plots were linear over the range of  $10^{-3}$  to  $10^{-6}$  M (absorbance:  $y = 3.15 (\pm 0.360) \times 10^2 x + 0.541 (\pm 0.176 \times 10^{-1})$ ; fluorescence:  $y = 9.33 (\pm 0.547) \times 10^3 x + 0.281 (\pm 1.18)$ ). Slopes and intercepts are given  $\pm$  S.D.). Depending on the method of sample pretreatment and handling employed, determinations can thus be made in terms of absolute amounts of formaldehyde in the nanomolar range. This is shown to be the case in the next section.

Lower limit of detection for formaldehyde with Fluoral-P

The lower limit of detection for formaldehyde, using the flow-injection analysis system, gave the data shown in Fig. 4-30. The difference in the two spectrophotometric parameters monitored, absorbance and fluorescence, can be more fully appreciated by examining the signal-to-noise ratio (SNR) against the amount of formaldehyde injected (Fig. 4-30). The signal is taken as the mean peak height from



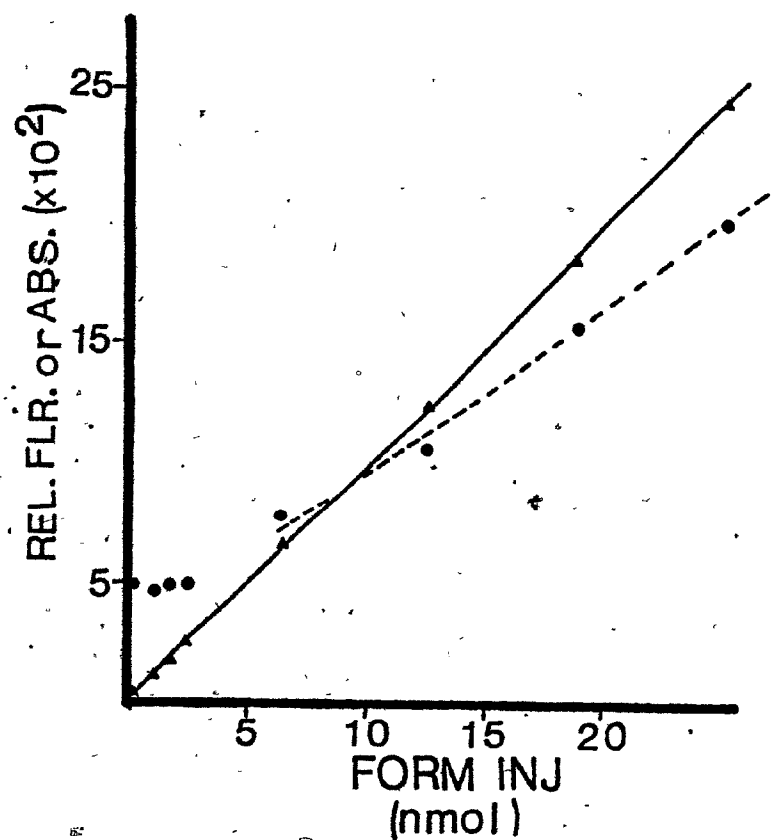


Figure 4-30. Comparison of absorbance (410 nm, ●) and fluorescence intensity (410,510 nm, ▲) signal from formaldehyde using Fluoral-P in the flow-injection analysis system.

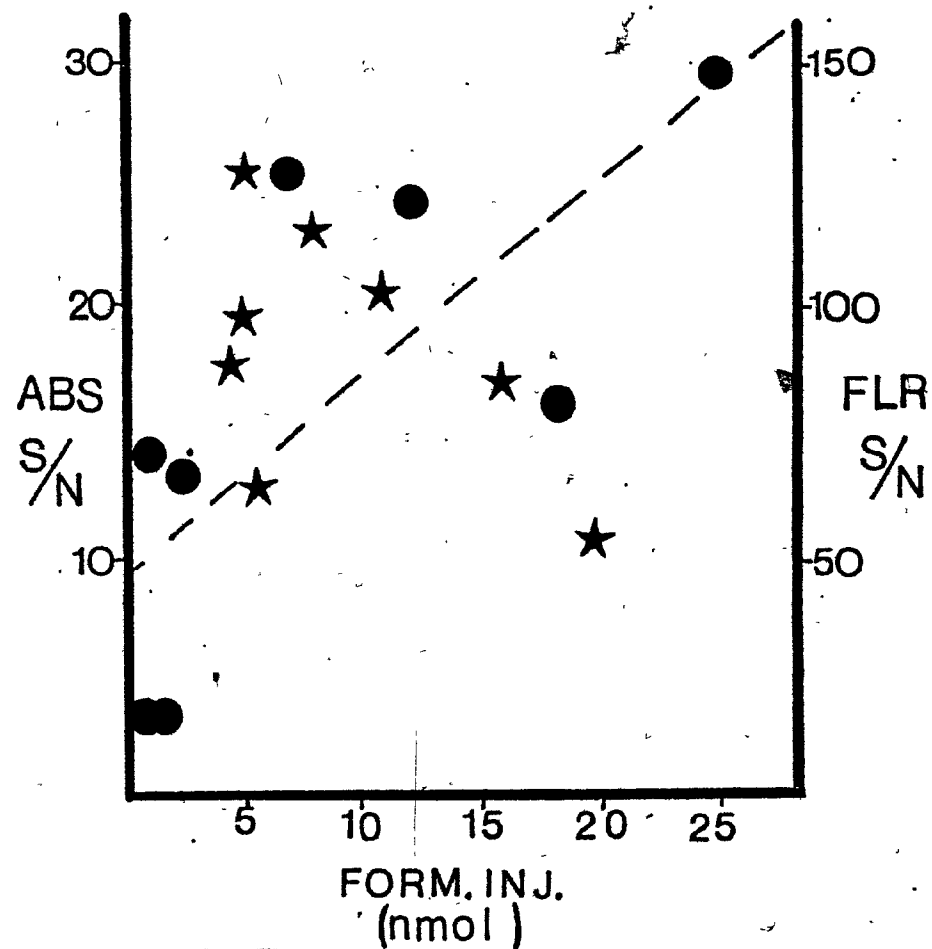


Figure 4-31. Signal-to-noise comparison between absorbance (★) and fluorescence (●) detection. The data is presented in the form of signal to standard deviation of signal at the respective formaldehyde amounts shown.

at least four injections into the analyzer while noise is taken as the standard deviation about the mean. The correlation coefficient assuming a linear relationship is -0.497 for absorbance and 0.74 for fluorescence. Using absorbance detection, the concentration range over which this experiment was conducted is seen to rival the detection limit of the analyzer. Thus in this concentration range the system is baseline noise limited. On the other hand fluorescence detection shows some correlation between SNR and signal and much greater SNR values than for absorbance. Fluorescence detection is not limited by baseline noise above about 3 ng of injected formaldehyde. This is reflected by the fact that the relative standard deviation of fluorescence measurements above 3 ng is on the average 0.88% while below this level it averages 3.8%. While this is a limited noise analysis study and is certainly system dependent, formaldehyde levels in the low nanomol per injection range can be measured using Fluoral-P and the flow injection system employed here.

This detection limit can be improved since the system is baseline noise limited and thus limited by the background fluorescence of the entire analysis system. For instance, measurements of the amount of formaldehyde in solvents commonly used in this laboratory are summarized in Table 4-9. These data show relatively high levels of formaldehyde contamination. Other improvements can be made on the entire

Table 4-9: Formaldehyde content of some solvents used in this laboratory

Solvent	nmole Formaldehyde per 25 $\mu$ L injection*	Formaldehyde ( $\times 10^4$ M)
H <sub>2</sub> O	9.6 $\pm$ 1.4	3.8 $\pm$ 0.56
Acetonitrile	6.1 $\pm$ 0.2	2.4 $\pm$ 0.08
2-Propanol	8.3 $\pm$ 1.8	3.3 $\pm$ 0.72
Methanol	25.4 $\pm$ 4.1	10.2 $\pm$ 0.16
Acetone	7.7 $\pm$ 2.2	3.1 $\pm$ 0.88

\* Mean  $\pm$  S.D. for four determinations.

analyzer system which was made from available hardware and was not optimized for this application.

#### 4.3.5 The Chemistry of the Post-Column Reactor, Stage II and III

Periodate oxidation of organic compounds is normally considered a selective process involving 1,2-diols. General reviews on the use of periodate (100-104) indicate that direct analytical usage is limited to a few cases (105,106) and the reagent is mainly used for synthetic work or structural confirmation.

Periodate is used here for selective oxidation of glycerol and 1-glycerol phosphate. The oxidation of glycerol is well known and oxidation of 1-glycerol phosphate over the 2-positional isomer was one of the earliest uses of periodate for structural confirmation (107). Periodate oxidation is not limited to these two compounds or diols in general. The lack of specificity of the reagent was investigated by Fleury and Boisson (108-110) and Sprinson and Chargoff (111). Specificity for 1,2-diols is lost above 50°C and is greatest at 10°C.

Non-selective oxidation with periodate is also seen with dimedone, 1,3-cyclohexanedione (112) and to a lesser extent 2,4-pentanedione (113). Furthermore, oxidation of

lutidine has necessitated use of sodium arsenite or rhamnose to eliminate excess periodate in the manual and automated methods using the Nash reagent (48,50,114,115). The phosphate catalyzed over-oxidation of sugars is not seen for glycerol phosphate (116,117).

The structural features (118) and conditions for periodate use indicate oxidation occurs over the pH range 1-11 (4-5 optimum) in aqueous, methanolic, ethanolic and acetic acid solutions (119,120).

The oxidation stage of the reactor (stage II) traditionally utilizes periodate as the oxidizing agent. The wide variation in conditions has necessitated some experimental work on the role of this reagent in the reaction sequence. Particular attention was dedicated to the oxidation of lutidine by the excess periodate and alternative reactor configuration and conditions was investigated.

The methods of saponification and transesterification are widely used today for the determination of hydrolyzable lipids in conjunction with gas chromatography. Some recent and complete reviews on esterification procedures for fatty acids (121), for gas chromatographic analysis (122), and saponification-transesterification (123) indicate that the transesterification procedure is faster than the saponification for deacylating acylglycerides (124). In anhydrous sodium methoxide solution glycerides, phospholipids, and wax esters

were hydrolyzed in less than 20 sec (124).

Catalysis of transesterification has been accomplished, for example, by borontrifluoride (125).

To remove the orthophosphate from the 1-phosphoglycerol portion of a phospholipid requires acid thermolytic cleavage (255°C, 10 min (c.f. 121, 126-129)) and base hydrolysis is ineffective (130). Saponification does not remove the fatty acid from the amide of sphingolipids nor long-chain aldehydes from plasmalogens (131), the latter being acid labile (132). Deacylation is thus a complex process and whether acid or base catalysis is used depends on the application. Acid hydrolysis would be preferred here since the mobile phases used for phospholipid elution are usually acid and the step after hydrolysis involves periodate oxidation in acidic medium. Thus it was investigated along with saponification and linked to periodate oxidation. Since periodate can oxidize 1-phosphoglycerol, the less ambitious deacylation, and not dephosphorylation, was of interest when investigating phospholipids.

The equation of Snyder (section 4.2.1.2) predicts the dispersion in the c.f.a. system is a function of the experimental parameters encountered in chromatography. The effects of temperature on dispersion were not included directly into the equation but viscosity, surface tension, and  $D_{w,25}$  are all temperature dependent physiochemical

properties. Consequently, besides increases in reaction rate, increases in temperature should affect dispersion of the sample bolus. The relation of temperature to dispersion was thus investigated.

Consideration of pH effects on reaction rate of Stage I was the determining factor setting the pH of the periodate reagent. Phosphoric acid was originally used to adjust reagent pH but due to precipitation of phosphate salts in the acetonitrile mobile phase, perchloric acid was substituted. The effect of changing perchloric acid concentration on the detector response was investigated.

#### 4.3.5.1 Experimental

##### Periodate oxidation, stage II

The oxidation of lutidine by periodate was investigated by observing the lutidine equilibrium concentration during the determination of a sample of phospholipid, triglyceride and formaldehyde. Thus,  $1.0 \times 10^{-3}$  M of L-3-phosphatidylcholine distearyl in isopropanol,  $5.0 \times 10^{-4}$  M tristearyl in isopropanol and  $1.0 \times 10^{-3}$  M aqueous formaldehyde standard, along with water and isopropanol blanks, were used in the following reaction sequences:

- i) 0.5 mL standard or blank was incubated for 5 min at 60°C following the addition of 0.20 mL of 0.5 M KOH in H<sub>2</sub>O.

ii) to this was added 0.5 mL of 0.0125 M  $\text{NaIO}_4$  and 0.5 mL Fluoral-P reagent (0.18 M 4-amino-3-penten-2-one in acetonitrile) and the reaction (at  $60^\circ\text{C}$ ) was monitored using absorbance spectroscopy (410 nm). This sequence was repeated three times.

A major concern was the reliability of taking the maximum of the concentration of lutidine as a value which reflects formaldehyde concentration. To see if this approach was experimentally sound various concentrations of 1-glycerol phosphate ( $1.4\text{--}2.9 \times 10^{-4}$  M) were first incubated at  $60^\circ\text{C}$  for 5 min and then oxidized with periodate for 10 min and allowed to react with Fluoral-P reagent. Color development was monitored (at  $\lambda_{410}$ ) and absorbance versus phosphoglycerol concentration (measured at 2 min) were reported.

Another experiment was designed to investigate the effect of periodate concentration on the oxidation of chromophore independent of the formation of the chromophore. This was investigated using a flow analysis system identical to the system eventually used as the p.c.r. detector. Conditions in the reactor were such that the only variable was the concentration of periodate. The experimental system consisted of:

i) Combining the following reagents at the respective flow rates: a)  $\text{H}_2\text{O}$  (0.5 mL/min); b) 0.5 N KOH in  $\text{H}_2\text{O}$  (0.23 mL/min); c) 0.0125 to 0.10 M  $\text{NaIO}_4$  in 0.125 M phosphoric acid



(0.42 mL/min).

ii) Adding through the final reactor stage  $5.8 \times 10^{-6}$  M lutidine in methanol at a rate of 0.42 mL/min.

The final stage had a volume of 0.994 mL which corresponded to a delay time of 38 sec.

The reactor manifold was heated to 60°C and the effluent stream debubbled and monitored with absorbance and fluorescence detectors.

Another study investigated the effect of temperature on the reactor's response. To the system used above, a 10  $\mu$ L sample of  $5 \times 10^{-3}$  M formaldehyde was injected. The change to the above system was that the  $5.6 \times 10^{-6}$  M lutidine in methanol was replaced by Fluoral-P reagent. The temperature range investigated was 22-60°C.

In a study using the same system as with the temperature study,  $9.87 \times 10^{-4}$  M phosphatidylcholine dipalmitoyl in isopropanol replaced  $H_2O$  and was pumped continuously into the c.f.a. (maintained at 60°C) and 0.2 M  $NaIO_4$  made up in different concentrations of perchloric acid (0.1-1.0 M) was used for oxidation. The other reagents consisted of 0.5 M KOH and 0.16 M Fluoral-P. The steady-state response heights (i.e. background increases) versus concentration of perchloric acid in the periodate reagent were measured.

### Deacylation stage III

The following samples:

- i) 1,3-phosphatidylcholine dilinolenoyl ( $6.4 \times 10^{-3}$  M)
- ii) Trilinolenin ( $6.89 \times 10^{-3}$  M) and standards
- iii) Methyl linolenate ( $7.93 \times 10^{-3}$  M)
- iv) Linolenic acid ( $8.48 \times 10^{-3}$  M)

were first separated using an h.p.l.c. method involving an Altex C-18, 10  $\mu$ m-column (Chapter 2) and a step gradient from 85 methanol/15 H<sub>2</sub>O/0.1 conc. H<sub>3</sub>PO<sub>4</sub> v/v/v switched to 100% methanol 3 min after injection. The chromatographic system was described in Chapter 2.

The hydrolysis systems and conditions are shown in Table 4-10 and were investigated at 60°C using a Pierce Reacti-Therm<sup>TM</sup> Heating module (Pierce Chemical Co., Rockford, Ill., 61105) as the incubating system.

#### 4.3.5.2 Results and discussion

The separation and detection of the lipid standards used in the deacylation study is shown in Fig. 4-35. The results of the investigation are shown in Table 4-11 where the mean of duplicate runs for each hydrolysis system is given.

This work indicates that acid hydrolysis is too slow under the conditions employed to be of use in the p.c.r. The thermal conditions normally used with acid hydrolysis cannot be duplicated in a p.c.r. Base hydrolysis at 60°C is complete within 10 min and is the best method.

Table 4-10: Summary of the experimental conditions used to investigate deacylation of triglycerides and phospholipids.

	I		II	III		IV**		
	50 $\mu$ L*		10 $\mu$ L				20 $\mu$ L	
	TG	PC	NaOH	H <sub>3</sub> PO <sub>4</sub> NaIO <sub>4</sub>	H <sub>2</sub> SO <sub>4</sub>	H <sub>2</sub> O	H <sub>2</sub> O	MeOH
1	x		x				x	x
2		x	x				x	x
3	x			x			x	x
4		x		x			x	x
5	x				x		x	x
6		x			x		x	x
7	x					x	x	x
8		x				x	x	x

25  $\mu$ L aliquots were taken at 10, 20 and 30 min quenched with 25  $\mu$ L cold methyl acetate and stored at 0°C. Analysis was carried out immediately by injecting 10  $\mu$ L of quenched reaction mixture into the HPLC.

\* The 50  $\mu$ L of CHCl<sub>3</sub> in which the sample was dissolved was evaporated and replaced with 50  $\mu$ L of methanol before reaction. This was easily accomplished because the reaction vials were initially pre-heated to 60°C.

\*\* I. 0.5 N NaOH in 50% MeOH.  
 II. 0.5 N H<sub>3</sub>PO<sub>4</sub> and 0.4 M NaIO<sub>4</sub> in H<sub>2</sub>O.  
 III. 0.5 N H<sub>2</sub>SO<sub>4</sub> in 50% MeOH.  
 IV. Distilled H<sub>2</sub>O.

Table 4-11: Summary of the results of the experimental systems in Table 4-10.

Conditions		10 min			20 min			30 min		
		FA	FAME	TG	FA	FAME	TG	FA	FAME	TG
NaOH (I)*	1)	20.7	1.9	-	19.7	1.1	-	19.2	0.4	-
H <sub>3</sub> PO <sub>4</sub> (II)	3)	-	-	1.9	-	-	5.7	-	-	.4
H <sub>2</sub> SO <sub>4</sub> (III)	5)	-	-	13.2	.1	.1	18.5	.4	.2	14.5
Control (IV)	7)	-	-	14.8	-	-	11.9	-	-	15.7
				PC			PC			PC
NaOH (I)	2)	15.6	-	-	17.2	-	-	16.2	-	-
H <sub>3</sub> PO <sub>4</sub> (II)	4)	-	-	3.8	-	-	3.7	-	-	1.4
H <sub>2</sub> SO <sub>4</sub> (III)	6)	.08	-	2.6	1.3	-	2.7	.4	-	1.7
Control (IV)	8)	-	-	4.5	-	-	5.0	-	-	1.1

\* See Table 4-10 for details. Values are given as measured peak heights and are thus in relative units. The use of standard curves was deemed unnecessary because these results are interpretable without exact quantitation.

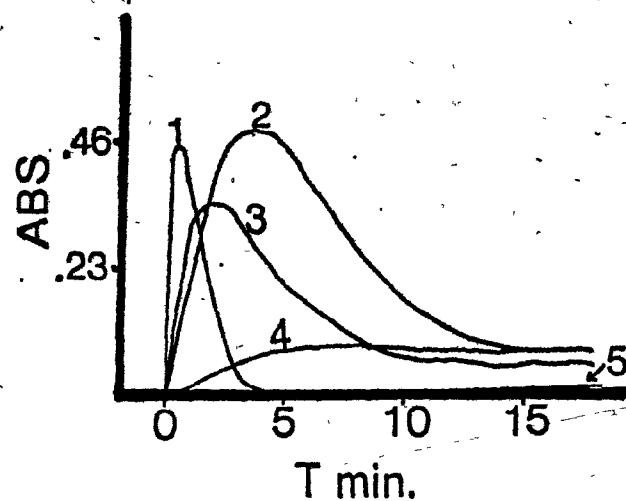


Figure 4-32. Production and destruction of lutidine derived from formaldehyde (1), tristearyl (2) and PC distearyl (3). Isopropanol (4) and water (5) were also used as blanks.

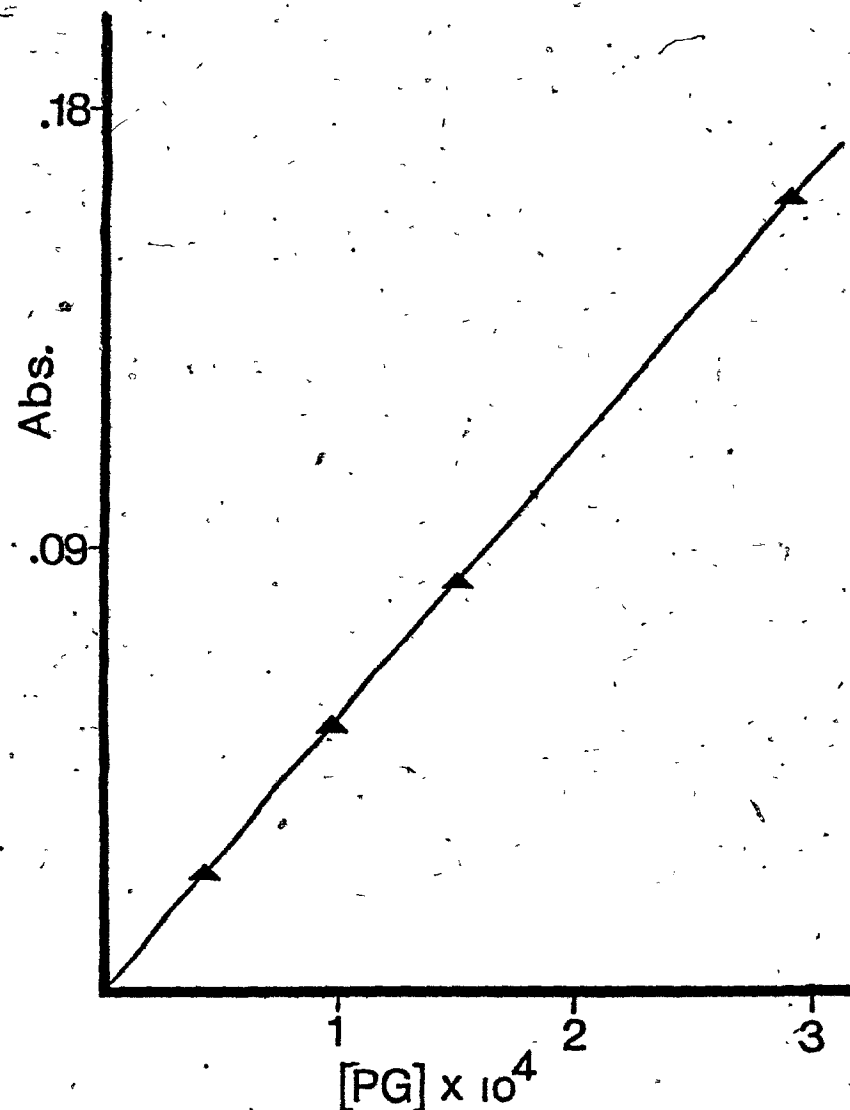


Figure 4-33. Absorbance (410nm) at 2 min. versus initial phosphoglycerol concentration.

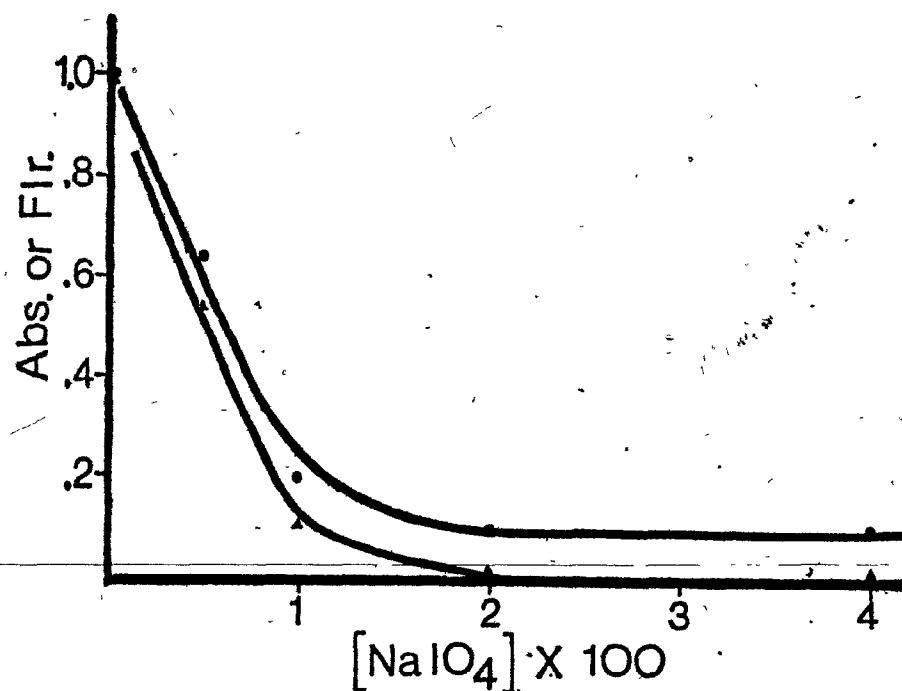


Figure 4-34. Relative decrease in background signal as a function of sodium periodate concentration. Details presented in text. (●) absorbance and (▲) fluorescence signal.

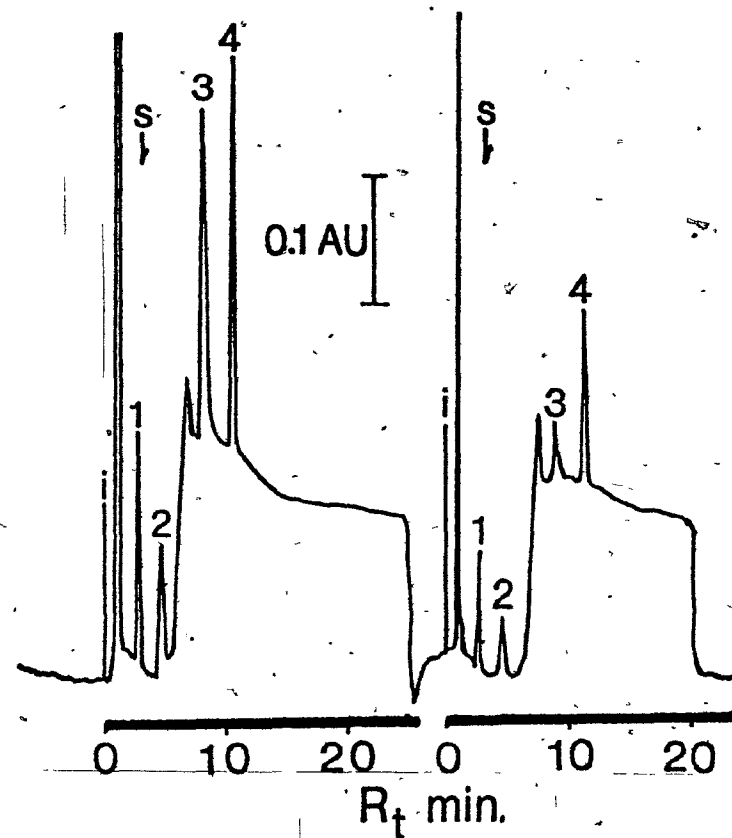


Figure 4-35. Some typical test runs on the reversed-phase h.p.l.c. separation and detection of fatty acid (1), fatty acid methyl ester (2), phospholipid (3) and triglyceride (4) as described in the text. S refers to where solvent is changed over in the Waters 6000A pump. Conditions were 60°C column temperature, 2 mL/min solvent flow rate, detection at 200 nm with the Sefel SP770.

Transesterification, which requires anhydrous conditions, is not possible in the p.c.r. system being developed. The hydrolysis reagent used for the p.c.r. was 0.5 N KOH made up in distilled water and stored in a polypropylene bottle.

For the periodate oxidation studies, representative reaction profiles are shown in Fig. 4-32 where it is seen that a maximum absorbance occurs within 5 min and then a decrease in absorbance to a very low level occurs.

The absorbance measured (y), versus phosphoglycerol concentration (X) correlated linearly with  $y = 5.09 (\pm .60) \times 10^{-3} X - 1.23 \pm 1.01$  ( $y = X \pm \text{S.D.} + y\text{-inter} \pm \text{S.D.}$ ) and correlation coefficient of  $= 0.990$ . Data is presented in Fig. 4-33.

The effects of varying periodate concentration are shown in Fig. 4-34 as the relative change in the background fluorescence or absorbance versus the initial signal (when no periodate is present) taken as 1.0. The difference in the two profiles can be accounted for by the 8-sec delay time (0.21 mL) between the absorbance and fluorescence detector. Significant amounts of lutidine were degraded at periodate concentrations greater than 0.02 M and this was taken as the highest acceptable periodate concentration for use in the reactor. The reactor design was such that the periodate and chromophore developing stages (II and III, respectively) were separate and the periodate stage was optimized to give

greater than 95% reaction. The delay time of the chromophore stage was then made to coincide with the maximum of the chromophore profile (Fig. 4-32).

The use of arsenite in an additional stage of the reactor was attempted but abandoned when it was found that the high concentrations (greater than 1 M) required for reaction with periodate were not attainable in the mobile phase systems being used (c.f. 61). Sodium arsenite precipitated from solution when high alcohol or acetonitrile concentrations were present. A bench reaction using rhamnose for periodate scavenging gave results which indicated periodate levels did not decrease significantly.

Fig. 4-36 shows the experimentally determined relationship between band width ( $W_{1/2}$ ) and response as a function of temperature. As can be seen for the c.f.a. unit studied here,  $W_{1/2}$  decreased while response increased with temperature. Thus increasing temperature generally aided in reducing band width and increasing response of the eluting sample. The temperature of 60°C was chosen since this was also the temperature used for the chromatography.

The results of the pH study are shown in Fig. 4-37. Perchloric acid of 0.3 M was used to prepare the periodate reagent.

With the minimization of background and noise in the system and the choice of temperature, pH and concentration of



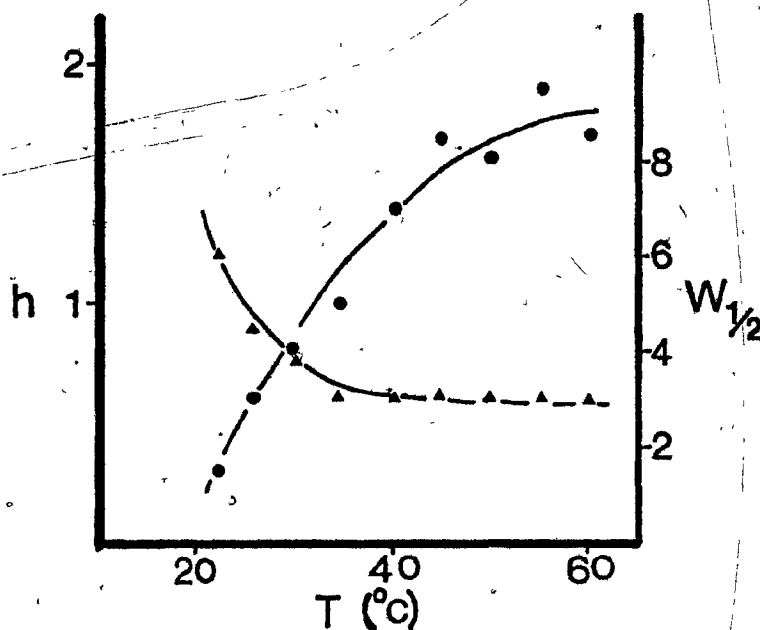


Figure 4-36. Experimentally determined relationship of  $w_{1/2}$  ( $\Delta$ ) and  $h$  ( $\bullet$ ) to the reactor temperature  $T$ .

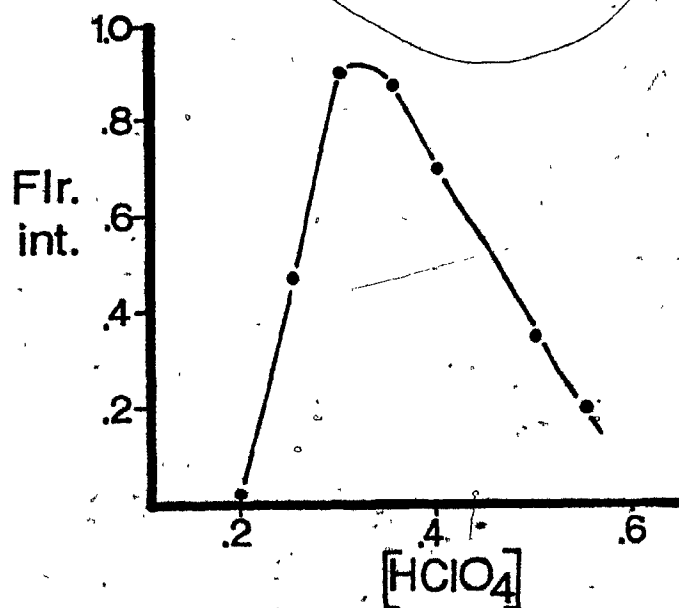


Figure 4-37. Affect on fluorescence background of varying concentrations of perchloric acid in the periodate Stage II.

KOH,  $\text{NaIO}_4$  and Fluoral-P, optimization of the various reactor stages was straightforward and involved application of the Stop-Flow Analysis optimization scheme to be presented.

#### 4.4 OPTIMIZATION OF THE POST-COLUMN REACTOR

##### 4.4.1 General Introduction

Diagnosing and optimizing the reaction conditions used in the widely applied methods of continuous-flow and flow-injection analysis was initially found to be tedious. Unfortunately, information pertaining to the theoretical (22,24,33,36,133) and practical (134,135) aspects of these two methods was of little aid in alleviating this problem.

A few systematic approaches have been taken to optimize flow-analysis systems. The exponential dilution technique (136) popular in the characterization of gas chromatographic detectors and residual gas analyzers, has been applied to optimization in c.f.a. (137-140). In this method a starting level of the reagents whose concentration is to be optimized is either increased (from zero concentration) or decreased (from some upper starting concentration) by the use of an exponential dilution flask (example 141). The optimum concentration of reagent for the system can be calculated from the characteristics of the task and the response generated. This method has not been used extensively

because the complexity of the c.f.a. system does not allow the system to be reduced to being a function of concentration of one reagent. A more realistic approach to optimization of these systems involved the use of the Simplex Optimization method (142). This method, while simple to use, was tedious to execute. An alternative method for optimization of the c.f.a. system was devised.

#### 4.4.2 The Optimization Scheme Based on Stop-Flow Analysis

A new approach to c.f.a. and f.i.a. optimization was developed specifically for this work. It was based on the method of Stop-Flow Analysis (142,143), stopping the flow of a c.f.a. or f.i.a. stream and following the reaction occurring in the detector cell. This enables predictions on the time required for the last reaction in the analyzer to go to completion. However, in most analyzers many reaction stages are present and what is needed is a method to evaluate the efficiency of all stages simultaneously. To do this the stop-flow analysis method was extended. The term "optimization" as used here refers to developing a reactor manifold which gives performance only achievable with much greater effort if using a random method.

In order to use Stop-Flow Analysis (s.f.a.) effectively, it was rationalized that all variables in the system should

be reduced to a point where reaction delay times in the manifold delay coils were the only manifold variables needing attention. This was accomplished by first applying steps 1-4 below. These steps were concerned with limiting dispersion and dilution while increasing reaction rates for each manifold stage. Stop-Flow Analysis was then used to determine the needs of the manifold with respect to delay times as explained in step 5. The scheme for reducing variables was executed as follows: Step,

1. Optimize reaction tubing size and bubble rate, presented in section 4-2.

2. Tentatively choose one or two pump tube sizes for use with all reagents. This aided in the stocking of such an expendable item. The choice was not arbitrary but based on experience with the manual method and information obtained from step 1. It was kept in mind that sample dilution characteristics dictate that flow rates in the lower ranges ( $< 0.5 \text{ mL min}^{-1}$ ) should be used.

3. Based on the manual method and with due consideration to solubility, pH, etc., choose the highest reagent concentration that may be used. This was done to increase reaction rates and minimize sample dilution by allowing lower pumping rates.

4. Considering the boiling points of the solvents

used, employ the highest temperature which can be tolerated. This generally increased reaction rates, mixing and solubility of the reagents while decreasing sample dispersion.

5. Stop-Flow Analysis was used to determine the exact reaction coil delay times necessary to simultaneously achieve nearly complete reactions ( $> 95\%$ ) in each manifold stage. This was illustrated as follows. The manifold delay coils were chosen to be of low volume compared to what would be dictated by the manual method. A continuous stream of the compound to be determined (triglyceride in this case) was then fed into the manifold (as opposed to being injected or sampled). With reference to Fig. 4-38 a baseline shift was observed ( $A_0$ ) corresponding to the steady-state response for the initial manifold design. At time  $t_0$  the system flow was halted. The observed rise in detector response corresponded to unreacted reactant in the final stage of the reactor. From this response the delay time required to yield 95% completion of the reaction in the final manifold stage was determined directly. Of greater interest, however, was what occurred after flow was resumed ( $t_{60\text{ s}}$  or  $t_{90\text{ s}}$ ). Plateaus ( $A_d$ ) appeared superimposed on the original baseline shift. These plateaus corresponded to additional reaction products produced in each manifold stage during the stop time. Thus, the Stop-Flow Analysis method effectively increased

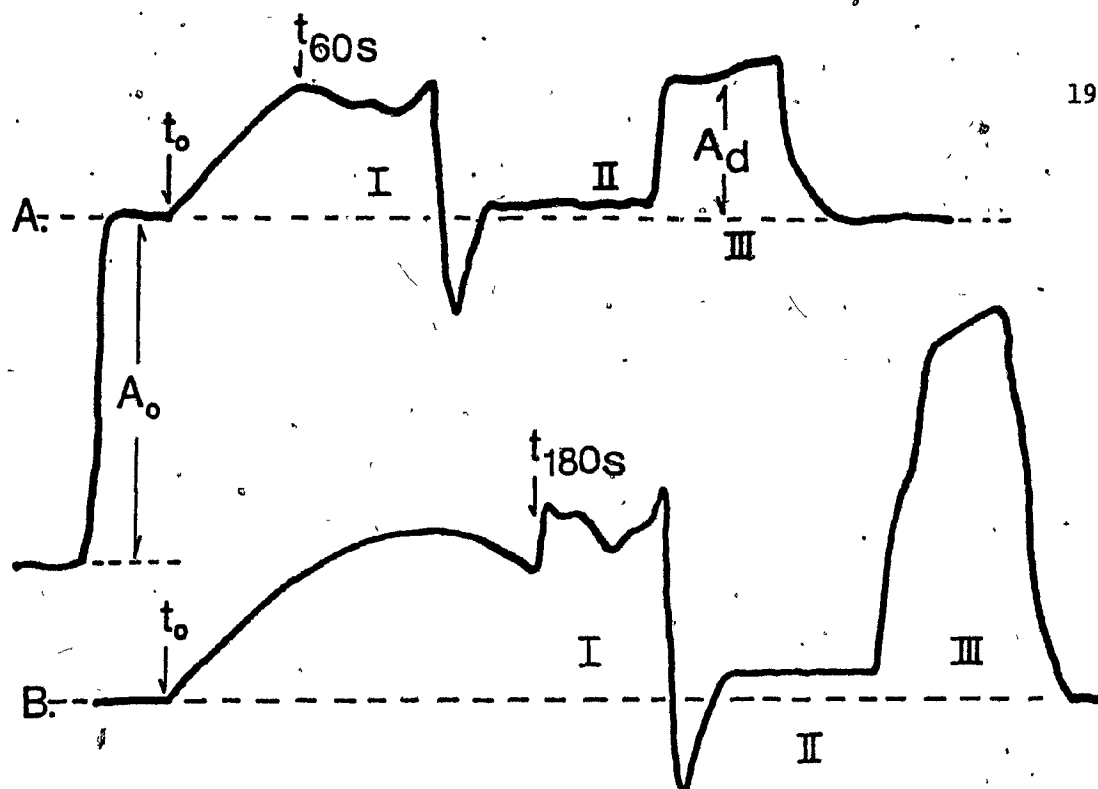


Figure 4-38. Detector output (410 nm) after s.f.a. of 60s (A) and 180s (B).  $A_0$  refers to absorbance change upon introduction of triglyceride,  $t_0$  is when reactor flow is interrupted,  $A_d$  is additional absorbance due to delay, and the numbers refer to each manifold stage.

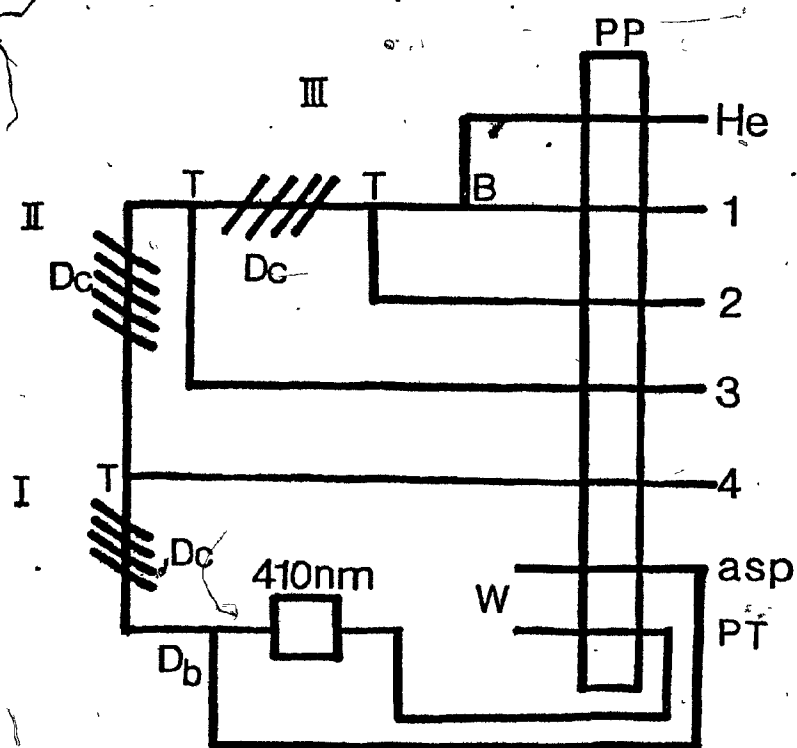


Figure 4-39. Schematic representation of the c.f.a. manifold and associated equipment, unoptimized. Details are presented in Table 4-11.

the volume of the delay coils by an amount equivalent to the product of the stop time and the reagent flow rate at the stage of observation. This was done simultaneously for all stages in the manifold and required no further manifold manipulation.

#### 4.4.3. Experimental

##### Apparatus

A Technicon Pump III (Technicon Instrument Corp., Tarrytown, NY), Schoeffel Spectroflow Monitor SF 770 (Schoeffel Instrument Corp., Westwood, NJ) and Honeywell Electronik 196 recorder were used. The c.f.a. manifold was the all stainless steel construction described in section 4.2. The reactor was run in the debubbled mode, at  $60 \pm 1^\circ\text{C}$ .

##### Operating conditions

Tributylglycerate (Sigma Chemical Co., St. Louis, Mo.) was used in the c.f.a. system schematically represented in Fig. 4-39. Details are given in Table 4-12.

##### Reagents

All reagents used are present in Table 4-12. The concentrations given were based on the work previously presented. Possible sources of formaldehydes (alcohols, acetic acid, etc.) normally associated with automated triglyceride analysis were eliminated.

Table 4-12: Summary of the optimized p.c.r. system.

Stage	measured* DC vol (mL)	Nominal flow rate through stage (mL/sec)	Calculated** delay time
III KOH	2.48	0.020	125 sec
II NaIO <sub>4</sub>	3.17	0.027	120 sec
I Flr-P	0.99	0.033	30 sec

	Nominal Pump**Flow rate (mL/sec)	Pump tube
III 0.5 M KOH in H <sub>2</sub> O	0.0038	PVC-0/W
II 0.02 M NaIO <sub>4</sub> in 0.3 M HClO <sub>4</sub>	0.0070	PVC-0/0
I 0.18 cm Fluoral-P in CH <sub>3</sub> CN	0.0070	Silicon-0/0
HPLC	0.0083	Waters 6000A
He (gas)	0.0070	Silicon 0/0

concentration of each reagent as it occurs in the reaction  
(assuming no reaction)

III 0.16 M KOH

II 0.0073 M NaIO<sub>4</sub>

I 0.048 M Flr-P

\* Measured by repetitive (10) injections of lutidine into a unit using the Waters 6000A pump, delay cell of interest and FS970 detector. Precision was to less than 1% relative standard deviation.

\*\* Due to pump tubing aging and variations these values are reproducible to  $\pm 5\%$ . The total flow rate of 1.99 mL/min was evaluated by pumping water through all lines and determined to be 1.97 mL/min.



### Procedures

Stages II and III were optimized simultaneously by using the system described, stopping flow at the times indicated in Fig. 4-40, and measuring  $A_d$ . Optimization of stage I was done independent of II and III by passing  $1.2 \times 10^{-3}$  M formaldehyde through a 0.37 mL DC. After stopping flow, 19 sec was required for 95% reaction (100% taken as maximum of the  $A_{410}$  profile). This additional delay time was added to stage I and conditions in Table 4-12 are for optimized conditions.

### 4.4.4 Results and Discussion

When the stop-flow method was applied to the system the results as shown in Fig. 4-40 indicated that an additional 120 sec was required for stage III and an additional 65 sec for II. Thus for stage III 1.46 mL and II 1.25 mL of additional reactor volume was calculated to be required.

After addition of the required volume a check was done on the c.f.a. by using the stop-flow method. The data, shown in Fig. 4-41, indicate that stopping the flow up to 120 sec gave a negligible increase in signal. The signal decreased rather than increased in Stage I, this being due to the periodate oxidation of lutidine. Also, a small plateau for the saponification stage (Stage III) was tolerated

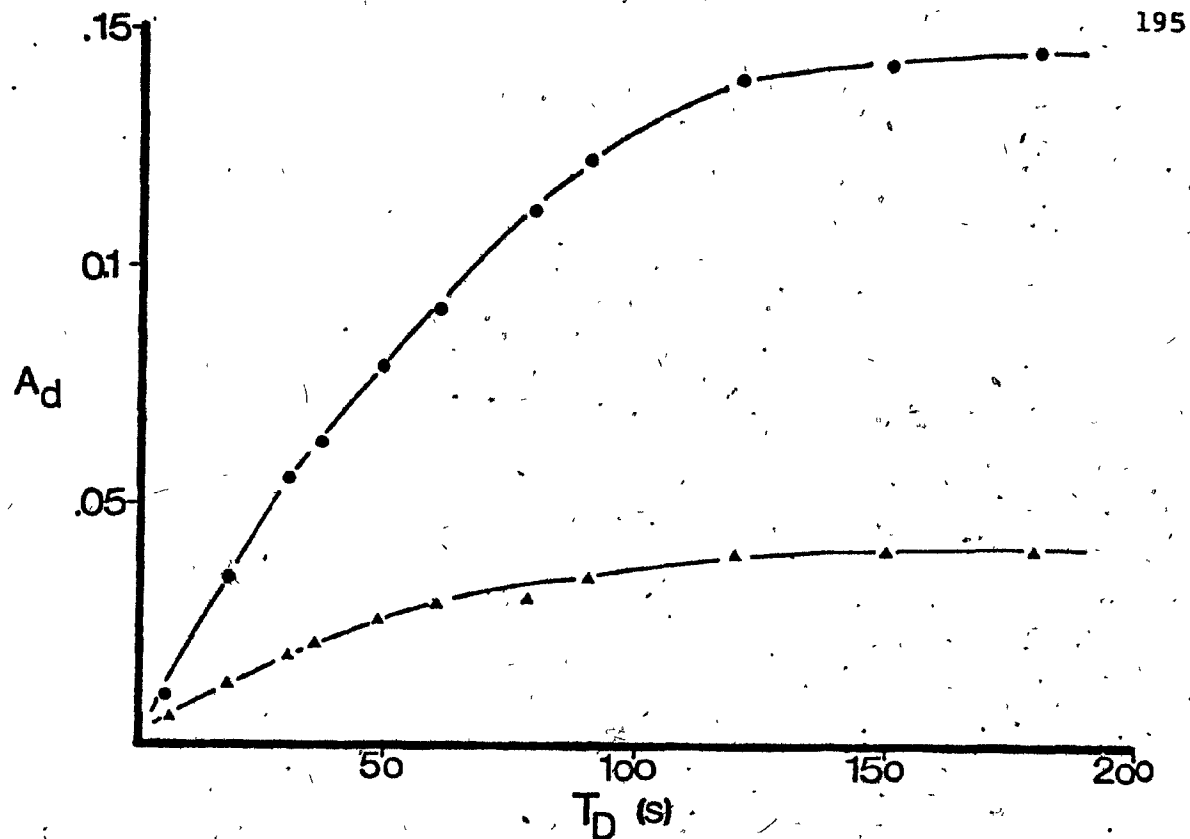


Figure 4-40. Stop-flow analysis results of the c.f.a., conditions given in text and Table 4-11.

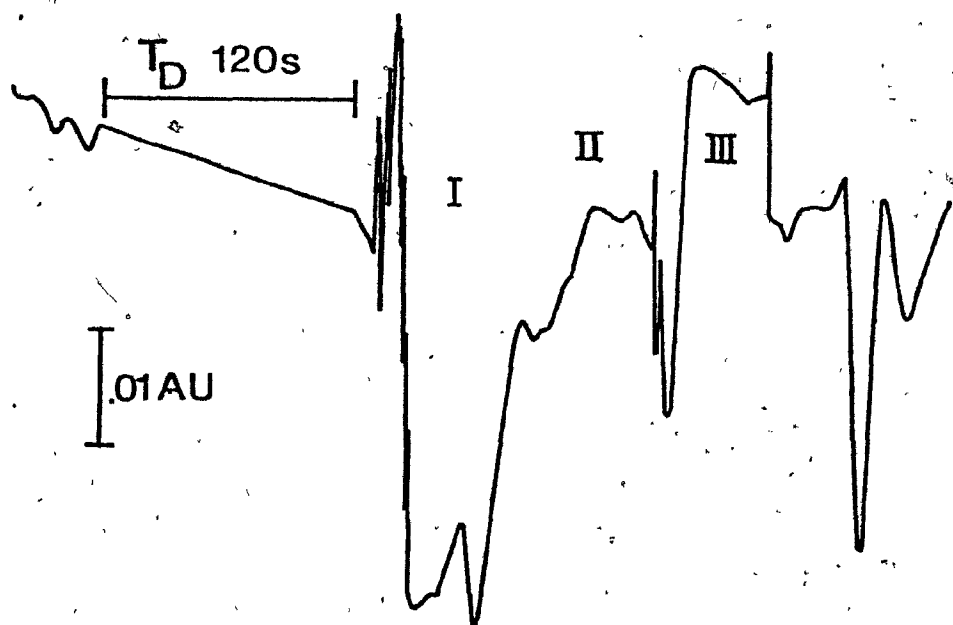


Figure 4-41. The final optimized c.f.a. design analyzed by s.f.a. The time delay (120s) resulted in significant oxidation of lutidine (I) and little change in II or III.

because only a slight increase in signal was anticipated by adding 120 sec additional delay time.

The use of the Stop-Flow Analysis optimization method developed here is new and thus evidence of general acceptance of the method is lacking. The method was simple to use and centered around step 5. It required only basic chemical knowledge and bench experience with the manual method. Stop-flow analysis involved fewer steps than would be involved in the 'Simplex' optimization method (142). For complicated manifolds such as the one presented here, this scheme was very helpful in permitting the rapid choice of reaction conditions and was used to "optimize" (in the limited definition given previously) the c.f.a. used for p.c.r. of triglycerides and phospholipids.

#### 4.5 DESCRIPTION OF THE TOTAL OPTIMIZED c.f.a. POST-COLUMN REACTOR SYSTEM

Figure 4-42 is a photograph of the c.f.a. manifold used for the p.c.r. work. Details and a summary of the system are presented in Table 4-12. This manifold design was used as described for detection of phospholipids and triglycerides following h.p.l.c. separation. The full evaluation of the manifold as a post-column reactor is given in the next chapter. This design was found to be very

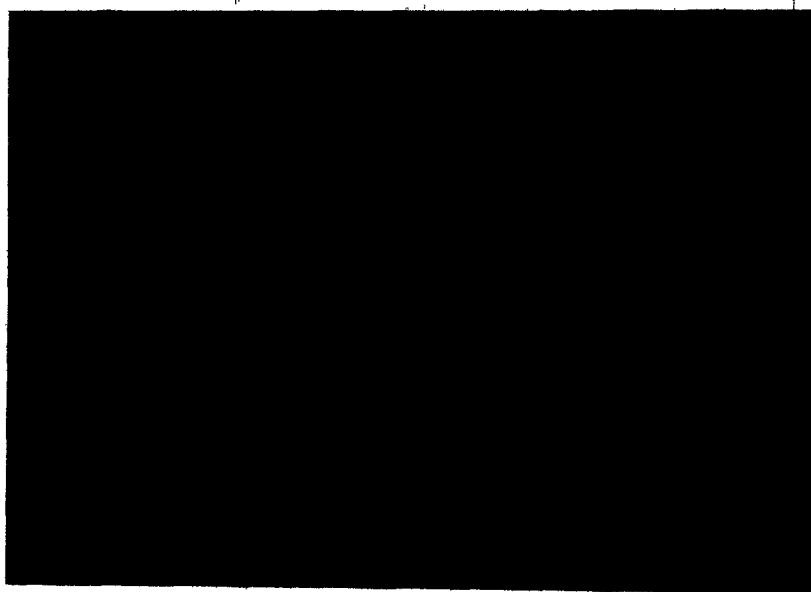


Figure 4-42. Photograph of the c.f.a. manifold used for the p.c.r. detection work.

rough and unlike most commercially available c.f.a. units, was very insensitive to positioning of its components. The band broadening contributions of this system are presented in the next chapter. The unit was found very suitable for use as a post-column reactor for h.p.l.c.

REFERENCES

1. Lofland, H.B., Jr., Anal. Biochem. 9 (1964) 393.
2. Lofland, H.B., Jr., Addendum, Anal. Biochem. 10 (1965) 178.
3. Kessler, G. and Lederer, H., in "Automation in Analytical Chemistry, Technicon Symposia 1965", (L.T. Skeggs, Jr., ed.) Mediad Incorp., New York, 1966, p. 341.
4. Bucolo, G. and David, H., Clin. Chem. 19 (1973) 476.
5. Bucolo, G. and McCroskey, R., Clin. Chem. 21 (1975) 424.
6. Annoni, G., Dioguardi, M.L., Tripodi, A. and Zuin, M., Clin. Chem. 26 (1980) 670.
7. Anaokar, S., Gary, F.J., Standefer, J.C., Clin. Chem. 23 (1979) 103.
8. Kennedy, D.A., Parker, C.W. and Sullivan, T.J., Analyt. Biochem. 98 (1979) 123.
9. Wetmur, J.G. and Wilson, C.R., U.S. Clearinghouse for Federal Scientific and Technical Information (1969), AD-695635, p. 22. C.A. 72:87005p.
10. Mandl, R.H., Goldman, J.F. and Weinstein, L.H., in "Automation in Analytical Chemistry, Technicon Symposia 1966", Vol. 1, Mediad, Inc., White Plains, N.Y., 1967, p. 167.
11. Furman, W.B., in "Continuous Flow Analysis: Theory and Practice", Marcel Dekker, Inc., New York, 1976.
12. Scott, R.P.W., in "Liquid Chromatography Detectors", Journal of Chromatography Library - Vol. II, Elsevier Scientific Publ. Co., New York, 1977, p. 41.
13. Frei, R.W. and Scholten, A.H.M.T., J. Chromatogr. Sci. 17 (1979) 152.
14. Lawrence, J.F., J. Chromatogr. Sci. 17 (1979) 147.
15. Kissinger, P.T., Bratin, K., Davis, G.C. and Pachia, L.A., J. Chromatogr. Sci. 17 (1979) 137.

16. Deelder, R.S., Koll, M.G.F., Beeren, A.J.B., and Van den Berg, J.H.M., *J. Chromatogr. Sci.* 149 (1978) 669.
17. Schwedt, G., *Angew. Chem. Int. Ed. Engl.* 18 (1979) 180.
18. Skeggs, L.T., Jr., *Amer. J. Clin. Path.* 28 (1957) 311.
19. Ruzicki, J. and Hansen, E.H., *Anal. Chim. Acta* 78 (1975) 145.
20. Little, C.J., Whatley, J.A. and Dale, A.D., *J. Chromatogr. Sci.* 171 (1979) 63.
21. International Conference on Flow Analysis, Sept. 11-13, 1979, Amsterdam, *Anal. Chim. Acta* 114 (1980).
22. Ruzicki, J. and Hansen, E.H., *Anal. Chim. Acta* 99 (1979) 37.
23. Van den Berg, J.H.M., Deelder, R.S. and Egberkink, H.G.M., *Anal. Chim. Acta* 114 (1980) 91.
24. Snyder, L.R., *Anal. Chim. Acta* 114 (1980) 3.
25. Schwartz, M.K., in *"Continuous Flow Analysis: Theory and Practice"*, (W.B. Furman, author), Marcel Dekker Inc., New York, 1976, p. iii.
26. Thiers, R.E., in *"Clinical Chemistry"*, (R.J. Henry, D.C. Cannon and J.W. Winkelman, Eds.), Chapter 10, Harper and Row, Hagerstown, Md., 1974.
27. Thiers, R.E. and Oglesby, K.M., *Clin. Chem.*, 10 (1964) 246.
28. Thiers, R.E., Bryan, J. and Oglesby, K., *Clin. Chem.* 12 (1966) 120.
29. Habig, R.L., Schlein, B.W.; Walters, L. and Thiers, R.E., *Clin. Chem.* 15, (1969) 1045.
30. Thiers, R.E., Meyn, J. and Wildermann, R.F., *Clin. Chem.* 16 (1970) 832.
31. Everson, M.A., Hicks, G.P. and Thiers, R.E., *Clin. Chem.* 16 (1970) 606.
32. Thiers, R.E., Reed, A.H. and Delander, K., *Clin. Chem.* 17 (1971) 42.

33. Begg, R.D., Anal. Chem. 43 (1971) 854.
34. Snyder, L.R. and Adler, H.J., Anal. Chem. 48 (1976) 1017.
35. Snyder, L.R. and Adler, H.J., Anal. Chem. 48 (1976) 1022.
36. Snyder, L.R., J. Chromatogr. 125 (1976) 287.
37. Taylor, G., Proc. Royal Soc. London, Ser. A, 219 (1953) 186.
38. Scott, R.P.W., and Kucera, P., J. Chromatogr. Sci. 9 (1971) 641.
39. Bender, M.K., American Lab., May (1980) 119.
40. Furman, W.C., in "Continuous Flow Analysis: Theory and Practice", Marcel Dekker, Inc., New York, 1976, p. 128.
41. Habig, R.L., Schelin, B.W., Walters, L. and Thiers, R.E., in "Advances in Automated Analysis", Vol. 1, Clinical Research, Mediad Inc., White Plains, NY, 1970, p. 139.
42. Neeley, W.E., Wardlaw, S.C., Yates, T., Hollingsworth, W.G., and Swinnen, M.E.T., Clin. Chem. 22 (1976) 227.
43. Furman, W.C., in "Continuous Flow Analysis: Theory and Practice", Marcel Dekker, Inc., New York, 1976, p. 223.
44. Sardesai, V.M., and Manning, J.A., Clin. Chem. 14 (1968) 156.
45. Royer, M.E., and Ko, H., Anal. Biochem. 29 (1969) 405.
46. Noble, R.P., and Campbell, F.M., Clin. Chem. 16 (1970) 116.
47. Levy, A.L., and Keyloun, C., in "Advances in Automated Analysis, Technicon International Congress 1969", (E.C. Barton, Ed.), Mediad, New York, NY 1970, p. 497.
48. Soloni, F.G., Clin. Chem. 17 (1971) 529.
49. Holub, W.R., Clin. Chem. 19 (1973) 1391.
50. Martin, P.J., Clin. Chim. Acta 62 (1975) 79.
51. Thomas, J.F., Sanborn, E.N., Mukai, M. and Tebbens, B.D., Ind. Eng. Chem. 51 (1959) 774.



52. Wayne, L.G. and Bryan, R.J., DHEW (NIOSH) Publication No. 77-117, Cincinnati, OH, 1976.
53. Finklea, J.R., DHEW (NIOSH) Publication No. 77-126, Cincinnati, OH, 1976.
54. Kane, L.E. and Alarie, Y., Am. Ind. Hyg. Assoc. J. 38 (1977) 509.
55. Yao, C.C. and Miller, G.C., DHEW (NIOSH) Publication No. 79-118, Cincinnati, OH, 1979.
56. Heylin, M. (Ed.), Chem. Eng. News, Oct. 22, 1979, p. 7.
57. Heylin, M. (Ed.), Chem. Eng. News, March 31, 1980, p. 28.
58. Lindstedt, G., Nature 156 (1945) 448.
59. Guthrie, R.D., in "Methods in Carbohydrate Chemistry", Vol. 1, (R.L. Whistler and M.L. Wolfrom, Eds.), Academic Press, New York, 1962, p. 432.
60. Vaskovsky, V.E. and Isay, S.V., Anal. Biochem. 30 (1969) 25.
61. Bell, D.J., J. Chem. Soc. (1948) 992.
62. Sawicki, E. and Sawicki, C.R., in "Aldehydes-Photometric Analysis", Vol. 1, Academic Press, New York, 1975, p. 10.
63. Nash, T., Biochem. J. 55 (1953) 416.
64. Sawicki, E. and Carnes, R.A., Mikrochim. Acta (1968) 148.
65. Sawicki, E. and Carnes, R.A., Mikrochim. Acta (1968) 602.
66. Hantzsch, A., Ber. 17 (1884) 1515.
67. Hantzsch, A., Ber. 18 (1885) 2579.
68. Belman, S., Anal. Chim. Acta 29 (1963) 120.
69. Vorländer, D. and Strauss, O., Justus Liebig's Ann. Chem. (1899) 375.
70. Vorländer, D. and Kalkow, F., Justus Liebig's Ann. Chem. (1899) 356.

71. Vorländer, D. and Erig, J., Justus Liebig's Ann. Chem. (1897) 284.
72. Vorländer, D., Z. Anal. Chem. 77 (1929) 241.
73. Vorländer, D., Z. Angew. Chem. 42 (1929) 46.
74. King, F.E. and Felton, D.G.I., J. Chem. Soc. (1948) 1371.
75. Ericson, C., Acta Pharm. Suecica 5 (1968) 283, C.A. 80: 16903c.
76. MacFadyen, D.A., Watkins, H.D. and Anderson, D.R., J. Biol. Chem. 158 (1945) 107.
77. Winter, M. and Demole, E., Helv. Chim. Acta 44 (1961) 271.
78. Sasamura, Y. and Morita, S., Tomakomai Koggokto Semmon Gakko Kigo 10 (1975) 21, C.A. 86:164855j.
79. Gray, G.M., in "Lipid Chromatographic Analysis", 2nd Ed. (Ed. G.V. Marinetti), Marcel Dekker, N.Y., 1976, p. 897.
80. Branther, A., Vamos, J. and Vegh, A., Gyogyszereszet 17 (1973) 457, C.A. 80:90931h.
81. Young, J.C., J. Chromatogr. Sci. 130 (1977) 392.
82. Selin, S., J. Chromatogr. Sci. 136 (1977) 271.
83. Compton, B.J. and Purdy, W.C., Anal. Chim. Acta (1980) in press.
84. Compton, B.J. and Purdy, W.C., Can. J. Chem. (1980) in press.
85. Combes, A. and Combes, C., Bull. Soc. Chim. Fr. 3 (1892) 778.
86. Lacy, M.J., Aust. J. Chem. 23 (1970) 841.
87. Erikson, J.M. and Biggs, H.G., J. Chem. Ed. 50 (1973) 631.
88. Greenhill, J.V., J. Chem. Soc. C (1971) 2699.
89. Haley, C.A.C. and Maitland, P., J. Chem. Soc. (1951) 3155.
90. Wilson, B.D., J. Org. Chem. 28 (1963) 314.

91. Horning, E.C. and Horning, M.G., J. Org. Chem. 11 (1946) 95.
92. Pitea, D. and Favini, G., J. Chem. Soc., Perkins Trans. II. 291 (1971).
93. Vanag, G.Y. and Stankevich, E.I., Zhur. Obshcheikhim. 30 (1960) 3287.
94. Dioxon, K. and Greenhill, J.V., J. Chem. Soc., Perkins Trans. II (1973) 164.
95. Pitea, D. and Favini, G., J. Chem. Soc., Perkins Trans. II (1972) 142.
96. Eiden, F. and Iwan, J., Arch. Pharm. 306 (1973) 470.
97. Balicki, R. and Nantka-Namirski, P., Pol. J. Pharmacol. Pharm. 26 (1974) 647.
98. Holtclaw, H.F., Jr., Collman, J.P. and Alire, R.M., J. Amer. Chem. Soc. 80 (1958) 1100.
99. Brown, N.M.D. and Nonhebel, D.C., Tetrahedron 24 (1968) 5655.
100. March, J., in "Advanced Organic Chemistry: Reactions, Mechanisms, and Structure", McGraw-Hill Book Co., N.Y., 1968.
101. Jackson, E.L., Org. Reactions 2 (1944) 341.
102. Benton, C.A., in "Oxidation in Organic Chemistry", Vol. 1, Academic Press, Inc., N.Y., 1965, pp: 367-407.
103. Bobbit, J.M., Adv. Carbohydrate Chemistry 11 (1956) 1.
104. Dryhurst, G., in "Periodate Oxidation of Diol and Other Functional Groups", Pergamon Press, Oxford, 1970.
105. Jefferies, D. and Fresco, J., J. Chem. Ed. 51 (1974) 545.
106. Dixon, J.S. and Lipkin, D., Anal. Chem. 26 (1954) 1092.
107. Pyman, F.L. and Stevenson, H.A., J. Chem. Soc. 78 (1956) 2489.
108. Fleury, P. and Boisson, S., Compt. Rend. 204 (1937) 1264.

109. Fleury, P. and Boisson, S., J. Pharm. Chim. 30 (1939) 145, 307.
110. Fleury, P. and Boisson, S., Compt. Rend. 208 (1939) 1509.
111. Sprinson, D.B. and Chargoff, E., J. Biol. Chem. 164 (1946) 433.
112. Wolfram, M.L. and Bobbit, J.M., J. Am. Chem. Soc. 78 (1956) 2489.
113. Biggs, H.G., Erikson, J.M. and Morrehead, W.R., Selected Methods of Clinical Chemistry, Vol. 8, (J.S. King, Ed.) AACC, Washington, D.C., 1977.
114. Vaskovsky, V.E. and Isay, S.V., Anal. Biochem. 30 (1969) 25.
115. Godicke, W. and Gerike, U., Mikrochim. Acta (1972) 603.
116. Hough, L. and Woods, B.M., Chem. and Ind. (1957) 1421.
117. Lindstedt, G., Nature 56 (1945) 448.
118. Crouthamel, C.E., Meek, H.V., Martin, D.S. and Banks, C.V., J. Am. Chem. Soc. 71 (1949) 3031.
119. Fieser, L.F., Fields, M. and Lieberman, S., J. Biol. Chem. 156 (1944) 191.
120. Karrer, P. and Hirohata, R., Helv. Chim. Acta 16 (1933) 959.
121. Christie, W.W., in "Topics in Lipid Chemistry", Vol. 3 (F.D. Gunstone, Ed.), John Wiley, N.Y., 1972, p. 171.
122. Sheppard, A.J. and Iverson, J.L., J. Chromatogr. Sci. 13 (1975) 448.
123. Glass, R.L., Lipids 6 (1971) 919.
124. Christopherson, S.W. and Glass, R.L., J. Dairy Sci. 52 (1969) 1289.
125. Nandet, M., Rev. Ferment. Ind. Aliment. 14 (1959) 268.
126. Hanahan, D.J., in "Lipide Chemistry", John Wiley, N.Y. 1960.

127. Rollet, A.Z., *Physiol. Chem.* 61 (1909) 210.
128. Shinowara, G.Y. and Brown, J.B., *Oil Soap* 15 (1938) 151.
129. Bottcher, C.J.F., Woodford, F.D., Boelsmavan Hante, E. and van Gent, C.M., *Rec. Trav. Chim.* 78 (1959) 794.
130. Weigel, W., *Hoppe-Seyler's Z. Physiol. Chem.* 353 (1972) 113.
131. Kuksis, A., in *"Handbook of Lipid Research"*, Vol. 1 (A. Kuksis, Ed.), Plenum Press, N.Y. (1978) p. 2.
132. Dawson, R.M.C., *Biochem. J.* (1960) 75.
133. Snyder, L.R. and Adler, H.J., *Anal. Chem.* 48 (1976) 1017.
134. Furman, W.C., in *"Continuous Flow Analysis: Theory and Practice"*, Marcel Dekker, Inc., New York, 1976, pp. 119-169.
135. Snyder, L., Levine, J., Stoy, R. and Conetta, A., *Anal. Chem.* 48 (1976) 942A.
136. Lovelock, J.E., in *"Gas Chromatography"* (R.P.W. Scott, Ed.) Butterworth, London, 1960, p. 26.
137. Gehrke, C.W., Baumgartner, J.H. and Ussary, J.P., *J. Ass. Offic. Anal. Chem.* 49 (1966) 1213.
138. Gehrke, C.W., Kaiser, F.E. and Ussary, J.P. in *"Automation in Analytical Chemistry, Technicon Symposia 1967"*, Vol. 1 Mediad, Inc., White Plains, N.Y., 1968, p. 239.
139. Gehrke, C.W., Killingley, J.S. and Wall, L.L., Sr., *J. Ass. Offic. Anal. Chem.* 55 (1972) 467.
140. Gehrke, C.W., Kaiser, F.E. and Ussary, J.P., *J. Ass. Offic. Anal. Chem.* 51 (1968) 200.
141. Nozoye, H., *Anal. Chem.* 50 (1978) 1727.
142. Olansky, A.S. and Deming, S.N., *Clin. Chem.* 24 (1978) 2115.
143. Ruzicka, J. and Hansen, E.H., *Anal. Chim. Acta* 106 (1979) 207.

APPENDIX 4-AComparison of Lutidine Standards with Age

The standard lutidine was made up as 1 mg/mL in methanol and compared seven months later with another newly made standard. The comparison procedure was to dilute 50  $\mu$ L of the standards to 2 mL with methanol. Results are expressed as absorptivity of the sample.

	a	S.D.	(n=5)
Old (7 months)	$6.89 \times 10^3$	( $\pm 0.338$ )	
New (1 h old)	$7.37 \times 10^3$	( $\pm 0.092$ )	

The literature value is  $7 \times 10^3$ . The standard is expected to be sensitive to light and thus stored in a bottle blacked out with aluminum foil.

APPENDIX 4-B

In standardization of formaldehyde the reaction sequence was applied to P.C. dipalmitoyl trilaurate, glycerol, phosphoglycerol and the old and new lutidine standards.

The standards were made up as:

				$a(\pm S.D.) \times 10^{-3}$
P.G.	$1.00 \times 10^{-3} M$	in water		2.17 ( $\pm 0.04$ )
P.C.	$1.00 \times 10^{-3} M$	in isopropanol		2.65 ( $\pm 0.11$ )
T.G.	$5.07 \times 10^{-4} M$	in isopropanol		4.71 ( $\pm 0.14$ )
Glycerol	$5.00 \times 10^{-4} M$	in isopropanol		5.87 ( $\pm 0.21$ )
Old lutidine	$5.20 \times 10^{-3} M$	in methanol		3.68 ( $\pm 0.18$ )
New lutidine	$5.30 \times 10^{-3} M$	in methanol		4.18 ( $\pm 0.22$ )
Formaldehyde	$1.0 \times 10^{-3} M$	in water		4.11 ( $\pm 0.50$ )
Methanol, isopropanol and water blanks				
Procedure (n=4).				

To 0.5 mL of sample was added 0.2 mL NaMeO\* and allowed to sit 10 min. Next 0.5 mL NaIO<sub>4</sub> was added and allowed to react 10 min. Then Flr-P was added (0.5 mL) and read at  $\lambda_{410}$  after 30 sec with a solvent blank. The apparent molar absorbances are given above for (n=4) runs. The results are taken as indicating that the formaldehyde standard made from

the 36% stock was adequate for use in these studies.

\*NaOMe 9.0 gm/L MeOH and filtered before use.

NaIO<sub>4</sub> 5.32 gm/L in 114 mL/L acetic acid-water.

Flr-P 0.18 M in CH<sub>3</sub>CN.



## 5. EVALUATION AND COMPARISON OF TWO CHROMATOGRAPHIC DETECTORS FOR THE DETERMINATION OF TRIGLYCERIDES AND PHOSPHOLIPIDS

### 5.1 INTRODUCTION

In this chapter two detectors are evaluated for use as chromatographic monitoring systems for triglycerides and phosphatidylcholine molecular species. One is the commercially available Schoeffel SF770 ultraviolet absorbance detector (UV) used in Chapter 2. The other is the post-column reactor detector (p.c.r.) described in Chapter 4.

The features of these detectors of interest are:

- 1) Selectivity-measured as response ( $R_D$ ).
- 2) Sensitivity-measured as the solute detection limit ( $C_{SDL}^D$ ).
- 3) Linear-dynamic range.
- 4) Sources and magnitude of noise.
- 5) Practical considerations of availability and ease of operation of the detector.

### 5.2 THE ULTRAVIOLET ABSORBANCE DETECTOR (UV)

Detectors based on ultraviolet absorption are most widely used of all for h.p.l.c. (1, page 142). The general operating characteristics of h.p.l.c.-UV detectors have been investigated (2,3) and reviewed (4). The unit used in this

study was the Schoeffel Model SF770 with GM770 monochrometer, a variable wavelength unit schematically represented in Fig. 5-1. This unit is marketed by Schoeffel Instrument Corp., 24 Booke, St., Westwood, NJ 07675).

This detector's mode of operation is by measuring transmitted light through two matched "Zee" type flow cells (Fig. 5-2), one the analytical and the other the reference cell, and taking the difference of the log intensity of transmitted light as the basis for analyte quantitation. This process can be described in terms of the absorption of radiation starting with the Boltzmann distribution

$$I = I_0 \exp(-\epsilon_{\lambda} bc) \quad (5-1)$$

where  $I$  = intensity of transmitted radiation at  $\lambda$ ,  
 $I_0$  = intensity of incident radiation at  $\lambda$ ,  
 $\epsilon_{\lambda}$  = absorptivity of the absorbing analyte at  $\lambda$ ,  
 $b$  = radiation path length through the sample,  
 $c$  = concentration of absorbing analyte.

Since  $A$ , the absorbance, is defined (5) as

$$A = \log I_0 / I \quad (5-2)$$

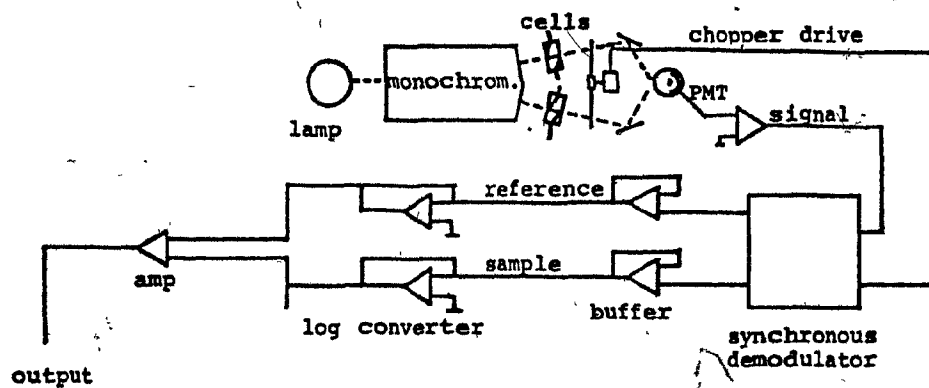


Figure 5-1. Scheffé SF770 schematic of signal flow and function diagram. Modified from the manual.

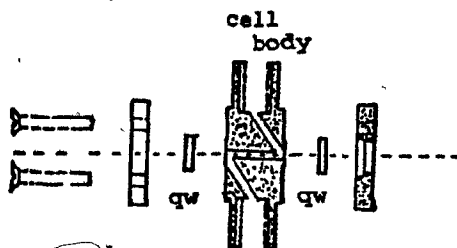


Figure 5-2. Scheffé SF770 absorption detector "Zee" cell design. (qw are the quartz windows).

and from Eqn. (5-1)

$$\ln I_0 I^{-1} = \epsilon_{\lambda} bc \quad (5-3)$$

combining Eqn. (5-2) and Eqn. (5-3) gives the usual form of the Beer - Lambert Law

$$A = abc \quad (5-4)$$

where  $a$  is the absorptivity of the absorbing analyte and is dependent on the wavelength of the absorbed radiation.

Because the SF770 is designed symmetrically with respect to the reference and sample cell (Fig. 5-1),

$$I_0(\text{sample}) = I_0(\text{reference}) \quad (5-5)$$

and thus if 1 refers to sample and 2, reference, then

$$\log I_0 I_1^{-1} = A_{\text{solvent}} - A_{\text{sample}} \quad (5-6)$$

$$\log I_0 I_2^{-1} = A_{\text{solvent}} \quad (5-7)$$

or on subtracting Eqn. (5-6) from Eqn. (5-7)

$$A_{\text{sample}} = \log I_1 - \log I_2 \quad (5-8)$$

The logarithmic amplifiers of the SF770 do the log conversion shown in Eqn. 5-8 and the subtraction is done using an operational amplifier circuit.

#### 5.2.1 Selectivity

The selectivity of the ultraviolet absorbance detector is one of its distinguishing features and can be discussed in reference to the Beer-Lambert Law, Eqn. (5-4). Since  $a$  is a function of the wavelength of the transmitted radiation as well as the nature of the analyte, the detector selectivity is a function of the experimental parameter of wavelength setting of the detector and the intrinsic absorptivity of the analyte. The class of compounds studied here all contain acyl moieties and are derivatives of either glycerol or substituted phosphoglycerol. The detector response  $R_{uv}$  can be described by

$$R_{uv} = a_{\lambda} C_s DV \quad (5-9)$$

where  $a_{\lambda}$  is the absorptivity of the analyte at the detector wavelength setting,  $C_s$  is the concentration of the sample of triglyceride or phospholipid,  $D$  is the chromatographic dilution factor, and  $V$  is the volume of sample injected while  $b$  in Eqn. (5-4) is assumed to be unity. The absorptivity  $a_{\lambda}$  can be expressed by

$$a_{\lambda} = \sum a_x, a_y, a_z, a_g \quad (5-10)$$

where  $a_x, a_y$  refer to absorptivity of isolated and conjugated double bonds,  $a_z$  to other chromophores substituted on the acyl moieties (i.e., epoxides, hydroxyl, etc.) while  $a_g$  refers to the absorptivity of the glycerol or phosphoglycerol moiety. Equation (5-10) assumes the respective chromophores are not an auxochrome of the other. Some representative absorptivities for polyenes are shown in Table 5-1.

The absorptivity of  $a_x$  and  $a_y$  can be predicted from the quantum mechanical "particle in a box" model by the relationship (6)

$$a_{x,y} = \frac{32Ne^2 l^2 \nu}{3\pi h c^2,000} \quad (5-11)$$

where  $l$  is the length of the box,  $N$  is Avogadro's number,  $e$  is the electronic charge,  $h$  is Planck's constant,  $c$  is the velocity of light and  $\nu$  is the frequency of the incident radiation. For the purpose of simplifying notation,  $a_x$  and  $a_y$  are combined as  $a_{x,y}$ . If  $l$  is assumed to be approximated by

$$l = kD_b \quad (5-12)$$

where  $k$  is the unit length of the carbon double bond and  $D_b$  is the number of double bonds in the total molecule, then

Table 5-1: Lowest energy  $\pi$ - $\pi^*$  absorption bands of polyene aldehydes  $[\text{CH}_3-(\text{HC}=\text{CH})_n-\text{CHO}]$  and acids  $[\text{CH}_3-(\text{HC}=\text{CH})_n\text{CO}_2\text{H}]$ . Taken from reference 5, page 72.

Aldehydes	n	$\lambda_{\text{max}}$ (nm), dioxane	a
	1	217	15,000
	2	270	27,000
	3	312	40,000
	4	343	40,000
	5	370	57,000
	6	393	65,000

Acids	n	$\lambda_{\text{max}}$ (nm), hexane	a
	1	208	12,500
	2	261	25,600
	3	303	36,500
	4	332	~48,00

Eqns. (5-11) and (5-12) combine to give

$$a_{x,y} = cD_b^2 \quad (5-13)$$

where  $c$  is the constant  $^{32}\text{Ne}^2 k^2 v (3\pi h c l, 000)^{-1}$ .

The usefulness of Eqn. (5-13) resides in the ability to predict the value of  $a_{x,y}$  for the acyl portion of triglycerides or phospholipids at constant wavelength ( $c/v$ ). The absorptivities presented in Table 5-1 indicate that both  $\lambda_{\text{max}}$  and  $a$  increase with increasing  $D_b$ . This information is of little use with fixed wavelength measurements. As will be experimentally shown, the major contributing chromophores to  $a_\lambda$  at the experimentally chosen wavelength of 195 nm are those whose absorptivities are represented by  $a_{x,y}$ .

### 5.2.2. Sensitivity

The sensitivity of the detector can be described in terms of its lower detection limit, which in turn is determined by the detector response, Eqn. (5-9), and the baseline noise in the same frequency domain as  $R_{uv}$ . As was discussed in Chapter 1, the signal-to-noise ratio (SNR) can be used as a basis for describing the lower detection limit.



The signal ( $R_{uv}$ ) can be predicted from Eqn. (5-9) and Eqn. (5-13). The noise of interest is described in the following sections. The lower detectable signal is defined as twice the  $2\sigma$  noise and is given from Eqns. (5-9) to (5-13) to be, as a SNR expression,

$$SNR = 32Ne^2 k^2 D_b^2 v C_s DV (3,000\pi hc(25))^{-1} \quad (5-14)$$

or if  $C_{SDL}^{uv}$  is the solute concentration at  $SNR = 2$ ,

$$C_{SDL}^{uv} = 6000\pi hc 26 (32Ne^2 k^2 D_b^2 v DV)^{-1} \quad (5-15)$$

Inspection of Eqn. (5-15) indicates that the detection limit for glycerides and phospholipids is predicted to be inversely proportional to the square of the number of double bonds in the molecular species.

### 5.2.3. The Linear Dynamic Range

The upper analytically useful range of the detector, as presented in Chapter 1, was given as the upper concentration where the linear relationship of signal to concentration varies by greater than 5%. This value can be experimentally determined by the appropriate standard concentration versus response determination over a large concentration range. The

SF770 has a lower and upper range of  $4 \times 10^{-4}$  AU (the typical measured  $2\sigma$  noise) to 2 AUFS. Deviations from the Beer-Lambert law depend on both experimental and chemical characteristics of the system. The instrumental characteristics are non-linearity in the detector optical-electronic components due to the very high absorbances and thus low transmittances of light through the flow cells at high sample concentrations. The chemical limitations originate at high solute concentrations and cause deviations from ideal solution behavior.

An additional consideration unique to the use of detectors for on-line chromatographic monitoring is the effect of column saturation (column loading on the partition isotherm) on eluting band shape. When column saturation occurs the assumption allowing use of peak height measurements for quantitation no longer applies and the non-linear relationship between peak height and sample amount is interpreted as non-linear detector response.

In summary, while the detection limit was presented as being an inverse function of  $a_{x,y}$  Eqn. (5-8), the upper detection limit is not expected to be a function of  $a_{x,y}$  but rather a function of concentration  $C$  or, more specifically, when  $C$  is no longer related to  $R_{uv}$  in Eqn. (5-9) due to either chemical or chromatographic reasons. The upper range of the detector is dependent on  $a_{x,y}$  only when instrumental deviations are responsible for non-linearity of

$R_{uv}$  versus C.

#### 5.2.4 Operating Characteristics of the SF770

The general operating characteristics of h.p.l.c. absorbance detectors (2,3) are summarized in Table 5-2. The SF770 was previously described in some detail (7) and its operating characteristics are summarized in Table 5-3. The SF770 compares favourably to other absorbance detectors with respect to the 2σ noise reported for typical absorbance detectors. The optical band pass (5 nm) and cell volume (8 μL) are typical of h.p.l.c. detectors and emphasize the nature of the signals as arising from molecular absorbance bands and highly efficient columns, respectively. The Schoeffel SF770 is not expected to be unique and can be substituted with any number of commercially available units. Wavelength calibration of the SF770 monochromator is given in Appendix 5A.

#### 5.3 THE POST-COLUMN REACTOR

The design and development of the post-column reactor (p.c.r.) was described in Chapter 4. The actual detector response originates from fluorescence intensity measurements and thus this aspect of the detector will be discussed here. The fluorescence detector used in conjunction

Table 5-2: Typical Operating Characteristics of Ultraviolet Absorption Detectors.

Linear dynamic range	$.5-1 \times 10^4$
Lower detection limit	$1 \times 10^{-9} \text{ gm} \cdot \text{mL}^{-1}$
$2\sigma$ noise	$2 \times 10^{-4} \text{ AU}$
drift (low frequency noise)	less than $5 \times 10^{-5} \text{ AU} \cdot \text{h}^{-1}$
Optical density range	0.01-2.54 AU full scale deflection

Table 5-3: Operating Characteristics of the Schoeffel Model  
SF770.

Wavelength range	190-630 nm
source	deuterium (190-400) and tungsten (350-630) lamps
Optical bandpass	5 nm half band width
2 $\sigma$ noise ( $\lambda_{280}$ nm)	$5 \times 10^{-4}$ AU*
Drift	$5 \times 10^{-4}$ AU·h <sup>-1</sup>
Cell Volume	8- $\mu$ L
Optical Path length	1.0 cm

\*Measured with dry nitrogen.

with the p.c.r. was the Schoeffel Spectrofluorometer Model FS970 with GM770 monochromator (Schoeffel Instrument Corp., 24 Booke St., Westwood, NJ).

A schematic representation of the operation and design of the FS970 and its cell is shown in Fig. 5-3 and Fig. 5-4, respectively. The signal from the detection cell is monitored by a photo-multiplier tube and associated amplifier circuit.

The relationship of fluorescence signal to analyte concentration is (5)

$$F = k_{f,n} \phi_{fn} (abc) \quad (5-16)$$

where  $\phi_{fn}$  is the fluorescence quantum efficiency of species  $n$  defined as

$$\phi_{fn} = \frac{\text{photons emitted} \cdot \text{sec}^{-1}}{\text{photons absorbed} \cdot \text{sec}^{-1}} = \frac{\text{photons emitted}}{\text{photons absorbed}} \quad (5-17)$$

and the term  $(abc)$  is derived from the Beer-Lambert law and accounts for the photons absorbed. The constant  $k_{f,n}$  is an instrumental factor accounting for the total efficiency of the FS970 in monitoring the fluorescence signal and is dependent on the optical and electrical design of the unit.

The Eqn. (5-16) is used in the response expression

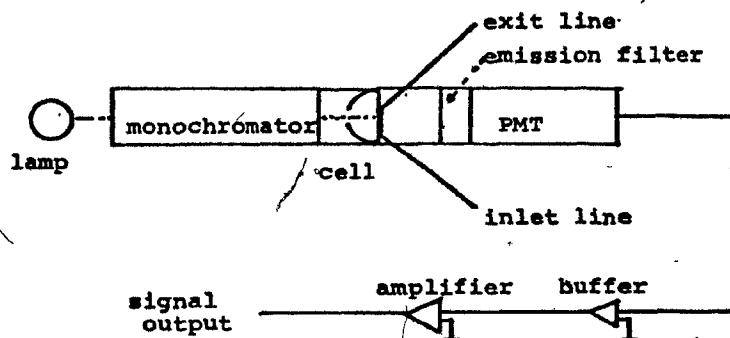


Figure 5-3. Scheeffel FS970 schematic of signal flow and function diagram.

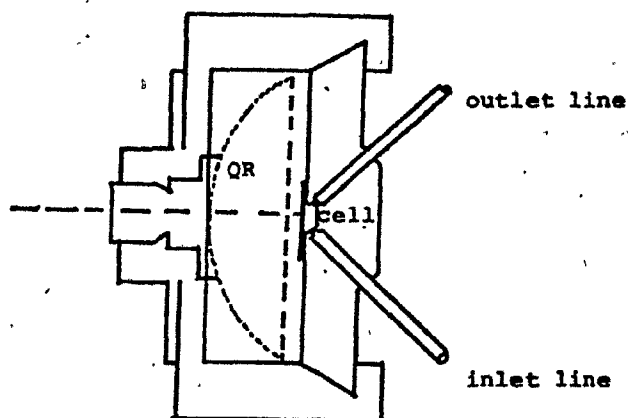


Figure 5-4. Scheeffel FS970 frontal fluorescence cell and chamber design.

$$R_{FLR,n} = k'_n C_s DV \quad (5-18)$$

where  $k'_n$  is  $abk_{f,n} \phi_{fn}$  and DV are the chromatographic dilution and injected volume terms as in Eqn. (5-9). Equation (5-18) is only applicable in describing fluorescence response for dilute (less than  $10^{-4}$  M) solutions of  $C_s DV$  since at higher concentrations changes in  $k'_n$  are expected.

The use of Eqn. (5-18) in this work requires an additional term to account for the p.c.r. portion of the detector. The effect of the p.c.r. is

$$C_{PCR,n} = k_{PCR,n} C_{s,n} \quad (5-19)$$

where  $C_{PCR,n}$  is the concentration of formaldehyde resulting from the chemical reactions of the p.c.r. on n, and  $k_{PCR,n}$  is the efficiency of the p.c.r. with respect to conversion of n to formaldehyde as well as the additional effects of band-spreading and solute dilution in decreasing  $C_{PCR}$ . The term  $k_{PCR,n}$  thus has two components, one resulting from the chemistry and the other the hydrodynamics of the p.c.r. Combining Eqn. (5-18) and Eqn. (5-19) gives

$$R_{Flr,n} = k'_n k_{PCR,n} C_{s,n} DV \quad (5-20)$$



or

$$R_{Flr,n} = k_n C_{s,n}^{DV} \quad (5-21)$$

where  $k_n$  is the combined constant  $k_n' k_{PCR,n}$  and  $C_{s,n}$  refers to species  $n$ .

When doing fluorescence measurements, some factors to consider are the role of impurity quenching (such as oxygen, which at the  $10^{-3}$  M concentration level decreases fluorescence by approximately 20% (8)), and the role of temperature (approximately a 1% decrease in  $F/^\circ\text{C}$  increase in temperature (8)).

### 5.3.1 Selectivity

The selectivity of the p.c.r. detector is determined by the p.c.r. and the FS970 portion of the detector. Thus the detector will detect any compound convertible by the p.c.r. or with endogenous fluorescence excitation and emission similar to lutidine ( $\lambda_{410}^{510}$ ). The response of the detector to triglycerides and phospholipids can be determined, by Eqn. (5-21). If  $k_n$  is the same for all TG and PL then the detector is a molar response detector for these two classes of compounds. This p.c.r. detector was specifically designed for this role.

### 5.3.2 Sensitivity

The sensitivity of the detector, if defined as for the UV detector, is determined by the SNR expression. The noise associated with the detector can be expressed as

$$N_{2\sigma} = k'_b k_{PCR,b} C_b P_b \phi_{cb} \quad (5-22)$$

where  $k'_b k_{PCR,b}$  are as for Eqns. (5-18) and (5-19) except here refer to  $b$  rather than  $n$ ,  $C_b$  is the concentration of chemical species  $b$  in the system as background, and  $P_b \phi_{cb}$  is a function associated with the peristaltic pump noise and mixing in the p.c.r., respectively, a general function describing the overall efficiency of the p.c.r. units reagent delivery and mixing components. This function is expected to have a complex nature and is made up of the sum of the fundamental noise components associated with the p.c.r.

The SNR expression is, from Eqns. (5-21) and (5-22)

$$SNR = k_n C_{s,n} (k'_b k_{PCR,b} C_b P_b \phi_{cb})^{-1} \quad (5-23)$$

where  $k'_b k_{PCR,n}$  and  $k_n$  may not be identical.

Equation (5-23) can be simplified to

$$SNR = K_{SNR} C_{s,n} C_b^{-1} \quad (5-24)$$

where  $K_{\text{SNR}} = k_n (k'_b k_{\text{PCR},b} P_b \phi_{cb})^{-1}$ . Thus the sensitivity of the detector is directly related to the ratio  $C_{s,n}/C_b$ . The lower detection limit for the detector can be defined in terms of the 2 $\sigma$  noise level so that

$$C_{\text{SDL},n}^{\text{FLR}} = 2C_b K_{\text{SNR}}^{-1} \quad (5-25)$$

where  $C_{\text{SDL},n}^{\text{FLR}}$  is the concentration of analyte detected at the detection limit.

### 5.3.3 Linear Dynamic Range

The linear dynamic range of the detector is determined by the p.c.r. and fluorescence contributions to this detector characteristic. Optimization of the p.c.r. chemistry was done assuming each reaction stage involved kinetics which remained constant (with respect to order) regardless of the degree of reaction. For the linearity of Eqn. (5-21) to be valid,  $k_{\text{PCR},n}$  must be independent of concentration. This is not expected to be true for high concentrations of the solute  $n$ , specifically when the concentration of  $n$  approaches the concentration of the reagents used in the p.c.r.

The linearity of Eqn. (5-21) also depends on  $k'_n$  being independent of concentration. At high concentrations of  $n$

the inner filter effect (also called concentration quenching effect (8)) is expected to affect  $k_{f,n}$  and thus  $k'_n$  and  $k_n$  are not expected to be constant at high solute concentrations. The lower range of the detector is determined by the lower detection limit as described in the context of the detector sensitivity.

#### 5.3.4 Operating Characteristics of the Schoeffel FS970

The operating characteristics of the FS970 have not been described previously. The novel feature of this detector, compared to other spectrofluorometric detectors for h.p.l.c., is the cell design. The frontal fluorescence design is unique since most fluorescence detectors are based on cylindrical flow cells with detection of emitted radiation occurring at right angles to excitation. This conventional design is convenient from the standpoint of detector construction but has limitations with respect to instrumental sensitivity since only a small fraction of the emitted radiation is detected. The frontal fluorescence cell enables, with the use of the quartz reflectance sphere (Fig. 5-4), a larger percentage of emitted radiation to be detected. Thus the FS970 is expected to have greater sensitivity than other spectrofluorometric detectors if the detector SNR is signal limited and the predominant contribution to noise is from

dark current. If the detector is noise limited from the same source as the signal then the FS970 will have similar sensitivities to other spectrofluorometric detectors.

The FS970 used for excitation a Corning filter 7-59 (transmission max. 370 nm, band pass 140 nm) and monochrometer set at excitation 410 nm, 0.5 nm half band pass (calibrated as described in Appendix 5A). For emission filters 480 and 550 nm (standard from Schoeffel) which are both high pass filters with 50% T at the wavelengths cited, were ganged together. The excitation band pass of the instrument was such that it did not overlap with the emission profile to greater than an estimated 0.001%.

#### 5.4 A COMPARISON OF THE DETECTOR RESPONSES

Experimental and theoretical based comparisons of the absorbance and fluorescence detectors (9) for h.p.l.c. have indicated that the order of sensitivity for these detectors is the reverse of the order of their selectivities. The expected detection limits for these detectors are shown in Table 5-4. The response ( $R_D$ ) and detection limit expressions ( $C_{SDL}^D$ ) for these detectors are summarized in Table 5-5 in their extended forms.

When comparing each detector expressions, it is apparent that selectivity plays a very large role in the response and detection limit expression. The UV detectors

Table 5-4: Reported detection limits for h.p.l.c. detectors

	$C_{SDL}^D$ <sup>1</sup> , theoretical	$C_{SDL}^D$ , practical
Filter photometer	$2 \times 10^{-10}$	$2 \times 10^{-9}$
Spectrophotometer	$6 \times 10^{-10}$	$6 \times 10^{-9}$
Spectrofluorometer	$1.8 \times 10^{-14}$	$1 \times 10^{-10}$

<sup>1</sup>In moles/L.

Table 5-5: Summary of the detection limit and response expressions for the ultraviolet absorption and p.c.r. detectors.

$$C_{SDL}^{uv} = \frac{Z_{uv} \sigma}{D_b^2 DV}, \quad Z_{uv} = \frac{6000 \pi h c}{32 N e^2 \lambda^2 v} \quad (5-26)$$

$$C_{SDL,n}^{Flr} = \frac{Z_{Flr} C_b^P (\phi_{cb})}{K_{PCR,n} DV}, \quad Z_{Flr} = \frac{2 k_b^k k_{PCR,b}}{2.3 K_{f,n} \phi_{f,ab}} \quad (5-27)$$

$$R_{uv} = \frac{32 N e^2 k^2 D_b^2}{3000 h c} C_s DV \quad (5-28)$$

$$R_{Flr,n} = (2.3 a b k_{PCR,n}^k k_{f,n} \phi_{f,n}^k k'_n) C_s DV \quad (5-29)$$

$R_{UV}$  and  $C_{SDL}^{UV}$  are a function of  $D_b^2$  of the compound detected. The fluorescence detector is the more selective and, because of the post-column reactor chemistry, the  $R_{FLR,n}$  and  $C_{SDL,n}^{Flr}$  are independent of the molecular weight of the acyl glyceride or phospholipid. All the detectors are expected to give responses which change in a direct proportion with the concentration or solute present in the eluent.

Because the post-column reaction is a molar-response detector, a relationship based on this molar response can be derived and may be useful in determining the identity of the solute being detected. This relationship is the detector's response ratio taken from Eqns. (5-28) and (5-29) and is

$$R_{Flr}^{uv} = \frac{C}{a} D_b^2 \quad (5-30)$$

where  $a = 2.3 ab k_{PCR,n} k_{f,n} \phi k'_n$

$$C = 32Ne^2 k^2 v (3000hc)^{-1}.$$

This expression is generally useful, being independent of the chromatography of the system as well as the amount of solute injected.



## 5.5 EXPERIMENTAL

The experiments described here were designed to evaluate the UV and p.c.r. detectors for the on-line detection of triglycerides and phospholipids. This involved utilizing the chromatographic information and equipment described in Chapter 2 and the detectors described previously in this and Chapter 4. Primary emphasis is placed on the evaluation of the p.c.r. detector since it is novel.

### 5.5.1 Equipment

The same equipment described in Chapters 2 and 4 was used in this section. The detector arrangements were such that the UV detector (Schoeffel SF770) was always placed directly after the column, the post-column reactor of Chapter 4 next, replacing the refractive index detector in Fig. 2-1. Data involving detector response ratios were taken from this configuration.

### 5.5.2 Chemicals

All solvents and standards were identical to those used in Chapters 2 and 4. Numerous triglyceride or phospholipid standard mixtures were made by combining volumes of the standards listed in Tables 2-1 to 2-3. The standard mixtures.

referred to in this chapter are listed in Table 5-6. The mixtures were stored desiccated at  $-20^{\circ}\text{C}$  when not in use. P.C. dilinoleoyl or P.C. dilinolenoyl were ordered from Sigma in anticipation of their being used. Some standards were received in partially degraded form and were discarded. Those which contained only minor amounts of degradation products (total amount estimated to be less than 5% of the parent lipid) were used without further purification. As mentioned in Chapter 2, the degradation of these unsaturated lipids has been the subject of much study and the degradation products are detectable using h.p.l.c. and the UV detector. In the standards used these products were not detectable with either the differential refractive index (Chapter 2) or p.c.r. detectors. All other synthetic lipids were found to give one band using the RI and p.c.r. detectors.

### 5.5.3 Methods

The sources of noise and background in the p.c.r. of Chapter 4 were investigated in a descriptive manner. This was done by noting noise and background in the optimized continuous-flow analyzer (exact conditions in text) under a variety of conditions such as during successive addition of reagents, cycling of the pumps and heaters and observing the effect of gas bubbles clearing through the flow cells.

Table 5-6: Triglyceride and phospholipid standards used for the detector evaluations.

N	TG-I Concentration (M)	N	PL-I Concentration (M)
13	Triolein $2.25 \times 10^{-3}$	1	Dihexanoyl $5.24 \times 10^{-4}$
11	Trilinolein $2.30 \times 10^{-3}$	3	Didecanoyl $2.10 \times 10^{-3}$
		8	Dioleoyl $1.51 \times 10^{-3}$
		9	Dilinoleoyl $1.50 \times 10^{-3}$
		10	Dilinolenoyl $1.50 \times 10^{-3}$
	TG-II		
5	Trimyristin $5.53 \times 10^{-3}$		
4	Trilaurin $6.26 \times 10^{-3}$		
10	Tripalmitolein $4.99 \times 10^{-3}$		
11	Trilinolein $4.60 \times 10^{-3}$		
	TG-III		
3	Tricaprin $7.20 \times 10^{-3}$		
4	Trilaurin $6.26 \times 10^{-3}$		
5	Trimyristin $5.53 \times 10^{-3}$		
10	Tripalmitolein $4.99 \times 10^{-3}$		
	Separate TG Standards		
4	Trilaurin $6.26 \times 10^{-3}$		
10	Tripalmitolein $4.99 \times 10^{-3}$		
13	Triolein $4.50 \times 10^{-3}$		
14	Tripetroselinin $4.52 \times 10^{-3}$		

The observations on the effects of gas bubbles led to an alternative to gas-debubbling described in Chapter 4. This was to allow bubbles to pass through the detector cell by applying electronic filtering to select for the desired signal. A choice between using the absorbance or fluorescence detector for monitoring the p.c.r. was made on the basis of experimentation with comparing the responses of the two detectors in the optimized p.c.r.

The general method employed for detector evaluation was to inject varying amounts of standard into the chromatographic system. Three general classes of experiments were run.

1) Detector Response versus Sample Amount Injected.

Standards TG-I and PL-I were used to determine the relationship between amount of standard injected and detector response,  $R_D$ . This was done by injecting between 2 and 25  $\mu\text{L}$  of a standard mixture into the system and monitoring the detector responses. Chromatographic conditions for all experiments are summarized in Table 5-7. Responses are reported as peak height measured from a line defining the top boundary of the baseline noise to the upper most deflection of the detector response. These responses are reported as absorbance units (at 195 nm) and relative fluorescence intensity response and are self consistent within each experiment.

Table 5-7: Chromatographic conditions used to evaluate the detectors.

Column: 5  $\mu\text{m}$   $\text{C}_6$  reversed phase, in-lab designed.

Temperature:  $60 \pm 1^\circ\text{C}$

Flow Rates: 1  $\text{mL}\cdot\text{min}^{-1}$  for UV detector

0.5  $\text{mL}\cdot\text{min}^{-1}$  when the PCR is used

Eluent: varied as follows

Standard	Eluent Composition*
TG-I	100% $\text{CH}_3\text{CN}$
TG-II and III	90 $\text{CH}_3\text{CN}/10\text{H}_2\text{O}$
TG-10 and 11	95 $\text{CH}_3\text{CN}/5\text{H}_2\text{O}$
TG-4 and 6	90 $\text{CH}_3\text{CN}/10\text{H}_2\text{O}$
PL-I	95 $\text{CH}_3\text{CN}/5\text{H}_2\text{O}/0.1$ conc. $\text{H}_3\text{PO}_4$

\*See Chapter 2 for full description.

Noise levels were measured directly off the chromatograms by drawing two parallel lines that border the peak-to-peak noise. The noise was measured over three peak base widths of the broadest chromatographic band.

2) Response Ratio of the Detectors.

The detector response ratio,  $R_{Flr}^{UV}$  was investigated using standards TG-II and PL-I. This involved making injections of 2-10  $\mu$ L of standard mixture into the chromatographic unit. Injections were repeated between 6 and 15 times ( $n = 6$  to 15) and the mean and standard deviation are reported.

3) The Evaluation of the p.c.r. Detector.

The standard mixtures TG-III and PL-I as well as the separate TG standards were used to evaluate the p.c.r. detector response  $R_{Flr,n}$  and selectivity. This involved repetitive ( $n = 5$ ) injections of 10- $\mu$ L volumes of the separate TG standards or PL-I mixture ( $n = 3$ ). The mixture TG-III and PL-I were also used to illustrate the selectivity of the p.c.r. with respect to detection of these lipids in the presence of large amounts of the solvent chloroform.

The response of the p.c.r., when given in terms of peak areas, was calculated using the relationship of height ( $h$ ) to base ( $b$ ) of an equilateral triangle ( $area = 1/2 hb$ ). This method was used because of the relatively low SNR encountered with the amounts of sample used in these studies. The use of low concentrations of standards was necessary

and is discussed at the end of this chapter.

## 5.6 RESULTS AND DISCUSSION

### 5.6.1 Origins of Noise in the P.C.R.

Possible sources of noise were observed to be:

- a) Proportioning pump pulsations
- b) Heating bath cycling
- c) Particles in the detector cells
- d) Bubbles in the detector cells
- e) Switch or relay noise and 60 Hz line pick-up

and are illustrated in Fig. 5-5.

#### Proportioning Pump Pulsations

The proportioning pump (Technicon Pump III) used in this study was not pulseless and a periodic noise (Fig. 5-5A) of frequency approximately .1 Hz was noted from this source. However, due to the nature of the p.c.r. unit being multi-channel, each line contributed noise of a slightly different phase. Thus, adding additional lines to the p.c.r. gave a variety of noise patterns. For instance, when adding reagent Fluoral-P through each of the three stages in succession, the traces shown in Fig. 5-6 showed that the frequency characteristics and amplitude of the noise varied as a function of the fundamental noises and their relative phase. This

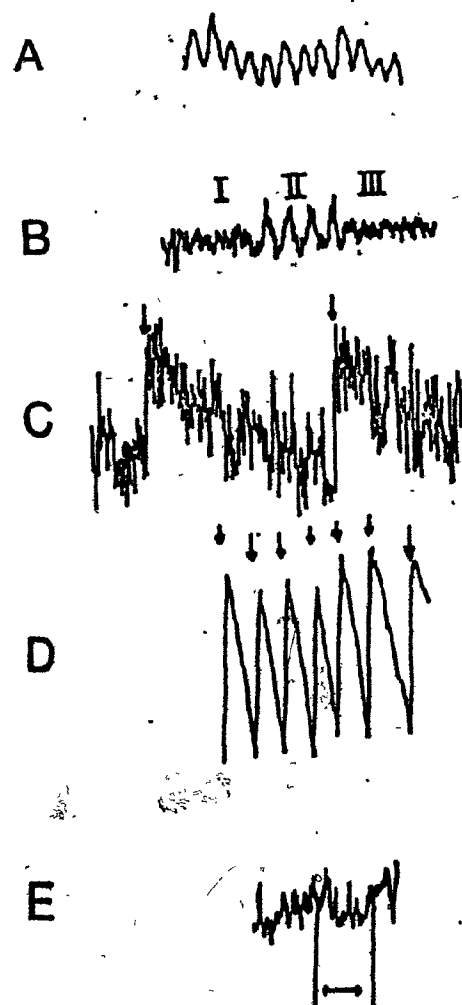


Figure 5-5. Recorder traces of some representative noise patterns observed for different sources in the p.c.r. Arrows in C and D indicate where bubble was observed to be dislodged from the cell. Arrow in E indicates spikes from electrical source.

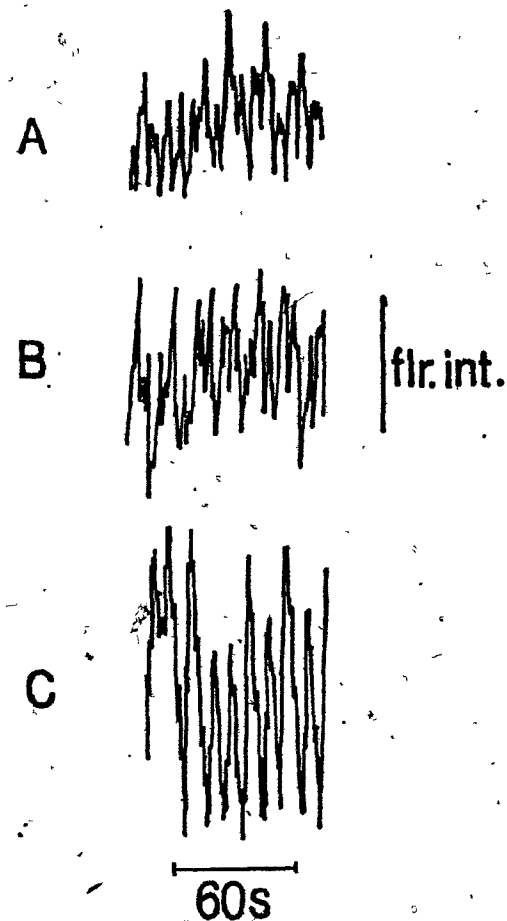


Figure 5-6. Effect of adding reagent Fluoral-P successively through reactor stages III (A), II (B), and I (C) on baseline noise.



is also shown in Fig. 5-7 where Fluoral-P reagent was added through one channel of the peristaltic pump while the Waters 6000A pump (a pulseless source) was used to vary the background signal by varying the amount of acetonitrile used to mix with the Fluoral-P reagent. The range of 1.1-2.0 mL/min  $\text{CH}_3\text{CH}$  is shown and illustrates that while white noise is decreasing in general (as seen by a lowering of average background) the amplitude and frequency of the noise was variable and corresponded to phasing of the various fundamental noise sources. Generally speaking,  $1/f$  noise was observed to decrease as white noise decreased if  $1/f$  noise originated from the same source as the white noise. However, the effects of fundamental noise complicated the relationship.

Proportioning-pump noise was found to be the greatest single source of noise in the p.c.r. because of the frequency over which it occurred. Since signals for the p.c.r. were of the same order of frequency as the proportioning pump noise, discriminating against this noise was not possible.

#### Heating Bath Cycle

A very common source of noise was that due to cycling of the heating bath. As illustrated in Fig. 5-5B, the on-off cycle of the bath used to incubate the p.c.r. manifold contributed noise in the 0.01 Hz range. In this baseline

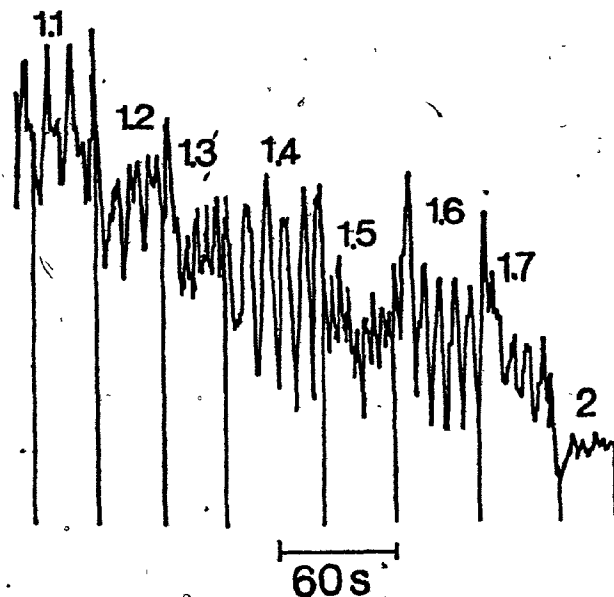


Figure 5-7. Baseline noise as a function of different dilution levels of Fluoral-P reagent (0.42 mL/min). Dilution was accomplished using the Waters 6000A pump and water with flow rates indicated (mL/min).

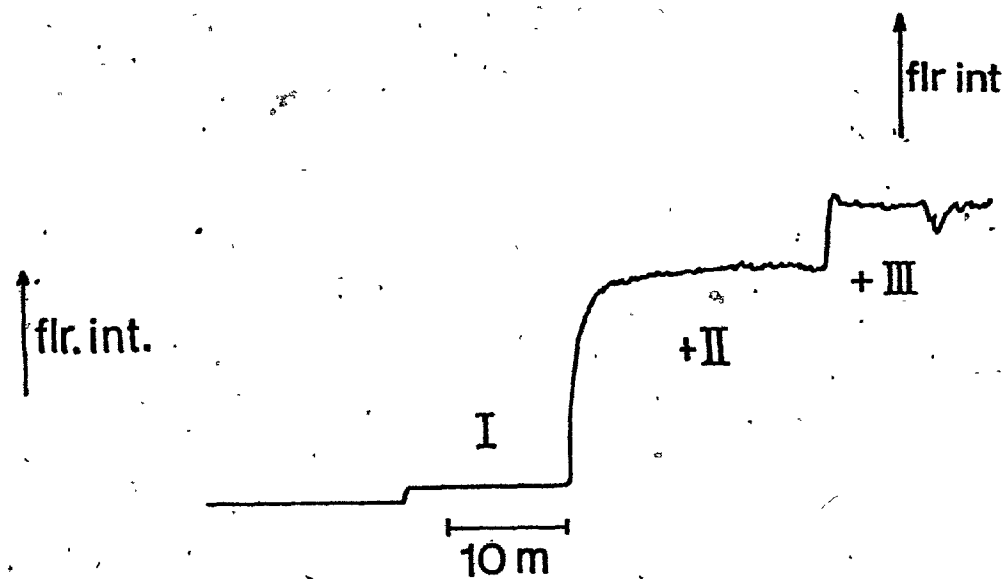


Figure 5-8. Successive addition of reagents (Stages indicated) and the effect on baseline and noise. Conditions are for the optimized manifold.

trace I corresponds to the heating approaching the thermostat set-point of 60°C. When cycling begins (II) periodic noise is seen. In III the heater has been turned off. To eliminate this source of noise the heating bath was insulated and kept full at all times. This resulted in longer bath cycles, outside the frequency range of interest.

#### Particles in the Detector Cell

Particles in the optical path of the spectrophotometer were characterized by extremely high background (white noise) and originated from precipitation of reagents in the p.c.r. and the leaching of plasticizers from pump tubing (especially polyvinyl chloride). Changing reagent composition or tubing eliminated this source of noise.

#### Bubbles in the Cells

The type of noise associated with bubble formation in the detector cells was characterized by high absorbance and background in the absorbance detector and by 1/f noise in the fluorescence detector. Examples of the formation of a bubble in the fluorescence detector cell are illustrated in Fig. 5-5C and Fig. 5-5D. In the first example (Fig. 5-5C) bubble growth in the fluorescence cell can be seen to occur by the decrease in background signal and then the sudden shift to greater background as the bubble is dislodged. A fundamentally similar process is shown in Fig. 5-5D except that much greater background (as white noise) is present

due to the application of reagents to the p.c.r. The noise associated with this type of process was noted to always be a function of background. This is not surprising when considering the mechanism of the noise being a function of change in the fluorescence cell surface and volume. This source of noise was eliminated by allowing bubbles to pass through the fluorescence detector cell. Thus this  $1/f$  noise was replaced by one of much greater frequency (from approximately 0.01 Hz to 3 Hz) and was treated by electronic filtering.

#### Switch and Relay Noise and 60 Hz Line-Pickup

This source of noise was usually synchronous and could vary from relatively high (60 Hz line) to low (0.01 Hz heater or refrigerator cycling) frequency. The heater noise previously discussed was due to temperature effects of the p.c.r. Relay noise associated with the heating cycle is shown in Fig. 5-5E and is characterized by spikes in the detector response. Line pick-up at 60 Hz was also noted for the recorder and was characterized by hum. Neither of these noise sources were treated by filtering since they originated in the recorder. Isolating the detector and recorder leads, however, was effective in minimizing this source of noise.

### 5.6.2 Sources of Background and the Effects on Detection Limit

Figure 5-8 shows the contributions to fluorescence background that occur as each reagent line in the p.c.r. is added. The minimization of background is imperative in the p.c.r., because of the intimate relationship between background and noise.

To minimize background and the associated noise from this source a radical departure from the normal triglyceride manifold design was required. This involved elimination of all major sources of formaldehyde contamination such as alcohols and acetic acid. These were replaced with acetonitrile and phosphoric or perchloric acid, respectively.

The normal physiological range for triglycerides in serum is from zero to 1.5 gm/L (10). In terms of triolein the lower detection limits for the clinical triglyceride analyzers can be calculated for a recent system to be on the order of  $5 \times 10^{-5}$  moles injected (11). This illustrates that the conventional manifolds are concerned with upper rather than lower ranges in the analysis. The p.c.r. system described here should be far superior to the conventional models because of the care given to minimizing band spread and lowering detector noise. Investigating the p.c.r. with distilled water flowing through all channels and injecting standard lutidine gave a lower limit of detection (based on

0.0008  $\mu$ A being the  $2\sigma$  noise) of  $1.6 \times 10^{-10}$  moles lutidine. In the f.i.a. study of the Fluoral-P reagent (Chapter 4), formaldehyde was detected at the  $3 \times 10^{-9}$  moles per injection level. This system contained Fluoral-P and dilute phosphoric acid as the reagents and with the higher background compared to distilled water higher detection limit was found. The value of  $1.6 \times 10^{-10}$  moles can be taken as the absolute lower limit of detection for the system based on the Fluoral-P reagent and using fluorescence detection. A more realistic value for detection limit is  $3 \times 10^{-9}$  moles per injection because of the general nature of the experimental system and the requirement for the presence of reagents in the p.c.r.

### 5.6.3 Comparison of the Absorbance and Fluorescence Detectors for Use with the Post-Column Reactor

The complete p.c.r. was used for this evaluation and typical recorder output is shown in Fig. 5-9. The fluorescence detector was found to be far superior to the absorbance detector from the standpoint of signal-to-noise ratio. Thus the absorbance detector was only used with the p.c.r. during the optimization (Chapter 4).

The main problem associated with the absorbance detector was low frequency noise due to Schlieren bands in the p.c.r. stream. The design of the cell is such that it is

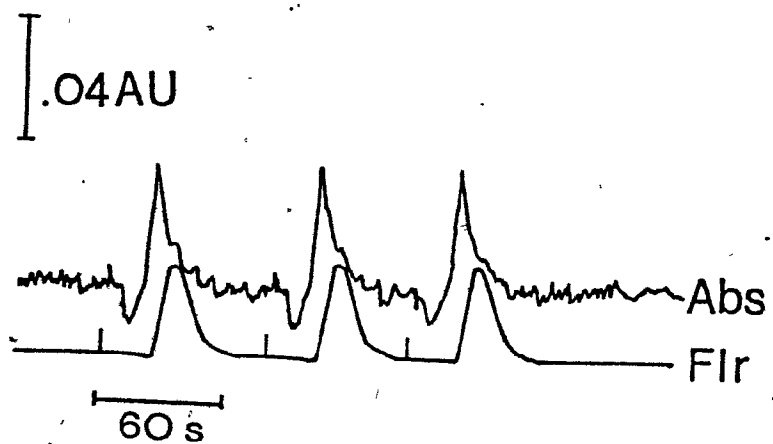


Figure 5-9. Direct comparison of absorbance (440nm) and fluorescence (410, 510 nm) detection of 25 nanomoles formaldehyde added to the optimized manifold. Baseline noise for fluorescence detection matched the absorbance at 50 times amplification.

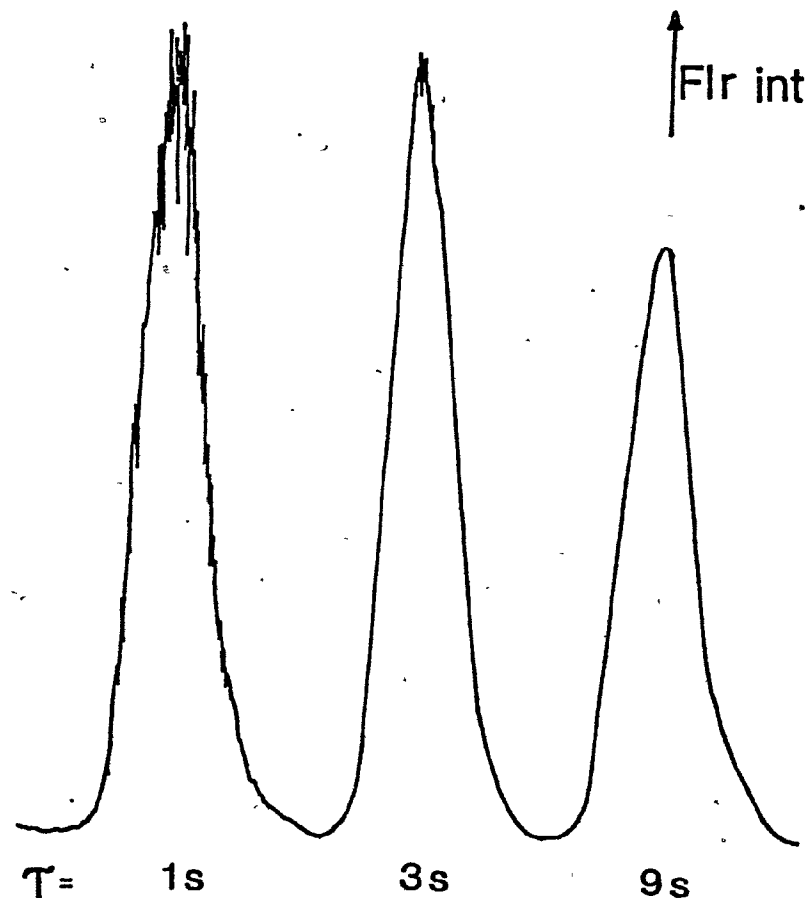


Figure 5-10. Recorder traces of fluorescence response to bubbled flow through at 1, 3, and 9 s filter time constant. The outputs were used to generate the results presented in Figure 5-11 and Table 5-8.

very sensitive to refractive index changes in the effluent and thus also effluent temperature. One cell design, the Taper cell<sup>TM</sup> of the Waters Model 440 Absorbance Detector (Waters Associates Inc., Maple Street, Milford, Mass. 01757) is claimed to be less sensitive to refractive index changes; however, attempts to fit such a cell to the SF770 failed. The Waters Model 440 was used in other parts of this work such as in monitoring the separations of the Nash and Sawicki reagents (Chapter 4).

#### 5.6.4 Evaluation of Bubbled and Debubbled Response in the SF970

The parameters which determine the sensitivity of the p.c.r. are:

- 1)  $2\sigma$  noise,
- 2) band dispersion properties ( $w_{1/2}$ ),
- 3) Signal (S).

The signal-to-noise ratio (SNR) determines to a great extent the sensitivity of the system.

When comparing the fluorescence and absorbance detectors, one finds a fundamental difference in the effects of gas bubbles on their respective responses. In the case of the SF770, a bubble scatters the sample beam causing a maximum absorbance signal to be measured. In the fluorescence



detectors (FS970) a negative response corresponding to a decrease in the frontal fluorescence cell surface area is seen. In both cases the frequency of the disturbance is the bubble frequency.

With respect to absorbance detection, the effect on the detector of a bubble is independent of the absorbance background. This is not true for the fluorescence detector since a decrease in emission rather than scatter causes the noise. Thus decreasing the background fluorescence ( $S_B$ ) can be used as a means of enabling bubbled flow to pass through the detector cell and thus eliminate the need for a debubbler. The bubbled versus debubbled mode of operating the fluorescence detector was examined.

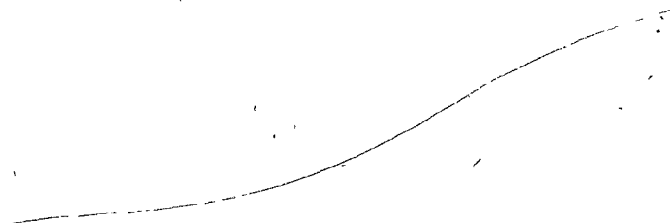
First, some justification should be given for eliminating the debubbler described in the previous sections. The FS970 was evaluated with and without the debubbler. Two features of the signal, signal height (H) and dispersion (here  $W_{1/2} = 2.354 \sigma$ ), were measured. The experimental data are summarized in Table 5-8. What is immediately apparent is that the debubbler increases band width at  $W_{1/2}$  by approximately 50% over the bubble-through-detector mode while the entire c.f.a. increases band width relative to the signal measured with the SF770 by 19%. Thus, the main contribution to band broadening in the p.c.r. is the debubbler.

Table 5-8: Comparison of various detector modifications on band dispersion ( $\bar{w}_{1/2}$ ) and concentration ( $\bar{H}$ ).

Mode	$\bar{w}_{1/2}$ (s)	(n)	$\bar{H}$	(n, %S.D.)**
1. Bubbles through detector	$17.5 \pm 0.89$	(8)	$123.6 \pm 7.6$	(8, 6.1%)
2. Bubbles eliminated	$26.0 \pm 0.76$	(8)	$33.5 \pm 5.4$	(8, 16.1%)
3. SF770 response ( $\lambda_{195nm}$ )	$14.7 \pm 0.78$	(19)	$0.097 \pm 0.0036$	(18, 3.7%)

\*  $\tau = 4$  s.

\*\* Fluorescence intensity for 1 and 2, not comparable to absorbance units for 3.



The development of electronic debubblers and bubble-gates as mentioned in the previous Chapter are thus quite understandable.

Another parameter of interest, peak height ( $H$ ), is affected greatly by debubbling where it is seen that a substantial signal decrease (approximately to 28% of the former value) is seen when the debubbler is used. This attenuation of  $H$  is due to dispersion and lack of efficient pull-through.

The relative standard deviation (S.D.) of the response was also affected by debubbling and as can be seen in Table 5-8 the SF770 has an S.D. of 3.7% and after the p.c.r. 6.1% for bubbled and 16.1% for the debubbled mode. An explanation for the high S.D. when using the debubbler is that even though all reagents are degassed and the segmentation gas is helium, bubble formation occurs in the SF970 and thus affects the effective volume and surface area of the cell. Thus elimination of the debubbling can be justified on the grounds of attaining better signal, less dispersion and better reproducibility. It is also noteworthy that the p.c.r. gives an increase in band dispersion of 11 sec (Table 5-8).

The Schoeffel FS970 is equipped with a one-stage active filter with variable time constant ( $\tau$ ) from 0-10 sec. The effect of varying  $\tau$  on detector response ( $H$ ) and dispersion

( $W_{1/2}$ ) is shown in Fig. 5-10 and summarized in Fig. 5-11 where a plot of  $\tau$  versus  $H$  and  $W_{1/2}$  is presented. The values as presented in Fig. 5-11 are normalized to 100.

An investigation of the associated peak-to-peak noise (represented as  $2\sigma$  noise from Chapter 1) versus  $\tau$  as measured over a two minute interval is shown in Fig. 5-12 for the conditions of low background ( $H_2O$  on-line) and the operating background (reagents on-line) when bubbled and debubbled. The results indicate that  $\tau = 4$  is sufficient for eliminating the major high-frequency portion of the noise and little is gained with respect to noise decrease at greater  $\tau$ . It is of interest to note that the noise profiles approximately parallel each other. This indicates that in both cases a high frequency noise is superimposed on a low frequency noise and is independent of effluent background signal. At  $\tau = 4$  a noise decrease of approximately 74% is seen when debubbling is used. This decrease is not enough to justify using a debubbler when one considers the effects of debubbling on  $H$ ,  $W_{1/2}$ , and the effect of gas bubbles on precision of  $S$ . Bubble formation in the cell did not occur with the SF770 detector if helium degassing and segmentation were used. It should be mentioned that the SF770 had inlet and outlet tubing of large diameter compared to the very small interior diameter of the inlet and outlet tubing of the FS970

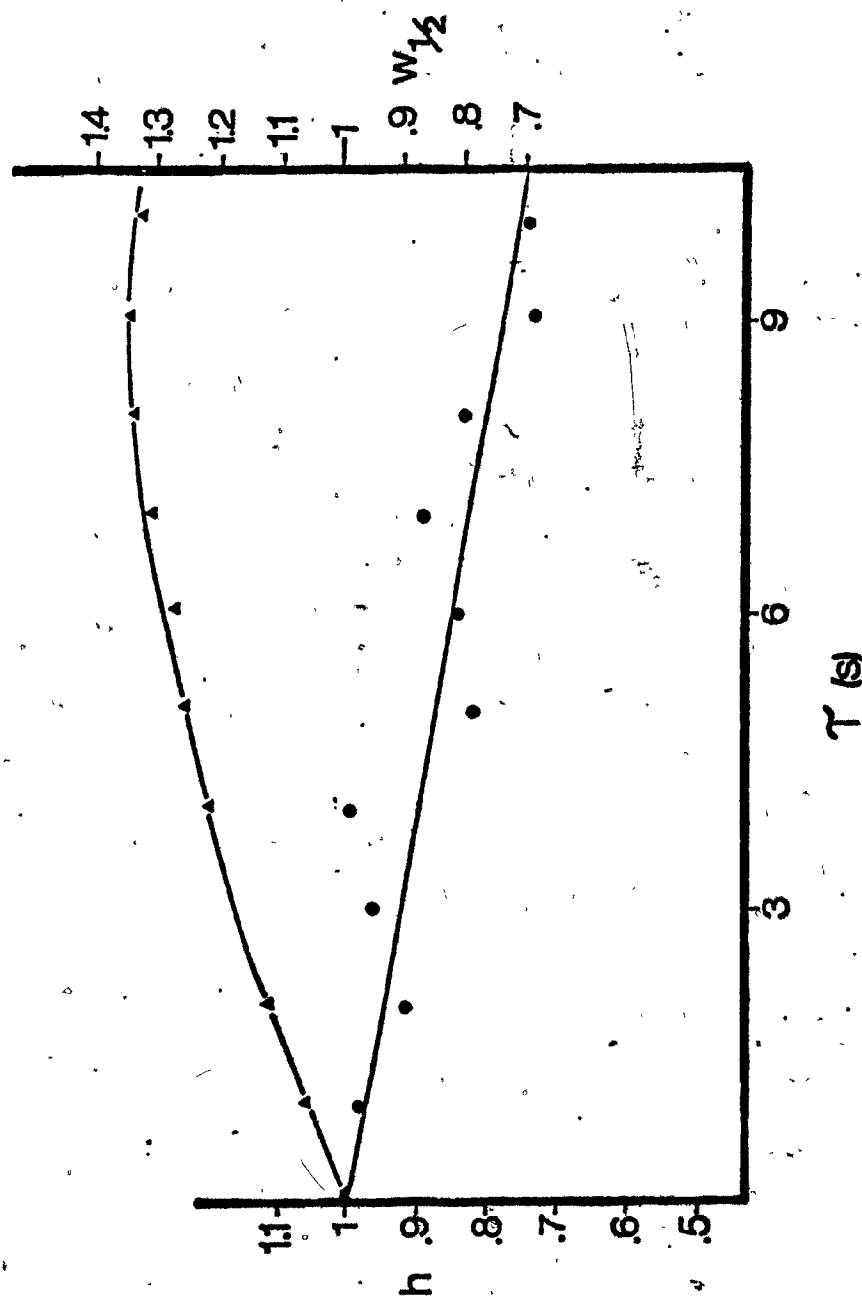


Figure 5-11. Effect on eluting bands height ( $h$ ) and dispersion ( $w_{1/2}$ ) of applying various filtering time constants  $\tau$ . ( $\circ$ ) =  $h$  and ( $\Delta$ ) =  $w_{1/2}$

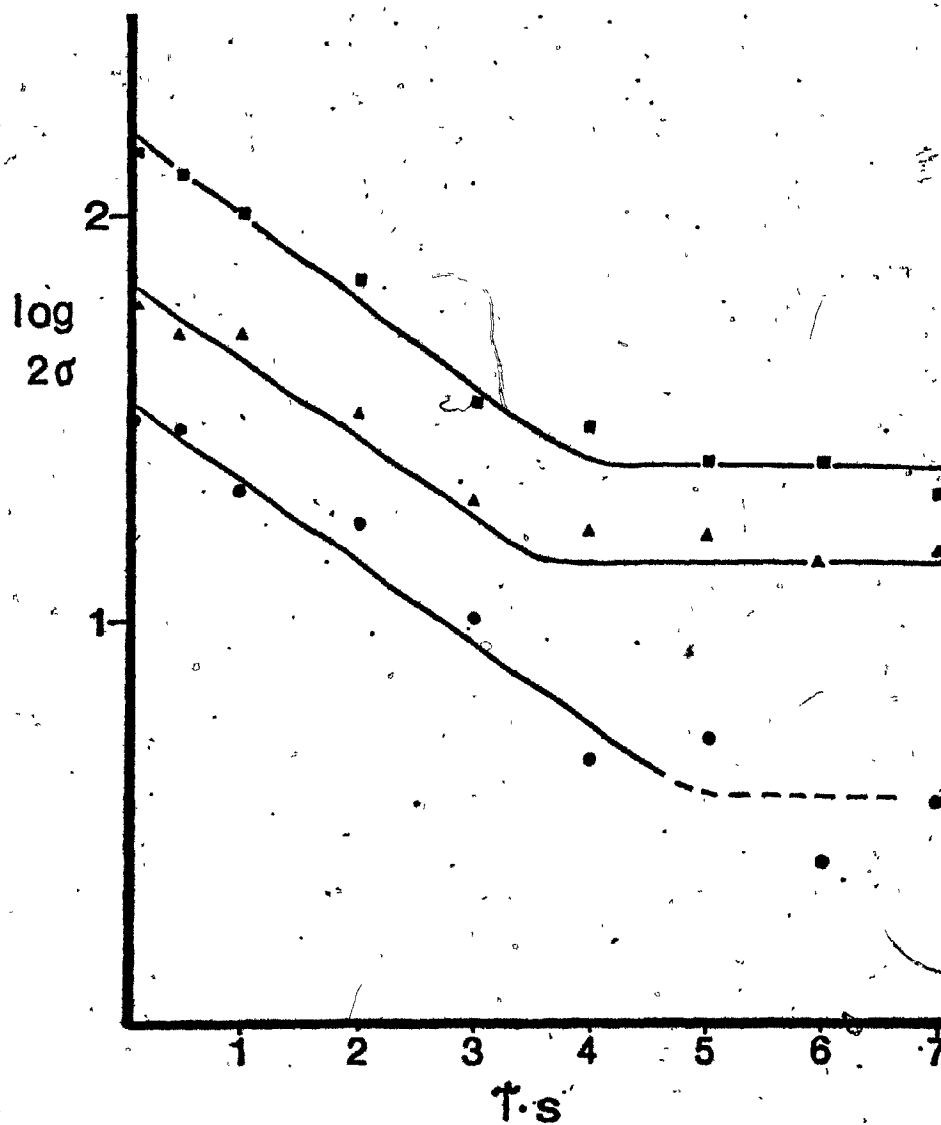


Figure 5-12. Relationship of filtering  $\tau$  on measured  $2\sigma$  noise of the RS970 with bubbled flow for water (●), only Fluoral-P (▲) and the total reagent system (■) through the optimized manifold.

(approximately 0.018 cm). This narrow diameter tubing was easily clogged and created additional problems of variable pull-through. Detector cells having moderately wide diameter tubing (approximately 0.03 cm) would not suffer from the unique problems of bubble formation and clogged inlets. However, for evaluation of the p.c.r. response, the debubbler was eliminated and bubbles were allowed to pass through the FS970 cell, filter time constant of 4 sec.

#### 5.6.5 Evaluation of the Detectors for H.P.L.C. of Triglycerides and Phospholipids

##### Evaluation of $R_D$

Reference to Eqns. (5-28) and (5-29) shows that  $R_D$  is expressed by the general form:

$$R_D = DF_D C_s V \quad (5-31)$$

where  $D$  is the chromatographic dilution factor,  $F_D$  is the respective detector response constant given in parenthesis in Eqns. (5-28) and (5-29), and  $C_s$  is the concentration of the standard. Thus a direct relationship between detector response  $R_D$  and volume of sample injected ( $V$ ) is expected.

The results showing  $R_D$  versus volume injected (given as amount of standard injected in moles, calculated

from the product  $VC_s$ ) are presented in Figs. 5-13 to 5-16, and summarized in Table 5-9. The 2 $\sigma$  noise levels are also indicated on each figure and enable calculation of the detection limit for each detector under the experimental conditions used to generate each standard curve.

The results show that good correlation exists between amount of lipid introduced and detector response  $R_D$ . Thus the general form of Eqn. (5-31) is correct. Inspection of Eqn. (5-31) also predicts that for any given detector condition ( $F_D$ ) and amount of solute injected ( $C_s V$ ), the chromatographic dilution factor  $D$  will determine  $R_D$ . This is seen for the p.c.r. data of the triglycerides and the p.c.r. and UV data of the phospholipids where the later eluting bands have lower detector responses (measured as  $B$ ).

The concentration ranges used for evaluating  $R_D$  were narrow. This was because of the limited solubility of the standards in the chromatographic mobile phase and the effect that chloroform, used to make up the standards, had on the p.c.r. It was noted that sample injections greater than 25  $\mu$ L gave a high probability of causing precipitation and blockage in the p.c.r. This effect is expected to be minimized if sodium hydroxide rather than potassium hydroxide is used for saponification. The precipitate is most likely potassium periodate; its sodium salt is more soluble in organic solvents.



Table 5-9: Linear regression analysis summary of standard curve data for Figures 5-13 to 5-16.

$$R_D = BV + A$$

Detector	Fig. 5-	Standard N	B	A	Linear condition Coefficient
Triglycerides					
UV	13	13	$3.4(\pm 0.63) \times 10^5$	$1.8(\pm 1.44) \times 10^{-3}$	0.9391
PCR	14	13	$9.9(\pm 0.74) \times 10^8$	$3.1(\pm 5.53) \times 10^{-1}$	0.9918
PCR	14	11	$2.5(\pm 0.10) \times 10^9$	$4.9(\pm 7.73) \times 10^{-1}$	0.9976
Phospholipids					
UV	15	9	$1.5(\pm 0.18) \times 10^6$	$4.1(\pm 4.2) \times 10^{-3}$	0.9735
UV	15	10	$5.3(\pm 0.30) \times 10^6$	$1.2(\pm 0.69) \times 10^{-1}$	0.9936
PCR	16	9	$3.8(\pm 0.17) \times 10^8$	$5.9(\pm 0.22)$	0.9972
PCR	16	9	$6.7(\pm 0.56) \times 10^8$	$7.5(\pm 0.73)$	0.9899

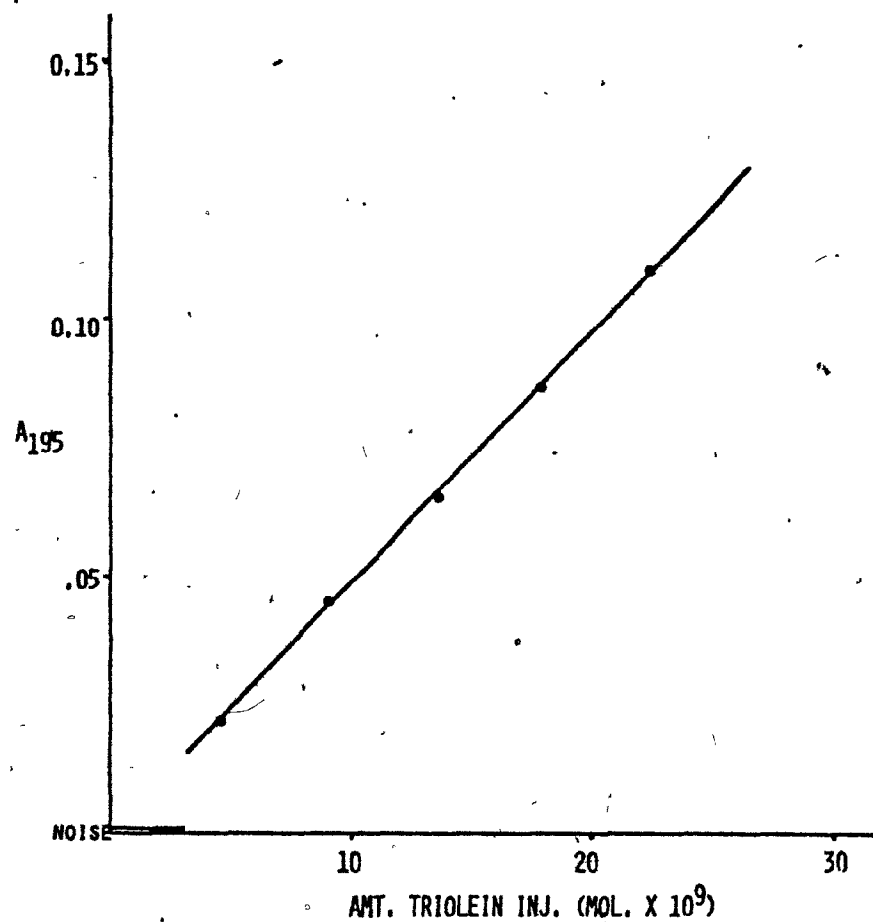


Figure 5-13. Response of Triolein (N-13) in the SP770 detector at 195 nm.

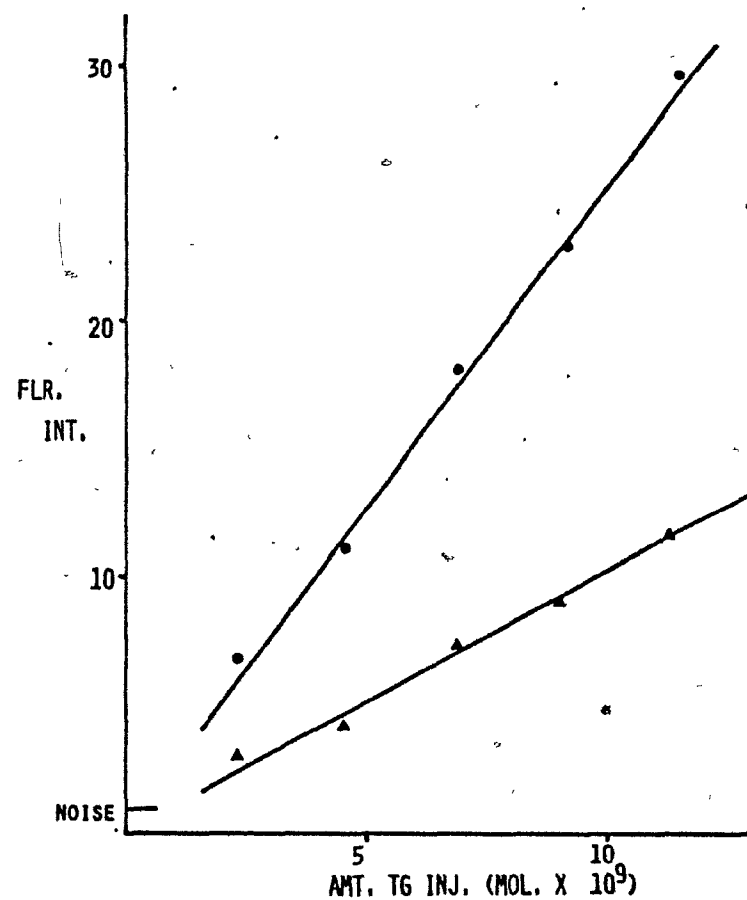


Figure 5-14. Response for Triolein (N-13) and Trilinolein (N-11) in the p.c.r. detector. (▲) = 13 and (●) = 11.

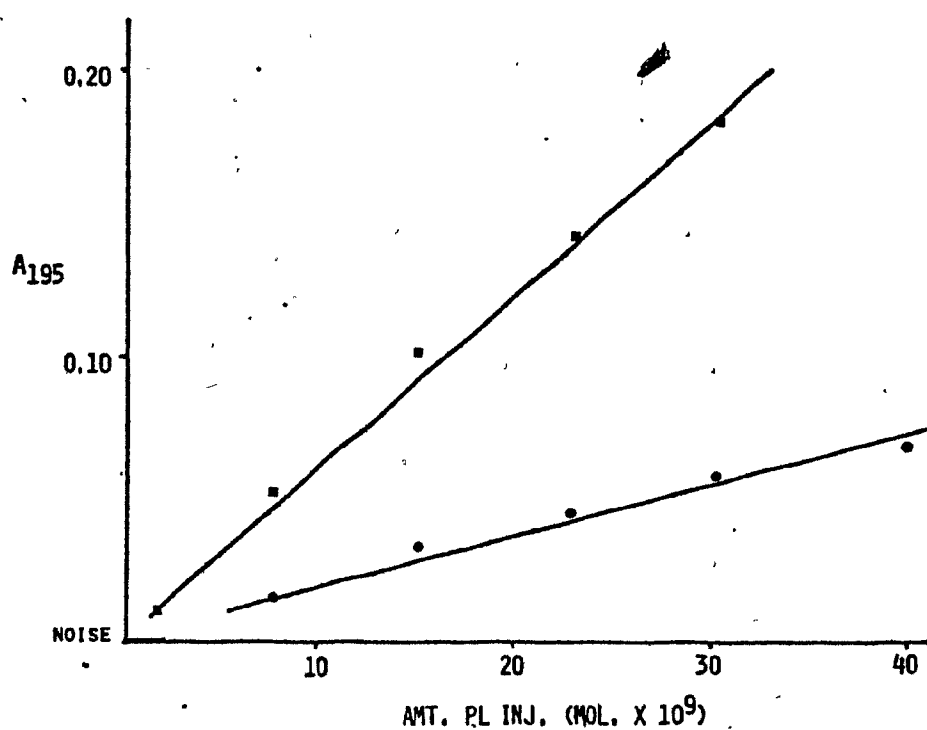


Figure 5-15. Response of PC-dilinoeoyl (•, N=9) and PC-dilinolenoyl (■, N=10) in the UV detector, 195 nm.

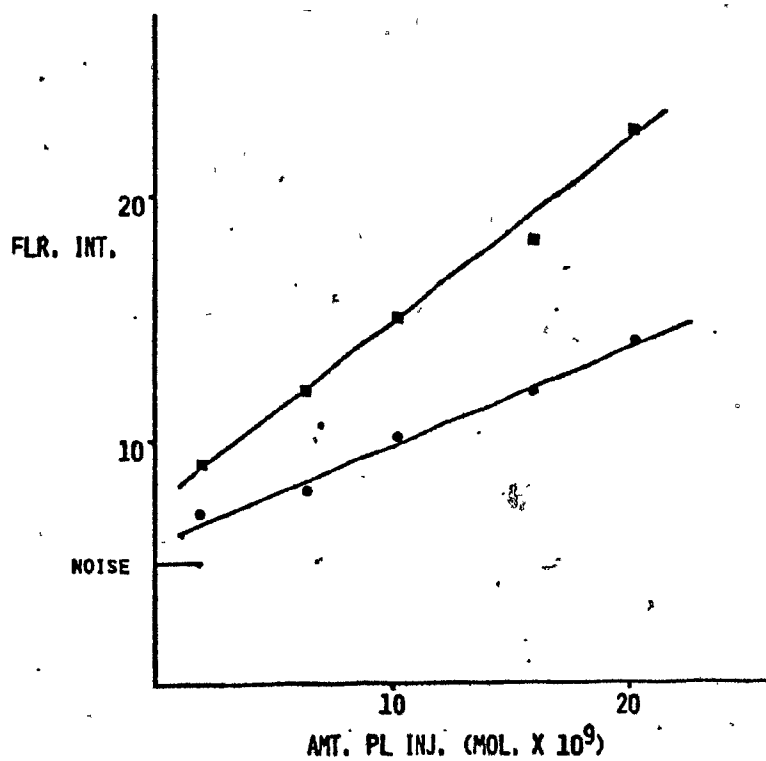


Figure 5-16. Response of PC-dilinoeoyl (•, N=9) and PC-dilinolenoyl (■, N=10) in the p.c.r. detector.

The concentration range used in this study shows the great sensitivity of the post-column reactor. Standards were characterized in the lower nanomole range.

#### Evaluation of $C_{SDL}^D$

The detection limits are presented in Table 5-10. These values are inversely related to  $D$ , the chromatographic dilution factor and the values calculated for Table 5-10 were based on eluting bands with  $k'$  values of between 5-15. The most useful  $k'$  ranges are from 1-10 (1, page 69) and thus these detection limits are realistic if not conservative figures. One detector characteristic of interest and related to improvement (decrease) in  $C_{SDL}^D$  is the stability of the detector baseline. The uv detector, at high sensitivity settings, showed some drift. This drift is associated with fundamental noise sources such as long term thermal fluctuations and pressure changes. The p.c.r. detector on the other hand showed no drift and was noise limited by higher frequency noise.

The  $C_{SDL}^D$  data are expressed in units of moles/L and correspond to the concentration of standard in the detector, and not the amount injected being detectable and giving  $R_D$  of twice the  $2\sigma$  noise. The use of concentration units is for ready comparison of  $C_{SDL}^D$  since the chromatographic dilution factor is taken into account. The results indicate that the p.c.r. detector is at least as sensitive as the UV detector

Table 5-10: Detection Limits ( $C_{SDL}^D$ )Triglycerides

N			UV	p.c.r.
4	Trilaurin	$C_{12}$	$3 \times 10^{-6}$	
5	Trimyristin	$C_{14}$	$3 \times 10^{-6}$	$4-5 \times 10^{-7}$
13	Triolein	$C_{18:1}$	$2 \times 10^{-7}$	
11	Trilinolein	$C_{18:2}$	$2 \times 10^{-8}$	

Phospholipids

N	PC-			
1	Dihexanoyl	$C_6$	$2 \times 10^{-6}$	
3	Didecanoyl	$C_{10}$	$2 \times 10^{-6}$	
8	Diolein	$C_{18:1}$	$2 \times 10^{-7}$	$1-2 \times 10^{-6}$
9	Dilinolein	$C_{18:2}$	$8 \times 10^{-8}$	
10	Dilinolenin	$C_{18:3}$	$2 \times 10^{-8}$	

\*Calculated as concentration of sample in the detector by

$$C_{SDL}^D = \frac{(VC_s)(2\sigma \text{ noise})}{(F_L W_{\text{base}})(H)} \text{ where } V, C_s, F_L \text{ and } H \text{ are as previously}$$

defined,  $2\sigma$  noise is the noise amplitude in response units and  $W_{\text{base}}$  is the signal base width in time units.

for standards containing no double bonds. This is important if both detectors are to be used simultaneously as in the use of the value  $R_{Flr}^{uv}$  for determining the double bond number of a sample. The  $C_{SDL}^D$  data of Table 5-10 can be changed from concentration to approximate amount of standard injected by multiplying the given values by  $1 \times 10^{-3}$ , the dilution factor of the h.p.l.c. While the resultant values are approximate, they show that the p.c.r. detector, as mentioned in the previous section, is conservatively sensitive to nanomolar quantities of triglycerides and phospholipids. The p.c.r. used here is approximately  $10^4$  times more sensitive than the continuous flow analyzers used in clinical chemistry laboratories.

#### Evaluation of $R_{PCR}^{uv}$ and $R_{Flr,n}$

The expression for  $R_{Flr}^{uv}$  (Eqn. (5-30)) can also be expressed as:

$$\log R_{Flr}^{uv} = 2 \log D_b + Ca^{-1} \quad (5-32)$$

and predicts that the ratio of  $\log R_{Flr}^{uv}$  to  $\log D_b$  has a value of 2. The values for  $R_{Flr}^{uv}$  are summarized in Table 5-11. The value  $d \log R_{Flr}^{uv} / d \log D_b$  for triglyceride standards N 10 and 11 (3 and 6 double bonds, respectively) gave a value of 2.2.

Evaluation of  $R_{Flr}^{uv}$  for phospholipids was done using

Table 5-11: Detector response ratios for triglycerides.

Triglycerides

N	$R_{Flr}^{uv}$	n	$D_b$
4 Trilaurin	$0.06 \pm 0.007$	(15)	0
5 Trimyristin			0
10 Tripalmitolein	$2.98 \pm 0.14$	(15)	3
11 Trilinolein	$13.58 \pm 1.03$	(6)	6

Phospholipids

N	$R_{Flr}^{uv}$	n	$D_b$
3 P.C.-dicaprinoyl	$0.88 \pm 0.13$	(4)	0
8 P.C.-dioleoyl	$1.42 \pm 0.34$	(4)	2
9 P.C.-dilinoleoyl	$6.77 \pm 1.67$	(4)	4
10 P.C.-dilinolenoyl	$14.70 \pm 1.86$	(6)	6

$\log R_{Flr}^{uv} = 2.36 \pm 0.177 \log D_b - 0.64 \pm 0.105$  (correlation coefficient 0.9972).

an alternative graphical method, plotting the results of Table 5-11 in Fig. 5-17 and evaluating the relationships of  $\log R_{Flr}^{uv}$  to  $\log D_b$  by linear-regression analysis. These results are presented in Table 5-11.

The value  $R_{Flr}^{uv}$  is a parameter independent of the concentration or chromatography of the system. This value was investigated since it is of diagnostic value for evaluating the operation of the p.c.r. compared to the commercially available UV detector. The results indicate that the p.c.r. is acting as a molar sensitive detector independent of the triglycerides, of phospholipids molecular species identity. Furthermore, the relationship Eqn. (5-32) is important in using the UV and p.c.r. detectors together for total lipid analyses. The correlation between  $\log R_{Flr}^{uv}$  and  $\log D_b$ , 2.21 and 2.36 for triglycerides and phospholipids, respectively versus 2 predicted, is in contradiction with previously reported (11) results, where a linear relationship was shown without any theoretical basis.

The standards used here were well suited for determination of  $R_{Flr}^{uv}$  since they were conjugated alkenes. The predictive value of  $R_{Flr}^{uv}$  will have to be studied in greater detail and for other standards before it can be practically applied.

The p.c.r. detector is expected to have  $R_{Flr,n}$  independent of sample identity as long as the sample is



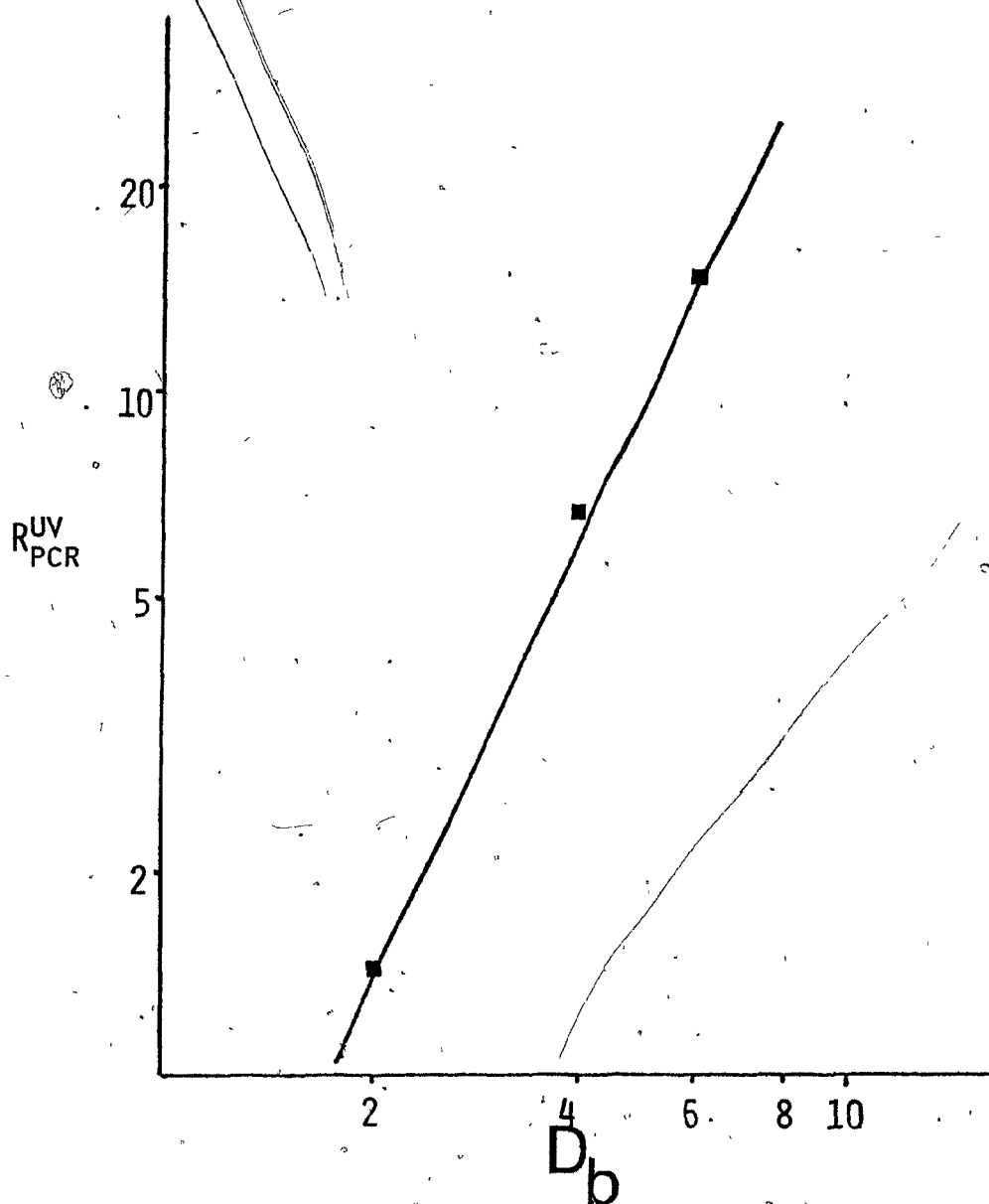


Figure 5-17. Plot of  $\log R_{PCR}^{UV}$  versus  $\log D_b$  for evaluation of equation 5-51.

triglyceride or phospholipid. The peak areas of four triglycerides were calculated and presented in Table 5-12. The p.c.r. detector is also characterized as being relatively selective for acyl-glycerides or phosphoglycerides. Chromatograms presented in Figs. 5-14 and 5-15 show the difference in selectivity of the p.c.r. to the UV detector.

The data in Table 5-12 were predicted by the results for  $R_{Flr}^{uv}$  since, if  $R_{Flr}$  is constant, this parameter is analogous to molar absorptivity and predicted by Eqn. (5-32). The p.c.r. response  $R_{Flr}$ , when reported as area, is independent of the chromatography. The data in Table 5-12 show within experimental error that the p.c.r. gives the response that was expected. Thus the detector gives the same response for any triglyceride and half the response for phospholipids. The chromatograms shown in Figs. 5-18 and 5-19 show the selectivity of the p.c.r. versus that of the UV detector. The p.c.r. does not appreciably detect the solvent chloroform and, in fact, is able to detect triglyceride co-eluting in the solvent band. Thus the p.c.r. behaves in every aspect as it was intended to.

Table 5-12: Molar response ( $R_{Flr}$ ) of the PCR measured as area.TRIGLYCERIDES

N			$R_{Flr}^1$ (S.D.), n=6
4	Trilaurin	$C_{16}$	140 ( $\pm 6$ )
10	Tripalmitolein	$C_{16:1}$	149 ( $\pm 18$ )
13	Triolein	$C_{18:1}$	170 ( $\pm 6$ )
14	Tripetroselinin	$C_{18:1}$	<u>152</u> ( $\pm 25$ )
		mean	152 ( $\pm 13$ )

PHOSPHOLIPIDS

N			$R_{Flr}^1$ (S.D.), n=3
3	Dicaprinoyl	$C_{10}$	79 ( $\pm 6$ )
8	Dioleoyl	$C_{18:1}$	67 ( $\pm 5$ )
9	Dilinoleoyl	$C_{18:2}$	67 ( $\pm 5$ )
10	Dilinolenoyl	$C_{18:3}$	<u>88</u> ( $\pm 6$ )
		mean	75 ( $\pm 10$ )

<sup>1</sup>Mean of n measurements ( $\pm 1$  S.D. unit).

$$\frac{R_{Flr} \text{ Triglyceride}}{R_{Flr} \text{ Phospholipid}} = 2.02.$$

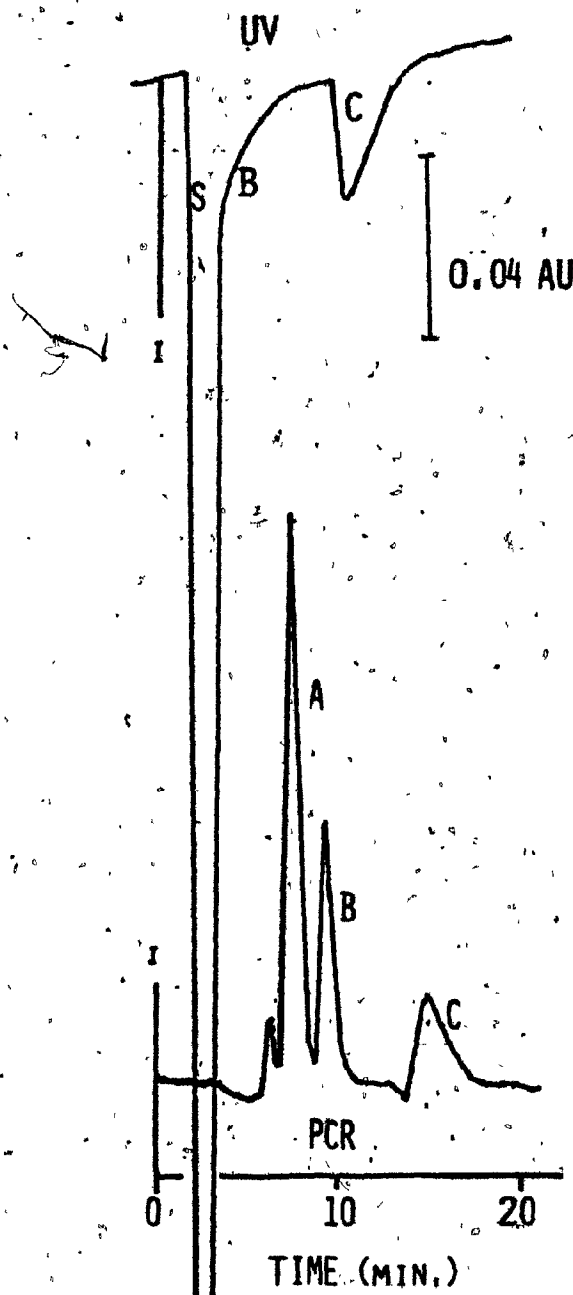


Figure 5-18. h.p.l.c. of triglycerides Tricaprin (A, 12.5 nmoles), Trilaurin (B, 11.1 nmoles) and Tripalmitolein (C, 9.98 nmoles) using the SF770 at 195 nm (UV) and the p.c.r. detector. The difference in occurrence of the responses is due to the dwell time of the p.c.r. S is the chloroform solvent response and I refers to when sample was injected.

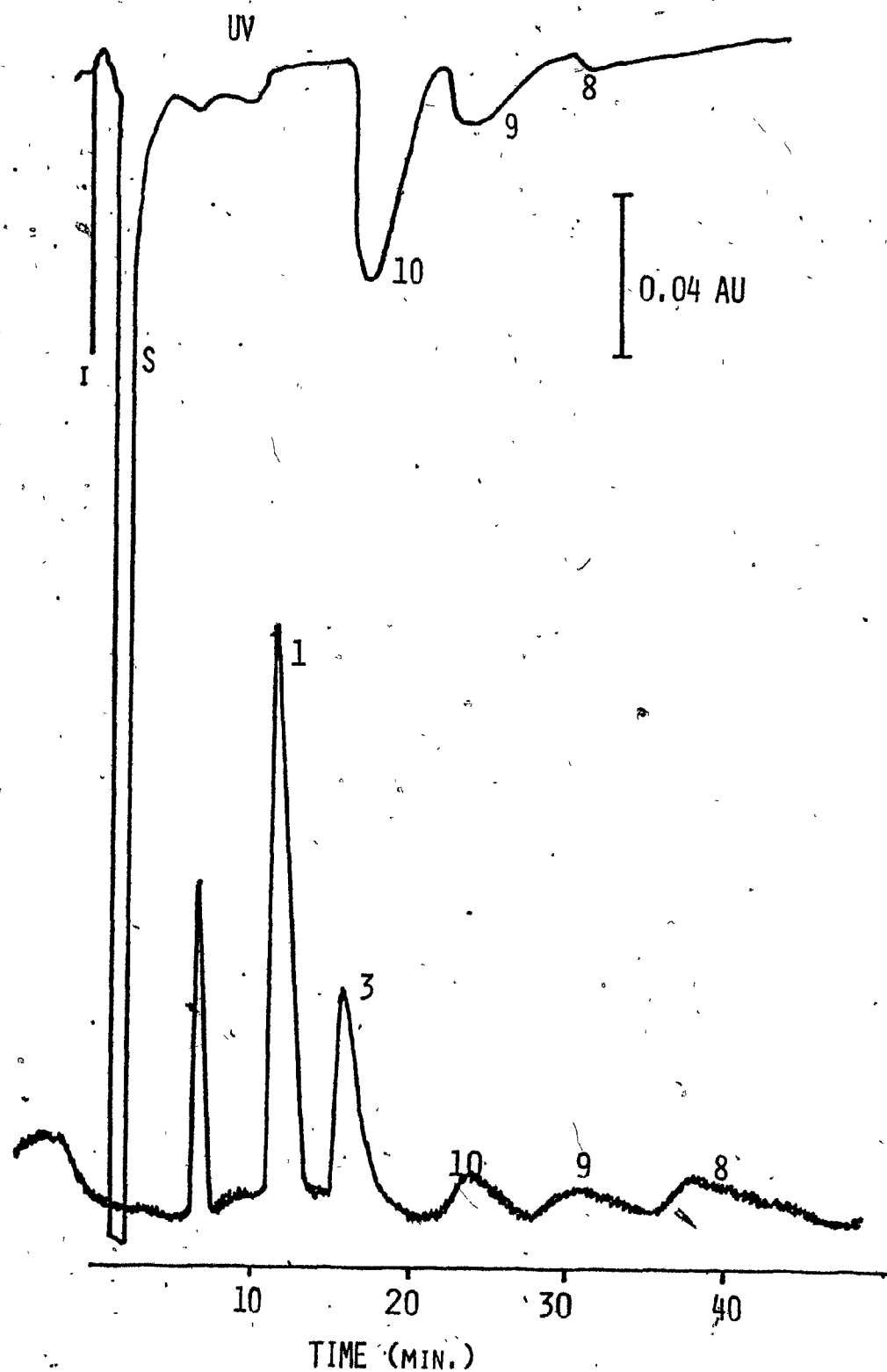


Figure 5-19. h.p.l.c. of phospholipids, 5- $\mu$ L of PL-I mixture was injected and bands are labelled with standard number N. S is the chloroform solvent, and I represents where sample was injected.

REFERENCES

1. Snyder, L.R. and Kirkland, J.J., in *"Introduction to Modern Liquid Chromatography"*, J. Wiley, New York, 1974.
2. Munk, M.N., *J. Chromatogr. Sci.*, 8 (1970) 491.
3. Krejci, M. and Pospisilova, N., *J. Chromatogr.*, 73 (1972) 105.
4. Magg, R.J., in *"Practical High Performance Liquid Chromatography"*, (C.F. Simpson, Ed.), Heyden and Son, Ltd., Hillview Gardens, London, 1978 p. 276..
5. Schenk, G.H., in *"Absorption of Light and Ultraviolet Radiation"*, Allyn and Bacon, Inc., Boston, 1973, p. 15-19.
6. Barrow, G.M., in *"Introduction to Molecular Spectroscopy"*, McGraw-Hill International Student Ed., Kogakusha Co., Ltd., Tokyo, Japan, 1962, pp. 276-279.
7. Lawrence, J.F. and Frei, R.W., *J. Chromatogr. Library*, Vol. 7, Elsevier, N.Y., 1976, p. 90.
8. Guilbault, G.G., in *"Practical Fluorescence"*, Marcel Dekker, Inc., New York, 1973, p. 18.
9. Baumann, W., *Fvesenins Z. Anal. Chem.*, 284 (1977) 31.
10. Tietz, N., in *"Fundamentals of Clinical Chemistry"*, W.B. Saunders; Philadelphia, 1976, p. 1225.
11. Holub, W.R., *Clin. Chem.*, 19 (1973) 1391.
12. Jungalwala, F.B., Evans, J.E. and McCluer, R.H., *Biochem. J.*, 155 (1976) 55.

APPENDIX 5-A

The SF770 and FS970 detectors have the same design of monochrometer. The bandpass (half-height) was given in Table 5-3 as 5 nm. The calibration of both detectors monochrometers involved using an atomic line source mercury discharge pen lamp (pen-ray<sup>®</sup> Quartz lamp, Ultra Violet Products, Inc. San Gabriel, Ca.) as replacement for the deuterium discharge lamp normally used with the detectors. The FS970 was calibrated by removing the low bandpass excitation filter (used to eliminate higher orders of the grating) and high band pass emission filter. Because the FS970 is a frontal fluorescence instrument the pen lamp radiation, after exiting from the monochrometer, was directly detected.

The SF770 was calibrated by directly monitoring the lamp current water on the front of the SF770 electronics module. When a line source was detected, the lamp current would decrease. This meter is normally used to judge the total radiation throughput to the photomultiplier tube.

Wavelengths were scanned by hand and are reported to the nearest 0.5 nm.

The expected and measured ( $\lambda_{\max}$ ) for the SF770 and FD970 are shown below in Table 5-A. The monochrometers are within the expected specifications for the bandpass of these units.

Table 5-A: Wavelength calibration of the SF770 and FS970.

	<u>Source</u>	<u>Expected <math>\lambda</math> (nm)</u>	<u>Measured <math>\lambda</math> (nm)</u>
SF770	Hg Lines	253.6	256.5
		289.4	292.0
		302.2	306.0
FS970	Hg Lines	253.6	254.0
		365.0	369.0
		404.7	407-408*
		407.8	
		435.83	437-441
		546.1	550.0

---

\*Not resolved.



### Claims to Originality

The research presented here had as its goal the development of an h.p.l.c. detector specific for triglycerides and phospholipids. This goal was attained, but the long-term goal of a system for total lipid analysis awaits further development.

By their very nature, preliminary investigations often necessitate many innovations. A list of the innovations presented in this thesis follows:

1) The concept of correlating  $R_{PCR}^{UV}$  to solute unsaturation and chromatographic retention data. The present work lays a firm foundation for implimenting further studies that may result in a system for the positive identification of the individual triglyceride or phospholipid species that are present in a complex matrix.

2) Detailed studies on the reversed-phase h.p.l.c. retention of phospholipids using mobile phases compatible with low wavelength ( 200 nm ) ultraviolet absorption detectors.

This was a prerequisite to the first claim, and also clarified the role of solute adsorption in the reversed-phase mode.

3) Construction of a phosphorus-sensitive transport detector by a modification of a commercial instrument. This detector was novel and further illustrated the limitations of transport-type detectors especially when dealing with non-volatile organophosphorus

compounds.

4) Construction of a molar-sensitive post-column reaction detector selective for triglycerides and phospholipids.

The entire unit was developed to be reliable and easy to use. A reliable bubbler was also developed. The use of a fluorescence detector with the segmenting bubbles passing through the cell was also inovative. This detector should find extensive use in the field of triglyceride and phospholipid analysis.

5) A practical experimental protocol (the Stop-Flow Optimization Scheme) for optimization of continuous flow analyzers. This scheme is novel and should be of great aid in automated analysis.

6) Investigations on the mechanism of the Nash method and the Sawicki and Carnes method for aldehyde analysis.

This represents a significant contribution to the field of aldehyde analysis since the elucidation of the mechanism of these two reagents led to the development of a totally new class of selective, sensitive, and rapid reagents. The Fluorals have the potential for superceding all other aldehyde reagents now in use.